

Monitoring reverse osmosis membrane integrity and virus rejection in water reuse

Marie-Laure Pype

▶ To cite this version:

Marie-Laure Pype. Monitoring reverse osmosis membrane integrity and virus rejection in water reuse. Life Sciences [q-bio]. University of Queensland [Brisbane]; Université Montpellier 2 (Sciences et Techniques), 2013. English. tel-02806818

HAL Id: tel-02806818

https://hal.inrae.fr/tel-02806818

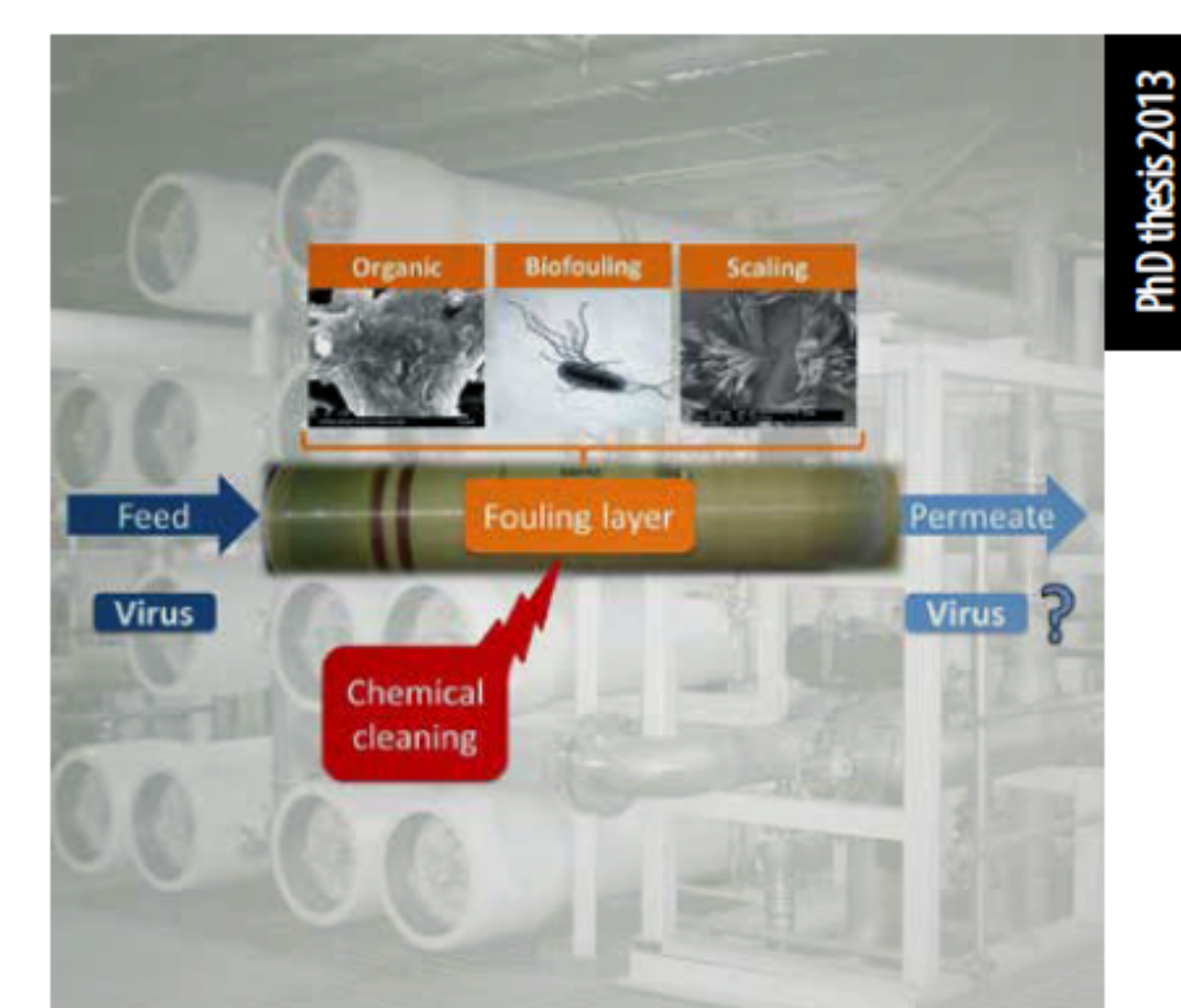
Submitted on 6 Jun 2020

HAL is a multi-disciplinary open access archive for the deposit and dissemination of scientific research documents, whether they are published or not. The documents may come from teaching and research institutions in France or abroad, or from public or private research centers.

L'archive ouverte pluridisciplinaire **HAL**, est destinée au dépôt et à la diffusion de documents scientifiques de niveau recherche, publiés ou non, émanant des établissements d'enseignement et de recherche français ou étrangers, des laboratoires publics ou privés.



Marie-Laure PYPE





CONTRÔLER L'INTÉGRITÉ DES MEMBRANES À OSMOSE INVERSE ET LE REJET DE SUBSTITUTS DE VIRUS DANS LES EAUX RECYCLÉES

MONITORING REVERSE OSMOSIS MEMBRANE INTEGRITY
AND VIRUS REJECTION IN WATER REUSE







Monitoring reverse osmosis membrane integrity and virus rejection in water reuse

Marie-Laure Pype

BSc Biochemistry

MSc Analytical chemistry

A thesis submitted for the degree of Doctor of Philosophy at

The University of Queensland in 2013
School of Chemical Engineering

&

L'université de Montpellier II in 2013

Ecole Doctorale Science des Procédés – Science des Aliments



Field of study: Chemical Engineering

Research centres: UQ/AWMC

INRA-LBE Narbonne

Oral defence: Brisbane, the 18th of December 2013

JURY

A/Prof Corinne Cabassud, Examiner

INSA Toulouse (France)

A/Prof Mikel Duke, Examiner

Victoria University (Australia)

Prof Jurg Keller, Chair

The University of Queensland (Australia)

A/Prof Raymond Steptoe, Convenor

The University of Queensland (Australia)

Dr Wolfgang Gernjak, Principal advisor

The University of Queensland (Australia)

Dr Dominique Patureau, Joint principal advisor

INRA-LBE Narbonne

Dr Nathalie Wéry, Associate advisor

INRA-LBE Narbonne

One of the major applications of reverse osmosis (RO) process is the production of high quality recycled water by providing a barrier to remove organic and inorganic contaminants as well as pathogens including viruses. In order to protect public health, validation and monitoring of the RO process integrity are necessary to ensure its correct operation. During operation a certain degree of fouling is inevitable and can reduce RO membrane performance. Thus, chemicals are often used in water treatment plants to prevent or remove the membrane fouling. However, these chemicals can modify the integrity of the polyamide layer on RO membrane over time. To date, the impact of membrane's physical change on its virus removal efficiency caused by the chemical use during operation is still not well understood.

A minimum virus removal efficiency of intact and impaired (e.g. by fouling) RO membranes can be ascertained by measuring the rejection of MS2 phage and membrane integrity indicators such as salt measured by conductivity, rhodamine WT (R-WT) or sulphate. However, conductivity measurement is the only full-scale standard monitoring technique. The removal of dissolved organic matter (DOM), which has been used as an indicator of water quality, can possibly be used for this purpose.

The first objective of this work was to assess the suitability of DOM as a membrane integrity indicator and to determine the impact of process failure on salt and DOM rejection in full-scale plants. A change of the conductivity does not necessarily mean that the membrane integrity has been breached. Thus, DOM monitoring has been tested and combined with the conductivity monitoring in order to distinguish between leaks and changes in membrane performances. It was concluded that DOM could be used as new monitoring technique. Moreover, a variation of DOM rejection can help identifying leaks better than just conductivity profiling alone.

The second objective was to determine the effect of membrane impairments on the rejection of one virus surrogate (MS2 phage) and four indicators (R-WT, DOM, sulphate and salt) using lab-scale RO set-ups. To this aim, two different cross-flow set-ups were used: a flat-sheet and a single 2.5" spiral-wound module.

Firstly, the effects of organic fouling and scaling on the rejection of virus surrogate and

indicators were studied separately. Organic fouling was created using a mix of organic foulants. The result of this study showed an increase of the rejection by more than 0.1 log for R-WT, salt and DOM. The general increase of the compounds' rejection might be due to the cavities blocking of the polyamide membrane and/or to the sorption of compounds to the fouling layer, which was observed by different autopsy techniques.

Scaling was created using a mix of inorganic salts in order to reconstitute the composition of a RO feed water and avoiding the presence of organic foulants. Scaling was found to have no impact on the rejection of all tested virus surrogates except for salt. Salt rejection showed a change of behaviour between different set-ups: with the 2.5" module set-up the inorganic layer led to a stabilisation of the salt rejection, whereas the salt rejection increased with the flat-sheet set-up. This could be explained by the variations of the systems configuration (i.e. spiral module versus flat-sheet, feed spacer height, etc.).

Secondly, the long-term impact of membrane ageing by exposure to chlorine, either active under filtration or passive by soaking, on the rejection of the virus surrogate and four indicators was studied. After a contact time of 9000 ppm·h NaOCl at pH 7, the membrane surface chemistry changed. The introduction of chlorine in the membrane chemistry and the breakage of amide bonds caused an increase of the water permeability and a decrease of the virus surrogate and indicators rejection. Despite the membrane damage being very strong a resulting reduction of salt rejection to 1.2 log (94%), the minimum rejection of MS2 phage was still of 3 log.

The last objective of this thesis was to evaluate the effect of the different experimental setups and impairments on the membrane integrity indicators' rejection to determine the most suitable lab-scale set-up to imitate full-scale and indicator(s) to monitor RO membrane integrity. The results of the two-way analysis of variance (ANOVA) showed that the type of set-ups and impairments had significant effect on the indicators' rejection. The statistical analyses confirmed that the stainless-steel flat-sheet cross-flow set-up was the most suitable set-up to imitate the full-scale regarding DOM rejection. Finally, a combination of DOM routine monitoring and R-WT challenge testing could be the best way to ascertain RO membrane integrity.

This PhD thesis adds several novel contributions relevant to science and industry. From a scientific perspective, this thesis demonstrated the application of fluorescence EEM to analyse organic rejection during RO filtration, the influence of organic fouling on the

rejection of different compounds by blocking the cavities of the membrane and also how chlorine attack affects RO monitoring techniques. From an industry perspective, this thesis will help develop novel monitoring techniques to control the RO process by adding knowledge on the rejection mechanisms of the different compounds as functions of the state of the membrane.

<u>Keywords:</u> Membrane ageing, membrane fouling, membrane integrity, membrane integrity indicators, reverse osmosis, virus surrogate, water reuse.

Les procédés d'osmose inverse (OI) permettent la production d'eau recyclée de très haute qualité grâce à l'élimination de contaminants organiques et inorganiques et de microorganismes. Le suivi du bon fonctionnement de ce procédé est nécessaire pour valider la rétention des virus pathogènes afin de protéger la santé des usagers. La présence de minéraux et matières organiques dans les effluents rend inévitable le colmatage des membranes lors de leur fonctionnement et diminue ainsi leur performance. Afin d'éviter et d'éliminer ces colmatages, les stations de traitements des eaux utilisent des produits chimiques. Ces derniers vont modifier les performances globales des membranes en polyamide comme par exemple la diminution de la perméabilité à l'eau, et plus particulièrement les performances de rétention des virus, or l'ensemble de ces perturbations n'est que très peu compris et donc peu maitrisé.

L'abattement des virus par OI sur des membranes intègres ou modifiées (ex : colmatage) ont donc été déterminés en mesurant la rétention d'un substitut de virus de type phage MS2 et d'indicateurs d'intégrité membranaire comme les sels (mesurés par conductivité), la rhodamine WT (R-WT) ou les sulfates. La conductivité est, en effet, la technique de contrôle standard dans les stations de traitement des eaux (échelle industrielle).

Le premier objectif de ce travail est d'évaluer l'utilisation d'un autre paramètre, les matières organiques dissoutes (DOM) comme nouvel indicateur et de déterminer l'impact du dysfonctionnement des procédés d'OI sur l'abattement des DOM et des sels à l'échelle industrielle. Les DOM peuvent en effet également être utilisées comme indicateur de qualité des eaux en fonction de leurs compositions et de leurs concentrations. L'abattement des DOM est donc testé comme nouvelle technique de surveillance afin de distinguer les fuites des changements de performance des membranes. Il est conclu que les DOM peuvent être utilisées comme nouvelle technique de suivi. De plus, une variation de l'abattement des DOM peut aider à identifier des fuites de manière plus robuste que par l'abattement des sels.

Le deuxième objectif est de déterminer l'effet des défauts membranaires sur les abattements d'un substitut de virus (phage MS2) et de quatre indicateurs d'intégrité (R-WT, DOM, sulfate et sels) à l'échelle de systèmes de laboratoire. Deux systèmes à flux longitudinal sont utilisés : une membrane plane et un module à spirale.

Dans un premier temps, l'effet du colmatage sur les abattements de ces différents substituts de virus et indicateurs est étudié.

Le colmatage organique, créé en utilisant un mélange de matières organiques, a pour effet d'augmenter de plus de 0,1 log les abattements de la R-WT, des sels et des DOM. Cette augmentation générale peut être due au blocage des cavités de la membrane et/ou par la sorption des composés sur les matières organiques.

Le colmatage inorganique, créé en utilisant un mélange de sels, n'a pas d'effet sur le rejet des composés sauf pour les sels qui montre un comportement différent entre les deux systèmes. Dans le système à membrane plane, la couche inorganique permet d'augmenter le passage des sels à travers la membrane. Par opposition, il n'y a pas d'effet sur leur abattement avec le module à spirale. Cette variation entre les deux systèmes peut être causée par la différence de configuration (module à spirale contre membrane plane).

Dans un deuxième temps, l'effet du chlore (modes passif et actif) sur la rétention de ces cinq composés est mesuré. Après un contact de 9000 ppm.h de NaOCl à pH 7, la surface membranaire change chimiquement. La formation de liaison Cl dans la couche en polyamide et la rupture des liaisons NH provoquent l'augmentation de la perméabilité à l'eau et diminuent l'abattement de l'ensemble des composés. Malgré une forte diminution de 1,2 log de l'abattement en sel, l'abattement minimum du phage MS2 reste de 3 log.

Le dernier objectif de cette thèse est de déterminer quel dispositif expérimental de laboratoire est le plus proche du fonctionnement de l'échelle industrielle et quel indicateur permet le mieux de caractériser l'intégrité du procédé d'OI. L'analyse de variance à deux facteurs (ANOVA) montre que le type de système et le type de défauts membranaires ont un impact significatif sur la rétention des composés. Les analyses statistiques révèlent que le système à membrane plane imite le mieux l'échelle industrielle pour l'abattement des DOM et que finalement, une combinaison DOM/R-WT peut être la meilleure façon de surveiller l'intégrité des procédés d'OI.

Cette thèse apporte des connaissances tant fondamentales qu'appliquées. Du point de vue scientifique, cette thèse démontre la possible application de la fluorescence tridimensionnelle pour l'analyse de la rétention des DOM par OI, l'influence du colmatage organique sur la rétention des différents composés en bloquant les cavités de la membrane et aussi comment l'attaque au chlore affecte les techniques de contrôle du procédé OI. Du point de vue industriel, cette thèse aidera à développer une nouvelle technique de suivi du procédé OI en

apportant des connaissances sur le mécanisme de rétention des différents composés en fonction de l'intégrité des membranes.

<u>Mots clés : Colmatage</u> des membranes, intégrité des membranes à osmose inverse, osmose inverse, source alternative d'eau potable, substitut de virus, vieillissement membranaire

Les devises Shadok



EN ESSAYANT CONTINUELLEMENT ON FINIT PAR REUSSIR. DONC: PLUS 4A RATE, PLUS ON A DECHANCES QUE GA MARCHE.

(http://www.lesshadoks.com/)

I would firstly like to express my deep gratitude to my three advisors Dr Wolfgang Gernjak (UQ/AWMC), Dr Dominique Patureau (UMII/INRA-LBE) and Dr Nathalie Wery (INRA-LBE).

Thank you Wolfgang for the chance you gave me to work on this project. Thank you for your patience and the discussions we had during these three years.

Merci Domi pour, encore une fois, m'avoir suivie sur ce nouveau projet. Merci pour toutes ces remarques constructives et ces encouragements même à plus de 15000 km. C'est toujours un plaisir de travailler avec toi.

Merci Nathalie pour tes encouragements et de ton aide à retrouver mon chemin dans le monde implacable de la microbiologie. Merci également pour tous ces commentaires et remarques qui m'ont aidée à mener cette thèse jusqu'à sa fin.

I would like to thank the directors of the two centres Prof Jurg Keller (UQ/AWMC) and Dr Jean-Philippe Steyer (INRA-LBE, Yop Yop) to welcome me in their respective laboratories. I thank also A/Prof Damien Batstone for having been my assessor during these 3 years.

Thank you very much Prof Cabassud (INSA-LISBP, France) and A/Prof Duke (VU, Australia) to have accepted to review this work. Your inputs during the examination process were valuable to improve this manuscript.

I would also like to thank Seqwater and Veolia Water Australia for the financial support obtained to perform this study in the context of the Water Recycling Research Program at The University of Queensland. I would like to give particularly thanks to Mr Yvan Poussade (Veolia Water Australia) for his help during these 3 years and for having been my assessor during year 1 and 2. I would like also to thank Mrs Annalie Roux (Seqwater) and Mr Cedric Robillot (Seqwater) for the interesting discussions we had. I would like to thank also Veolia Water staff working at the AWTP's (in particular Bradley Rhodes and Kersval Naidoo) and Queensland Urban Utilities (in particular Neville Jones) for their help to access the plants, information about the full-scale processes and their kindness.

Huge thanks must go to Dr Marc Pidou (MacGyver I) and Dr Bogdan C. Donose, for your help in the lab, for sharing your scientific point of view, your availability and your kindness. Thanks also to the drinking and recycling water team (or the French/European team) and especially to my little hands Llucia Marti. Thanks Markus (MacGyver II) to save my

experiments so many times and Ampon to have spent months and months on the data logger.

Thank you to the ASL lab especially Dr Beatrice Keller-Lehmann and Mr Nathan Clayton; to Mr Robert Simpson and Dr Michael Nefedov (SCMB RT-PCR facilities) to introduce me to the qPCR world. Thanks Alyshia Lyon for your help in the PC2 lab.

Thank you to all AWMC and LBE staffs and students. Big up to Viv, Jess, Sarah, Christine and Emma C., but also to my proof-readers Apra, Katrin D, Katrin S, Shao, Ilje and Claudio. Merci au bureau des pleurs alias Dr Kristell Le Corre et Dr Victoria Flexer. Ce fût un plaisir d'aller pleurer dans vos jupons. Un énorme merci à Nadine D, Mélanie and Maialen du LBE pour tout ce que vous m'avez apportée.

To my awesome friends, the PhD mafia alias: Adrian, Ann-Kathrin, Claudio, Emma, Fabien, Janske, Julie, Katrin, Marga, Selene and Victoria; but also Carly, Magda and Ilje. Mille mercis à Man & Julie, Nico, Mélan, Binomette, les Tchoups, les BB, les SM et Math.

Pour finir, merci à toute ma famille et tout particulièrement à mes parents, Benoit & Cécile & Chloé, Emmeline & Sébastien, tata Brigitte & Parrain. Merci de votre support, de vos encouragements et d'avoir cru en moi.

Bref MERCI!

Publications during candidatures

PEER-REVIEWED PAPER:

Pype, M.-L., Patureau, D., Wery, N., Poussade, Y., Gernjak, W. (2013). Monitoring reverse osmosis performance: Conductivity versus fluorescence excitation-emission matrix (EEM). *Journal of Membrane Science* 428, 205-211.

CONFERENCE PRESENTATIONS:

Pype, M.-L., Poussade, Y., Patureau, D., Wery, N., Gernjak, W. (2011). Fluorescence Excitation-Emission: a New Tool for Monitoring the Integrity of Reverse Osmosis Membrane? 6th IWA Specialist Conference on Membrane Technology for Water & Wastewater Treatment, 4-7th October 2011, Aachen, Germany. (Oral presentation)

Pype, M.-L., Patureau, D., Wery, N., Gernjak, W. (2012). Development of surrogates to monitor reverse osmosis membrane integrity and performance during filtration of pre-treated secondary effluent. *2012 UQ Engineering Postgraduate Research Conference*, 4th June 2012, Brisbane, Qld, Australia. (*Oral presentation*)

Pype, M.-L., Patureau, D., Wery, N., Donose, B. C., Gernjak, W. (2012). Virus surrogate in reverse osmosis membrane. Membrane Society Australasia 3rd Early Career Research Symposium, 28-30th November 2012, Brisbane, QLD, Australia. (*Oral presentation*)

Pype, M.-L., Patureau, D., Wery, N., Donose, B. C., Gernjak, W. (2013). Influence of different reverse osmosis membrane impairments on the rejection behaviour of virus surrogates – lab-scale study. *AWWA/AMTA Membrane Technology Conference & Exposition*, 25-28th February 2013, San Antonio, TX, USA. (*Oral presentation*)

Pype, M.-L., Patureau, D., Wery, N., Donose, B. C., Gernjak, W. (2013). Is Ageing Hard? A Study of Aged RO Membranes and their Integrity to Remove Virus Surrogates. *International Membrane Science and Technology Conference*, 25-29th November 2013, Melbourne, VIC, Australia. (*Oral presentation*)

Table of contents

Abstract	v
Résumé	ix
Acknowledgments	xiii
Publications during candidatures	xvii
List of figures	. xxiii
List of tables	xxix
List of nomenclature & abbreviations	xxxiii
Introduction	1
1. Literature review	7
1.1. Water recycling or reuse	8
1.2. Risk assessment in water reuse	12
1.3. Reverse osmosis	15
1.3.1. Principal failures in RO process	17
1.3.1.1. Process failures	17
1.3.1.2. Membrane impairments and failures	18
1.3.2. Monitoring RO membrane integrity	27
1.3.2.1. Direct monitoring	28
1.3.2.2. Indirect monitoring	28
1.4. Rejection of virus by membrane filtration process	29
1.4.1. Virus	29
1.4.2. Mechanisms of virus rejection by membrane	32
1.5. Application of virus surrogates and indicators for membrane integrity testing	36

	1.5.1. Su	errogates & indicators used to study virus LRV during filtration	36
	1.5.2. Ef	fect of failure modes on testing RO Membrane integrity	38
	1.6. Conclu	sion and thesis objectives	44
2.	Materials &	the methods	47
	2.1. Virus s	surrogate and membrane integrity indicators	48
	2.2 Lab-sca	ale experimental apparatus	50
	2.2.1. Sta	ainless-steel flat-sheet cross-flow set-up (SS flat-sheet set-up)	51
	2.2.2. Pla	astic flat-sheet cross-flow set-up (plastic flat-sheet set-up)	52
	2.2.3. Sp	viral-wound module set-up (2.5" module set-up)	54
	2.2.4. Me	embrane characteristics	55
	2.2.5. Me	embrane impairment protocols	56
	2.2.5.1.	Organic fouling	58
	2.2.5.2.	Scaling	60
	2.2.5.3.	Ageing	60
	2.3. Analyti	ical methods	61
	2.3.1. Ar	nalysis of virus surrogate and membrane integrity indicators	61
	2.3.1.1.	MS2 quantification	61
	2.3.1.2.	R-WT quantification	66
	2.3.1.3.	DOM analysis	66
	2.3.1.4.	Sulphate quantification	68
	2.3.1.5.	Electrical conductivity	68
	2.3.2. Ot	her chemical analysis	69
	2.3.3. Mo	embrane autopsies	69
	2.3.3.1.	Atomic force microscopy (AFM)	70
	2.3.3.2.	Scanning electron microscopy-energy dispersive spectroscopy (SEM-l	EDS)70
	2.3.3.3.	Attenuated total reflection-Fourier transform infrared (ATR-FTIR)	70

	2.4.	Stat	tistical data analysis	71
3.	Mo	onito	ring RO performance: Conductivity versus EEM	73
	3.1.	Rev	verse osmosis plant description, sampling protocols and general water quality.	74
	3.2.	Det	ermination of membrane defects through measurement of salt and organ	nics
	rejec		by conductivity and fluorescence profiling	
			derstanding the blue-shift of the fluorescence of humic substances from feed	
			nclusions and implications for practice	
4.	Eff	ect o	of membrane impairments: Organic fouling & Scaling	87
	4.1.	Org	anic fouling	88
	4.1	.1.	Membrane characteristics	88
	4.1	.2.	Membrane autopsy	89
	4.1	.3.	Rejection of virus surrogate and membrane integrity indicators	93
	4.2.	Sca	ling	97
	4.2	.1.	Membrane characteristics	97
	4.2	2.	Membrane autopsy	98
	4.2	3.	Rejection of virus surrogate and membrane integrity indicators	.100
	4.3.	Cor	nclusions	.102
5.	Eff	ect o	of membrane impairments: Ageing	.105
	5.1.	Me	mbrane characteristics	.106
	5.2.	Me	mbrane autopsy	.109
	5.3.	Rej	ection of virus surrogate and membrane integrity indicators	.114
	E 1	Cor	aclusions	110

6. St	ratistical comparison of experimental set-ups & membrane impairments	119
6.1.	Correlation between the rejection of the different membrane integrity indicators	121
6.2.	Effect of membrane impairment and set-up	123
6.3.	Comparison of the different lab-scale set-ups with the full-scale plant	129
6.4.	Conclusions	132
7. C	onclusions & recommendations for future research	133
7.1.	Conclusions	134
7.2.	Recommendations for future research	136
Refere	nces	141
Appen	dix A. Résumé en français	159
Appen	dix B. R program	173

Figure 1: Conceptual diagram of the 7 barriers approach to the planned indirect potable reuse
of water scheme in South East Queensland (Seqwater, 2011)
Figure 1.1: Schematic representation of the RO membrane process
Figure 1.2: SEM of a cross section of a thin film composite membrane. (1) shows a typical
chemistry of a cross-linked polyamide polymer, but variations are possible. (2) and (3)
are often made of poly (ether) sulfone and polyester
Figure 1.3: Simplified schematic of an RO train.
Figure 1.4: Typical spiral-wound module pressure vessel (from (USEPA, 2005))18
Figure 1.5: Schematic illustration of scale formation schemes (from (Antony et al., 2012)). 20
Figure 1.6: Excitation and emission wavelength boundaries (dash lines) for five EEM regions
(adapted from (Chen et al., 2003))22
Figure 1.7: Typical LC-OCD profile with the five fractions: biopolymers, humics, building
blocks, low molecular weight (LMW) acids and neutrals (adapted from (Huber et al.
2011))22
Figure 1.8: Proposed mechanism of polyamide membrane impairment by hypochlorite
(adapted from (Kwon et al., 2006; Do et al., 2012a))25
(adapted from (Kwon et al., 2000, Do et al., 2012a))2
Figure 1.9: Principle of deposition mode filtration (USEPA, 2005)39
Figure 1.10: Principle of suspension mode filtration (USEPA, 2005)
Figure 2.1: Summary of the virus surrogate and membrane integrity indicators analysed in the
different feed waters
umerem recu waters49
Figure 2.2: (a) photo and (b) drawing of the SS flat-sheet set-up

Figure 2.4: (a) photo and (b) drawing of the 2.5" module set-up
Figure 2.4. (a) photo and (b) drawing of the 2.3 module set-up
Figure 2.5: General experimental protocol developed for the impaired RO membrane experiments
Figure 2.6: R-WT rejection as a function of filtration time with three different membrane
coupons. Error bars = standard error of 5%
Figure 2.7: Typical LC-OCD chromatograms of (a) RO feed and RO permeate from a South East Queensland AWTP and (b) organic foulants (black line) (from (Fujioka et al., 2013))
Figure 2.8: The qRT-PCR principle using TaqMan probes (Bustin and Mueller, 2005)63
Figure 2.9: Amplification curves (a) and standard curve (b) of 10-fold diluted MS2 from 10^6 to 10^2 ng· μ L ⁻¹ 65
Figure 3.1: Simplified schematic of an RO train in plant A with online conductivity sensors (red triangle) and sampling points used to measure offline conductivity and fluorescence (green circle). *In plant B, the total perments conductivity is manitored online for entire
(green circle). *In plant B, the total permeate conductivity is monitored online for entire RO trains
Figure 3.2: Typical RO (a) feed diluted 50 times and (b) permeate EEM. The location of the three regions evaluated is delimited by solid lines
Figure 3.3: Percentage of salt rejection using conductivity and percentage of organic rejection using the FRI method for two RO trains (3 stages) during a single sampling event. Examples of (a) a drop of salt rejection in a train without major leaks and (b) a drop of both salt and organic rejections in a train with a broken interconnector in stage 3. PV 1.X: pressure vessel X pertaining to stage 1; PV2.X pressure vessel X pertaining to stage 2 and PV3.X: pressure vessel X pertaining to stage 3
Figure 3.4: SEC chromatograms of (a) RO feed, and (b) RO permeate from stage 3 train 2 plant A. Note: the ordinate scale in arbitrary fluorescence units differs by a factor of 100 xxiv

Figure 2.3: (a) photo and (b) drawing of the plastic flat-sheet set-up......53

between (a) and (b).
Figure 3.5: DOM rejection calculated from SEC chromatograms of RO feed diluted 50 time and undiluted RO permeate for (a) 305 / 385 nm and (b) 335 / 440 nm ($\lambda_{excitation}$ $\lambda_{emission}$) from stage 3 train 2 plant A
Figure 4.1: (1) Digital photographs, (2) SEM (bar scale = 50 μm) and (3) AFM (30 x 30 μm height scale bar: 300 nm) images of (a) intact and organically fouled membranes with (b) the SS flat-sheet set-up and (c) the 2.5" module set-up92
Figure 4.2: ATR-FTIR spectra of intact and organically fouled membranes with the SS flat sheet set-up and the 2.5" module set-up. Vertical black lines = characteristic peaks of polyamide
Figure 4.3: Comparison between MS2 phage, salt (EC), R-WT, DOM and sulphate rejection by intact and organically fouled membranes using (a) the SS flat-sheet and (b) the 2.5 module set-ups. Error bars = standard deviation, $n = 9$ (3 measurements/coupon, membrane coupons) for SS flat-sheet set-up and $n = 6$ (1 membrane module) for the 2.5 module set-up. Black arrow (\rightarrow) = value determined limited by the LOQ of the analytical technique, i.e. permeate concentration below LOQ. Value above bar = t -test p value.
Figure 4.4: SEM images (bar scale = $50 \mu m$) and EDS results of (a) intact and scaled membranes with (b) the SS flat-sheet and (c) the 2.5" module set-ups99
Figure 4.5: Comparison between the overall MS2 phage, conductivity, R-WT, DOM and sulphate rejections by intact and scaled membranes using (a) the SS cross-flow set-up and (b) the 2.5" module set-up. Error bars = standard deviation, n = 9 (3 measurements/coupon, 3 membrane coupons) for SS flat-sheet set-up and n = (1 membrane module) for the 2.5" module set-up.
Figure 5.1: Evolution of water permeability (K _w , round) and salt rejection (R _{salt} , cross) with the SS cross-flow set-up (passive mode). System fed sequentially with DI water, NaC solution (1500 mg·L ⁻¹) and pre-filtered secondary effluent

Figure 5.2: AFM images (30 x 30 μm) of (a) intact membranes used to filtered (1) RO feed
synthetic (MS2, R-WT and salt) and (2) pre-filtered secondary effluent (DOM, sulphate
and salt), and aged membranes with (b) the plastic flat-sheet (1. active and 2. passive
modes), (c) the SS flat-sheet and (d) the 2.5" module set-ups. Height scale bar: 300 nm
for intact, 200 nm for active and passive ageing using the plastic flat-sheet set-up, and
400 nm for the SS flat-sheet and the 2.5" module set-ups
Figure 5.3: ATR-FTIR spectra of intact and aged membranes with the plastic flat-sheet
(active and passive modes), the SS flat-sheet and the 2.5" module set-ups. Black boxes =
peaks modified by the chlorine attack
Figure 5.4: Comparison between MS2 phage, R-WT, salt (EC), DOM and sulphate rejections
with intact and aged membranes using (a) the plastic flat-sheet, (b) the SS flat-sheet and
(c) the 2.5 " module set-ups. Error bars = standard deviation, $n = 12$ for the plastic flat-
sheet set-up (3 measurements/coupon, 4 membrane coupons), n = 6
(3 measurements/coupon, 3 membrane coupons) for the SS flat-sheet set-up and $n=6$ (1
membrane module; MS2 phage $n = 1$) for the 2.5" module set-up. Black arrow (\rightarrow) =
LRV value determined limited by the LOQ of the analytical technique, i.e. permeater
concentration below LOQ. Value above bars = t -test p - $value$
Figure 5.5: Picture of the 2.5" spiral-wound module ageing set-up116
Figure 6.1: Effect of the set-up scales on the LRV of indicators. Module = 2.5" spiral-
wound module set-up, Plastic = plastic flat-sheet cross-flow set-up, SS = stainless-
steel flat-sheet cross-flow set-up. The numbers in the graphs = number of sample
per impairment128
Figure 6.2: Effect of the different impairments on the LRV of indicators. I = intact
membrane, OF = organic fouling impairment, S = scaling impairment, PA = passive
ageing impairment and AA = active ageing impairment. The numbers in the graphs
= number of sample per impairment129

membranes. Module = 2.5" spiral-wound module set-up, Plastic = plastic flat-shee
cross-flow set-up, SS = stainless-steel flat-sheet cross-flow set-up. Numbers in graphs =
number of sample per impairment
Figure 7.1: LRV of MS2 phage and membrane integrity indicators by intact RO membranes
based on this thesis results138

List of tables

Table 1.1: IPR projects around the world.	10
Table 1.2: Physical parameters, potential chemical and pathogen risks associated of recycled water.	
Table 1.3: Australian Guidelines for Water Recycling definition for terms investigation pathogens.	
Table 1.4: Summary of studies on the impact of hypochlorite on RO	26
Table 1.5: Human viruses documented to be found in the wastewater.	31
Table 1.6: Log removal and concentration of viruses (C virus) in different secondary and tertiary wastewater treatment.	
Table 1.7: LRV of MS2 phage, microsphere and R-WT depending on the RO s and the type of impairment.	•
Table 2.1: Synthetic RO feed water characteristics.	49
Table 2.2: Pre-filtered secondary effluent characteristics (n = 15)	50
Table 2.3: Operating conditions used in the lab-scale apparatus	51
Table 2.4: Summary of the different analytical techniques and their limit of quantify the compounds	
Table 2.5: The qRT-PCR reaction mixture composition.	64
Table 2.6: Primers and probe used for the quantification of MS2 phage	64
Table 2.7: FRI parameters of each region	67
Table 2.8: Summary of the microscopy and spectroscopy techniques, their function use by type of membrane impairment	

Table 3.1: Mean water quality characteristics (± standard deviation) on the days samples (n=4)
Table 3.2: FRI parameters and average percentage share of fluorescence response of each region in feed and permeate ($P_{i,n} \pm \text{standard deviation}$) for plant A and B76
Table 3.3: Percentage of salt and DOM rejection (± standard deviation) by RO stage of the three delimited fluorescence regions
Table 4.1: Comparison of water permeability and NaCl rejection before and after organic fouling with the SS flat-sheet and the 2.5" module set-ups at an applied pressure of 7.5 bar and a cross-flow velocity of 10 cm·s ⁻¹ . Temperature normalised at 25°C
Table 4.2: Zeta potential values of organic foulant solutions, intact and fouled ESPA2 ROmembranes at pH 7.
Table 4.3: Comparison of water permeability and salt rejection before and after scaling at an applied pressure of 7.5 bar and a cross-flow velocity of 10 cm·s ⁻¹ . Temperature normalised at 25°C
Table 5.1: Comparison of water permeability ($K_w \pm standard deviation$) and NaCl rejection ($R_{salt} \pm standard deviation$) before and after ageing with the plastic flat-sheet (plastic set-up at an applied pressure of 5 bar and a cross-flow velocity of 10 cm·s ⁻¹ ; the SS flat sheet (SS) and the 2.5" module (module) set-ups at an applied pressure of 7.5 bar and cross-flow velocity of 10 cm·s ⁻¹ . Temperature normalised at 25°C
Table 5.2: RMS (± standard deviation) as a function of the ageing conditions112
Table 5.3: Principal peak assignment for FTIR of intact and aged polyamide RO membrane
Table 6.1: Summary of the different experiments done for each scale
Table 6.2: Pearson's cross-correlation matrix for each combination of indicators (LRV)123

Table 6.3: <i>p-values</i> of the indicators obtained from the two-way ANOVA124
Table 6.4: <i>p-values</i> of the <i>t</i> -tests for the comparison between the different types of set-up. 125
Table 6.5: <i>p-values</i> of the <i>t</i> -tests for the comparison between the different types of impairment
Table 6.6: p -values of the t -tests for the comparison between the full-scale and lab-scale
set-ups

List of nomenclature & abbreviations

Nomenclature

 Λ conductivity measurement (μS·cm⁻¹)

 $\Delta\lambda$ wavelength interval

 Λ wavelength (nm)

Φ volume of fluorescence intensity beneath of each region

 π osmotic pressure

C solute concentration (mg·L⁻¹ or equivalent)

d membrane thickness (m)

D dilution factor

Da dalton

E PCR efficientF Fisher's F-test

 $J_w \qquad \qquad \text{permeate flow } (L \cdot h^{\text{-}1} \cdot m^{\text{-}2})$

K constant characteristic of active layer membrane material

 K_s membrane permeability (m·s⁻¹)

 K_w water permeability $(L \cdot h^{-1} \cdot m^{-2} \cdot bar^{-1})$

MF multiplication factor

N number of plaque

 N_{PFU} number of plaque forming unit (PFU·mL⁻¹)

P Pressure (bar)

 $P_{i,n}$ percent fluorescence response of each region 'i' (%)

 Q_s rate of salt flow through the membrane $(m^3 \cdot s^{-1})$

r Pearson's correlation coefficient

R recovery (%)

R_% percentage rejection (%)
S membrane area (m²)

TCF temperature correction factor

V sample volume (mL)

Vnpnts number of height event

Y height of the peak

Subscripts

em emission ex excitation

f feed

i specific fluorescence region

in influent
meas measured
n normalized
out effluent

p permeate

T cumulative volume

Abbreviations

AFM: atomic force microscopy DALY: disability-adjusted life year

AGWR: Australian Guidelines for DBP: disinfection by-product

Water Recycling DI: de-ionised

ANOVA: analysis of variance DOC: dissolved organic carbon ATR-FTIR: attenuated total reflection- DOM: dissolved organic matter

Fourier transform infrared

spectroscopy EC: electrical conductivity

AWTP: advance water treatment EDS: energy dispersive

plant spectroscopy

EEM: excitation emission matrix

BNR: biological nutrient removal ELISA: enzyme-linked

immunosorbent assay

CA: cellulose acetate

CCP: critical control point FRI: fluorescence regional

CP: concentration polarisation integration

xxxiv

qRT-PCR: quantitative reverse IC: ion chromatography

transcriptase polymerase **ICP-OES**: inductively coupled plasma-

chain reaction optical emission spectrometry

R-WT: rhodamine WT LC-OCD: liquid chromatography-

> RMS: root-means-square organic carbon detector

RO: reverse osmosis LOQ: limit of quantification

LRV: log removal value SEC: size exclusion

LMW: low molecular weight

scanning electron microscopy M_F: SEM: microfiltration

chromatography

SEQ: South East Queensland MW: molecular weight

SIM: spiked integrity monitoring MWCO: molecular weight cut off

SS: stainless-steel

N/A: not available TCF: temperature correction factor

TMP:

N.A: not applicable TEM: transmission electron

N-Nitrosodimethylamine NDMA:

microscopy NF: nanofiltration

transmembrane pressure TOC: total organic carbon

PA: polyamide

PAC: powdered activated carbon UF: ultrafiltration

PES: poly (ether sulfone) UV: ultraviolet

PFU: plaque forming unit

pressure vessel

pI: isoelectric point WHO: World Health Organisation PV:

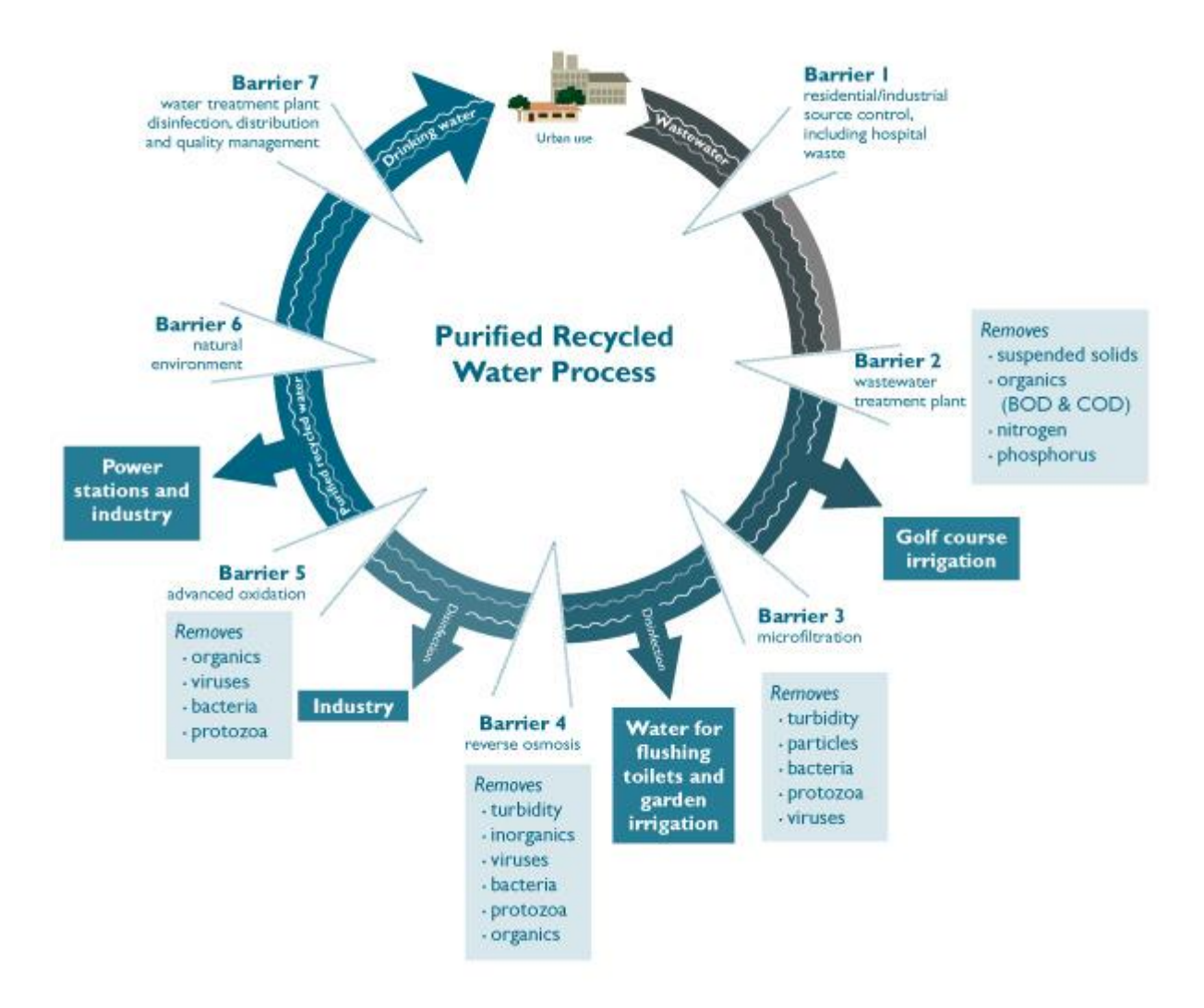
XPS: **QPCR**: quantitative polymerase chain X-ray photoelectron

> reaction spectroscopy

Introduction

With an increasing demand for water due to global climate change, urbanisation and population growth, alternative sources of water supply have to be used in order to supplement conventional water sources (i.e. surface water and groundwater) (Semiat, 2008). Considering the social, economic and environmental impacts, water recycling is a part of the solution for water scarcity and therefore becomes an increasingly important source of water (Shannon et al., 2008; Grant et al., 2012). Recycled water is used for industry, agriculture, public space irrigation, dual pipe reticulations systems in households and augmentation of drinking water supplies by indirect potable reuse (IPR).

Using wastewater as water supply may pose a potential risk due to chemicals and pathogen contamination. Wastewater recycling is not a new practice. Since the 1970s, IPR has been practised in several parts of the USA like California and Virginia (Salinas Rodriguez et al., 2009). Nowadays, applications are implemented around the world in Africa, Asia, Australia and Europe (Radcliffe, 2004). The share of potable water provided by IPR is dependent on the area. For example, IPR constitutes 4.8% of the potable water for the Orange County Water District (California, USA), and 2.5% in Singapore (Radcliffe, 2004; Bastian, 2006). The majority of IPR plants use microfiltration (MF) or ultrafiltration (UF) followed by reverse osmosis (RO) and ultraviolet (UV) sometimes coupled with hydrogen peroxide (H_2O_2) (Radcliffe, 2004). These barriers are designed to collectively prevent the infiltration of contaminants from the wastewater into drinking water supplies prior to supplementation of the water supply reservoir (dams or groundwater). The reservoir is considered as an environmental barrier which facilitates elimination of any remaining contaminants by physical or biological processes. It also permits to reduce any potential risk by decreasing the concentration of contaminants by dilution in case of any failure occurring during treatment process (USEPA, 2012). Figure 1 presents the largest recycled water scheme constructed in Australia using seven barriers system to ensure the highest standard of water quality to the South East Queensland (SEQ) population (Seqwater, 2011). The multiple barrier system is the chosen way to reduce the potential chemical and pathogen risks to an acceptable level. The greatest pathogen risks are associated with ingestion of water contaminated with faeces from humans and animals. Moreover, some organisms can grow in piped water distribution systems (e.g. Legionella) (WHO, 2011). With the aim of public health protection and increased public acceptance, the treatment processes should be validated according to specific guidelines (NRMMC et al., 2008; WHO, 2011). However, legislation regarding the validation of treatment processes for water recycling purpose is typically country or even state dependent.



<u>Figure 1:</u> Conceptual diagram of the 7 barriers approach to the planned indirect potable reuse of water scheme in South East Queensland (Seqwater, 2011).

The Australian Guidelines for Water Recycling (AGWR), based on the risk assessment from sewage to IPR, requires a log removal above 9.5 for pathogenic viruses and a log removal above 8 for pathogenic bacteria and two protozoa: *Giardia* and *Cryptosporidium* (NRMMC et al., 2006, 2008). The membrane filtration processes used in IPR plants aim to remove microorganisms including bacteria and viruses but to a different extent. MF can remove from 1 to > 7 log of bacteria and 0 to 2 log of viruses (Jacangelo et al., 1995; Lovins III et al., 2002; Lebleu et al., 2009). UF processes can remove from 1.5 to > 7 log of bacteria and viruses (Jacangelo et al., 1995; Asano, 2007). The removal efficiency of these two processes

depends on the type of membrane and the quality of water effluent. RO membranes are commonly used in tertiary treatment for water reuse applications as the last physical disinfection process due to their theoretical capacity to remove completely viruses (Shannon et al., 2008). However, several studies showed the passage of viruses across RO membrane due to a lack of membrane integrity (Adham et al., 1998b; Kitis et al., 2003; Lozier et al., 2003; Mi et al., 2004). To monitor the integrity of RO membranes and continuously assess their rejection performance, conductivity profiling is generally used (Adham et al., 1998b). Although this technique can be applied online, conductivity is neither very sensitive (1.7 - 2 log) nor a good predictor of virus rejection (Kitis et al., 2003). Thus, there is an urgent need to develop a direct online monitoring method to assess the efficiency of RO membrane to remove viruses. Dissolved organic matter (DOM) is generally used as an indicator of water quality. Therefore, Henderson *et al.* (2009) mentioned that DOM could be used as a new monitoring technique for recycled water systems.

Thesis objectives – *general:*

In order to develop an efficient method to monitor RO membrane virus integrity, it is essential to firstly understand the mechanisms of virus removal by intact but also impaired membranes. Thus, the objectives of this thesis were to:

- Assess the suitability of dissolved organic matter (DOM) as a novel integrity indicator and to determine the impact of process failure on the salt and DOM rejections in full-scale plants;
- Understand the effect of membrane impairments on monitoring techniques for virus rejection;
- Compare the different experimental set-ups and membrane impairments on the rejection of the compounds used in this thesis.

This knowledge will help to select a single or a combination of several indicator(s) to monitor RO systems effectively. Assessing the potential rejection of processes correctly will contribute to increasing the confidence of government authorities and consumers and the acceptability of potable reuse schemes employing RO membranes.

Thesis organisation:

This thesis comprises seven chapters and two appendices. Chapter 1 begins with the description of the scientific context through an overview of water reuse and its risk assessment. Then, RO membrane filtration and its potential failures are presented followed by a discussion on virus removal and the application of virus surrogates in validation and monitoring of RO processes. The chapter ends with the presentation of the thesis objectives. Chapter 2 details the materials and methods used in this work. The next four chapters present the results and discussion of the thesis. Chapter 3 investigates the effect of RO process integrity using two indicators (salt by electrical conductivity and dissolved organic matter) in two full-scale AWTPs. Chapters 4 and 5 study the effect of membrane impairments such as fouling (organic fouling and scaling; Chapter 4) and ageing (Chapter 5), on virus surrogate and membrane integrity indicators rejection at lab-scale. Chapter 6 analyses the impact of the operational parameters and usage of different experimental set-ups and scales on compounds rejection with statistical tests such as *t*-tests and two-way analysis of variance (ANOVA). Finally, Chapter 7 presents the overall conclusions of this work and proposes several recommendations for future research that may result from this work.

1. Literature review

1.1.	Wa	ater recycling or reuse	8
1.2.	Ris	sk assessment in water reuse	12
1.3.	Rev	verse osmosis	15
1.3	3.1.	Principal failures in RO process	17
	1.3.1	.1. Process failures	17
	1.3.1	.2. Membrane impairments and failures	18
1.3	3.2.	Monitoring RO membrane integrity	27
	1.3.2	2.1. Direct monitoring	28
	1.3.2	2.2. Indirect monitoring	28
1.4.	Rej	jection of virus by membrane filtration process	29
1.4	4.1.	Virus	29
1.4	4.2.	Mechanisms of virus rejection by membrane	32
1.5.	App	plication of virus surrogates and indicators for membrane integrity testing	36
1.5	5.1.	Surrogates & indicators used to study virus LRV during filtration	36
1.5	5.2.	Effect of failure modes on testing RO Membrane integrity	38
1.6.	Cor	nclusion and thesis objectives	44

1.1. Water recycling or reuse

According to the guidelines of water reuse (USEPA, 2012), recycled water is "municipal wastewater that has been treated to meet specific water quality criteria with the intent of being used for a range of purposes. The term 'recycled water' is synonymous with 'reclaimed water'. Municipal wastewater is composed of water, salt, organics and nutrients at different concentrations. The wastewater quality depends on the type of population waste and the type of industry or hospitals present for example. Wastewater treatment is composed of a series of processes which permit to remove contaminants (Wilf, 2010). Briefly, preliminary treatment removes large solids and grit by physical processes such as screening. Primary treatment removes total suspended solids (TSS) and some biochemical oxygen demands (BOD). Secondary treatment removes colloidal and soluble organic contaminants. Advanced and tertiary treatments increase the removal of nutrients, pathogens and sometimes metals. Finally, disinfection is the last treatment before discharge of the water into the environment and permits to avoid the spreading of waterborne diseases.

Water recycling is not a new concept. Indeed, in ancient Greece, wastewater was already reused to irrigate agriculture by the elaborate design of sewerage systems (Angelakis and Spyridakis, 1996). In the 19th century, catastrophic epidemics of waterborne diseases took place due to the lack of adequate water and wastewater treatment. As a consequence, engineering solutions have been developed for alternative water sources and filtration systems have been progressively installed (Barty-King, 1992). However, it is only at the end of the 20th century that the USA and the European Union had accepted more broadly the idea to use wastewater as supplementing water resources (Asano and Levine, 1996). Nowadays, wastewater recycling has attracted worldwide interest due to the reduction of usual water supplies, global warming, urbanisation, population growth, and environmental problems due to the discharge of inadequately treated sewage effluent (Radcliffe, 2004).

Recycled water can be produced at different water quality depending on its end-use (Bastian, 2006):

- Non-potable water reuse for industry, agriculture, landscape irrigation (residence, golf club, parks and school grounds dual reticulation systems);
- Potable water reuse to increase drinking water supplies via direct or indirect potable reuse.

Direct potable reuse projects may be put in place temporally due to extreme circumstances such as severe drought; but it is the category of water reuse least accepted by population. An example of a continuously operating direct potable reuse plant is the one in Namibia. The Windhoek's Goreangab reclamation plant treats water and blends it with potable water distribution network to provide up to 25% of the Windhoek city consumption since 1968 (du Pisani, 2006). In contrast, different indirect potable reuse (IPR) schemes have been successfully implemented in the USA (e.g. California, Water Factory 21 and Orange County Water District Council), Europe and Asia and are presented in Table 1.1 (Rodriguez et al., 2009; USEPA, 2012).

In Australia, there are some projects considering the use of IPR through aquifer recharge or dam supplementation in Perth (Western Australia) and South East Queensland (SEQ), but none is implementing potable reuse as yet for a variety of reasons, among them concerns related to community acceptance. The city of Toowoomba (Qld) is a good example for demonstrating the importance of public opinion. Indeed, in this case the development of a potable water recycling project has not been fulfilled because of the opposition of the local community to this project (Hurlimann and Dolnicar, 2010). Hurlimann and Dolnicar (2012) demonstrated the power of the media on the public acceptance to water recycling in Australia and concluded on the fact that the media should use scientific evidence and be impartial in their statement. Nevertheless, the critical water supply situation in late 2007 and early 2008 in SEQ changed the public opinion towards water reuse as IPR to supplement the Wivenhoe dam. However, as rainfalls increased in late 2008, the community was less supportive and the Queensland Government changed its recycled water policy from continuous use of IPR to emergency use when the dam levels fall below 40% of its capacity (Rodriguez et al., 2009). In order to improve the acceptance of IPR by the population, it is important to demonstrate that the potential risks are well managed by implementing suitable monitoring of the different water treatment processes. In this context, it may seem an interesting observation that the community concerns about engineered potable reuse systems are generally much higher than the in principle similar practice of so-called unintentional potable reuse. This happens for instance along major river systems such as the River Rhine or the River Thames in Europe, where one community abstracts water from the river, uses it, treats it and discharges it back to the river to be used again by the community living downstream (Bixio and Wintgens, 2006).

<u>Table 1.1:</u> IPR projects around the world.

Project	Place	Treatment	Buffer	% Blended
Orange County Water District (OCWD). Water Factory 21	California (USA)	Lime clarification, recarbonation, multimedia filtration, granular activated carbon, filtration, RO and UV/ H_2O_2	Aquifer	3.2% total water 4.8% groundwater
OCWD Groundwater replenishment system (Upgrade of the Water Factory 21 plant)	California (USA)	MF/RO and UV/H ₂ O ₂	Aquifer	15 - 18%
West Basin Municipal Water District	California (USA)	MF/RO and UV/H ₂ O ₂	Aquifer	10 - 15%
Upper Occoquan Sewage Authority (UOSA)	Virginia (USA)	Lime clarification, two-stage recarbonation, flow equalization, sand filtration, granular activated carbon ion exchange, post carbon filtration and chlorination	Reservoir	10 - 45%
Montebello Forebay Groundwater Recharge Project	California (USA)	Secondary treatment, inert media filter, chloramination and injection	Aquifer	18.7 - 35%
San Diego Water Repurification Project*	California (USA)	MF/RO and UV/H ₂ O ₂	Reservoir	N/A
Hueco Bolson Recharge Project	Texas (USA)	Two-stage powdered activated carbon treatment, lime treatment, two-stage recarbonation, sand filtration, ozonation, granular activated carbon filtration, chlorination and storage	Aquifer	40 - 100%
The Chelmer Augmentation Wastewater Reuse Scheme	Essex (UK)	MF and UV	Reservoir	8 - 12%
Water Reclamation Study (NeWater)	Singapore	UF/RO, UV, Stability control and chlorination	Reservoir	2.5%

<u>Table 1.1:</u> IPR projects around the world (continued).

Project	Place	Treatment	Buffer	% Blended
Torreele Reuse Plant	Wulpen (Belgium)	MF/RO and UV disinfection	Aquifer	40%
Valley Integrated Water Resource Management	Bangalore (India)	Membrane treatment and granular activated carbon	Reservoir	N/A
Western Corridor Recycled Water Project*	SEQ (Australia)	UF/RO and UV/H ₂ O ₂	Dam	N/A
Llobregat Delta*	Barcelona (Spain)	UF/RO and UV	Aquifer recharge	N/A

MF: microfiltration.

N/A: Not available.

RO: reverse osmosis.

SEQ: South East Queensland.

UF: ultrafiltration.

UV: ultraviolet.

% blended: % of recycled water blended with alternate sources.

*: Water produced not yet use as IPR.

Adapted from (Rodriguez et al., 2009; USEPA, 2012).

1.2. Risk assessment in water reuse

The use of recycled water poses many risks. One of the main risks associated with recycled water is the potential damage to public health which obliges authorities to draft strict policies in order to protect community health (Radcliffe, 2004). Some of the risks or parameters that must be managed in water recycling are presented in Table 1.2. Recognising and managing these risks are critical to the successful implementation of recycled water schemes.

<u>Table 1.2</u>: Physical parameters, potential chemical and pathogen risks associated with the use of recycled water.

Physical parameters	Chemical Risks	Pathogen Risks		
Colour	Inorganic (e.g. cadmium,	Bacteria (e.g. Escherichia coli,		
Taste and odour	mercury)	Salmonella)		
Appearance	Organic compounds (e.g. endocrine disrupting	Viruses (e.g. adenoviruses, enterovirus)		
	compounds, disinfection by- products)	Protozoa (e.g. <i>Giardia,</i> <i>Cryptosporidium)</i>		
		Helminths (e.g. Ascaris)		

Adapted from (Radcliffe, 2004; Foley et al., 2007; WHO, 2011).

The transmission of infectious diseases by pathogenic organisms is the most common concern of health professionals in water reclamation and water reuse. Microorganisms associated with waterborne diseases are primarily enteric pathogens, including enteric bacteria, protozoa and viruses. These pathogens can survive in water and infect humans through ingestion of faecal-contaminated water or contact with contaminated surface and food. From a public health and process control perspective, enteric viruses are the most critical group of pathogenic organisms in the developed world due to the possibility of infection from exposure to low doses and the lack of routine, cost-effective methods for detection and quantification of viruses (Asano and Levine, 1996). The definition of the various terms related to pathogens is given in Table 1.3 (NRMMC et al., 2008).

<u>Table 1.3</u>: Australian Guidelines for Water Recycling definition for terms involved with pathogens.

Term	Definition
Pathogen	A disease-causing organism (e.g. bacteria, viruses and protozoa).
Enteric pathogen	Pathogen that infects the gut of humans and other animals.
Microorganism	Organism too small to be visible to the naked eye. Bacteria, virus, protozoa, and some fungi and algae are microorganisms.
Virus	Small obligate intracellular parasites containing either a RNA or DNA genome surrounded by a protective virus-coded protein coat.
Protozoa	A phylum of single-celled animals.

From (NRMMC et al., 2008).

In order to manage these risks, the processes used to produce high quality water have to be validated and monitored. However, there is no universal recycled water policy around the world as the legislation is area dependant. For example, in the USA, each state handles the validation rules independently. Some of them do not have any legislation; others use individual barriers validation as being part of a whole plant such as California which uses the same approach as in Queensland (Australia) (USEPA, 2012). For this reason, the concept of risk assessment presented in this sub-chapter is introduced as defined by the Australian Guidelines for Water Recycling (AGWR) (NRMMC et al., 2008). These principles may be applied and interpreted slightly differently according to the local legislation.

According to AGWR, rotavirus and adenovirus are the reference pathogens for enteric viruses for the following reasons:

- Rotavirus represents waterborne viruses (Khan and Roser, 2007). It is a good candidate for risk assessment because of its high capacity to cause gastrointestinal infection and an established dose-response model (WHO, 2011). However, there is no routine culture-based method permitting the quantification of the infectious units;
- Adenovirus is a virus that can be cultured, found in high numbers in sewage and is renowned for its resistance to UV light inactivation (Gerba et al., 2002; WHO, 2011; USEPA, 2012). However, there is no dose-response model established.

An advanced water treatment plant (AWTP) must monitor equipment and automation to

prove the required log rejection and ensure the correct functioning of the processes (NRMMC et al., 2008).

To determine the requirement for virus removal for a specific end-use of recycled water, AGWR used the disability-adjusted life year (DALY). DALY is a common metric for all types of hazard taking into account health outcomes including probabilities, severities and duration of effect (WHO, 2011). For example, the DALY of rotavirus in developing countries is 480 DALYs per 1000 cases (Havelaar and Melse, 2003; WHO, 2011). From this factor and the assumed concentration of a pathogen in the source water, the required log removal value (LRV) is calculated (NRMMC et al., 2006, 2008). LRV is a way to express the removal or inactivate efficiency for a specific target such as an organism, particulate or surrogate (1 LRV = 90% reduction in density of the target organism, 2 LRV = 99% reduction, 3 LRV = 99.9% reduction, etc.) and is calculated as presented in Equation 1.1 (USEPA, 2005; NRMMC et al., 2008; UNESCO and WRQA, 2009).

$$LRV = log(\frac{c_{in}}{c_{out}}) \tag{1.1}$$

where C_{in} and C_{out} are the concentrations of the pathogen in the influent and the effluent, respectively.

From DALYs associated to enteric viruses and their assumed concentrations in sewage, the minimum LRV required for the production of recycled water for potable purposes from sewage has been set to 9.5 in the AGWR (NRMMC et al., 2006, 2008).

Depending on the type of process such as clarification and membrane filtration, and the target such as virus or organic matter, different integrity tests¹ are selected. According to Table 1.1, membrane filtration processes are used in the majority of the IPR projects. Low pressure membranes (MF and UF) are difficult to validate continuously and have been widely studied. Moreover, viruses can go through these membranes which give a variable LRV (from 1 to > 7) depending on their pore size (Jacangelo et al., 1995; Asano, 2007).

RO membrane has been proven to be able to remove above 5 log for virus in laboratory and pilot studies (Kitis et al., 2003; Lozier et al., 2003; Mi et al., 2004). However, it has not been possible to prove such performance on full-scale. The assumed difference between the LRV

¹ Integrity test: test permitting to determine the state quality of a process.

that RO can currently be validated for and its actual performance is therefore largely proved. This is also an important perceived opportunity to increase current LRV associated to this barrier. This is one main reason, why this thesis and consequently the following sections of this literature review focus on RO validation.

1.3. Reverse osmosis

RO membranes are commonly used in tertiary treatment for water reuse applications as a physical filtration process. These types of membrane are non-porous and have the capacity to remove salt and other inorganic and organic contaminants (USEPA, 2005). Figure 1.1 presents schematically the principle of the RO membrane (Wilf, 2010). Briefly, a pressure is applied at the feed side and forces water to go through the membrane forming the permeate whereas salt and contaminants are retained by the membrane and remain dissolved in the water of the concentrate.

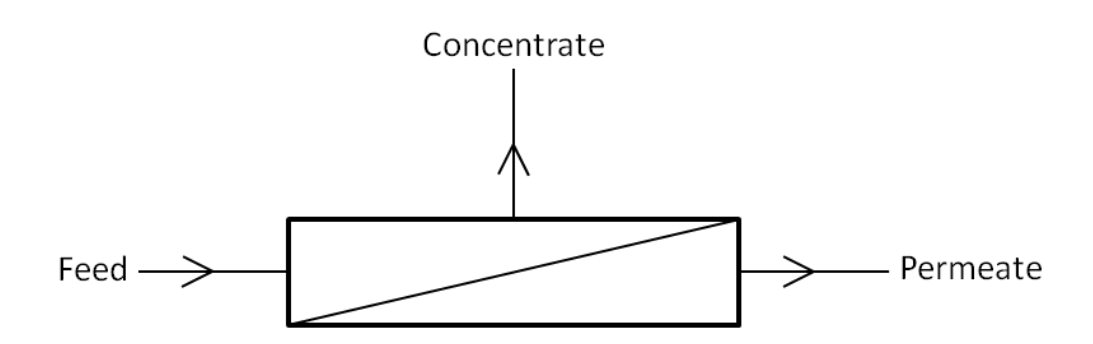
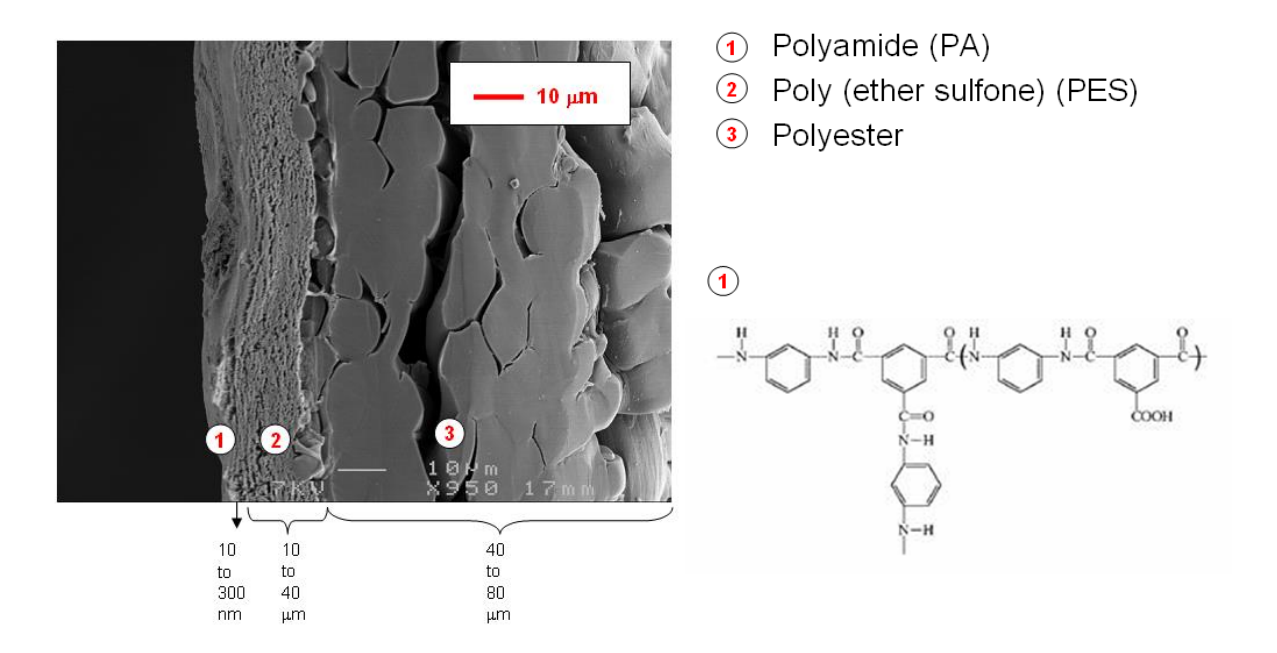


Figure 1.1: Schematic representation of the RO membrane process.

RO technology started as a scientific experiment in the 1950s at the University of Florida where Reid and Breton (1959) were able to demonstrate desalination properties of a cellulose acetate (CA) membrane. The first CA membrane was made from a cellulose diacetate polymer by Loeb and Sourirajan (1962) in the late 1950s. Later on, Peterson *et al.* (1982) introduced a composite membrane based on aromatic polyamide (PA) in the early 1980s. Since then, subsequent progress such as development of better membrane chemistry, development and optimization of membrane module configurations has been achieved. The composite PA membrane approach is preferentially used in commercial applications because it has a significant higher permeability and salt rejection than the CA membrane and also because composite PA tolerates a wide range of pH. PA, on the other hand, is less tolerant to

the exposure of oxidants like free chlorine. For this reason, CA membranes are still used in specific cases. A scanning electron microscopy (SEM) picture of a cross section of a Toray TML 20 membrane is shown in Figure 1.2. RO membranes consist of a film of polymeric material composed of three layers:

- 1. Semi-permeable membrane layer: this barrier is responsible for the passage of water and rejection of dissolved species;
- 2. Thick and spongy supporting layer: it has a pore size corresponding to a UF membrane (0.001 0.1 μm), which permits a high water permeability;
- 3. Fabric backing.



<u>Figure 1.2:</u> SEM of a cross section of a thin film composite membrane. (1) shows a typical chemistry of a cross-linked polyamide polymer, but variations are possible. (2) and (3) are often made of poly (ether) sulfone and polyester.

RO membrane manufacturers typically offer membrane elements in a spiral-wound geometry. This configuration consists of two sheets of membrane separated with a permeate tube collector and glued at three ends. A varied number of such membrane sheets can be included in a membrane module depending on its size. Further descriptions on the use of RO membranes in engineering systems are introduced in Section 1.3.1.1.

The semi-permeable RO membrane has the ability to retain salt, microorganisms and DOM in feed water because it is not porous. However, some passage of particulate matter may occur due to manufacturing imperfections; therefore, RO membranes should not be considered per se an absolute barrier without further validating the process (USEPA, 2005). Its molecular weight cut off (MWCO) is in the range of 100 - 300 Dalton (Da) for organic molecules and it rejects in theory around 99% or greater of inorganic ionic solutes (Wilf, 2010). The principal mechanism to remove compounds with a molecular weight (MW) greater than MWCO is size exclusion. Other removal mechanisms can contribute such as charge repulsion (or electrostatic repulsion), sorption and diffusion, especially for solutes having a MW lower than the MWCO (NRMMC et al., 2008). Moreover, the integrity of the RO process can be diminished over time and the principal failures are presented in the next part. Further details on the theory of RO membrane can be found in the USEPA "membrane filtration guidance manual" (2005) and the guidebook to "membrane technology for wastewater reclamation" by Mark Wilf (2010).

1.3.1. Principal failures in RO process

Membrane filtration is a physical barrier for pathogens that are larger in size than the cavity size of the membrane. However, any anomaly on the membrane process may result in microbial risk of the product water (Antony et al., 2012). In a full-scale plant, some failures may occur over time depending on the RO process or the membrane itself and are presented in this part.

1.3.1.1. Process failures

In an AWTP, the RO process is constituted of units called RO trains, of which several may be operated in parallel. One RO train can contain from 1 to 3 stages in which the combined concentrate of one stage is the feed of the next stage (Figure 1.3). A different number of pressure vessels (PV) in parallel are assembled to form a stage. A PV is designed to contain from 1 to 8 elements by vessel connected together with an O-ring and an interconnector to assure the watertightness of the system (Figure 1.4).

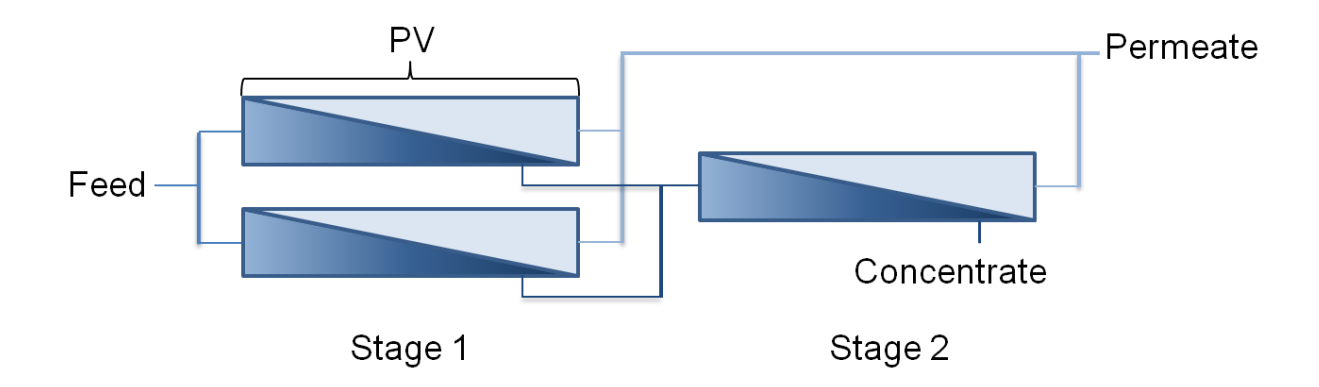


Figure 1.3: Simplified schematic of an RO train.

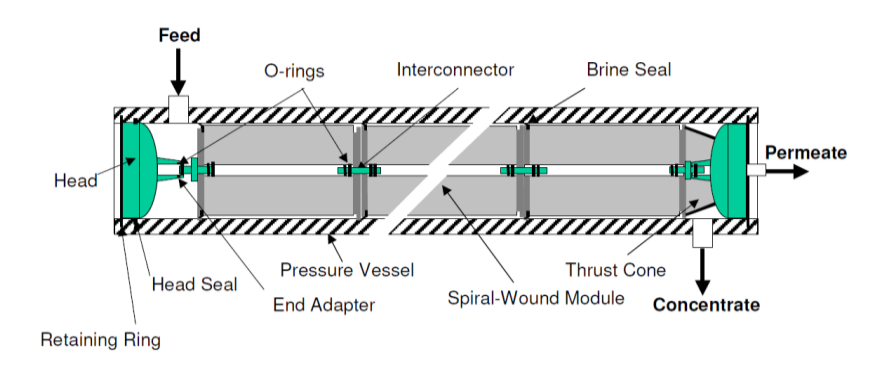


Figure 1.4: Typical spiral-wound module pressure vessel (from (USEPA, 2005)).

Over time, process failures might appear: interconnectors may break and create a leak decreasing the water quality; an O-ring may be compressed at the time of the module installation in the PV or may be compressed or cut during system operation with the movement of module. Nevertheless, major interconnector and O-ring breakages can be detected by electrical conductivity (EC) resulting in an increase of salt concentration in permeate, as feedwater passes to the permeate side unfiltered.

1.3.1.2. Membrane impairments and failures

Membrane defects can have two origins: from manufacturing or as a consequence of assembly/commissioning and operation.

The typical manufacturing defects are holes and glue-line problems. A faulty glue-line may cause leaks to appear. Both of these defects cause a decrease of salt rejection and can be detected easily by EC. Nevertheless, these problems are generally detected during the

manufacturer's quality control process and can be avoided.

Over time, fouling can appear, resulting in an increase of feed channel pressure drop, decline of water permeability and/or increase of salt passage. Fouling is dependent on feed water quality and can be characterized according to the nature of the constituent responsible. The literature distinguishes four categories of fouling (Malaeb and Ayoub, 2011; Guo et al., 2012): colloidal fouling, inorganic fouling or scaling, organic fouling and biofouling.

Colloidal fouling:

Colloids are fine particles having a size range of 1 to 1000 nm. Buffle *et al.* (1995a, 1995b; 1998) classified them into two categories:

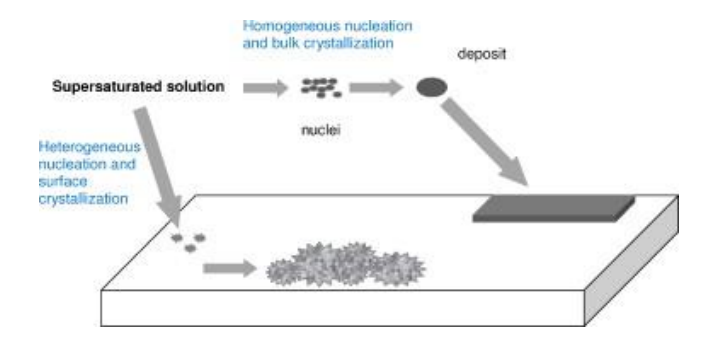
- Rigid inorganic colloids such as silica, iron (oxy) hydroxide and aluminium silicate minerals;
- Organic macromolecules such as biopolymers and fulvic compounds.

Interactions between colloids and/or between colloid and surface are bound by Van der Waals and electrostatic forces. Depending on the particles size and type of interaction, colloids can form a cake layer on the surface of the membrane which can have an impact on the permeate membrane flux. Colloidal fouling causes a decline of the water permeability, an increase of the salt passage and a decrease of the differential pressure between feed and concentrate in RO membrane. This water permeability can also be affected by the concentration polarisation (CP) effect. The CP is a result of an accumulation of dissolved species next to the membrane surface forming a boundary layer where the solute concentration exceeds the one in the bulk solution. Colloidal fouling is affected by feedwater composition, membrane properties and operational conditions such as low cross-flow velocity and high flux (Tang et al., 2011). This fouling can be controlled by pre-treatment such as UF or by chemical cleaning.

Scaling:

Scaling or inorganic fouling is the crystallization or precipitation due to super-saturation of dissolved salts, oxides and hydroxides on the membrane surface and in the bulk solution by two mechanisms (Lee and Lee, 2005; Oh et al., 2009; Antony et al., 2011) (Figure 1.5):

- Surface crystallization: inorganic compounds growth laterally blocking the membrane cavities;
- Bulk crystallization: crystals formed in the bulk solution may deposit onto the membrane to form a cake layer.

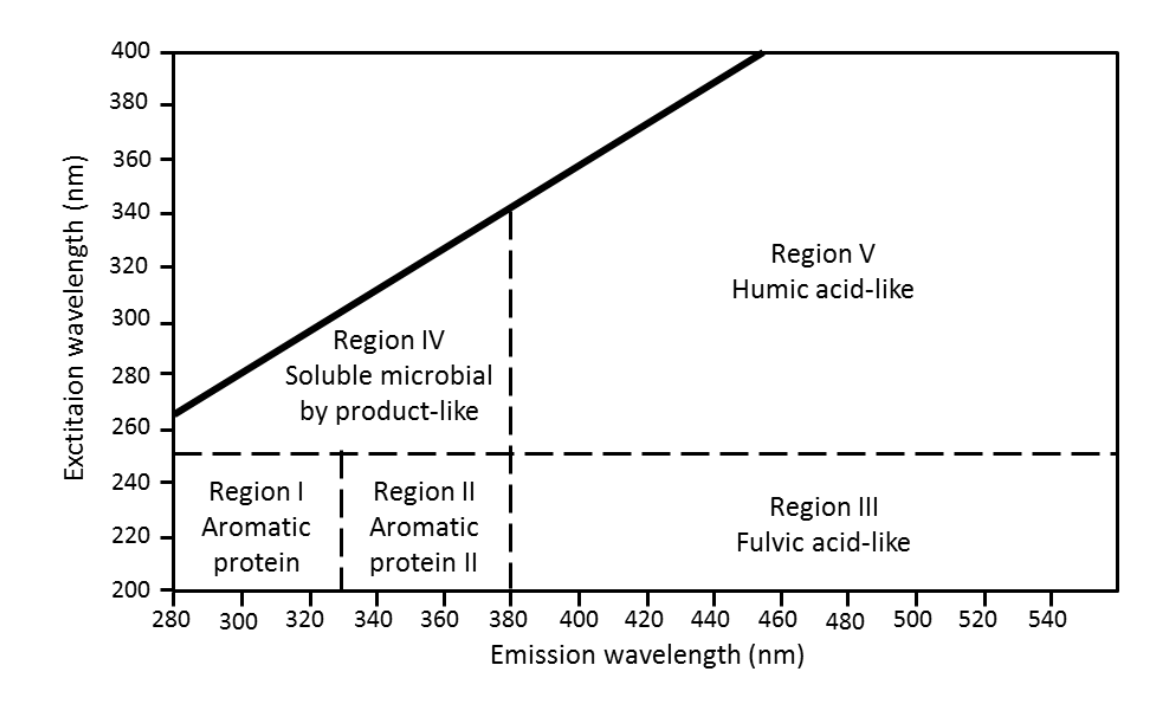


<u>Figure 1.5</u>: Schematic illustration of scale formation schemes (from (Antony et al., 2012)).

Scaling causes a water permeability decline, a decrease of salt rejection, a decrease of the differential pressure between feed and concentrate and also can have an irreversible impact by destroying the membrane (Dow, 2010). Scaling depends on the type of inorganic constituent present in the feed water. Scaling is an important problem in desalination and can also appear on the surface of the membrane in water reuse application. The most common scales are calcium carbonate (CaCO₃), calcium phosphate (CaPO₄), calcium sulphate (CaSO₄), barium sulphate (BaSO₄) and silica (Antony et al., 2011). Several parameters affect salt precipitation such as operating conditions (pressure, permeate rate, flow velocity), temperature, pH, presence of other salts or metal ions and most importantly the concentration polarisation. The cross-flow velocity has an impact on the CP which plays an important role in scale formation. In fact, by increasing the velocity, the CP decreases and therefore surface crystallization formation decreases (Lee and Lee, 2005). To control scaling, anti-scalants are generally used in full-scale plants combined with added pH control. For most scale forming salts inorganic crystallization is decreased at lower pH. The performance of a scaled membrane can partially or completely be restored by acidic chemical cleaning-in-place (CIP) procedures employing for example citric acid, which can be complemented by other chelating agents. Depending on feedwater quality and operational conditions, CIPs regimes may be required at varying frequency, ranging from monthly to close to yearly.

Organic fouling:

This fouling is characterized by the adsorption of DOM onto the membrane surface by physicochemical bonds (e.g. Van der Waals force, electrostatic attraction). DOM is a heterogeneous mixture of aromatic and aliphatic hydrocarbon structures containing three main functional groups: carboxylic acids (COOH), phenolic alcohols (ρ -OH; ρ = phenol) and methoxy carbonyls (C=O). By the presence of these functional groups, DOM can be negatively charged like the polyamide RO membrane resulting in electrostatic repulsions (Peter-Varbanets et al., 2011). However, the presence of divalent ions such as Ca²⁺ or Mg²⁺ permits to neutralize DOM and to form aggregation. Its composition and concentration in aquatic samples are highly variable and depend on the water source (Chen et al., 2003; Leenheer and Croue, 2003). Three-dimensional (3D) fluorescence excitation-emission matrix (EEM) and liquid chromatography-organic carbon detection (LC-OCD) are two types of method analysis permitting to classify DOM in function of their chemical and size specificities. Chen et al. (2003) proposed to classify DOM in five categories depending on their fluorescence characteristics (Figure 1.6). LC-OCD quantifies and separates DOM based on the size of the compounds by gel permeation chromatography coupled to an organic carbon detection (Figure 1.7) (USEPA, 2012). Analysis of DOM provides a good indication of water quality. Organic fouling is one of the predominant problems in membrane process causing a decrease of the water permeability (Dow, 2010). Concentration polarisation plays a role in the aggregation of humic substances in the boundary layer (Peter-Varbanets et al., 2011). The performance of the membrane can be partially or completely restored by basic chemical cleaning such as sodium hydroxide.



<u>Figure 1.6:</u> Excitation and emission wavelength boundaries (dash lines) for five EEM regions (adapted from (Chen et al., 2003)).

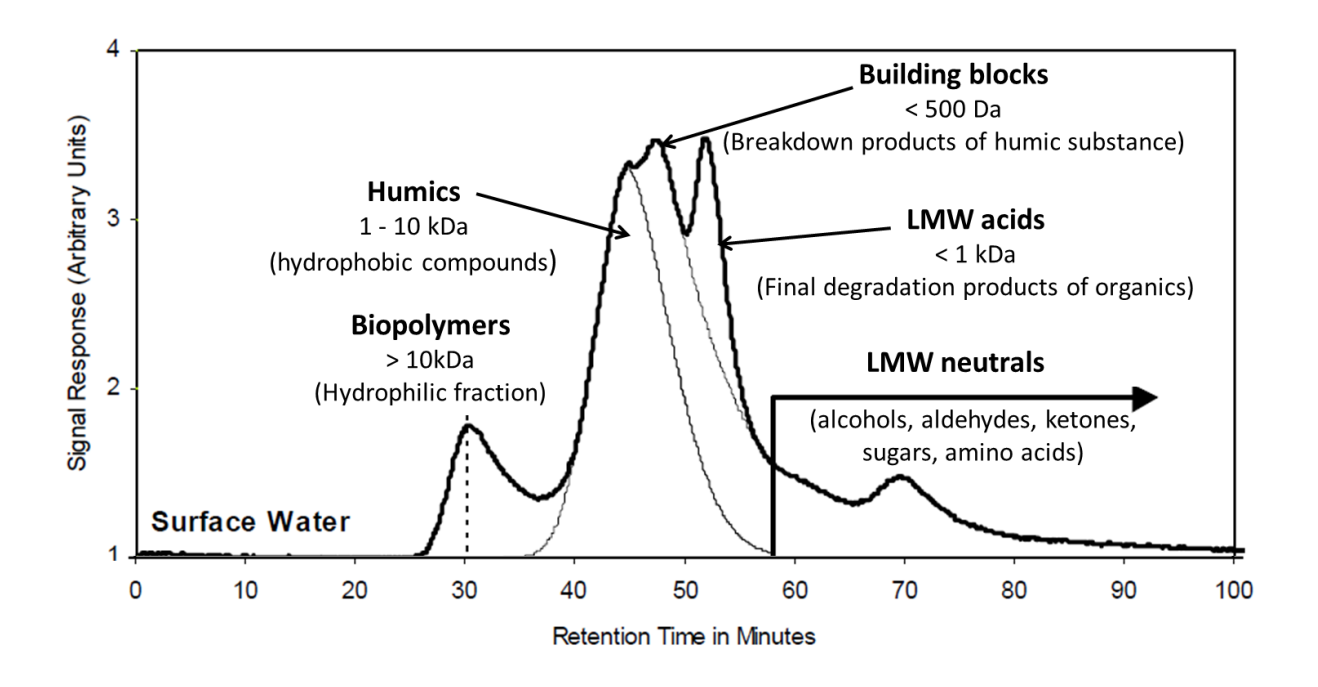


Figure 1.7: Typical LC-OCD profile with the five fractions: biopolymers, humics, building blocks, low molecular weight (LMW) acids and neutrals (adapted from (Huber et al., 2011)).

Biofouling:

Biofouling is a microbial colonisation forming a biofilm on the membrane surface. It is a dynamic process because additionally to an accumulation, it is also determined by growth and metabolism of microorganisms on the membrane (Guo et al., 2012). Biofouling is formed by several steps including (i) the attachment of bacteria onto a surface or other bacteria; (ii) the formation of micro-colony; and finally (iii) the formation of biofilm (Watnick and Kolter, 2000; Guo et al., 2012). Biofouling is one of the predominant problems in RO membrane process and causes a decline of the water permeability and an increase of the differential pressure between feed and concentrate (Dow, 2010). Early biofouling can be detected by monitoring drifts in the evolution over time of longitudinal differential pressure along the feed channels of RO trains. Wolf et al. (2001) demonstrated the possible use of online twodimensional (2D) scanning fluorometry to monitor complex biosystems permitting the detection of biofouling at an early stage. Several parameters affect the formation of biofouling such as substrate concentration, substrate load and hydrodynamic shear force (Vrouwenvelder et al., 2009). The removal or the inactivation of microorganisms by pretreatment is not sufficient to avoid biofouling; it is also necessary to control the nutrient load in order to avoid cells growth (Vrouwenvelder et al., 2009; Vrouwenvelder et al., 2010). Indeed, Vrouwenvelder et al. (2010) have demonstrated that the absence of phosphate limits the formation of biofouling. It has been reported that biofouling is better controlled by applying several approach such as the use of appropriate equipment design and operation, the control of biomass growth conditions, and the application of cleaning agents (Vrouwenvelder et al., 2010).

To conclude, fouling phenomena is often complex and include several foulants simultaneously. Indeed, whereas productivity, energy consumption, salt rejection and contaminants rejection of a membrane may be worsened by fouling, an increase of virus removal has been observed and it has been suggested that the fouling layer may cover membrane imperfections (Kitis et al., 2003; Lozier et al., 2003). However, a proof of such a mechanism has not been supplied. Chemical cleanings are used to remove fouling in RO process, but the effect of these cleanings on the RO membrane integrity and virus removal has not been yet studied.

Chemical Ageing:

To remove organic fouling and scaling, bases or acids are used. If performed in agreement with the membrane supplier's instructions these chemical cleanings should have little impact on the polyamide membranes as they have a high tolerance to low and high pH. In order to limit the formation of biofouling on RO membrane, AWTP often use chlorine or monochloramine as pre-treatment. However, monochloramine can form NDMA (*N*-Nitrosodimethylamine), a carcinogenic disinfection by-product (DBP) by reacting with organic matter. As described previously in Section 1.3, free chlorine can react with the PA layer of RO membrane. Depending on the operating condition and especially pH condition, the effects on water permeability and salt rejection can increase or reduce (Kwon and Leckie, 2006a; Antony et al., 2010; Dow, 2010; Do et al., 2012a; Do et al., 2012c; Donose et al., 2013). However, no study so far has presented the effects of long term membrane operation on virus removal and to date, the effect of the chemical ageing on the membrane (e.g. decomposition or oxidation) is unknown regarding the virus removal (Antony et al., 2012).

The majority of the ageing studies analysed the impact of chlorine on the water permeability and salt rejection of RO membranes (Table 1.4). Very few studies analysed the impact of chloramine with or without ions and acid solution (Gabelich et al., 2005; da Silva et al., 2006; Cran et al., 2011; Liu et al., 2011). Several studies attempted modifying the RO membrane surface in order to increase their resistance to ageing (Iborra et al., 1996; Shintani et al., 2007; Buch et al., 2008; Shintani et al., 2009; Liu et al., 2011). The observations of the various studies of chlorine attack on the PA layer show contradictory impacts on the membrane characteristics (water permeability and salt rejection, see also Table 1.4). Usually, ageing decreases salt rejection, but increases or decreases water permeability depending on the experimental condition.

PA membranes have a structure based on amides bonded to benzenes. The vulnerable points of this type of membrane are nitrogen functional groups and aromatic rings (Glater et al., 1994). The incorporation of chlorine in the molecular structure leads to the breakage of hydrogen bonds, which affects the tertiary structure of the PA (Antony et al., 2010). To explain the chlorination of the PA, different mechanisms have been proposed and are presented in Figure 1.8. The chlorination of the aromatic ring can take place by direct electrophilic aromatic substitution (Shafer, 1970; Glater and Zachariah, 1985) or by indirect chlorination, known as the Orton rearrangement. In this last case, the chlorine species attacks

the amino NH group (N-chlorination) followed by inter-/intra-molecular rearrangement and formation of a ring-chlorinated product (Orton and Jones, 1909; Orton et al., 1928; Kawaguchi and Tamura, 1984).

As demonstrated by three different studies (Oh et al., 2007; Mitrouli et al., 2010; Donose et al., 2013), the effect of hypochlorite is pH dependent. At pH 4 - 8, the [HOCI] species is dominant which favours the N-chlorination and causes a decrease of the water permeability. By contrast, [OCI] species is abundant at basic pH which promotes the hydrolysis of the amide C-N bonds leading to the formation of COOH groups and increases the water permeability (Do et al., 2012b). The impact of chlorine on PA membrane has also been analysed by different membrane autopsy techniques such as attenuated total reflection-Fourier transform infrared spectroscopy (ATR-FTIR), zeta potential measurements and atomic force microscopy (AFM). In summary, chlorination modifies the surface roughness and surface chemistry of the membrane. This modification of surface chemistry has an impact on the hydrophobicity and charge of the membrane. However, as with water permeability, these surface modifications are dependent of the ageing conditions and also of the membrane type.

<u>Figure 1.8:</u> Proposed mechanism of polyamide membrane impairment by hypochlorite (adapted from (Kwon et al., 2006; Do et al., 2012a)).

<u>Table 1.4:</u> Summary of studies on the impact of hypochlorite on RO.

Reference	Membrane Type	Exposure (ppm·h)	Pressure (bar)	Analytical Techniques	Ageing type	рН	Kw	RSalt%
(Antony et al., 2010)	BW30-FR	400 - 10000	12	ATR-FTIR, Fujiwara	Active (stirring)	6	↑	\downarrow
				analysis	Passive (immersion)		\uparrow	\rightarrow
(Do et al., 2012a)	BW30	10 - 24000	6.8; 17.9; 4.8	XPS, ATR-FTIR, Zeta potential, contact angle	Passive (shaker)	5	\downarrow	\downarrow
(Donose et al., 2013)	TML20;	1000; 3000;	12	ATR-FTIR, SEM, AFM	Passive (Static)	4	\	\rightarrow or \uparrow
	BW-30 XFR,	6000				7	\downarrow or \rightarrow	^
	ESPA 2					10	\rightarrow or \uparrow	\rightarrow or \uparrow or \downarrow
(Ettori et al., 2011)	SW30HRLE- 400	up to 4000	55 - 60	ATR-FTIR, XPS	Passive (soaking)	5; 6.9; 8.0	\	\
(Kwon and Leckie,	LFC1	Up to 2000	15.2	XPS, contact angle, zeta	Passive (shaker)	4	\downarrow	\downarrow
2006a, 2006b)				potential, ATR-FTIR, AFM		9	\uparrow	\uparrow
(Mitrouli et al., 2010)	N/A	100 - 26000	10.3	AFM	Passive (soaking)	3.2 - 3.6	\downarrow	\downarrow
	•					9.2 - 11.2	↑	\downarrow
(Roh et al., 2002)	N/A	Up to 540; up	15	ATR-FTIR	Passive (immersion)	4	,	,
, ,	,	to 2000			,	10	<u> </u>	<u> </u>
(Shemer and Semiat, 2011)	ESPA 2	Up to 248	4 - 55		Passive (soaking)	8.2	\	\
(Shin et al., 2011)	SWC1	up to 25000	54	AFM, XPS, SEM	N/A	7 - 8	\uparrow	\downarrow
(Simon et al., 2009)	BW30	9000; 36000	6.8	contact angle, AFM, zeta potential	Passive (immersion)	10.5	\downarrow	\rightarrow

N/A: not available.

infrared spectroscopy.

R_{salt%}: salt rejection.

XPS: X-ray photoelectron spectroscopy.

K_w: water permeability.

SEM: scanning electron microscopy.

AFM: atomic force microscopy.

ATR-FTIR: attenuated total reflection-Fourier transform

In summary, fouling in full-scale RO membrane is very challenging to control. It is generally diagnosed by following the water permeability and salt rejection over time. Some studies analysed the impact of fouling on the rejection of virus, but the mechanism is still poorly understood (Kitis et al., 2003; Lozier et al., 2003). On the other hand, the nature of the changes to membranes induced by membrane ageing and its consequences and mechanisms are poorly understood in general. To date, the impact of chlorine or chemical attack on the rejection of virus by PA membrane is unknown. Thus, it is crucial to improve the understanding of the virus removal mechanism by impaired membrane.

1.3.2. Monitoring RO membrane integrity

The RO process must be continuously monitored to ensure its correct operation to prove the log rejection that it has been validated for. To monitor the integrity of RO membranes and continuously assess their rejection performance, online electrical conductivity (EC) and total organic carbon (TOC) measurement are generally used to measure performance of critical control points (CCPs) (Adham et al., 1998a; Kumar et al., 2007). CCPs are validated preventive measures associated with removal of target criteria (such as viruses). The performance (sometimes expressed by 'log removal') of CCPs can be validated by once-off challenge testing using the target contaminant or a surrogate (such as a virus or virus-like particle), and this performance is then related to a set-point for the operational performance measure (usually EC) that can be measured online. This operational performance set-point is referred to as the critical limit for the process, which needs to be maintained to reduce high risks to acceptable levels (NRMMC et al., 2008).

EC is a good surrogate measurement for rejection of ions by the membrane, which is typically 1.7 - 2 LRV (98 - 99%). A major disadvantage is that rejection of ions measured by EC tends to underestimate the performance of RO membranes with regards to the rejection of microorganisms including viruses (Kitis et al., 2003). Other monitoring techniques have been studied to improve the monitoring of microorganisms rejection. In this sense, online TOC monitoring (2.3 - 3 LRV) has shown to be a better measure of their rejection than online EC (Adham et al., 1998b). Nowadays, for full-scale RO plants, rhodamine WT (R-WT; 2.75 - 4 LRV depending on its concentration in feed water among other things) has been successfully used during initial plant validation and online EC, online TOC and offline sulphate measurement (2.4 - 2.8 LRV) are used for operational monitoring of integrity (Zornes et al.,

2010).

Membrane integrity tests are classified into direct² and indirect³ methods. The system should be periodically verified by direct method testing and continuously by indirect method. The existing integrity methods are reliable and sensitive only for particle matter larger than 1 μm for low and high pressure membrane operations (USEPA, 2005). However, to protect public health from microbial risk, it is essential to develop a test in order to monitor and detect a loss of integrity of the RO membrane responsible for virus passage. These different tests are briefly presented in this part.

1.3.2.1. Direct monitoring

Vacuum decay test:

This test is performed in spiral-wound element to check the permeability of the wet membrane to air and to detect membrane leaks and imperfections (Adham et al., 1998a). However, this test is generally not used for full-scale practice, because of the inability to continuously monitor the integrity of the process and the difficulty to remove the air after test completion for example (USEPA, 2005).

1.3.2.2. Indirect monitoring

Particle counting and particle monitoring:

Particle counters use laser-based light scattering to count the particle as a function of size. However, the sensibility of this method does not permit to measure particle smaller than 1 µm and the resolution is dependent on number of particles in feed water, which is generally low due to successive pre-treatments.

Online monitoring and periodic testing:

² Direct method: "a physical test applied to a membrane unit in order to identify and/or isolate integrity breaches" (USEPA, 2005).

³ Indirect method: "monitoring some aspect of filtrate water quality that is indicative of the removal of particulate matter" (USEPA, 2005).

Measurement of constituents already present in feed water and removed to a high degree are performed periodically or continuously to measure the membrane integrity. Online EC, online TOC and offline sulphate are currently available and used, but as mentioned above, these techniques can only ascertain a limited LRV, typically below 3 (Kumar et al., 2007).

Challenge testing:

This test is required to demonstrate the ability of a membrane process to remove a specific target organism or surrogate (e.g. rhodamine). Challenge testing is discussed in detail later in this chapter.

The presented monitoring techniques underestimate the efficiency of the RO membrane to remove virus. By consequence, it is necessary to find a better monitoring method to assess the effectiveness of membranes to remove viruses which require a good understanding of the virus removal mechanisms.

1.4. Rejection of virus by membrane filtration process

1.4.1. Virus

A virus is a small infectious agent able to multiply only within a host-specific cell. Its size ranges from 10 to 300 nm in cross-section and is composed of two or three parts:

- Genetic material (DNA or RNA);
- Protein coat to protect the genetic material (capsid);
- Envelope of lipoproteins (facultative).

A wide variety of viruses may be found in an aqueous environment and a non-exhaustive list is presented in Table 1.5 (Bosch et al., 2008). There are more than 120 identified human enteric viruses, and some of the better known viruses include the enteroviruses (polio-, echo- and coxsackieviruses), hepatitis A, rotaviruses and human caliciviruses (noroviruses). Some of the commonly viruses found in wastewater are human adenovirus, enterovirus, norovirus and hepatitis type E (Ottoson et al., 2006; Hewitt et al., 2011; Masclaux et al., 2013). In recycled water, the concentration of viruses is very low (Table 1.6), which makes their direct measurement difficult. Different techniques can be used to quantify viruses such as plaque-

assay, enzyme-linked immunosorbent assay (ELISA), quantitative polymerase chain reaction (qPCR) and transmission electron microscopy (TEM), but only some of these techniques are applicable for one specific virus. Furthermore, these detection and quantification techniques are time-consuming such as plaque-assay and TEM, and can be difficult to implement due to the requirements of cleanliness and expertise (e.g. qPCR). The virus counter is a new quantification technique able to measure viruses in a non-specific manner. The principle of this technique is to stain the genetic material and the protein coat of the virus with fluorescent dyes to determine the total number of virus particles per mL by laser (Stoffel et al., 2005). However, this technique has not been yet used to quantify viruses from RO feed. No references are available that show the application of this technique in AWTPs clarifying the limit of quantification (LOQ) of this method and the possible interferences. For these reasons, it is important to find/develop a virus surrogate to monitor the integrity of the different AWTP processes. Nevertheless, the mechanism of virus removal by failure modes of RO process (e.g. fouled membrane or O-ring broken) has to be understood firstly in order to define its best surrogate.

<u>Table 1.5:</u> Human viruses documented to be found in the wastewater.

Genus	Popular name	Disease caused	pI	Size (nm)	Form
Enterovirus	Poliovirus	Paralysis, meningitis, fever	~ 6.5 - 8.3, 4	25	Icosahedral non-enveloped
	Coxsackie A, B virus	Herpangina, meningitis, fever, respiratory disease, hand-foot-and-mouth disease, myocarditis, heart anomalies, rush, pleurodynia, diabetes	4.8, 6.1 - 6.8	30	
	Echovirus	Meningitis, fever, respiratory disease, rush, gastroenteritis	4.0 - 6.4	24-30	
	Enterovirus types 68-71	Meningitis, encephalitis, respiratory disease, paralysis	N/A	25 - 27	
Hepatovirus	Hepatitis A virus	Hepatitis	2.8	27 - 32	Icosahedral non-enveloped
Rotavirus	Human rotavirus	Gastroenteritis	5.25 - 5.8	65 - 75	Icosahedral non-enveloped
Reovirus			N/A	N/A	Icosahedral non-enveloped
Norovirus	Norovirus	Gastroenteritis	5.9	35 - 39	Icosahedral non-enveloped
Hepevirus	Hepatitis E virus	Hepatitis	N/A	27 - 34	Spherical non-enveloped
Mastadenovirus	Human adenovirus	Gastroenteritis, respiratory disease, conjunctivitis	4.5	70 - 90	Icosahedral non-enveloped
Astrovirus	Human astrovirus	Gastroenteritis	N/A	28 - 30	Icosahedral non-enveloped
Coronavirus	Human coronavirus	Enterocolitis	N/A	120	Spherical non-enveloped

pI: isoelectric point.

N/A: not available.

Adapted from (Madaeni, 1997; Bosch et al., 2008; Gerba et al., 2008; Kaiser, 2009; Chung et al., 2010; Michen and Graule, 2010).

<u>Table 1.6:</u> Log removal and concentration of viruses (C virus) in different stages of secondary and tertiary wastewater treatment.

	Secondary treatment	UF/MF	RO	UV/H ₂ O ₂
Log removal	0 - 2	0.5 - 6	1.4 - >7	4 - 5
C virus (PFU·100 mL ⁻¹) after treatment step	1 - 1000*	< 1 - 300	0 - 10	≈ 0

^{*}before disinfection.

PFU: plaque forming unit. 1 PFU = 1 infectious virus particle.

Adapted from (Kitis et al., 2003; Asano, 2007; Kumar et al., 2007).

1.4.2. Mechanisms of virus rejection by membrane

Virus rejection by membrane process is predominantly achieved by size exclusion mechanism, influenced by the physicochemical properties of the membrane, the surface properties of the virus (electrostatic and hydrophobic interactions) and the solution environment (Antony et al., 2012). Virus rejection has been widely study by using low pressure membrane, but only few studies have been done using RO membrane. Bacteriophages⁴ are generally used as model viruses avoiding the complex manipulation of native viruses (e.g. lack of analysis methodology, pathogenic, etc.). Model viruses have also similar inactivation and adsorption behaviours than the native ones.

RO membrane:

A first study done by Sorber (1972) on the virus rejection by RO and UF membranes demonstrated the need to evaluate the virus removal using typical virus concentrations found in feed water. In fact, the higher the virus concentration in the feed water is, the higher is the possibility to obtain virus aggregates causing an increase of the measured LRV. The effect of membrane composition (cellulose acetate or PA RO membranes) on virus rejection was shown by Adham *et al.* (1998b).

⁴ Bacteriophage: a virus that infects and replicates within bacteria. They are not pathogenic for human.

Low pressure membrane:

In contradiction to the study conducted by Sorber (1972), Lovins III et al. (2002), studying the rejection of different bacteria and viruses by five membranes (two low pressure membranes: one MF and one UF; three high pressure membranes: nanofiltrations - NFs), suggested that the microorganism LRV was more dependent on the type of membrane than the organism size and concentration used in the challenge test. Farahbakhsh and Smith (2004) demonstrated that bacteriophage (coliphages) removal was affected by transmembrane pressure (TMP) and permeate flux which has not been the case in another study using MS2 bacteriophages (Jacangelo et al., 1995). Recently, a particle tracking model was developed to assess virus passage through compromised low pressure membranes (MF and UF) in a stirred-cell test using MS2 and PRD1 bacteriophages (Pontius et al., 2011). The conclusion of this study is that the influence of the hole on the virus rejection is depending on the hydrodynamics (flux and hole flow) which are principally functions of TMP, water temperature and membrane resistance. The effect of the TMP has been analysed by Arkhangelsky and Gitis (2008) using UF membrane. They showed that at higher TMP, the LRV reduces due to possible pore enlargement. Other studies using MF membrane have been reported. According to Madaeni (1997), the dominant mechanism of poliovirus retention (size: 25 nm) in MF membrane (MWCO: 0.22 µm) was standard blocking or adsorption onto the membrane. The sorption of virus onto the membrane is facilitated by the presence of salt in the effluent (Huang et al., 2012) which improves the hydrophobic interactions (van Voorthuizen et al., 2001). However, depending on the salt composition, the virus type and the membrane type, the hydrophobic interactions can increase, do not change or decrease (Lukasik et al., 2000). Herath et al. (1999) suggested a close relationship between isoelectric point (pI) and rejection. This study also suggested that a pI near to the pH of the water improves the virus rejection because of the equal positive and negative charge around the virus (zwitterionic form) which permits virus-virus and virus-impurity coagulation. The virus-impurity coagulation has been recently suggested by Huang et al. (2012) by demonstrating that in the presence of effluent organic matter and on a fouled membrane, the LRV of virus increased. Recent studies used fluorescent dye labelled MS2 bacteriophage (Gitis et al., 2002; Bakhshayeshi et al., 2011) or another biosynthetic tracer such as MS2 bacteriophage coupled by an enzyme (Soussan et al., 2011b) to simulate the viral transport during membrane filtration enabling alternative detection methods. The main advantage of these tracers is the ability to study the virus removal mechanism of membranes using fast

detection methods.

Although, it seems logical that the principal mechanism of virus rejection is size exclusion, the details of the process and what impacts of the response of the system to a defect on a membrane is difficult to understand and not well-established as it is a multi-factorial system. It is not only depending on the virus properties such as the pI and the size, but also depending on the type of membrane, the characteristics of the membrane operation such as flux and TMP, and water composition. Thus, it is important to properly understand the mechanism in order to better understand the impact of the different membrane/process impairments on the virus removal and to be able to monitor the membrane integrity. To find a non-biological alternative would be advantageous given the risk involved in performing the challenge tests with viruses or other human pathogens and other related difficulties in using live organisms such as bacteriophages.

A first study done by Sorber (1972) on the virus rejection by RO and UF membranes demonstrated the need to evaluate the virus removal using typical virus concentrations found in feed water. In fact, the higher the virus concentration in the feed water is, the higher is the possibility to obtain virus aggregates causing an increase of the measured LRV. In contradiction, Lovins III et al. (2002), studying the rejection of different bacteria and viruses by five membranes (two low pressure membranes: one MF and one UF; three high pressure membranes: nanofiltrations - NFs), suggested that the microorganism LRV was more dependent on the type of membrane than the organism size and concentration used in the challenge test. The effect of membrane composition (cellulose acetate or PA RO membranes) on virus rejection was also shown by Adham et al. (1998b). Farahbakhsh and Smith (2004) demonstrated that bacteriophage (coliphages) removal was affected by transmembrane pressure (TMP) and permeate flux which has not been the case in another study using MS2 bacteriophages (Jacangelo et al., 1995). Recently, a particle tracking model was developed to assess virus passage through compromised low pressure membranes (MF and UF) in a stirred-cell test using MS2 and PRD1 bacteriophages (Pontius et al., 2011). The conclusion of this study is that the influence of the hole on the virus rejection is depending on the hydrodynamics (flux and hole flow) which are principally functions of TMP, water temperature and membrane resistance. The effect of the TMP has been analysed by Arkhangelsky and Gitis (2008) using UF membrane. They showed that at higher TMP, the LRV reduces due to possible pore enlargement. Other studies using MF membrane have been reported. According to Madaeni (1997), the dominant mechanism of poliovirus retention (size: 25 nm) in MF membrane (MWCO: 0.22 µm) was standard blocking or adsorption onto the membrane. The sorption of virus onto the membrane is facilitated by the presence of salt in the effluent (Huang et al., 2012) which improves the hydrophobic interactions (van Voorthuizen et al., 2001). However, depending on the salt composition, the virus type and the membrane type, the hydrophobic interactions can increase, do not change or decrease (Lukasik et al., 2000). Herath et al. (1999) suggested a close relationship between isoelectric point (pI) and rejection. This study also suggested that a pI near to the pH of the water improves the virus rejection because of the equal positive and negative charge around the virus (zwitterionic form) which permits virus-virus and virus-impurity coagulation. The virus-impurity coagulation has been recently suggested by Huang et al. (2012) by demonstrating that in the presence of effluent organic matter and on a fouled membrane, the LRV of virus increased. Recent studies used fluorescent dye labelled MS2 bacteriophage (Gitis et al., 2002; Bakhshayeshi et al., 2011) or another biosynthetic tracer such as MS2 bacteriophage coupled by an enzyme (Soussan et al., 2011b) to simulate the viral transport during membrane filtration enabling alternative detection methods. The main advantage of these tracers is the ability to study the virus removal mechanism of membranes using fast detection methods.

Although, it seems logical that the principal mechanism of virus rejection is size exclusion, the details of the process and what impacts of the response of the system to a defect on a membrane is difficult to understand and not well-established as it is a multi-factorial system. It is not only depending on the virus properties such as the pI and the size, but also depending on the type of membrane, the characteristics of the membrane operation such as flux and TMP, and water composition. Thus, it is important to properly understand the mechanism in order to better understand the impact of the different membrane/process impairments on the virus removal and to be able to monitor the membrane integrity. To find a non-biological alternative would be advantageous given the risk involved in performing the challenge tests with viruses or other human pathogens and other related difficulties in using live organisms such as bacteriophages.

1.5. Application of virus surrogates and indicators for membrane integrity testing

1.5.1. Surrogates & indicators used to study virus LRV during filtration

According to the AGWR (NRMMC et al., 2008), the definition of surrogate is "the measurement parameter or combination of parameters that can be used to assess the quality of water; a specific contaminant, group of contaminants or constituent that signals the presence of something else (e.g. the presence of *Escherichia coli* can be taken to indicate the likely presence of pathogenic bacteria)".

A good virus surrogate is a particle or substance having the following characteristics:

- Defined size near to the size of viruses;
- Easily detectable;
- Reasonably priced;
- Representative of pathogen retention characteristics.

Up-to-now, only six RO studies were found testing only one scale and using two membrane integrity indicators: microsphere and rhodamine WT (R-WT) which were compared to MS2 bacteriophage. MS2 phage is one of the most used virus surrogates in virus removal studies performing challenge tests. It has been reported as the best process indicator for the following reasons (Golmohammadi et al., 1993; UNESCO and WRQA, 2009; Michen and Graule, 2010):

- Size: ~ 25 nm, which is similar to poliovirus (one of the smaller enteric viruses);
- Molecular weight = $3.6 \cdot 10^6 \text{ Da}$;
- Form: icosahedral, which is typical of many enteric viruses;
- Low isoelectric point = 3.1 3.9 (viruses are generally negatively charged at water pH);
- Easy to culture in large quantities;
- Multiplies only in host cells;
- Non-pathogenic to human.

MS2 phage is therefore the worst case scenario of the common viruses due to its small size. However, its negative surface charge at circumneutral pH (6 - 8) favours electrostatic repulsion with negative charged membranes. On the other hand, due to its low pI compared to other viruses, MS2 phage does not aggregate avoiding the increase of the LRV by size exclusion due to cluster formation (IAWPRC, 1991; Langlet et al., 2008; Michen and Graule, 2010). Unfortunately, the incorporation of this test on full-scale is impractical due to the high cost and effort required to culture and plate sufficient quantity of MS2 phage. Moreover, the techniques used to detect this phage can be time-consuming (24 - 48 h in plaque-assay).

The book "microbial removal and integrity monitoring of high-pressure membranes" by Lozier and co-authors (2003) describes three of these studies using different clean and compromised RO and NF membranes at bench-scale (flat-sheet cell and spiral-wound element experiments) and pilot-scale. A summary of all the RO studies to date is reported in Table 1.7 (Adham et al., 1998b; Kitis et al., 2003; Lozier et al., 2003; Mi et al., 2004; Zornes et al., 2010).

Microspheres are very small latex spheres with a size close to the virus one (~ 24 nm) and a possible variety of functional groups to alter surface properties such as charge or hydrophobicity. The ones used in the presented studies (Table 1.7 Studies 2, 3, 5, 6) are 20 nm fluorescent-dyed polystyrene microspheres detected by luminescence.

R-WT is a non-reactive tracer chemical approved by the US Environmental Protection Agency for use in drinking water (Zornes et al., 2010). Its molecular weight is 487 g·mol⁻¹ and it is expected to be well rejected by RO membranes, because it is considerably larger than the MWCO. Moreover, R-WT is negatively charged at water pH (pKa = 5.1) and it is expected to be removed by charge repulsion in addition to size exclusion. Due to its low cost and easy dosing, R-WT has been suggested as a non-microbiological alternative to MS2 phage.

Other indicators were studied with low pressure membranes (UF, MF) and might have a potential use in RO system. These novel integrity techniques can be classified in two groups:

Spiked integrity monitoring system (SIM):

In this method, a high concentration of powdered activated carbon (PAC) is spiked in the feed water and detected online in permeate by particle or turbidity monitoring (Guo et al.,

2010b). SIM test was conducted in pilot- and full-scale UF plants (Yorkshire Water Services, 90 MLD) and showed a LRV higher than 4.4. However, the test cannot be directly linked to pathogen removal because the size of PAC can vary considerably, agglomeration can happen, some interference with the particles present in water affect the sensitivity of the method and finally, PAC cannot be removed with a backwash.

An alternative of the SIM is the magnetic particle method. Magnetically susceptible particles were used instead of PAC (Deluhery and Rajagopalan, 2008; Guo et al., 2010b). The size of these particles is greater than the membrane pore size and they have low density. They can be detected by magnetorelaxometry or measurement of magnetic susceptibility. The advantages of this technique are the possibility for online detection, the ability to detect virus-size breaches and the low cost (Guo et al., 2010a). At this moment, only UF lab-scale results have been reported. Considering the advantages of this technique, a full-scale application might be possible.

Nanoscale probes:

In this method, two kinds of molecules were used: citrate- or thiol-stabilized gold nanoparticles and microspheres (Gitis et al., 2006). Gold nanoparticles are non-toxic and have a low background level in water system. Its mechanism of retention is size exclusion regardless of surface chemistry and these particles were detected electrochemically using anodic stripping voltammetry and these particles are a good surrogate to determine the integrity of the process (e.g. breaches in the membrane). The main advantage of nanoparticles is the possibility to modify their surface in order to have the same surface properties than virus and the possibility to add fluorescent dyes in order to allow their detection (Takimoto et al., 2010). However, nanoparticles may aggregate at the membrane surface and cause fouling (Lohwacharin and Takizawa, 2009). Moreover, due to the actual expensive cost of these nanoparticles, their use in full-scale is not possible nowadays (Kitis et al., 2003).

1.5.2. Effect of failure modes on testing RO Membrane integrity

Influence of the type of system used:

Adham *et al.* (1998b) (Table 1.7 Study 1) studied the rejection of MS2 phage with intact polyamide and cellulose acetate RO membranes using a flat-sheet dead-end system. The main

conclusion of this study is that MS2 phage LRV had a high variation with a same type of membrane. This high variability in rejection might be explained by the use of the dead-end system. This system uses the principle of deposition mode as there is only one feed stream becoming concentrated during the experiment due to the absence of a recycling loop, and one permeate stream (Figure 1.9) (USEPA, 2005). On a piece of flat-sheet used for the filtration, there is a probability to have some imperfections which are not detected and which will decrease the virus LRV due to the longitudinal pressure and flow. However, this possible imperfection can be easily covered up by the foulant cake layer.

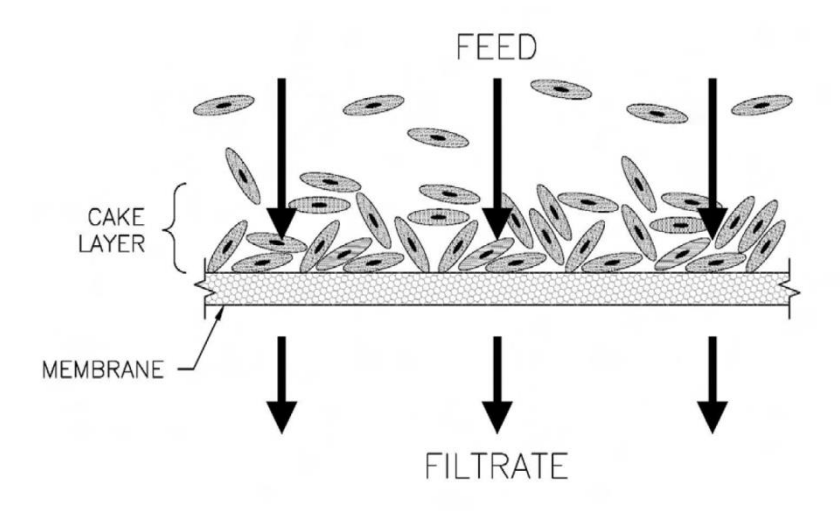


Figure 1.9: Principle of deposition mode filtration (USEPA, 2005).

Other studies (Adham et al., 1998a; Kitis et al., 2003; Lozier et al., 2003; Mi et al., 2004; Zornes et al., 2010) used cross-flow systems from flat-sheet membrane to spiral-wound module with the principle of suspension mode (Figure 1.10). The advantage of these systems is to have a tangential pressure and flow which decrease the formation of cake layer compared to the deposit mode. According to several studies (Table 1.7 Studies 2 to 6), the virus LRV (3.4 - 7.9) is more stable, which might be explained by the type of the system used. In fact, even if there were possible imperfections on the membrane, due to the tangential flow, the MS2 phage and microsphere were still retained by the membrane.

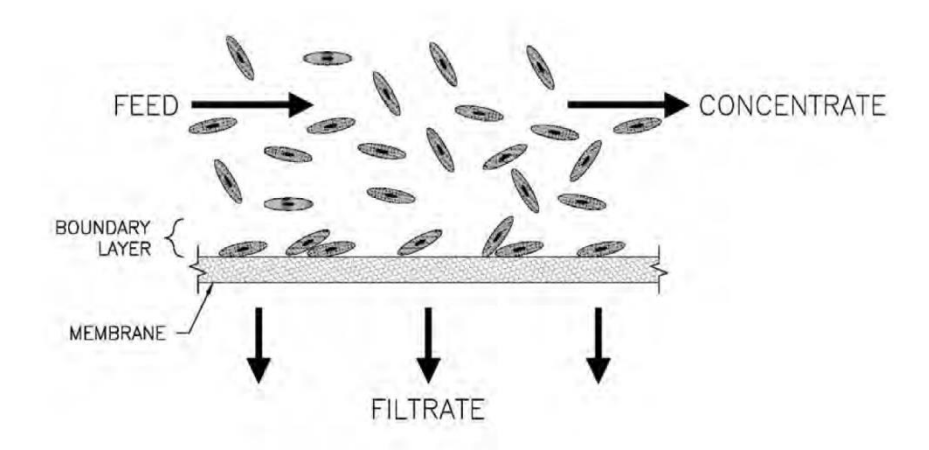


Figure 1.10: Principle of suspension mode filtration (USEPA, 2005).

Loss of integrity by scratch/hole in the membrane:

In the following studies (Table 1.7 Studies 2 - 3 and 5 - 6), the effect of pinholed membranes on virus surrogate (MS2 phage) and membrane integrity indicators (R-WT and microsphere) rejection was studied. According to Lozier et al. (2003) (Table 1.7 Study 2), a scratch on the PA layer was not sufficient to permit the passage of viruses through the membrane. Furthermore, if a hole did not go through the three layers, MS2 phage and microsphere were still maintained by the membrane which was the case for Table 1.7 Studies 2 and 3. This can be explained by the fact that the polysulfone layer, which is essentially of a similar composition and morphology than UF membranes, has the capacity to retain virus (Jacangelo et al., 1995; Asano, 2007). Also, if the pinhole is small, it can be clogged by the particles present in the feed water (Lozier et al., 2003; Mi et al., 2004). By consequence, the LRV is the same or higher than with the intact membrane (Lozier et al., 2003). However, if the pinhole is large enough not to cause a steric hindrance, particulate and dissolved compounds go through the hole independent of the compound physicochemical characteristics. This means that the passage of enteric virus through large hole can be mimicked by particulate and soluble indicators. The creation of pinhole has been also studied at pilot-scale (Kitis et al., 2003; Lozier et al., 2003). Two types of pilot were used in two different plant sites. The first pilot named DETU consisted of two pressure vessels in series containing one 4" spiral-wound module. The second pilot named MVTU consisted of three pressure vessels in parallel containing each three 4" spiral-wound modules. The feed water flow containing the indicators was directed to only two of the three pressure vessels. Fouling was formed on the pinholed membranes and the efficiency of cleaning solution were analysed. The cleaning of the fouled membrane restored the reduced LRV obtained with the pinhole for the DETU pilot. However, for the MVTU, the LRV was around the one obtained initially with an uncompromised membrane. This difference could be explained by the fact that it was not the same cleaning solution used for both systems and it might neither be the same fouling layer as it was two different feed waters. The efficiency of the MVTU cleaning solution might be lower, which then would not have removed all the foulants and by conclusion, would not have unclogged the pinhole.

O-ring:

In the following studies (Kitis et al., 2003; Lozier et al., 2003; Mi et al., 2004; Zornes et al., 2010) (Table 1.7 Studies 2 - 3 and 5 - 7), the effect of faulty O-ring on MS2 phage, R-WT and microsphere rejection was studied. Different degrees of impairment were induced on the O-ring from a crack to a removal of small section (i.e. 1, 2, or 4 mm) to one missing O-ring (full-scale study, Table 1.7 Study 7). According to Kitis et al. (2003), a cracked O-ring was not sufficient to decrease virus surrogate and indicators rejection. Other tests at pilot-scale (Table 1.7 Study 6) were performed to determine the impact of the compromised module and O-ring location (Kitis et al., 2003; Lozier et al., 2003). The compromised membrane location had a direct impact on compounds removal. The location of the compromised module in the last pressure vessel was more affected compared to the first pressure vessel. This could be explained by the difference in the net driving force pressure (NDP, differential pressure across the O-ring) along the process. A high NDP could compress the O-ring by closing the gap in the removed section of the O-ring and then 'repair' the faulty O-ring. In contrast, a lower NDP would increase the flow across the O-ring cut. However, the higher concentration of particulate compounds (MS2 phage and microsphere) in the last pressure vessel might clog the faulty O-ring and thus decreased the impact of the impairment. Finally, the size of the removing section from the O-ring would influence the passage of compounds. Indeed, the Oring with a 4 mm of removed section had the biggest impact on compounds removals.

1. Literature review

<u>Table 1.7:</u> LRV of MS2 phage, microsphere and R-WT depending on the RO system used and the type of impairment.

	Scale	Surrogate	Impairment	LRV (range)	Reference
1	Dead-end cell	MS2 phage	None	1.4 - > 7.4	(Adham et al., 1998b)
2	Cross-flow Flat-sheet cell	MS2 phage	None Scratch Pinhole (~150 μm)	5 - > 7 > 5.7 0.1 - > 8.6	(Lozier et al., 2003)
		Microsphere	None Pinhole (~150 μm) ^a	< 1 - > 2.8 0.15 - > 4.6	
3	Spiral-wound Element	MS2 phage	None Free chlorine (1000 ppm h) O-ring Pinhole	5.3 - 7.9 > 6 - 8 6.2 - 7.9 1.0 - 7.6	(Lozier et al., 2003; Mi et al., 2004)
		Microsphere	O-ring Pinhole	5 - 6 0.9 - 3.1	
4	Pilot	MS2 phage	None O-ring	3.4 3.4	(Adham et al., 1998a)
5	Pilot DETU ^b	MS2 phage	None O-ring (cracked and cut) Pinhole (300 - 500 μm) Pinhole/Fouling Pinhole/Fouling/Cleaning	6.8 6.8 3 7 2.9	(Kitis et al., 2003; Lozier et al., 2003)
		Microsphere	None O-ring (cracked only) Pinhole (300-500 µm) Pinhole/Fouling Pinhole/Fouling/Cleaning	> 4 2.6 - 4.3 2.2 - 2.5 > 4.3 2.6	

Table 1.7: LRV of MS2 phage, microsphere and R-WT depending on the RO system used and the type of impairment (continued).

	Scale	Surrogate	Impairment	LRV (range)	Reference
5	Pilot DETU (continued)	R-WT	None O-ring (cracked and cut) Pinhole (300 - 500 µm) Pinhole/Fouling Pinhole/Fouling/Cleaning	3.8 - 4 0.6 - 4.1 2.2 4.4 2.3	(Kitis et al., 2003; Lozier et al., 2003)
6	Pilot MVTU	MS2 phage	None O-ring - lead adaptor O-ring - trailing adaptor Pinhole - lead (300 - 500 µm) Pinhole - trailing (300 - 500 µm) Pinhole/Fouling Pinhole/Fouling/Cleaning	5.3 - 5.5 2.8 5.1 - 6.0 2.3 - 2.8 4.2 7.2 - 8 5.2	(Kitis et al., 2003; Lozier et al., 2003)
		Microsphere	None O-ring – lead adaptor O-ring - trailing adaptor Pinhole – trailing (300 - 500 µm) Pinhole/Fouling Pinhole/Fouling/Cleaning	> 4.2 2.6 3.7 2.3 3.8 - 4.3 > 4.3	
		R-WT	None O-ring - lead adaptor O-ring - trailing adaptor Pinhole - lead (300 - 500 µm) Pinhole - trailing (300 - 500 µm) Pinhole/Fouling Pinhole/Fouling/Cleaning	3.5 - 5.3 2.6 - 2.7 3.5 - 4.4 2.2 3.8 - 4.3 3.8 - 4.5 3.4 - 4.2	
7	Full-scale	R-WT	None O-ring removed	2.5 - 2.8 2.4	(Zornes et al., 2010)

In bolt: low LRV (< 3).

1.6. Conclusion and thesis objectives

This literature review has shown a lack of knowledge about the effect of RO process and membrane failures on the rejection of virus especially regarding the virus rejection mechanisms. Moreover, nowadays, there is no adequate method to monitor the integrity of RO membrane filtration process regarding virus removal beyond 2 LRV. Thus, the overall aim of this thesis was to better understand virus removal by (i) RO process failures; and (ii) different membrane impairments using different RO process scales and membrane integrity indicators. The last objective of this thesis was (iii) to compare the different set-up and the different indicators used in this thesis.

<u>Objective 1:</u> Monitor RO performance by conductivity and fluorescence excitation-emission matrix (Chapter 3).

As described previously, interconnectors and O-rings can break over time causing a decrease of the salt rejection measured by EC. However, it is not certain that with this type of failure, viruses will pass the membrane and by consequence will decrease the virus removal especially with a O-ring broken in the last pressure vessel (Lozier et al., 2003). To improve sensitivity and selectivity, Henderson et al. (2009) suggested the analysis of fluorescent DOM as potential surrogate due to its chemical properties. DOM is a heterogeneous mixture of aromatic and aliphatic hydrocarbon structures containing different functional groups. Its composition and concentration in aquatic samples are highly variable and depend on the water source (Chen et al., 2003; Leenheer and Croue, 2003). Analysis of DOM provides a good indication of water quality. For this reason, the use of EEM to analyse DOM in membrane organic fouling studies, to differentiate the water quality in the steps of recycled water treatment plants and to identify cross-connections in dual pipe distribution systems has recently gained a lot of attention (Her et al., 2008; Singh et al., 2009; Hambly et al., 2010; Peiris et al., 2010a; Peiris et al., 2010b). In 2009, Singh et al. showed that DOM in RO permeates can be characterized by fluorescence EEM allowing differentiation of the permeate quality among different stages of the RO trains. They also demonstrated that humic-like fluorescence can be detected sensitively in this matrix. Therefore, in the first part of the thesis, the use of DOM present naturally in feed water, measured by EEM and analysed using the fluorescence regional integration (FRI) technique, has been tested as a new monitoring technique and compared to EC monitoring in two full-scale plants.

<u>Objective 2:</u> understand the impact of membrane impairments on the rejection of virus surrogate and membrane integrity indicators (Chapters 4 & 5).

In the RO process, the major membrane failure is fouling (especially organic fouling and scaling). Different chemicals are used to remove or to avoid fouling. Chlorine containing disinfectants are generally used in AWTPs to avoid biofouling on RO membrane, which can have an impact on the integrity at long-term. Thus, the effect of short-term failures (organic fouling and scaling; Chapter 4) and long-term failure (ageing; Chapter 5) have been studied. To better understand the impact of these membrane failures on virus removal, one virus surrogate and four membrane integrity indicators have been tested in two lab-scales.

The purpose of this objective is to identify the main factors influencing virus surrogate and indicator removals in order to understand the impact of the impairments on their rejection and to propose removal mechanism of viruses by impaired membranes. These compounds were selected knowing that virus surrogate and indicators have different mechanisms of rejection due to their different chemistries (e.g. particulate versus solute).

The two lab-scales used are a flat-sheet cross-flow and a 2.5" spiral-wound module. These systems have been selected because of their use in previous studies (Adham et al., 1998b; Kitis et al., 2003; Lozier et al., 2003; Mi et al., 2004; Kwon et al., 2008; Zornes et al., 2010; Liu et al., 2011; Do et al., 2012a).

The virus surrogate and membrane integrity indicators selected are:

- MS2 phage: it has been mentioned previously that MS2 phage is the virus surrogate used in membrane technology research. In this study it is used as benchmark and all indicators were compared to it. The stock solutions of MS2 phage have been quantified by plaque-assay in order to have the result the day after making the solution. The feed and permeate samples were quantified by quantitative reverse transcriptase-polymerase chain reaction (qRT-PCR), because this technique is more sensitive than the plaque-assay technique;
- R-WT: This dye is a soluble surrogate authorised to be used in drinking water by the US Environmental Protection Agency (2005) and easy to be analysed by fluorescence. Its use permitted to compare the data obtained in this study to the ones obtained by Lozier *et al.* (2003);

- Salt as determined by EC measurement: EC reflects the contents of ions, which is usually dominated by the effect of monovalent ions due to their higher abundance in most waters, and it is currently used to monitor the integrity of the membrane. The sensitivity of this technique is only 1.7 2 LRV, because of the limited rejection of monovalent ions by RO membrane. However, EC is the only standard method used in full-scale plant to monitor the integrity of RO process;
- Sulphate (SO₄²⁻): sulphate is a doubly charged ion (bigger size than most monovalent ions) that is present naturally in feed water and can be easily detected by ion chromatography (IC). Sulphate is also currently evaluated at full-scale plants to periodically verify the correct operation of the RO process;
- DOM: in the previous objective, the efficiency to use DOM as monitoring technique has been determined. Its use in this objective permitted to determine its possible uses as novel membrane integrity indicator regarding virus rejection even if DOM properties are different to virus properties.

Objective 3: comparison of the different scales and the different compounds (Chapter 6).

In order to achieve the two previous objectives, two different scales have been used: full-scale plant (Chapter 3) and lab-scales (Chapters 4 & 5). In the lab-scale, three different set-ups have been used with different active membrane area and/or configuration (spiral-would element and flat-sheet cross-flow). In general, RO membrane studies used these different set-ups in addition to the dead-end filtration set-up. In this thesis, the dead-end filtration system has not been used because of its difference in filtration mode (deposition mode, Figure 1.9) compared to full-scale filtration system (suspension mode, Figure 1.10). To date, there is no study comparing different scales and the results obtained with them in challenge tests. For this reason, a first purpose of the last objective was to compare the different scales in order to estimate which lab-scale imitated best the full-scale. The other part of this objective was to select the best indicator(s) used in this study able to monitor effectively the integrity of RO membrane. For this purpose, a two-way analysis of variance (ANOVA) has been used to compare the effects of scale and impairment type on compounds rejection.

2. Materials & methods

2.1. Virus s	surrogate and membrane integrity indicators48
2.2 Lab-sc	ale experimental apparatus
2.2.1. St	ainless-steel flat-sheet cross-flow set-up (SS flat-sheet set-up)51
2.2.2. Pl	astic flat-sheet cross-flow set-up (plastic flat-sheet set-up)52
2.2.3. Sp	piral-wound module set-up (2.5" module set-up)
2.2.4. M	embrane characteristics
2.2.5. M	embrane impairment protocols
2.2.5.1.	Organic fouling58
2.2.5.2.	Scaling60
2.2.5.3.	Ageing60
2.3. Analyt	ical methods61
2.3.1. Aı	nalysis of virus surrogate and membrane integrity indicators61
2.3.1.1.	MS2 quantification61
2.3.1.2.	R-WT quantification
2.3.1.3.	DOM analysis
2.3.1.4.	Sulphate quantification
2.3.1.5.	Electrical conductivity
2.3.2. Ot	ther chemical analysis69
2.3.3. M	embrane autopsies69
2.3.3.1.	Atomic force microscopy (AFM)70
2.3.3.2.	Scanning electron microscopy-energy dispersive spectroscopy (SEM-EDS)70
2.3.3.3.	Attenuated total reflection-Fourier transform infrared (ATR-FTIR)70
2.4. Statisti	cal data analysis71

In this part, the physicochemical properties of the virus surrogate and membrane integrity indicators, the experimental apparatus including experimental systems and membrane, and membrane impairment protocols, the analytical techniques and the data analyses are described in detail.

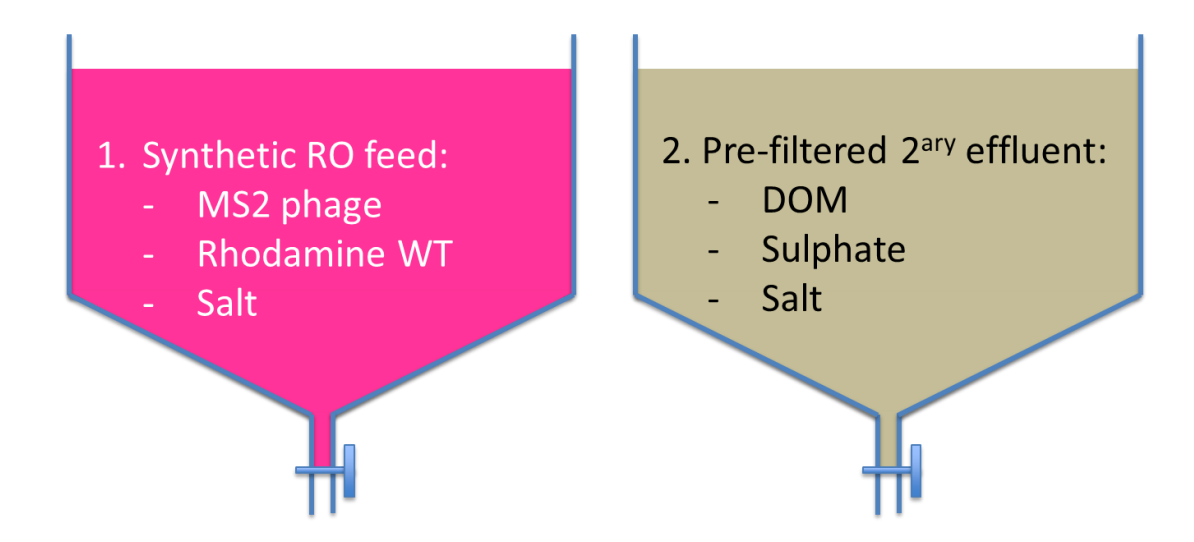
2.1. Virus surrogate and membrane integrity indicators

Tests were performed with one virus surrogate (MS2 phage) and four non-biological indicators (R-WT, salts, DOM and sulphate). MS2 phage, R-WT and salts were used together in one synthetic RO feed solution, whereas DOM and sulphate were applied as they are naturally present in the secondary effluent (Figure 2.1).

MS2 phage strain 15597-B1 (ATCC, Manassas, VA, USA) was cultured using the host *Escherichia coli* (*E. coli*) 15597 (ATCC, Manassas, VA, USA) following the ATCC product information sheet. Host and phage were received as freeze-dried pellets, were cultured following the procedure ISO 10705-1 (ISO, 1995) and were stored at - 80°C with 10% of glycerol. The target feed concentration for MS2 phage was 10⁸ - 10⁹ PFU·mL⁻¹.

The non-biological indicators used were R-WT (Ortho Chemical Australia Pty. Ltd., Newmarket, Australia) and a mixture of salts (ions) measured by electrical conductivity (EC). R-WT is a non-hazardous chemical tracer and was selected because of its acceptance by the US Environmental Protection Agency for use in drinking water (USEPA, 2005) and its use in numerous research studies (Kitis et al., 2003; Lozier et al., 2003; Zornes et al., 2010). The target feed concentration for R-WT was 100 μg·L⁻¹. A mixture of NaCl, NaHCO₃, KCl, CaCl₂ (Ajax Finechem Pty Ltd, Taren Point, Australia), KH₂PO₄ and MgSO₄ (Chem-Supply, Gillman, Australia) was dissolved in de-ionised (DI) water to constitute a typical ionic composition of RO feed water as determined from several average samples of South East Queensland AWTPs. Table 2.1 shows the detailed synthetic feed water characteristics.

Secondary effluent was taken before the step of disinfection of a wastewater treatment plant and then filtered in the lab with $0.45~\mu m$ filters. This pre-filtered secondary effluent was used as feed water to conduct the analysis of DOM and sulphate, the two last indicators, and salt (EC). Due to treatment plant problems (AWTP shutting down), it was impossible to use RO feed from the AWTP for the lab-scale set-up experiments (Chapters 4 and 5). Table 2.2 shows the detailed secondary effluent feed water characteristics from the AWTP.



<u>Figure 2.1:</u> Summary of the virus surrogate and membrane integrity indicators analysed in the different feed waters.

<u>Table 2.1:</u> Synthetic RO feed water characteristics.

Concentration
165 mg·L ⁻¹
275 mg·L ⁻¹
70 mg·L ⁻¹
50 mg·L ⁻¹
45 mg·L ⁻¹
40 mg·L ⁻¹
30 mg·L ⁻¹
10 mg·L ⁻¹
7 - 7.5

<u>Table 2.2:</u> Pre-filtered secondary effluent characteristics (n = 15).

Technique	Element	Concentration
рН		7.8 ± 0.3
Conductivity (µS·cm ⁻¹)		1090 ± 134
DOC (mg·L-1)		8.72 ± 0.81
IC (mg·L ⁻¹)	Cl-	146.5 ± 20.6
	SO_4^{2-}	77.3 ± 10.1
ICP-OES (mg·L-1)	Ca	29.9 ± 7.0
	K	15.0 ± 5.9
	Mg	13.6 ± 4.9
	Na	123.0 ± 47.0
	P	0.7 ± 0.9
	S	23.0 ± 9.2

DOC: dissolved organic carbon.

IC: ion chromatography.

ICP-OES: induced coupled plasma-optical emission spectrophotometer.

2.2 Lab-scale experimental apparatus

The different lab-scale apparatus presented in this section were operated at constant feed flux and pressure. The operating conditions selected were similar to those selected at the AWTPs of the Western Corridor Recycled Water Scheme. The operating conditions are summarised in Table 2.3. For the plastic flat-sheet set-up, a maximum pressure of 5 bar was used due to the limitation of the PTFE material used for tubing and connections.

<u>Table 2.3:</u> Operating conditions used in the lab-scale apparatus.

Operating conditions	SS	Plastic	Module
Pressure	7.5	5	7.5
Cross-flow velocity (cm·s-1)	10		
Feed flow (L·h-1)	30	40	540
Temperature (°C)		Normalised at 25°C	

2.2.1. Stainless-steel flat-sheet cross-flow set-up (SS flat-sheet set-up)

All experiments were performed using a stainless-steel (SS) flat-sheet test unit consisting of a membrane element cell (effective membrane area: 140 cm²; Sterlitech Corporation, Kent, WA, USA), a Hydracell pump (Wanner Engineering Inc., Minneapolis, MN, USA) and a 15 L feed tank (Rota Moulding, Midvale, Australia). The constant feed pressure controlled at 7.5 bar. The feed pressure and the differential pressure between feed and concentrate lines were measured with two digital gauge transmitters (Endress + Hauser, North Ryde, Australia). The concentrate flow rate was controlled at 30 L·h⁻¹ by adjusting the speed of the pump and by adjusting a needle valve (Swagelok, Brisbane, Australia) installed in the concentrate line. Permeate and concentrate flow rates were measured with a HPLC liquid flow meter (GJC Instruments Ltd, Cheshire, England) and a 1200 MPB flow meter (MPB industries Ltd, Kent, England), respectively prior to be returned to the feed tank. The temperature of the feed solution was measured in order to normalise the performance to 25°C. Sampling points (Swagelok, Brisbane, Australia) were located in the feed, permeate and concentrate lines. Figure 2.2 presents (a) a photo and (b) a drawing of the SS flat-sheet set-up.

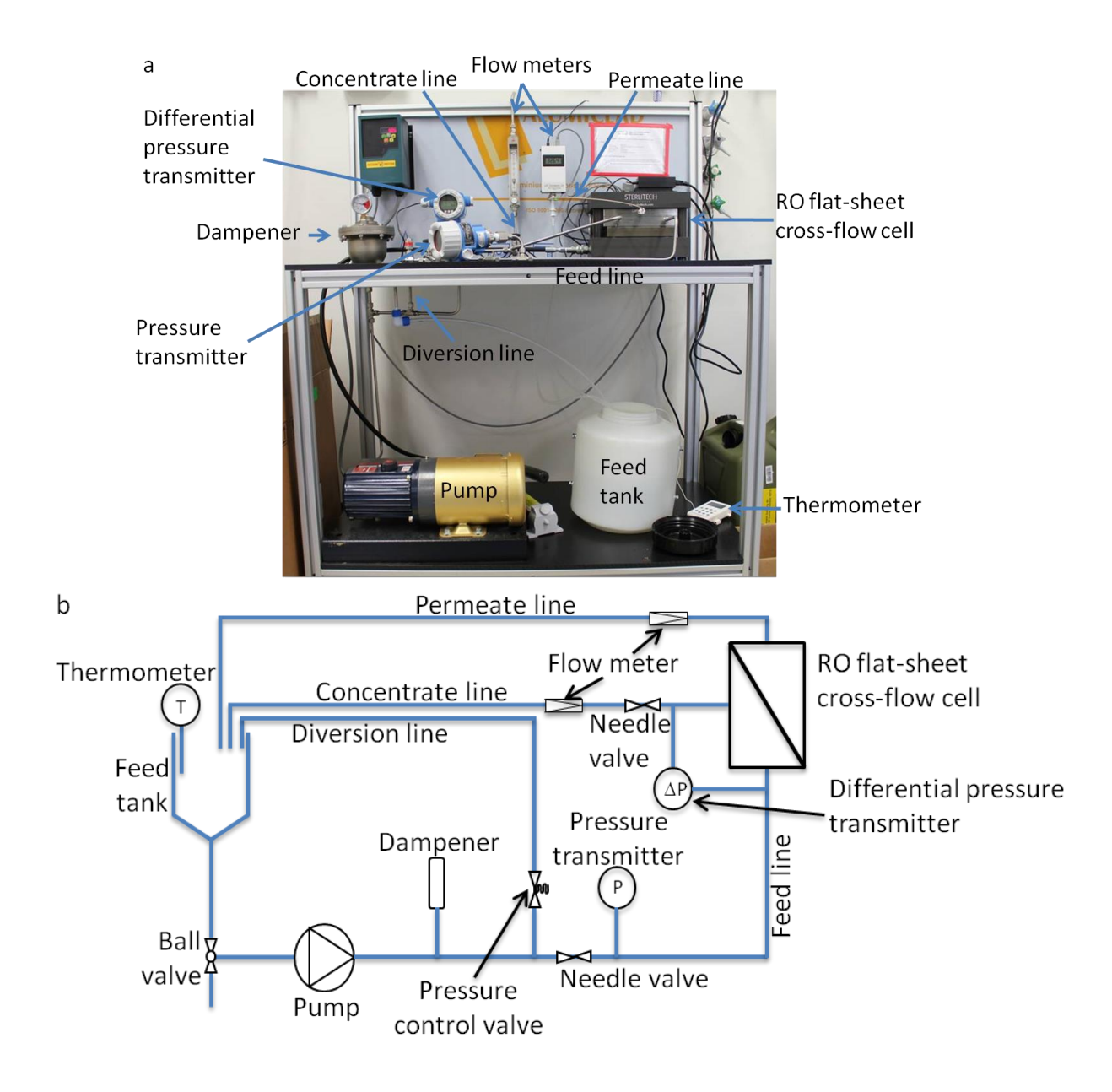
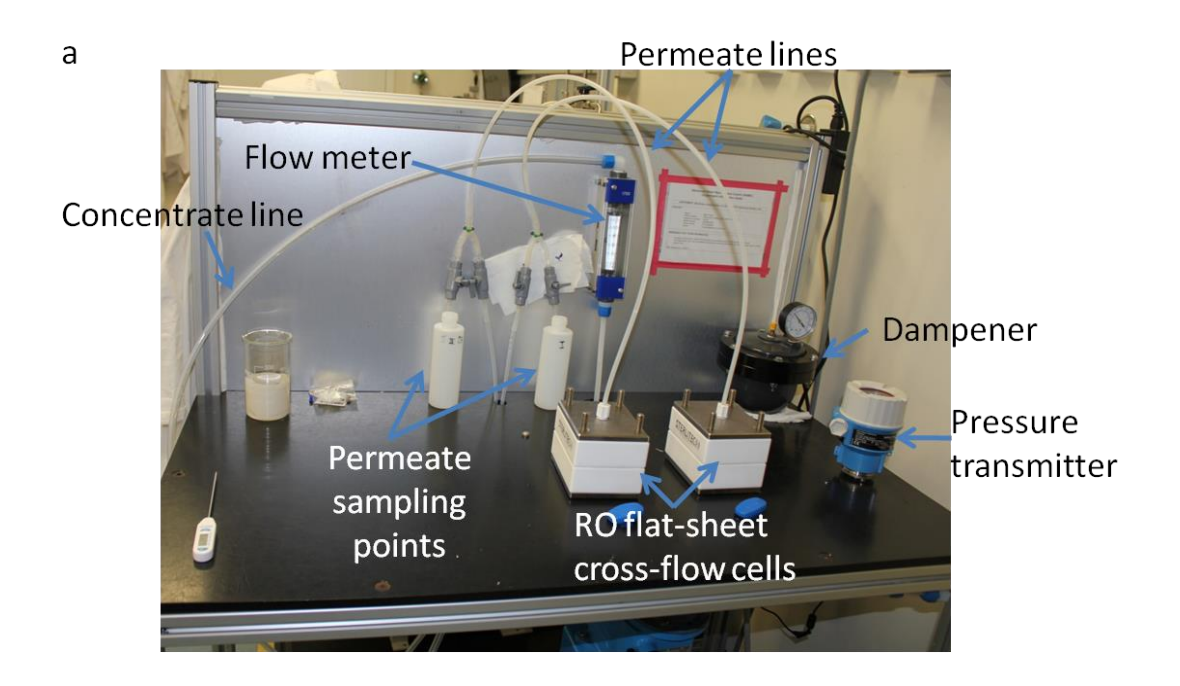


Figure 2.2: (a) photo and (b) drawing of the SS flat-sheet set-up.

2.2.2. Plastic flat-sheet cross-flow set-up (plastic flat-sheet set-up)

The ageing experiments were performed using a plastic flat-sheet test unit consisting of two resin flat-sheet cross-flow cells connected in parallel (effective membrane area: 42 cm²; Sterlitech Corporation, Kent, WA, USA), a metering pump Z series (Tacminam, Japan) and a 15 L polyethylene feed tank (Rota Moulding, Midvale, Australia). The constant feed pressure controlled at 5 bar. The feed pressure was measured with a digital gauge transmitter and the cumulative concentrate flow rate of the two cells was controlled at 80 L·h¹ by adjusting the speed of the pump and a needle valve installed in the concentrate line. The permeate flow rate

was measured by weight and the concentrate flow rates were measured with a 1200 MPB flow meter (MPB industries Ltd, Kent, England) prior to be returned to the feed tank. The temperature of the feed solution was measured in order to normalise the performance to 25°C. Sampling points were located in permeate and concentrate lines. Figure 2.3 presents (a) a photo and (b) a drawing of the plastic flat-sheet set-up.



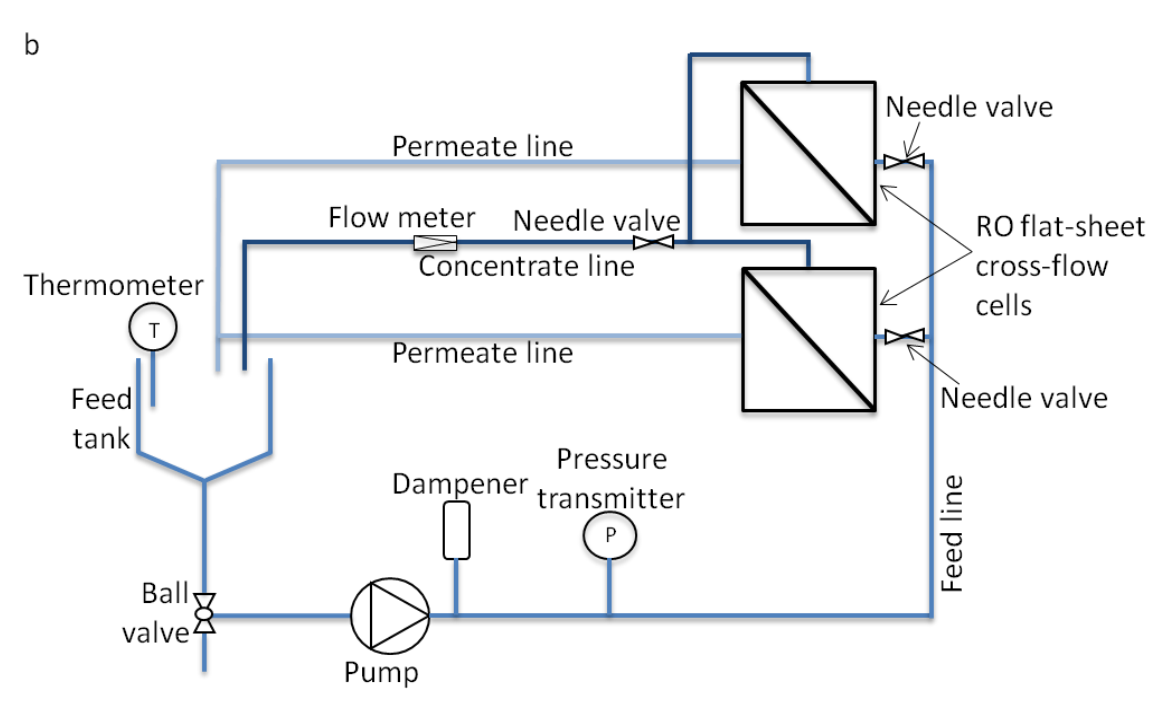


Figure 2.3: (a) photo and (b) drawing of the plastic flat-sheet set-up.

2.2.3. Spiral-wound module set-up (2.5" module set-up)

All experiments were performed using a single 2.5" spiral-wound module unit consisting of a stainless-steel pressure vessel (membrane shop, Australia), a Hydrovar CRN1-27 pump (Grundfos, Australia) and a 100 L feed tank. The constant feed pressure controlled at 7.5 bar. The feed pressure and the differential pressure between feed and concentrate lines were measured with two digital gauge transmitters. The concentrate flow rate was controlled at 540 L·h⁻¹ by adjusting the speed of the pump and by adjusting a needle valve installed in the concentrate line. Permeate and concentrate flow rates were measured with a TX50 flow meter and a 1750 MPB flow meter (MPB industries Ltd, Kent, England) respectively prior to be returned to the feed tank. The temperature of the feed solution was controlled using a cooling thermostat (Lauda, Australia). Sampling points were located in feed, permeate and concentrate lines. Figure 2.4 presents (a) a photo and (b) a drawing of the 2.5" module set-up.

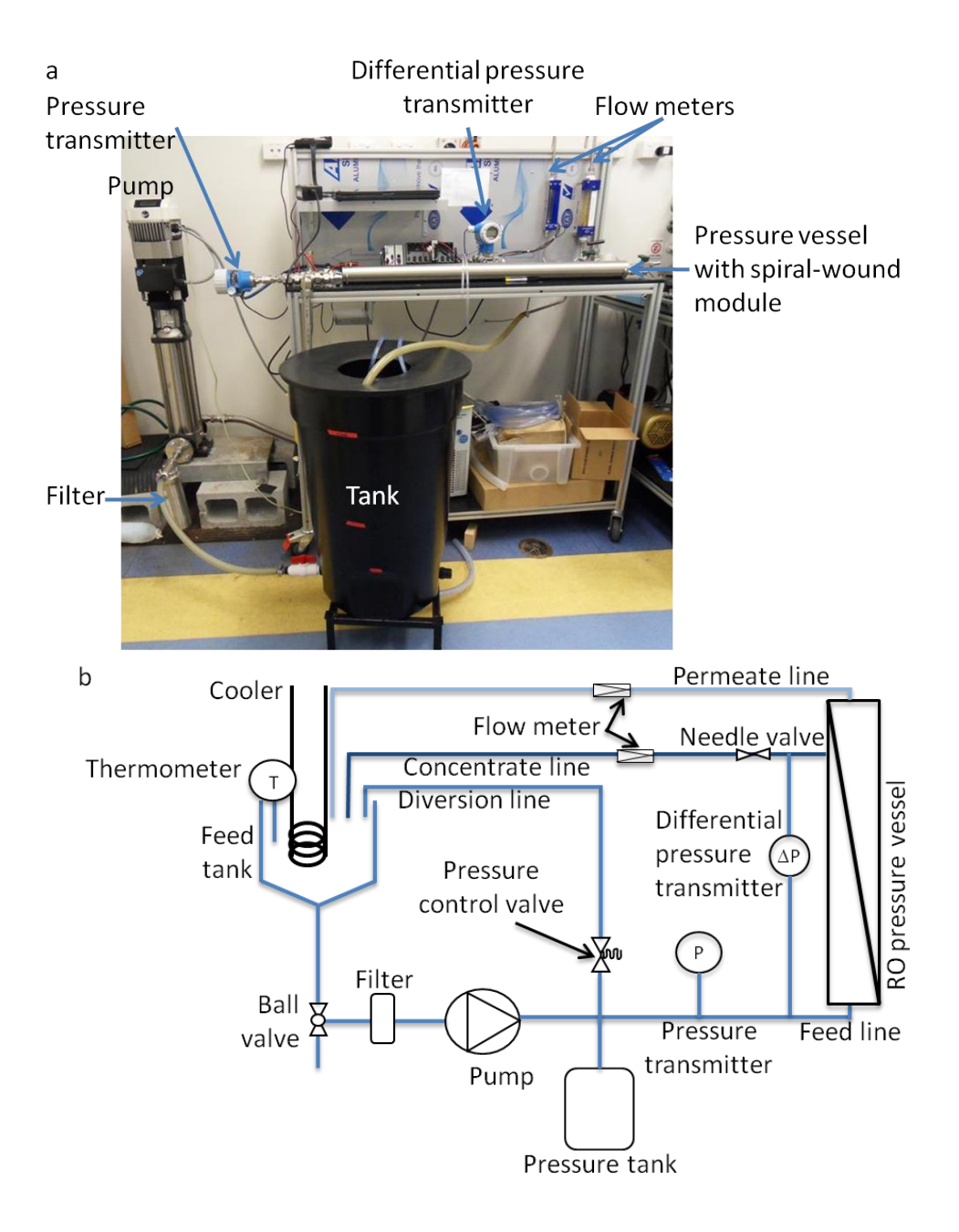


Figure 2.4: (a) photo and (b) drawing of the 2.5" module set-up.

2.2.4. Membrane characteristics

The membranes used in the three lab-scale experiments were a thin film composite energy saving polyamide RO membrane (ESPA2; Hydranautics, Oceanside, CA), which has a polysulfone supporting layer of 15 kDa MWCO. This membrane was selected because of its wide application in water reuse globally (e.g. by individual plants pertaining to the recycled water schemes operated by Orange County, California, PUB Singapore and in South East Queensland). Membrane sheets used for the flat-sheet set-ups were cut from a 4" spiral-

wound element and were stored in milli-Q water at 4°C. 2.5" spiral-wound membranes were used for the 2.5" module set-up. Water permeability and NaCl rejection were determined before each experiment using DI water and 1500 mg·L⁻¹ NaCl feed solution, respectively at an applied pressure of 7.5 bar (i.e. 5 bar with the plastic set-up) and a cross-flow velocity of 10 cm·s^{-1} . The performance specifications such as water permeability (K_w ; L·h⁻¹·m⁻²·bar⁻¹) and NaCl rejection ($R_{salt\%}$, %) were expressed as below (Equations 2.1 and 2.4, respectively).

$$K_{w} = \frac{J_{w}}{S} \times \frac{1}{NDP \times TCF}$$
 (2.1)

$$NDP = P_f - 0.5 \times TMP - \pi_f \tag{2.2}$$

$$TCF = \left(\frac{1}{\exp\left(K \times \left(\frac{1}{273} + T\right) - \left(\frac{1}{298}\right)\right)}\right) \tag{2.3}$$

$$R_{\text{salt}\%} = \left(1 - \frac{\Lambda_{\text{p}}}{\Lambda_{\text{f}}}\right) \times 100 \tag{2.4}$$

where J_w is the permeate flow (L·h⁻¹·m⁻²), S the membrane area (m²), NDP the net driving pressure (bar), TCF the temperature coefficient factor, P_f the feed pressure (bar), TMP the transmembrane pressure (bar), π_f the feed osmotic pressure (bar), K a constant characteristic of active layer membrane material, T the temperature (°C) at time t, $R_{salt\%}$ the salt rejection and Λ the normalised electrical conductivity value (μ S·cm⁻¹) in feed (f) and permeate (p) (Hydranautics, 2001; Mi et al., 2004; Wilf, 2010).

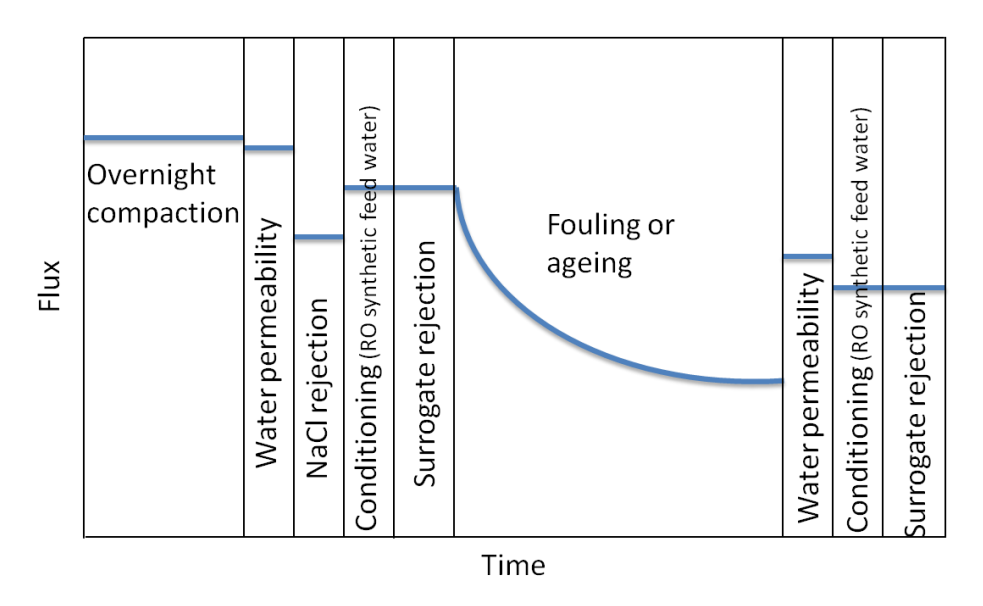
2.2.5. Membrane impairment protocols

The general experimental protocol developed for the three experiments (organic fouling, scaling and ageing) is shown in Figure 2.5. Prior to any experiments, the membranes were compacted overnight with DI water set to a pressure of 8.5 bar. This was followed by measurements of the pure water permeability (Equation 2.1) and salt rejection (1500 mg·L⁻¹ NaCl; Equation 2.4) at an applied pressure of 7.5 bar (cross-flow velocity: 10 cm·s⁻¹). An applied pressure of 5 bar was set for the compaction and filtration steps with the plastic flat-sheet set-up. Afterwards, the synthetic RO feed water or pre-filtered secondary effluent was added. In the case of synthetic RO feed, MS2 phage and R-WT were added after process stabilisation. Samples were taken hourly to determine the surrogate rejection by intact membranes. The surrogate rejection is expressed in LRV and calculated by Equation 2.5.

$$LRV = \log (C_f) - \log (C_p)$$
 (2.5)

where C_f and C_p are the concentrations of the compound in the feed and permeate samples, respectively.

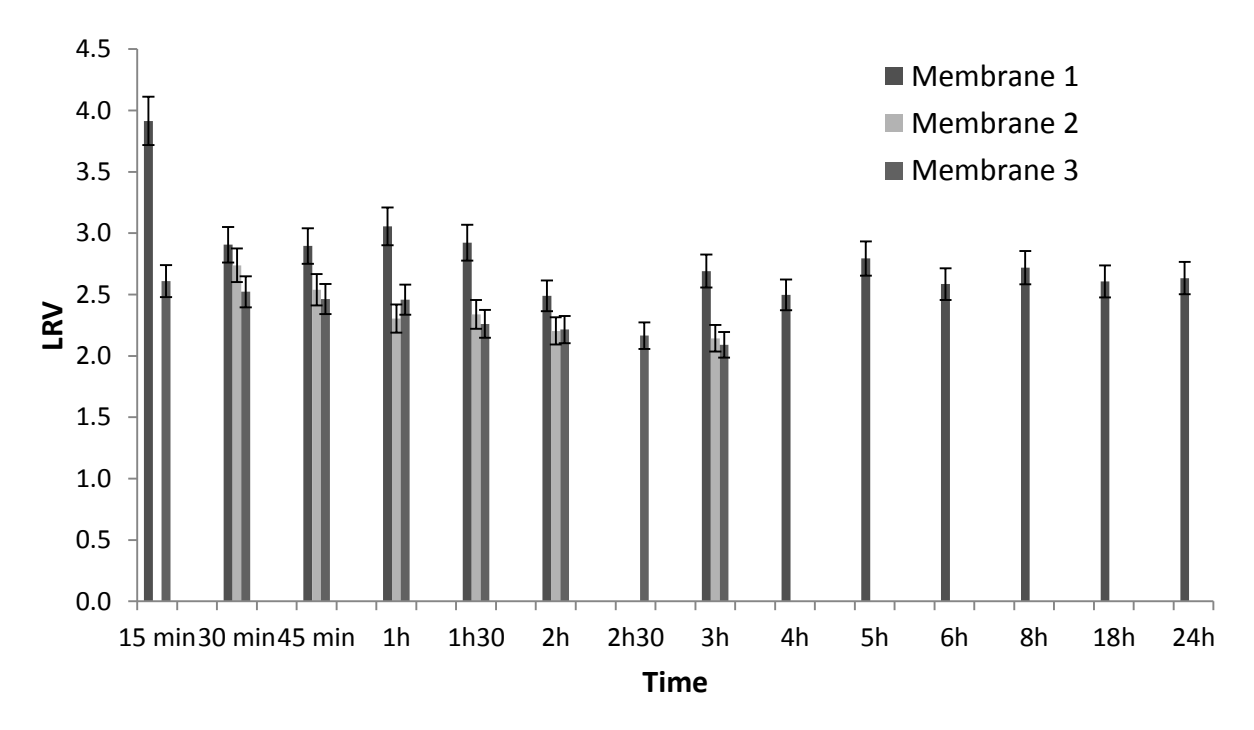
After cleaning the system, membrane impairment protocol was applied depending on the type of experiment conducted. The measurement of the pure water permeability (except for scaling experiments), salt rejection (except for organic fouling experiments) and surrogates rejection were determined for the membrane impairment as described previously (Equations 2.1, 2.4 and 2.5).



<u>Figure 2.5:</u> General experimental protocol developed for the impaired RO membrane experiments.

The different samples (feed and permeate) of virus surrogate and membrane integrity indicators were taken after 1 h, 2 h and 3 h of filtration with three different coupons for the SS flat-sheet set-up and four coupons with the plastic flat-sheet setups. Samples were taken after 1 h, 2 h, 3 h, 6 h, 18 h and 24 h with one membrane module for the 2.5" module set-up in order to have a sufficient number of samples to do a comparison. This sampling protocol was determined following a preliminary study done with intact membrane using the SS flat-sheet set-up. During this study, the evolution of the R-WT rejection was studied after different time of filtration from 15 min to 24 h. It has been determined that after 1 h, the system was stable with the standard error of 5% as showed in Figure 2.6. The decrease of R-WT LRV could be due to R-WT sorption on the membrane surface or the covering up of

possible imperfection in the polyamide membrane. However, as soon as the sorption sites are full, the rejection mechanisms of R-WT are size exclusion and electrostatic repulsion.

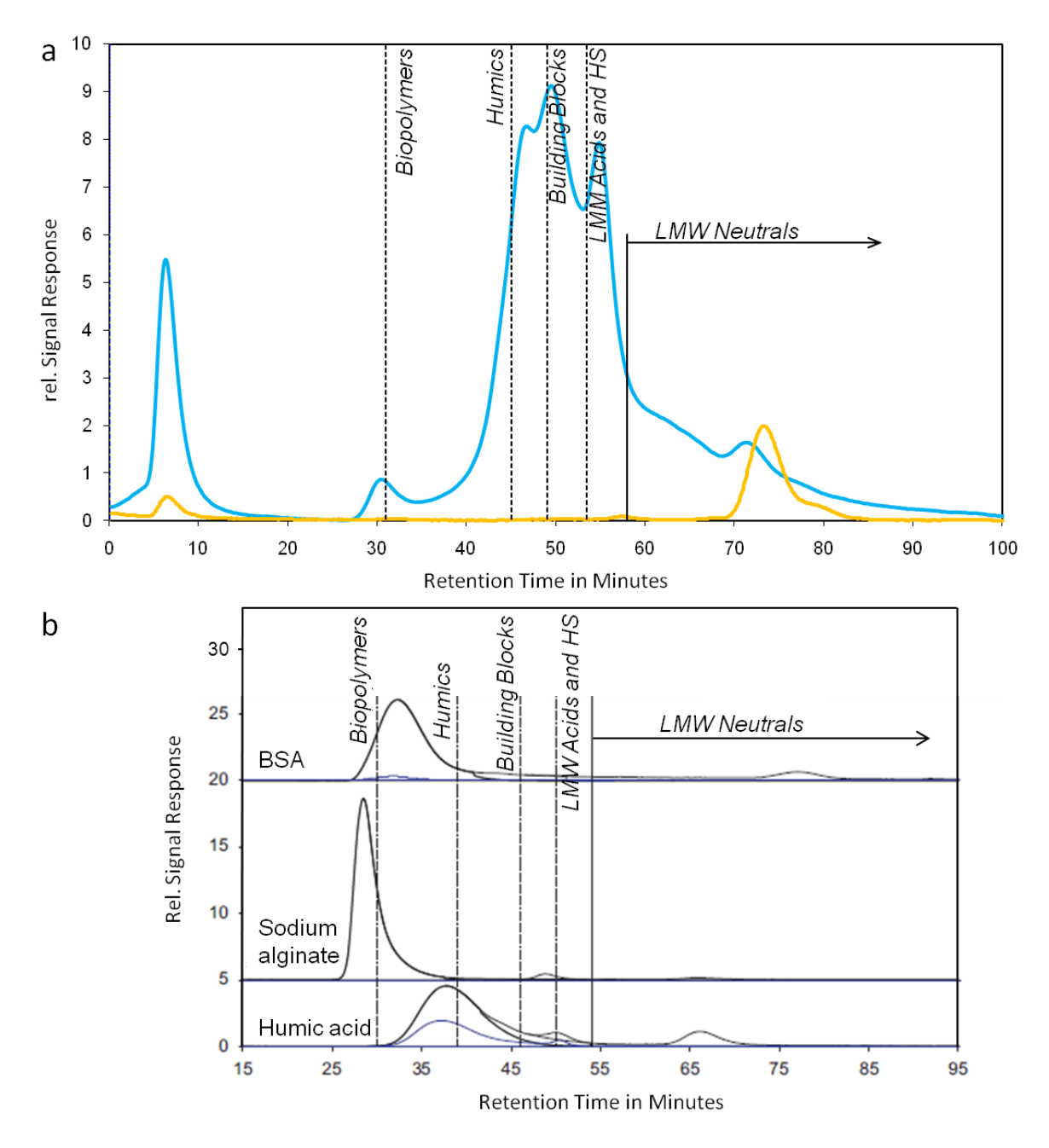


<u>Figure 2.6:</u> R-WT rejection as a function of filtration time with three different membrane coupons. Error bars = standard error of 5%.

2.2.5.1. Organic fouling

Three organic foulants at different concentrations were added to the synthetic RO feed solution to create an organic cake layer onto the membrane: 5 mg C·L⁻¹ humic acid (Sigma Aldrich, St Louis, MO, USA), 0.25 mg C·L⁻¹ bovine serum albumin (BSA, protein model foulant; Sigma Aldrich, St Louis, MO, USA) and 0.25 mg C·L⁻¹ sodium alginate (polysaccharide model foulant; Chem-Supply, Gillman, Australia) (Ang and Elimelech, 2008). This layer was created to mimic the organic fouling presence in a full-scale plant. The appropriate concentration of each foulant was taken from a previous study (internal data, not published). This study characterised the different feed waters from several tertiary treatment processes by different analytical techniques (e.g. TOC, fluorescence, etc.). Figure 2.7 presents typical LC-OCD chromatograms of the RO feed, RO permeate and different organic foulants (Fujioka et al., 2013). All organic foulants were received in powder form. Stock solutions of 2 g·L⁻¹ of humic acid, 1 g·L⁻¹ of sodium alginate and 1 g·L⁻¹ of BSA were prepared in milli-Q water. These stock solutions were mixed overnight to ensure the complete

dissolution of the foulant. They were then filtered with $0.45~\mu m$ nylon filters (Pm separations, Australia) and were conserved at 4°C. Organic foulants were filtered until the membrane permeability decreased by more than 20%. This impairment was studied with the SS flatsheet and the 2.5° module set-ups.



<u>Figure 2.7:</u> Typical LC-OCD chromatograms of (a) RO feed and RO permeate from a South East Queensland AWTP and (b) organic foulants (black line) (from (Fujioka et al., 2013)).

2.2.5.2. Scaling

In order to create a scaling layer, the synthetic RO feed solution was filtered through the membrane without recycling the permeate line until the concentration of the feed water was concentrated around 3-4 times. The permeate line was then recycled until the water permeability decreased by $\geq 10\%$. During the scaling, the pH of the feed water solution was maintained around pH 6-7 (i.e. normal operating pH in RO water recycling plant) by adding 0.5 M HCl as the scale formation is pH dependant. This impairment was studied with the SS flat-sheet and the 2.5° module set-ups.

2.2.5.3. Ageing

Accelerated damaging of the membrane was performed using a solution of sodium hypochlorite (Pool Resources, Smithfield, Australia) at 560 mg·L⁻¹ and at pH 7 during 16 h. These steps yield a chlorine exposure of 9000 ppm·h. The choice of the ageing protocol was done in order to ensure an impact on the polyamide layer and thus to decrease its efficiency to remove compounds. Donose *et al.* (2013) showed that 6000 ppm·h of chlorine exposure has a similar impact as 1000 and 3000 ppm·h on the salt rejection. From preliminary tests with the SS flat-sheet set-up, R-WT rejection by aged membrane did not change with a chlorine exposure time of 3000 and 6000 ppm·h. A higher chlorine exposure of 9000 ppm·h was tested and it was observed that the rejection of R-WT decreased by 0.1 LRV. For this reason, 9000 ppm·h of chlorine exposure time was selected. Also, the impact of the ageing is pH dependant. Therefore, the pH value was selected to obtain ageing that is similar in its mechanism of generation than the one which may occur in South East Queensland AWTP. Thus, the pH of the ageing solution was fixed at 7 by using a concentrated solution of HCl.

Two exposure modes were analysed:

- Dynamic mode: filtration of the chlorine solution across the membrane. Due to the chlorine attack on stainless-steel material, this method has been used only with the plastic flat-sheet system;
- Static mode: soaking of the membrane in a glass beaker containing the chlorine solution and protecting it from light. This impairment was studied with all three set-ups (SS flat-sheet, plastic flat-sheet and 2.5" module set-ups).

2.3. Analytical methods

2.3.1. Analysis of virus surrogate and membrane integrity indicators

Each compound has a specific detection method which is presented in Table 2.4 with the limit of quantification (LOQ).

<u>Table 2.4:</u> Summary of the different analytical techniques and their limit of quantification (LOQ) used to quantify the compounds.

Compound	Technique	LOQ
MC2 phage	Plaque-assay	30 PFU·mL ⁻¹
MS2 phage	qRT-PCR	$10^2copies\cdot\mu L^{1}$, $10^{1}copies\cdot mL^{1}$
R-WT	Fluorescence	25 ng·L ⁻¹
DOM	Fluorescence EEM	N/A
Sulphate	Ion chromatography	0.1 mg·L ⁻¹
Salt mixture	Electrical conductivity	1 μS·cm ⁻¹

qRT-PCR: quantitative reverse transcriptase-polymerase chain reaction.

EEM: excitation-emission matrix.

N/A: not available.

2.3.1.1. MS2 quantification

The concentration of MS2 phage was determined by the plaque-assay method (ISO, 1995) and quantitative reverse transcriptase-polymerase chain reaction (qRT-PCR).

Plaque-assay technique:

The plaque-assay method is a simple technique which permits to enumerate viable MS2 phage (phage being able to infect its host) by its culture. It was applied to determine the concentrations of MS2 phage stock solution, feed and permeate samples inoculated with *E. coli* using the double agar layer procedure described previously (ISO, 1995; Furiga et al., 2011). When necessary, logarithmic dilutions of MS2 phage samples were performed in order to obtain a number of plaques included between 30 and 300. After incubation overnight at a set temperature of 37°C, plates were examined to calculate the sample number of plaque

forming units (N_{PFU}; PFU·mL⁻¹) as defined in Equation 2.6.

$$N_{PFU} = \frac{N \times D}{V}$$
 (2.6)

where N is the number of plaque in one Petri dish, D the dilution factor and V (mL) the sample volume.

qRT-PCR:

Quantitative PCR (qPCR) is a sensitive and fast quantitative technique to target RNA and DNA. It allows the detection of all MS2 phage, both viable and broken. The principle behind this technique is to amplify and simultaneously quantify a targeted DNA molecule by fluorescence. The two most common methods for the detection of qPCR products are the detection using SYBR Green, which binds all double-stranded DNA; and the detection using TaqMan probes, which are specific to the target sequence. TaqMan probes were used in this study. The level of fluorescence depends on the initial quantity of DNA, the number of cycles and the reaction yield of the PCR. MS2 phage is a RNA virus. Thus, a prior reverse transcriptase step is necessary to convert RNA to DNA. The qRT-PCR principle is presented in Figure 2.8.

The RNA of MS2 phage was extracted from 140 μ L of sample using a QIAamp viral RNA kit (QIAGEN, Australia) and eluted with 60 μ L of buffer as described in the manufacturer's instruction guide. The extracted RNA was conserved at -80°C (Ogorzaly and Gantzer, 2006).

Calibration curves were created for each qRT-PCR and produced from a MS2 phage stock solution in broth yeast extract, pre-enumerated by the PFU method. The viral RNA of the stock solution was extracted and the RNA concentration was measured by absorbance (NanoDrop, Thermo scientifique, Australia). Afterwards, the extracted RNA stock solution was serially diluted to create 10-fold standard concentrations from 10⁶ to 10² ng·μL⁻¹. For each standard, 20 μL aliquots were frozen at -80°C. The LOQ of the technique was determined by the last standard value having a correct signal.

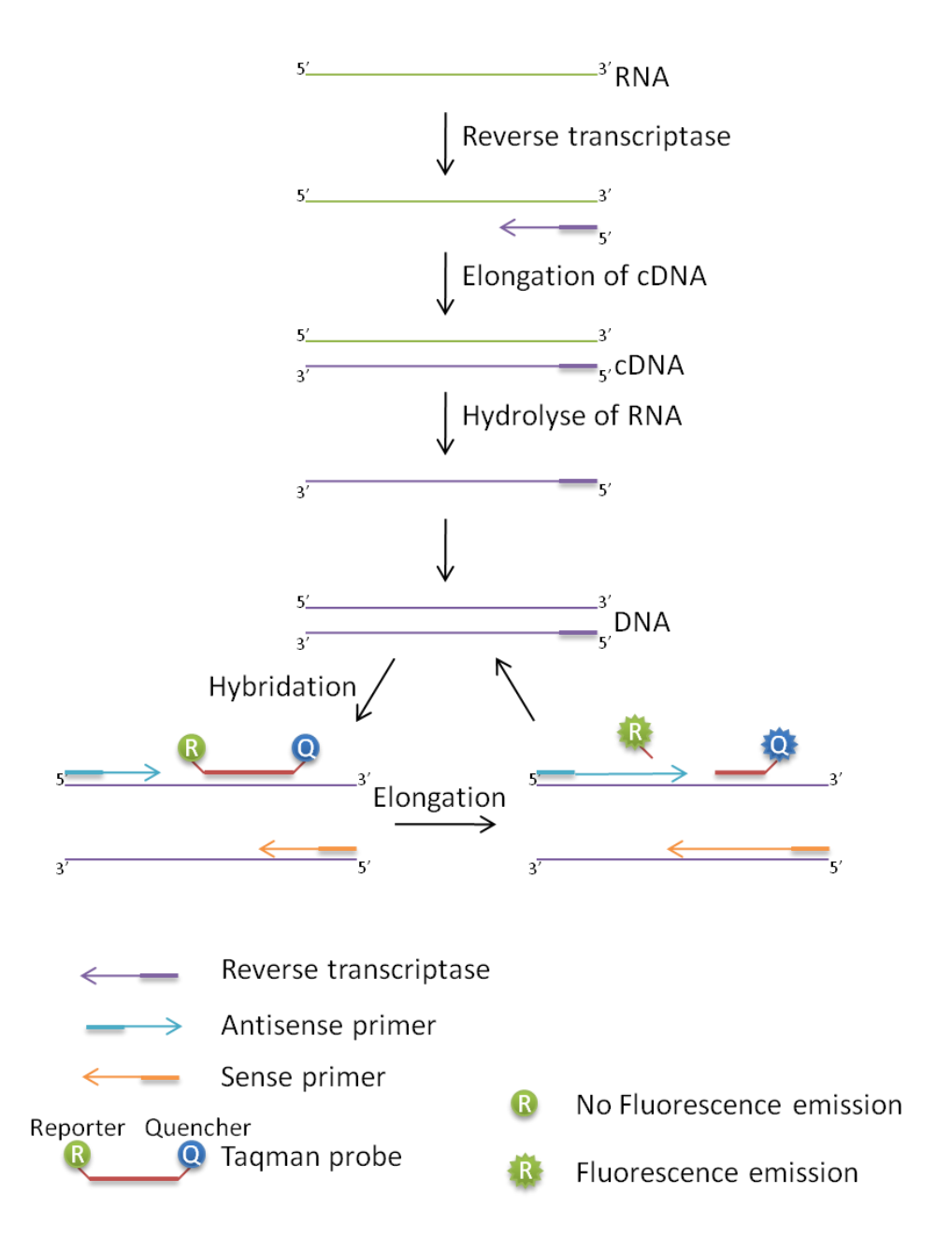


Figure 2.8: The qRT-PCR principle using TaqMan probes (Bustin and Mueller, 2005).

RNA quantification was performed using a one-step QuantiTect Probe RT-PCR kit (Qiagen, Australia) with 10 μL of reaction mixture containing 5 μL of Master mix (containing the enzyme in its buffer and dNTPs), 1 μL of 300 nM of each forward and reverse primers, 1 μL of 125 nM of TaqMan probe, 0.1 μL of RT-mix and 1.9 μL of RNA (Table 2.5). Primers and probe used for the quantification were the MS2-TM2-F, MS2-TM2-R and MS2-TM2JOE (Table 2.6) as described by Dreier *et al.* (2005). The qRT-PCR protocol was the following: reverse transcription at 50°C for 30 min, denaturation at 95°C for 15 min, followed by 45 cycles of annealing at 95°C for 15 s and elongation at 60°C for 60 s. The reaction was run

on an ABI Prism 7900 HT sequence detection system operated with the SDS 2.3 software (Applied Biosystems). The concentration of each sample was determined using standard curves plotted with the threshold cycle (C_T) of each dilution amplified in triplicates as a function of the logarithmic RNA concentration (Ogorzaly and Gantzer, 2006; Furiga et al., 2011). The PCR efficiency (E) was determined by the slope (s) of the standard curve following Equation 2.7 (Kubista et al., 2006). Thus, a slope of - 3.33 corresponds to 100% of reaction efficiency. Figure 2.9 presents typical amplification curves of MS2 phage standards and the standard curve of 10-fold diluted MS2 from 10^6 to 10^2 ng· μ L⁻¹.

$$E = 10^{-1/s} - 1 \tag{2.7}$$

For all assays, the efficiency was above 99%.

<u>Table 2.5:</u> The qRT-PCR reaction mixture composition.

Reagent	Final concentration (nM)	Volume (µL)
Master mix	N.A	5
Forward Primer	300	1
Reverse Primer	300	1
TaqMan probe	125	1
RT-mix	N.A	0.1
RNA matrix	N.A	1.9
Final volume		10

N.A: not applicable.

<u>Table 2.6:</u> Primers and probe used for the quantification of MS2 phage.

	Sequence	Position
MS2-TM2-F	TGCTCGCGGATACCCG	3169 - 3184F
MS2-TM2-R	AACTTGCGTTCTCGAGCGAT	3229 - 3210R
MS2-TM2JOE	ACCTCGGGTTTCCGTCTTGCTCGT	3186 - 3209

MS2-TM2JOE: sequence 5' (JOE), sequence 3' (BHQ1).

From (Dreier et al., 2005).

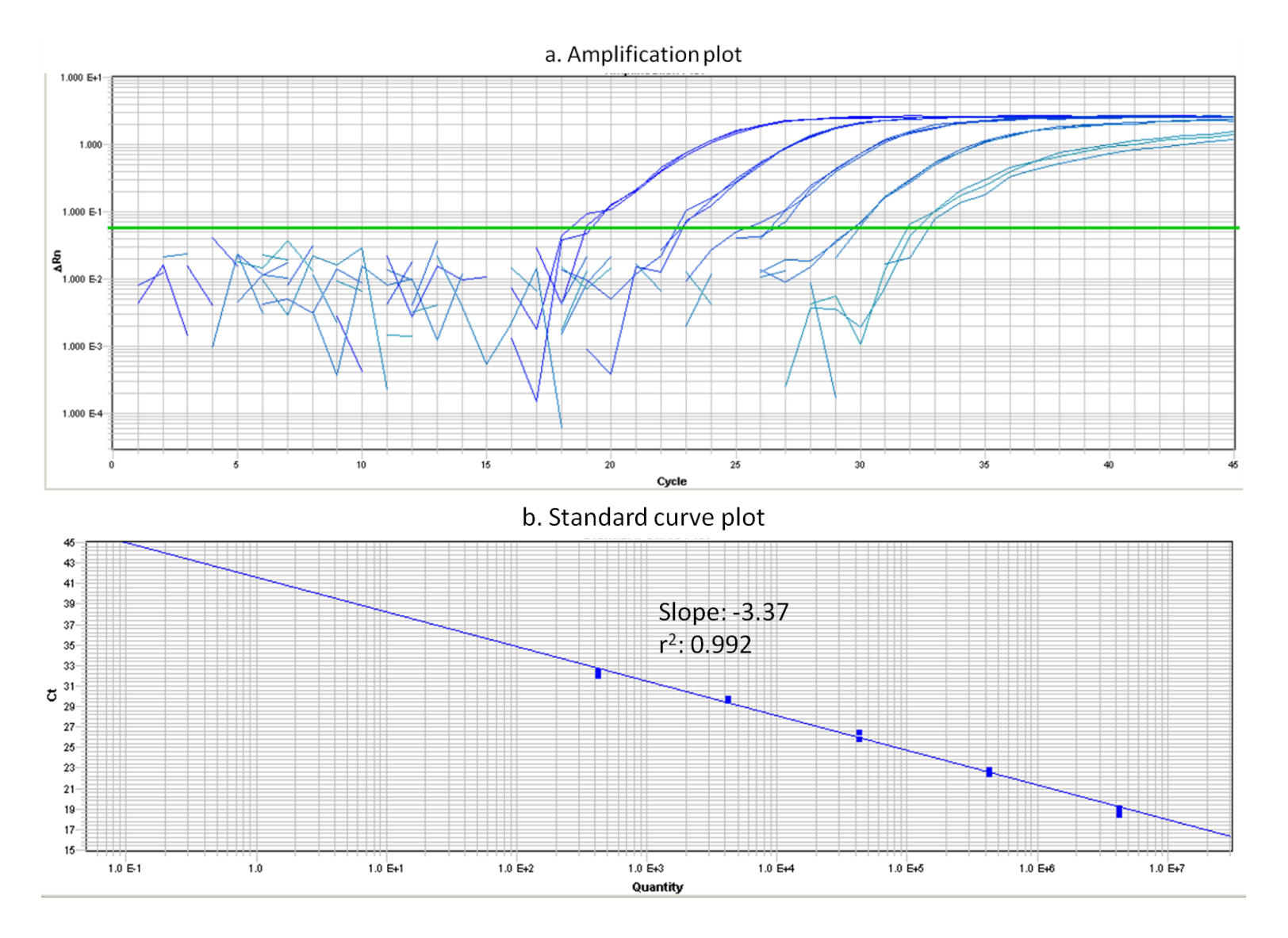


Figure 2.9: Amplification curves (a) and standard curve (b) of 10-fold diluted MS2 from 10⁶ to 10² ng·μL⁻¹.

2.3.1.2. R-WT quantification

Fluorescence measurements of R-WT were performed using a PerkinElmer LS-55 luminescence spectrometer (PerkinElmer, Australia) in a 1 cm quartz cuvette operated with the Winlab® software provided by PerkinElmer. Fluorescence intensity was recorded using excitation and emission wavelengths of 550 and 580 nm, respectively. Excitation and emission scan slits were set to 3 nm for feed and concentrate samples and to 10 nm for permeate samples in order to increase the sensibility of the instrument. The photomultiplier voltage was set to the automatic mode.

2.3.1.3. DOM analysis

Fluorescence measurements of DOM were performed using a PerkinElmer LS-55 luminescence spectrometer (PerkinElmer, Australia) in a 1cm quartz cuvette operated with the Winlab® software provided by PerkinElmer. Fluorescence intensity was recorded by varying excitation wavelengths (λ_{ex}) from 200 nm to 400 nm at steps of 5 nm, and emission wavelengths (λ_{em}) from 280 nm to 500 nm at 0.5 nm steps generating a three-dimensional fluorescence EEM as previously described by Chen *et al.* (2003). A cut-off at 290 nm was used to limit the second-order Raleigh scattering. Excitation and emission scan slits were set to 7 nm for the full-scale study (Chapter 3) and to 10 nm for the lab-scale study (Chapters 4 and 5), the scan speed was set to 1200 nm·min⁻¹ and the photomultiplier voltage was set to the automatic mode. Samples were equilibrated at room temperature (air conditioned at 23°C) prior analysis in order to minimise the temperature effect and all RO feeds were diluted 50 times to avoid the inner filter effect (absorption of photons of either incident or emitted light by the sample; $A_{230} < 0.05$) (Larsson, 2007; Lakowicz, 1999). This dilution allows measuring both types of samples (feed and permeate) in a similar chemical environment avoiding factors such as pH and salt concentration which could affect fluorescence.

For all fluorescence spectra, Raman normalisation ($\lambda_{ex} = 350$ nm, $\lambda_{em} = 371$ - 428 nm) and a blank subtraction (milli-Q water generated by Millipore Advantage fed by tap water previously filtered through activated carbon and RO) were applied as described previously (Lawaetz and Stedmon, 2009; Murphy et al., 2010). A fluorescence regional integration (FRI) technique from fluorescence spectroscopy was used to quantify the contribution to the EEM spectra (Chen et al., 2003; Singh et al., 2009) of three delimited regions (region I: λ_{ex} / λ_{em}

300 - 325 / 375 - 405 nm, region II: $\lambda_{ex} / \lambda_{em} 320 - 350 / 405 - 440$ nm defined as 'humic-like' by Coble *et al.* (1996) and region III: $\lambda_{ex} / \lambda_{em} 230 - 260 / 380 - 470$ nm) in both full-scale AWTPs (details given in Table 2.7). Peak volumes and ratios between volumes of the three selected EEM regions were calculated following equations described by Chen *et al.* (2003) using R software (adapted from (Lapworth and Kinniburgh, 2009)). Briefly, the volume of fluorescence intensity (Φ_i) of each region 'i' was calculated and normalised 'n' ($\Phi_{i,n}$) with a multiplication factor (MF_i) specific to each region 'i' (Equations 2.8 and 2.9). The cumulative volume 'T' of the normalised fluorescence intensity ($\Phi_{T,n}$) was calculated by Equation 2.10. The percent fluorescence response of each region 'i' ($P_{i,n}$) was calculated using Equation 2.11 (Chen et al., 2003).

$$MF_{i} = \left(\frac{(\Delta \lambda e \times \Delta \lambda e m)_{i}}{\sum (\Delta \lambda e \times \Delta \lambda e m)_{i}}\right)^{-1}$$
(2.8)

where $\Delta \lambda ex$ and $\Delta \lambda em$ are the interval of the excitation and emission wavelength, respectively.

$$\Phi_{i,n} = MF_i \Phi_i \tag{2.9}$$

$$\Phi_{T,n} = \sum_{i=1}^{3} \Phi_{i,n} \tag{2.10}$$

$$P_{i,n} = \frac{\Phi_{i,n}}{\Phi_{T,n}} \times 100 \tag{2.11}$$

The rejection of the organics ($R_{DOM\%}$) which are responsible for the fluorescence of each region by the RO membranes, was determined by calculating the removal of fluorescence intensity using Equation 2.12.

$$R_{DOM\%} = \left(1 - \frac{\Phi_{p,n}}{\Phi_{f,n}}\right) \times 100 \tag{2.12}$$

where $\Phi_{p,n}$ and $\Phi_{f,n}$ are the normalised volume of permeate and feed fluorescence intensity, respectively.

Table 2.7: FRI parameters of each region

EEM region	Excitation (nm)	Emission (nm)	Nº of EEM data points per region	Projected area (nm²)	MF_i
I	300 - 325	375 - 405	300	750	6.00
II	320 - 350	405 - 440	420	1050	4.29
III	230 - 260	380 - 470	1080	2700	1.67
Summation			1800	4500	

2.3.1.4. Sulphate quantification

Sulphate ions were measured as SO₄-S by a compact Dionex ICS-2000 ion chromatograph (IC; Dionex, Australia) with a DS6 heated conductivity detector (35°C). A potassium hydroxide gradient was applied with the Dionex automatic eluent generator using an EluGen cartridge (EGC II KOH). The gradient started at 12 mM KOH, was ramped up in 5 min to 34 mM where it was kept for 3 min, then in 1 min it was ramped up from 34 to 52 mM and kept at that concentration for another 11 min. The data acquisition time was 20 min and the total analysis time 25 min. The injection volume was 25 μL and the flow rate 1 mL·min⁻¹. The separation was achieved with a Dionex IonPac AG18 (4 x 50 mm) guard and an IonPac AS18 (4 x 250 mm) separating column. Both columns were heated to 35°C. The data processing was done with the Dionex Chromeleon software.

2.3.1.5. Electrical conductivity

EC was measured using a Mettler Toledo SevenEasy. Salt rejection (R_{salt%}) was calculated from conductivity measurements of each sample following Equation 2.4.

To calculate salt rejection, conductivity measurements (Λ_{meas}) were normalised as defined by Equations 2.13 and 2.14 for the average feed salinity (f) and permeate salinity (p), respectively. Feed salinity is an average value of the feed water salinity that increases during filtration within a pressure vessel due to the passage of feedwater to the permeate channel.

$$\Lambda_{f} = \frac{\Lambda_{\text{meas},f}}{\frac{\text{TCF}}{R}} \times \ln \frac{1}{1-R}$$
(2.13)

$$\Lambda_{\rm p} = \frac{\Lambda_{\rm meas,p}}{\rm TCF} \tag{2.14}$$

where R is the stage recovery (%) and TCF is the temperature correction factor as expressed

above in Equation 2.3 (Hydranautics, 2001).

2.3.2. Other chemical analysis

UV₂₃₀ was measured using a Cary 50 bio UV-vis absorption spectrophotometer (Varian, Australia). Dissolved organic carbon (DOC) was measured with a TOC-multi N/C 2100S (Analytik Jena, Australia) using the non-purgeable organic carbon method. Colorimetric tests (chlorine pocket colorimeterTM II, HACH Lange GmbH, Düsseldorf, Germany) were used to determine the concentration of chlorine. Metals were measured using inductively coupled plasma-optical emission spectrometry (ICP-OES). The sample was acidified with either 5% of concentrated nitric acid (HNO₃, trace metal analysis grade) in the absence of organic matter or 10% of HNO₃ in the presence of organic matter.

2.3.3. Membrane autopsies

At the end of each experiment, membranes were autopsied and analysed by different microscopy and spectroscopy techniques in order to characterise the impairment. Table 2.8 summarises the membrane autopsy techniques used for each type of impairment and their main function.

<u>Table 2.8:</u> Summary of the microscopy and spectroscopy techniques, their function and their use by type of membrane impairment.

Technique	Function	Impairment
AFM	Membrane surface visualisation	Organic fouling
Al'IVI	(roughness)	Ageing
SEM	Surface imaging	Organic fouling
SEM-EDS	Surface imaging and elemental	Scaling
SEM-EDS	composition	Scaring
ATR-FTIR	Surface chemical structures and	Organic fouling
AIN-I'IIN	functional groups modification	Ageing

AFM: atomic force microscopy.

SEM-EDS: scanning electron microscopy-energy dispersive spectroscopy.

ATR-FTIR: attenuated total reflection-Fourier transform infrared.

2.3.3.1. Atomic force microscopy (AFM)

The principle of AFM is to monitor the deflection of the probe as it contacts the sample surface and to convert deflection data into topographical information. Therefore, a cantilever beam terminated with a sharp tip scans the surface at constant force or fixed vibration frequency (Alford et al., 2007a).

AFM analysis was done following a previously described method (Donose et al., 2013). Briefly, imaging was performed on 10 x 10 µm dried samples in intermittent contact mode (Asylum MFP-3D-BIO, Asylum Research, USA). The roughness parameters of the membrane were determined by extracting the root-mean-square (RMS) roughness following Equation 2.15.

$$RMS = \sqrt[2]{\left(\frac{1}{\text{Vnpnts}}\sum Y_i^2\right)}$$
 (2.15)

where Vnpnts is the number of height events and Y is the height of the peak.

2.3.3.2. Scanning electron microscopy-energy dispersive spectroscopy (SEM-EDS)

The morphology of a sample is obtained by scanning an electron probe across the sample which produces a high resolution image. The elemental analysis of the sample is obtained by monitoring secondary X-rays produced by electron-specimen interaction. The X-rays energy is specific to the atomic structure of an element which allows assessing the elemental composition of the sample (Alford et al., 2007b).

Sample imaging was done employing a Philips XL30 scanning electron microscope. All samples were Pt coated (SPI) for 90 s and vacuum dehydrated for at least 24 h before imaging. Image acquisition was done at 5 kV accelerating voltage and approximately 10 mm working distance.

2.3.3.3. Attenuated total reflection-Fourier transform infrared (ATR-FTIR)

The principle of FTIR technique is to monitor the intensity of the transmitted radiation of a sample exposed to an electromagnetic radiation over a desired range of the incident radiation frequency (Jaddi and Vij, 2006). Depending on the chemical composition of the sample, a series of peaks in the spectrum appears due to the absorption of radiation at specific resonant

frequencies.

ATR-FTIR analysis was done using a previously described method (Donose et al., 2013). Briefly, spectra were collected by a Nicolet 5700 spectrometer (Thermo Electro Corporation, USA) using a Ge crystal as an internal reflection unit. All spectra were collected with a minimum of 128 scans at a resolution of 4 cm⁻¹ and analysed with Spekwin32 version 1.71.6.1 software.

2.4. Statistical data analysis

Plot and correlation factor, Student's *t*-test, two-way analyse of variance (ANOVA) and box plot were performed using the R software.

The Pearson's correlation coefficient was used to measure the strength of a linear association between two indicators and is noted with 'r'. The closer the value of r to 1 the greater was the correlation between the two variables. Plots were used to visualise these correlations.

Student's t-test was used to verify the statistical similarity between samples. If the p-value was below 0.05 (p-value < 0.05), the hypothesis that two samples were different was rejected with 5% of risk. Before running the t-test, Fisher's F-test was used in order to determine the homogeneity of the samples which allowed setting the parameters of the t-test.

Two-way ANOVA was used to compare the average differences between the LRV of R-WT, DOM and salt (called groups) that were split on two independent variables (called factors) such as the type of membrane impairment (intact, organically fouled, scaled and aged) and the type of set-up (SS, plastic or 2.5" module set-ups). The primary goal of a two-way ANOVA is to understand if there is an interaction between the two independent factors on the dependent variable. Thus, it allows verifying the null hypothesis (H_0) that all samples have the same average. The alternative hypothesis is that at least one samples average is different to the others. In this objective, F-test and its *p-value* were determined. If $F_{calculated}$ was higher than $F_{critical}$ ($F_{calculated} > F_{critical}$), the hypothesis H_0 was rejected.

Box plots were used to project groups of numerical data through their quartiles graphically. They present differences between groups without making any hypothesis of the underlying statistical distribution and are non-parametric.

3. Monitoring RO performance:

Conductivity versus EEM

This chapter is an edited version of the following peer-reviewed journal publication:

Pype, M-L., Patureau, D., Wery, N., Poussade, Y., Gernjak, W. (2013). Monitoring reverse osmosis performance: Conductivity versus fluorescence excitation—emission matrix (EEM). *Journal of Membrane Science* 428, 205-211.

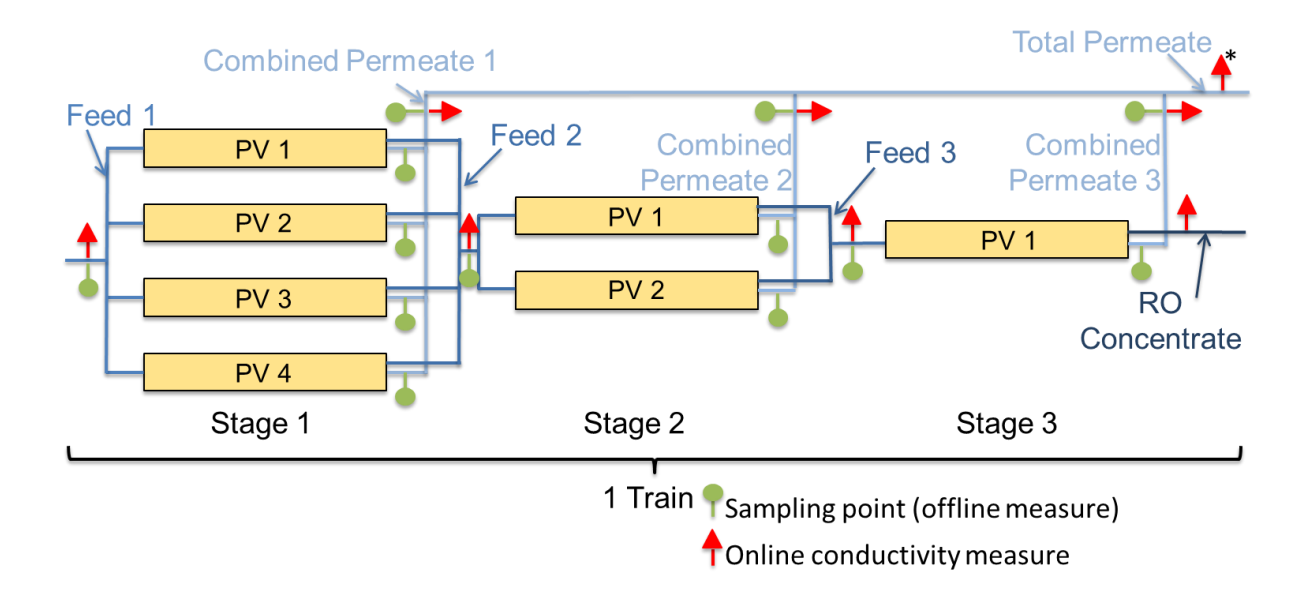
3.1.	Reverse osmosis plant description, sampling protocols and general water quality	74
3.2.	Determination of membrane defects through measurement of salt and organic	cs
reject	ion by conductivity and fluorescence profiling	76
3.3.	Understanding the blue-shift of the fluorescence of humic substances from feed	to
perm	eate	82
3.4.	Conclusions and implications for practice	85

In the present chapter, we propose to use DOM removal analysed by EEM coupled to a fluorescence regional integration (FRI) technique as a tool to monitor RO membrane integrity, which to the authors' best knowledge has not been published before. Feed and permeate waters from different pressure vessels (PV) in a RO train were analysed by conductivity and EEM fluorescence to analyse the variability of ion and DOM rejection. A FRI technique from fluorescence spectroscopy was used to calculate the area of three delimited regions (noted region I, II and III) in two full-scale advanced water treatment plants (AWTPs). In addition to the direct measurement of the samples by EEM, size exclusion chromatography (SEC) with fluorescence detection was used to further characterize the DOM in feed and permeate samples.

The objectives of this work are (i) to assess performance variability within RO trains and AWTPs as measured by conductivity and DOM rejection; and (ii) to evaluate EEM fluorescence and SEC with fluorescence detection as a monitoring tool for DOM rejection by RO membranes with high sensitivity, which could potentially be used as membrane integrity indicator for RO process validation and operational monitoring.

3.1. Reverse osmosis plant description, sampling protocols and general water quality

Samples were collected from the RO process of two AWTPs in South East Queensland (SEQ) over a period of 18 months from September 2010 to February 2012 (Figure 3.1). In plant A, 7 PVs in stage 1, 4 PVs in stage 2 and 2 PVs in stage 3 have been sampled 7 times in 5 campaigns; in plant B, 3 PVs in stage 1, 10 PVs in stage 2 and 8 PVs in stage 3 have been sampled 5 times in 4 campaigns. When different trains have been sampled on the same day, water quality for the combined feed and permeate of the RO process has been determined only once. Both RO processes are operated at 85% of recovery throughout three stages, use two different RO thin-film composite polyamide membranes and are fed by secondary effluent from biological nutrient removal plants pre-treated by ferric iron coagulation, clarification and ultrafiltration.



<u>Figure 3.1:</u> Simplified schematic of an RO train in plant A with online conductivity sensors (red triangle) and sampling points used to measure offline conductivity and fluorescence (green circle). *In plant B, the total permeate conductivity is monitored online for entire RO trains.

All samples were collected in 100 mL amber glass bottles, transported in cold storage and analysed within three days. The water quality of the RO feed and permeate for the sampling period is detailed in Table 3.1. All the analytical methods and data analysis are explained in Chapter 2 Materials and methods.

<u>Table 3.1:</u> Mean water quality characteristics (± standard deviation) on the days sampled (n=4).

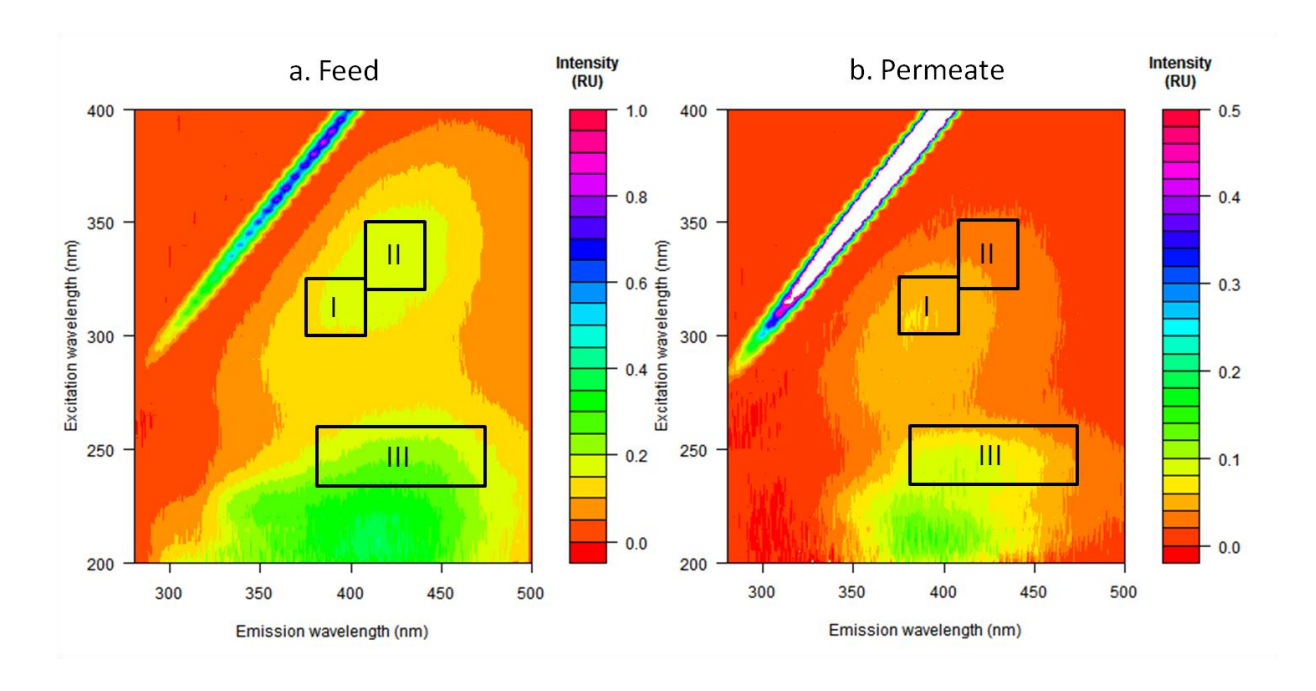
	RO feed		RO permeate	
	Plant A Plant B		Plant A	Plant B
Conductivity (µS⋅cm ⁻¹)	1066 (± 77)	1303 (± 203)	43 (± 6)	56 (± 9)
DOC (mg·L ⁻¹)	8.32 (± 1.26)	6.82(± 0.33)	< 0.1	< 0.1
рН	6.8 (± 0.3)	6.4 (± 0.1)	5.7 (± 0.2)	5.6 (± 0.1)

3.2. Determination of membrane defects through measurement of salt and organics rejection by conductivity and fluorescence profiling

Figure 3.2 shows a typical fluorescence EEM of RO permeate and feed. The maximum fluorescence of the humic-like peak in feed and permeate was located at two different wavelength pairs in the EEM (region II and I, respectively), whereas the region III was similar in both samples, but at different fluorescence intensity. Therefore, these three different regions were observed and delimited to quantify relative concentration using the FRI technique (Chen et al., 2003). The FRI parameters and the share of each region of total fluorescence are presented in Table 3.2. There is a significant difference between the distribution of fluorescence intensity among the three regions between feed and permeate. This trend is similar in both plants: the share of total fluorescence of region I increased from approximately 25% to 33% from feed to permeate, respectively, whereas the share of region II decreased from 31% to 22%. Region III was similar for all samples and was around 43%. Table 3.3 shows the average DOM rejection of the three delimited regions and salt rejection by RO stage for both plants. DOM rejection was constant throughout the 3 stages contrary to salt rejection which decreases stage by stage in both plants. In general, region II DOM removal was consistently around 99.5% and we can conclude that the DOM fluorescent in this region of the EEM was better rejected than DOM fluorescent in region I and III, and this difference of rejection causes the shift in the FRI distribution among the regions.

<u>Table 3.2:</u> FRI parameters and average percentage share of fluorescence response of each region in feed and permeate ($P_{i,n}$ ± standard deviation) for plant A and B.

	P	lant A	F	Plant B
EEM region	Feed Permeate $(n = 21)$ $(n = 91)$		Feed (n = 15)	Permeate (n = 105)
I	26.9 ± 0.9	34.7 ± 2.6	24.7 ± 2.8	32.8 ± 4.4
II	32.2 ± 1.2	21.8 ± 2.6	29.8 ± 2.7	22.6 ± 1.8
III	40.9 ± 1.3	43.5 ± 2.4	45.5 ± 5.2	44.6 ± 4.6
Summation	100	100	100	100



<u>Figure 3.2:</u> Typical RO (a) feed diluted 50 times and (b) permeate EEM. The location of the three regions evaluated is delimited by solid lines.

<u>Table 3.3:</u> Percentage of salt and DOM rejection (± standard deviation) by RO stage of the three delimited fluorescence regions.

	Plant A			Plant B		
% rejection	Stage 1 (n = 49)	Stage 2 (n = 28)	Stage 3 (n = 14)	Stage 1 (n = 15)	Stage 2 (n = 50)	Stage 3 (n = 40)
R _{DOM%} Region I	98.9 ± 0.2	99.1 ± 0.2	98.9 ± 0.5	98.5 ± 0.1	99.0 ± 0.5	99.2 ± 0.2
R _{DOM%} Region II	99.5 ± 0.2	99.5 ± 0.1	99.3 ± 0.5	99.5 ± 0.1	99.4 ± 0.4	99.6 ± 0.1
R _{DOM%} Region III	99.2 ± 0.2	99.2 ± 0.2	99.0 ± 0.5	99.4 ± 0.1	99.2 ± 0.4	99.4 ± 0.1
$R_{Salt\%}$	98.3 ± 0.5	98.2 ± 0.3	96.9 ± 0.9	98.2 ± 0.1	97.8 ± 0.4	97.5 ± 0.2

During the experiment, salt rejection can vary from 0.1 to 1.5% in an individual PV (data not shown). Two possible ways of increasing salt passage to the permeate were proposed: (i) loss in membrane filtration performance either due to scaling, fouling or polymer ageing or (ii) a leak around a seal, glue-lines or other physical membrane defects (Wilf, 2010). Assuming that all pressure vessels within the same stage in a RO train should, in theory, reject DOM to the same degree, a variation of organic rejection within a stage can help identifying leaks more sensitively than conductivity profiling alone since DOM rejection is higher than conductivity rejection. Increasing the sensitivity of the detection of leaks is of particular

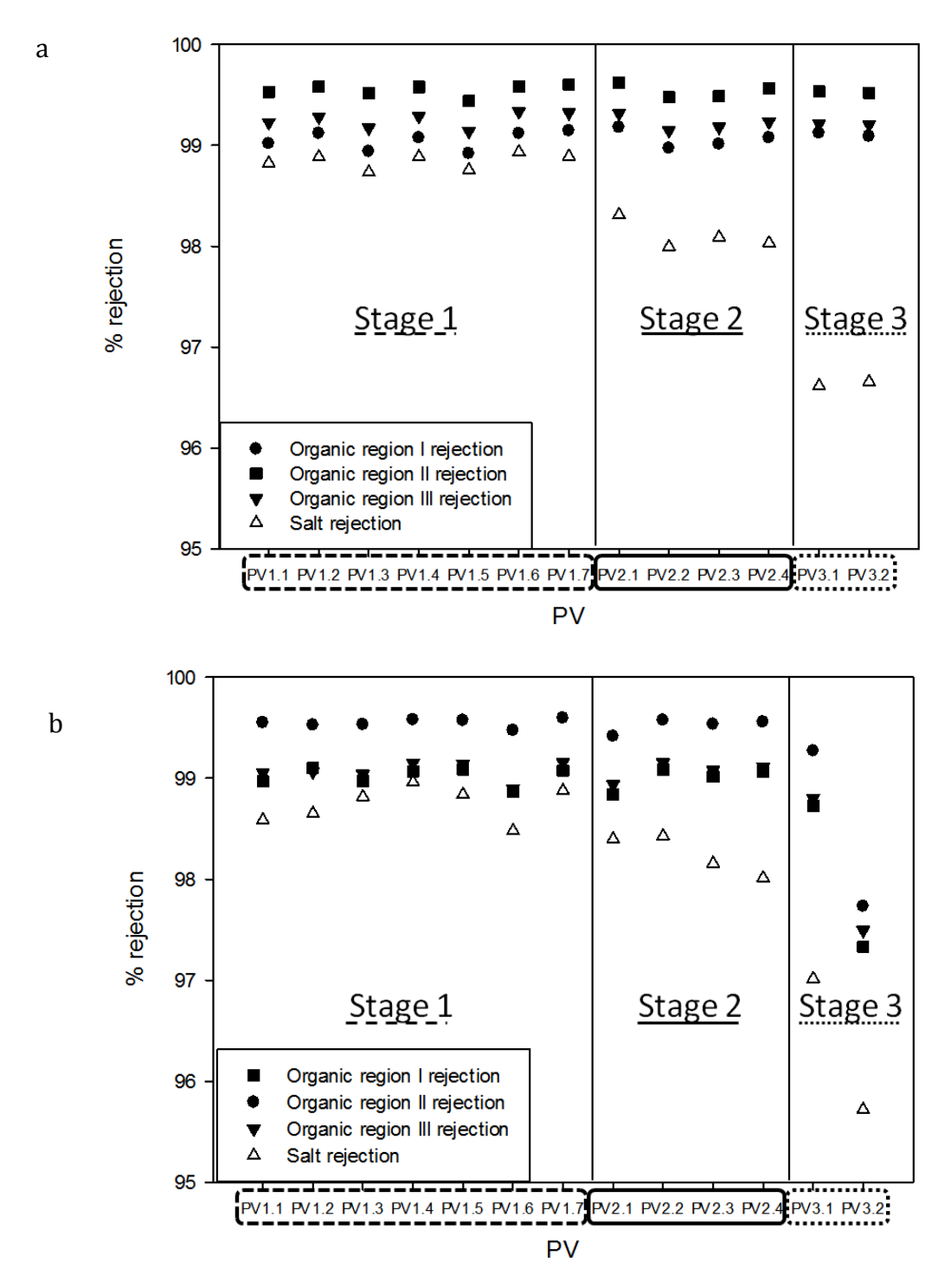
importance, if high virus rejection is a treatment goal of the RO filtration process.

Figure 3.3 shows the organic and salt rejection results for two different RO trains in Plant A during one sampling event. In one RO train (Figure 3.3 a), the organic rejection was constant (less than 0.3% of variation) during the process but the salt rejection decreased around 1.1% from stage 2 to stage 3. In contrast, in the other RO train (Figure 3.3 b), a drop of both, organic rejection and salt rejection, was observed.

Salts are rejected following different mechanisms, of which charge repulsion and sieving effect (or size exclusion) are the principals, and the rate of salt flow through the membrane $(Q_s, \text{m} \cdot \text{s}^{-1})$ follows Equation 3.1 (Wilf, 2010):

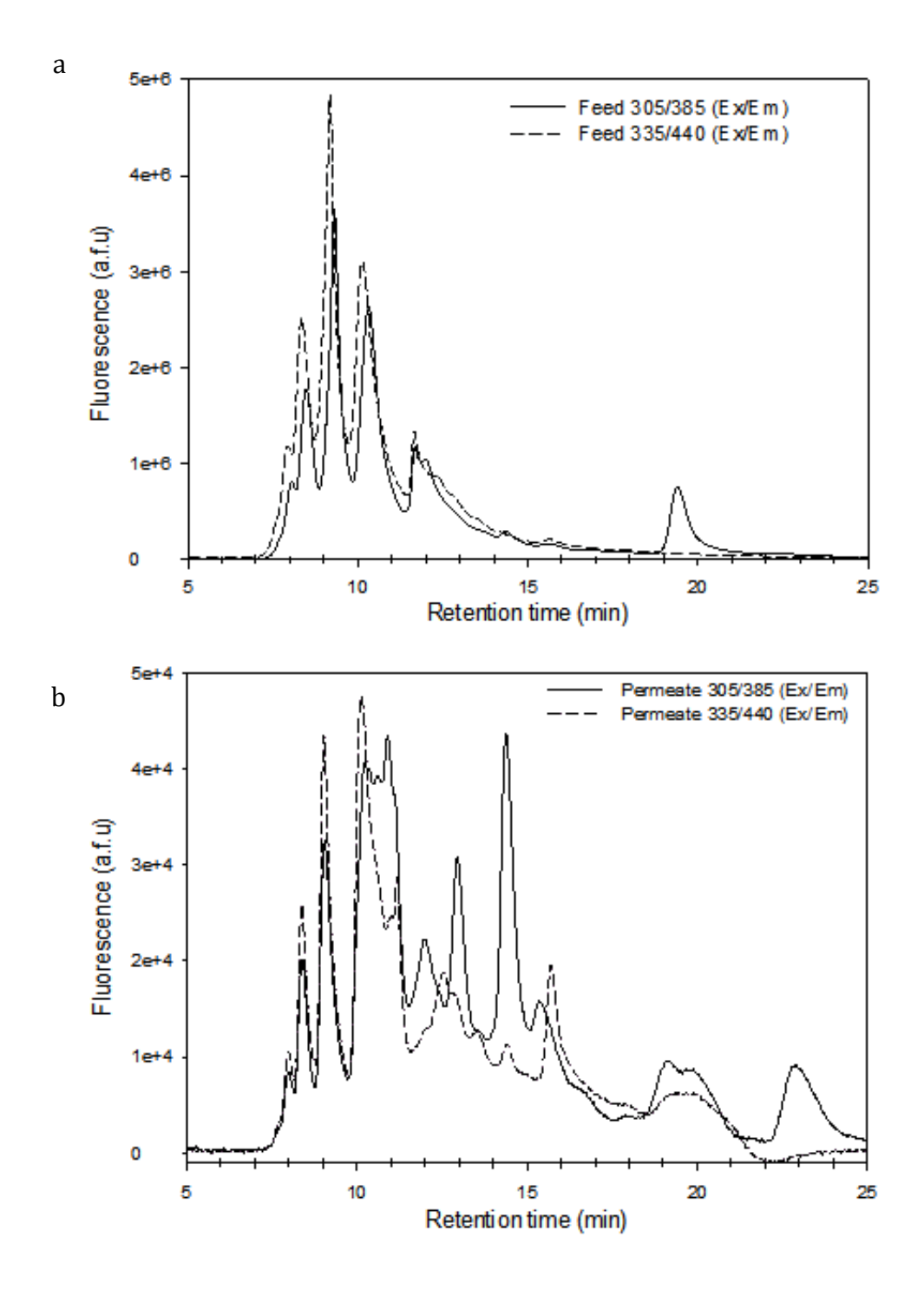
$$Q_s = (C_f - C_p) \times K_s \times \frac{S}{d}$$
(3.1)

Where (C_f - C_p) (mg·L⁻¹), K_s (m·s⁻¹), S (m²) and d (m) are feed and permeate salt concentration differential across the membrane, the membrane permeability coefficient for salt, the membrane area and the membrane thickness, respectively. Charge repulsion is dependant of the Donnan potential. Thus, cations are attracted on the negatively charged membrane and anions are repelled towards the bulk of the solution. However, a solution containing a high concentration of cations decreases the repulsive force of the membrane on the anions. This effect can increase the salt passage through a membrane (Peeters et al., 1998; Bartels et al., 2005). Also, during operation the concentration of salt at the membrane surface (CP effect) may increase causing reduction of water flow rate and increase of salt passage. In RO, pressure and feed conductivity increase through the process resulting in the increase of the osmotic pressure, which favours CP and scaling phenomena. However, other aspects can cause a change in salt rejection such as an adjustment in transmembrane flow among the stages (e.g. a higher transmembrane flow in stage 1 than in stage 2 and 3) or membrane damage occurred during operation.



<u>Figure 3.3:</u> Percentage of salt rejection using conductivity and percentage of organic rejection using the FRI method for two RO trains (3 stages) during a single sampling event. Examples of (a) a drop of salt rejection in a train without major leaks and (b) a drop of both salt and organic rejections in a train with a broken interconnector in stage 3. PV 1.X: pressure vessel X pertaining to stage 1; PV2.X pressure vessel X pertaining to stage 2 and PV3.X: pressure vessel X pertaining to stage 3.

The principal removal mechanisms for DOM are size exclusion, charge repulsion and adsorption which are further influenced by other molecular properties such as hydrophobicity and are therefore predicted to be consistently high as long as the integrity of the membrane process is high. For example, a statistically significant reduction of organic rejection may indicate a defective membrane or seal. Charge repulsion as well as changes in pressure and feed concentration may also have an effect on the DOM removal mechanism as described previously with the salt removal mechanisms. However, according to the results, the difference of pressure and concentration across the system did not affect the organics rejection. In the case of the RO train sampled in Figure 3.3 b, an interconnector was broken in this PV causing then a leak of feed water to permeate. As shown in Figure 3.3 and Table 3.3, the RO salt rejection is more variable than organic rejection. Thus, measuring organic rejection via fluorescence is more suitable than salt rejection to detect leaks during regular checks of plants, initial commissioning or after any manipulation of PVs. Moreover, fluorescence spectrometry allows selective measurement of organics that have particularly high rejections as will be demonstrated in the following section. The determination of rejection of fluorescent DOM can therefore be regarded as a more suitable membrane integrity indicator measurement for virus rejection compared to conductivity, because of its higher LRV approximating itself closer to the rejection behaviour of viruses. Due to virus properties such as size and surface charge, their rejection should be closer to organics rejection than salt rejection.



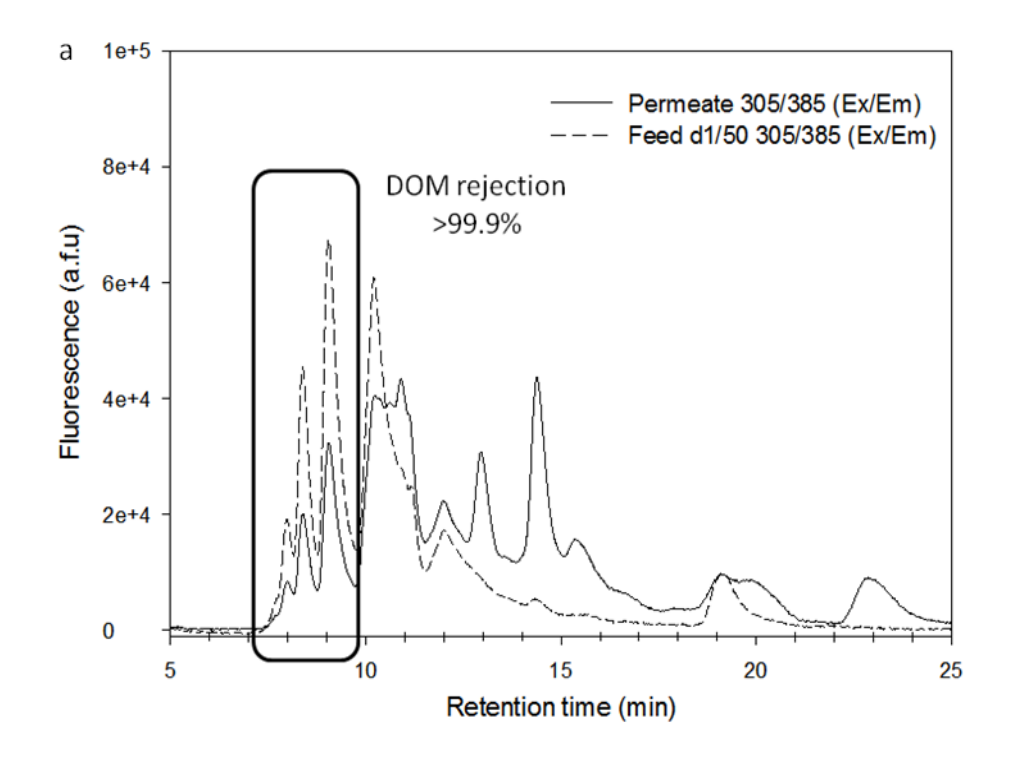
<u>Figure 3.4:</u> SEC chromatograms of (a) RO feed, and (b) RO permeate from stage 3 train 2 plant A. Note: the ordinate scale in arbitrary fluorescence units differs by a factor of 100 between (a) and (b).

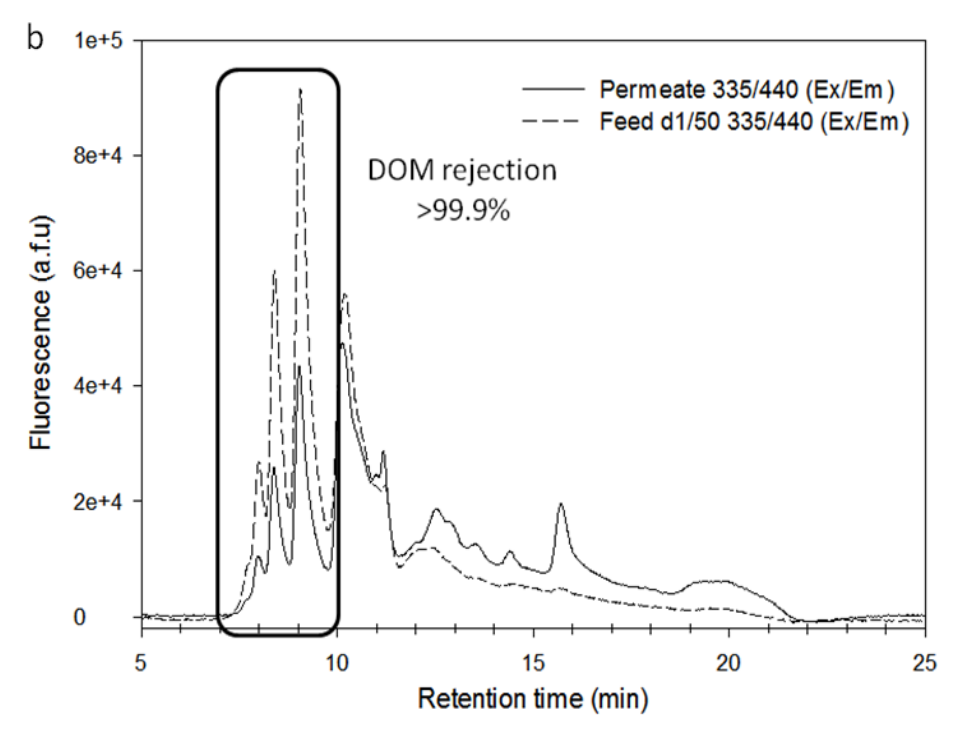
3.3. Understanding the blue-shift of the fluorescence of humic substances from feed to permeate

As described previously in this study, a comparison between feed and permeate EEM spectra demonstrated a shift of the maximum peak of the humic-like substances to lower wavelengths (from region II: λ_{ex} / λ_{em} 320 - 350 / 405 - 440 nm to region I: λ_{ex} / λ_{em} 300 - 325 / 375 -405 nm) from feed to permeate. To better understand the origin of this shift, samples were analysed by SEC with fluorescence detection by selecting two wavelength couples corresponding to EEM region I and II. The chromatograms of feed and permeate from stage 3 train 2 plant A were compared in Figure 3.4. The results indicate that this blue-shift is correlated to a change in size distribution between feed and permeate. Indeed, according to the permeate chromatogram the DOM concentration at low MW is higher than the one at high MW. The presence of high MW DOM in permeate can be explained by the presence of defects in an industrial sized RO plant (e.g. leaking seal as described previously) and also by the fact that the size of the cavity is not uniform. Previously, researchers have shown that cavity size of PA membranes follows log-normal distributions rather than having a uniform cavity size that would result in an absolute MWCO (Van Der Bruggen et al., 2000). However, the permeate samples from stage 1 and stage 2 were difficult to analyse with our analytical set-up due to their low DOM concentration.

Using SEC with fluorescence detector, we could verify that RO membrane removes more efficiently high MW substances than low MW substances. This conclusion is in accordance with a previous study using SEC with organic carbon detector (OCD) (Henderson et al., 2010). This showed that although MWCO's of RO membranes are typically reported as below 100 Da, a MW selective behaviour of RO membranes can be observed also for organics of much higher MW. The three first SEC peaks at a retention time from around 7 to 10 min correspond to an apparent MW around 5000 Da according to our calibration curve built from different MW polystyrene polymers (Sigma Aldrich, Australia) analysed with the UV detector at 254 nm (calibration not shown). Viruses have generally a molecular weight 1000 times or more than the DOM corresponding to these peaks (Golmohammadi et al., 1993). Thus, determining the DOM removal by SEC and especially from the peaks of the chromatograms associated to high MW can be proposed as another methodology to monitor membrane integrity. By this method, DOM rejections above 99.9% were determined for the first peaks (Figure 3.5), which is higher than those calculated by the FRI method (around

99.4% for region II for the same sampling). However, as mentioned above, the determination of DOM rejection in the two first stages can be challenging due to their weak concentration. We encourage further work on either concentrating permeate samples (e.g. by freeze drying) or improving the LOQ of the SEC method to enable quantification of DOM rejection for a wider range of samples.





<u>Figure 3.5:</u> DOM rejection calculated from SEC chromatograms of RO feed diluted 50 times and undiluted RO permeate for (a) 305 / 385 nm and (b) 335 / 440 nm ($\lambda_{excitation}$ / $\lambda_{emission}$) from stage 3 train 2 plant A.

3.4. Conclusions and implications for practice

In this study, the feasibility of coupling fluorescence EEM with FRI technique to calculate DOM rejection across a membrane during RO filtration has been proven. We identified an area of excitation and emission wavelengths where DOM rejection was highest (λ_{ex} / λ_{em} 320 - 350 / 405 - 440 nm) and consistently around 99.5% throughout all stages of the membrane treatment.

In addition, in combination with conductivity measurements, the utilisation of fluorescence measurements allowed a sensitive determination of the presence of potential defects in individual PV. In fact, with the underlying hypothesis that all PVs within the same stage in an RO train should, in theory, reject DOM to the same degree, a variation of organic rejection can help identifying leaks more sensitively than conductivity profiling alone.

Moreover, the results showed that the observed blue-shift between the fluorescence maxima of the region II in feed and region I in permeate was caused by increased rejection of organic substances of higher MW. In SEC chromatograms obtained by analysing feed and permeate stage 3 of a RO process, we measured DOM rejection in excess of 99.9% for three of the main peaks with the highest MW. Thus, analysis by SEC would verify a 3 log (99.9%) DOM rejection.

DOM rejection may also be used to determine in a conservative manner the maximum achievable log removal for pathogens in a RO process. DOM might be a good novel alternative indicator to prove the efficiency of RO membranes for pathogen removal in order to satisfy the current legislation in place to protect public health. However, further research is warranted to confirm a congruent behaviour of DOM and pathogen during the RO filtration process and, particularly, the suitability of DOM as a membrane integrity indicator for virus rejection.

4. Effect of membrane impairments: Organic fouling & Scaling

4.1 Or	ganic fouling	88
4.1.1.	Membrane characteristics	88
4.1.2.	Membrane autopsy	89
4.1.3.	Rejection of virus surrogate and membrane integrity indicators	93
4.2. Sca	aling	97
4.2.1.	Membrane characteristics	97
4.2.2.	Membrane autopsy	98
4.2.3.	Rejection of virus surrogate and membrane integrity indicators	100
4.3. Co	nclusions	102

Fouling is one of the major membrane failures in RO process. Its presence can have an impact on membrane integrity. In the present chapter, the removal of one virus surrogate (MS2 phage) and four indicators (R-WT, salt, sulphate and DOM) were analysed to monitor the integrity of RO membrane fouled by organic and inorganic foulants. Feed and permeate waters from organically fouled and scaled impaired membranes were analysed by different analytical techniques to determine the rejection of the different compounds with the SS flatsheet and 2.5" module set-ups. The analytical methods and the two set-ups have been described previously in Chapter 2 Materials & methods.

The objectives of this work are (i) to assess the performance of organically fouled and scaled RO membranes to remove the different compounds; and (ii) to better understand the compound's removal mechanisms with fouled membrane.

4.1. Organic fouling

<u>Note:</u> the organic fouling layer was created using a mixture of three organic foulants in DI water: $5 \text{ mg C} \cdot \text{L}^{-1}$ humic acid, $0.25 \text{ mg C} \cdot \text{L}^{-1}$ bovine serum albumin (BSA, protein model foulant) and $0.25 \text{ mg C} \cdot \text{L}^{-1}$ sodium alginate (polysaccharide model foulant).

4.1.1. Membrane characteristics

Table 4.1 presents the performance of the two set-ups before and after organic fouling. The organic fouling layer has been generated as described in Chapter 2 Section 2.2.5.1. Initially, the performance of the membranes employed was statistically different (*p-value* < 0.05). The averages of the water permeability and the NaCl rejection of the 2.5" module were higher than those of the SS flat-sheet. This difference could be explained by the manipulation of the membrane and the difference between set-ups configuration. For the 2.5" module set-up, the membrane was protected by a hard cover made in resin which decreases the chance to damage it. In contrast, the membranes of the flat-sheet set-up were highly manipulated. Firstly, the membranes were cut from a 4" membrane module and stored in milli-Q water at 4°C. Then, they were cut in coupons at the RO cell dimension before the experiment. All these manipulations and storage could reduce the integrity of the membrane. Also, imperfections due to the non-homogeneity of the membrane material have more impact on the flat-sheet set-up than the 2.5" spiral-wound module set-up because of its smaller active surface area. Moreover, membrane configuration/geometry affects membrane performances

due to hydraulic differences. The membrane geometry and also the height size of the feed spacer were different between the two set-ups. Feed spacer impacts on mass transfer and thus, the concentration polarisation effect (Kaufman et al., 2012).

As expected, the organic foulant layer caused a decrease of the water permeability (*p-value* < 0.05) which is considered typical (Dow, 2010) and has been observed in different studies (Ang and Elimelech, 2007; Ang et al., 2011; Kim and Dempsey, 2013). The decreases of the water permeability after organic fouling were of 36% and 48% for SS flat-sheet and 2.5" module set-ups, respectively. It has to be noted that the NaCl rejection after creation of the organic fouling layer has not been determined in order to avoid the removal of the organic foulants from the membrane surface. Indeed, during preliminary tests, we observed that, after creation of the organic layer on the membrane the addition of a solution of NaCl 1.5 g·L⁻¹ into the feed tank resulted in the release of organic matter in the water after less than one hour. This release of organics might be explained by the change of osmotic pressure between pure water and salty water which could remove foulants that are not strongly attached to the membrane surface or to other foulants.

<u>Table 4.1:</u> Comparison of water permeability and NaCl rejection before and after organic fouling with the SS flat-sheet and the 2.5" module set-ups at an applied pressure of 7.5 bar and a cross-flow velocity of 10 cm·s⁻¹. Temperature normalised at 25°C.

	SS flat-sheet set-up		2.5" module set-up	
	Before	After	Before	After
Water permeability (L·h-1·m-2·bar-1)	6.7 ± 0.5	4.3 ± 0.1	10.0 ± 0.2	5.2 ± 0.2
NaCl rejection (%)	98.2 ± 0.2	N.A	98.6 ± 0.1	N.A

N.A: not applicable.

SS flat-sheet set-up: average of six membrane coupons.

2.5" module set-up: average of 15 values of one membrane module.

4.1.2. Membrane autopsy

Figure 4.1 shows digital photographs, SEM (scanning electron microscopy) and AFM (atomic force microscopy) images. The digital photographs were used to show the membranes colour and the possible presence of organic deposition on the membranes surface.

SEM and AFM techniques were used to show the surface membrane microscopically and to determine the surface roughness, respectively. Figure 4.2 presents the ATR-FTIR (attenuated total reflection-Fourier transform infrared) spectra of intact and organically fouled membranes from the SS flat-sheet and 2.5" module set-ups. ATR-FTIR was used to analyse the membrane surface chemistry.

Digital photograph:

It has to be noted that the scale of the digital photographs of the three membranes are different. Also, the bottom of the picture of the intact and 2.5" module set-up membranes represents the glue-line of the spiral-wound module which explains the colour difference. The organically fouled membrane photos show the presence of brown substances on the membrane surface which constitute the organic foulant layer. However, this layer is not homogeneous and the pattern of the feed spacer can be seen. Thus, it can be concluded that the feed spacer played a role on the accumulation of these foulants on the membrane surface.

SEM image:

The comparison between intact and organically fouled membranes by SEM images shows also heterogeneity on the surface of the impaired membranes. The SEM of the SS flat-sheet set-up shows a membrane area more fouled than the one from the 2.5" module set-up.

<u>AFM image:</u>

AFM images show a change on the surface roughness of the membrane by increasing the RMS (root-mean-square) index which is caused by the presence of the organic foulants layer. The standards deviation of the RMS value of the fouled membranes shows a high variability. The scale of AFM image is $30 \times 30 \mu m$. Thus, depending on the spot where the image was taken, the thickness of the organic layer was different to another spot.

ATR-FTIR spectroscopy:

ATR-FTIR spectroscopy provides important qualitative and/or quantitative chemical information on the active layers and can be sensitive from a few hundred nanometres depth to a few micrometres in the high (4000 - 2600 cm⁻¹) and low (< 2000 cm⁻¹) wavenumbers, respectively (Tang et al., 2009). Thus, this technique permitted to compare the chemical

changes between intact and organically fouled membranes. Four peaks are specific to the polyamide layer and their frequencies are 1444 cm⁻¹ (broad chemical groups), 1541 cm⁻¹ (amide II band), 1609 cm⁻¹ (aromatic amide band) and 1664 cm⁻¹ (amide I band). In our case, the foulants deposited on the surface of the membrane covered up the ATR-FTIR peaks characteristic of polyamide membrane which is in accordance with the literature (Xu et al., 2006; Xu et al., 2010; Zhao et al., 2010). BSA, humic acids and alginate are constituted of carboxyl groups (COOH) measurable by IR due to their high polarity. On the spectra of organically fouled membrane, two absorption bands appeared in the range of 1700 -1600 cm⁻¹ (amide I band) and 1350 - 1215 cm⁻¹ (amide III band). Amide I band is mainly associated with the C=O stretching vibration. Amide III band is more difficult to interpret as it is constituted of a mixture of coordination displacement, but this band might correspond to phenolic groups (Guan et al., 2006). Two studies analysed BSA by ATR-FTIR and showed the presence of peaks at 1700 - 1600 cm⁻¹ (Maruyama et al., 2001; Tantipolphan et al., 2007). Humic acid also presents two absorption bands at around 1700 - 1500 cm⁻¹ (amide I and II bands) and 1500 - 1300 cm⁻¹ (amide III band) which might correspond also to C=O and phenolic groups (Guan et al., 2006; Her et al., 2008). To conclude ATR-FTIR spectra proved the sorption of organics on the surface of the membrane by changing the surface chemistry. However, it was not possible to determine precisely the type of organic foulants on the membrane.

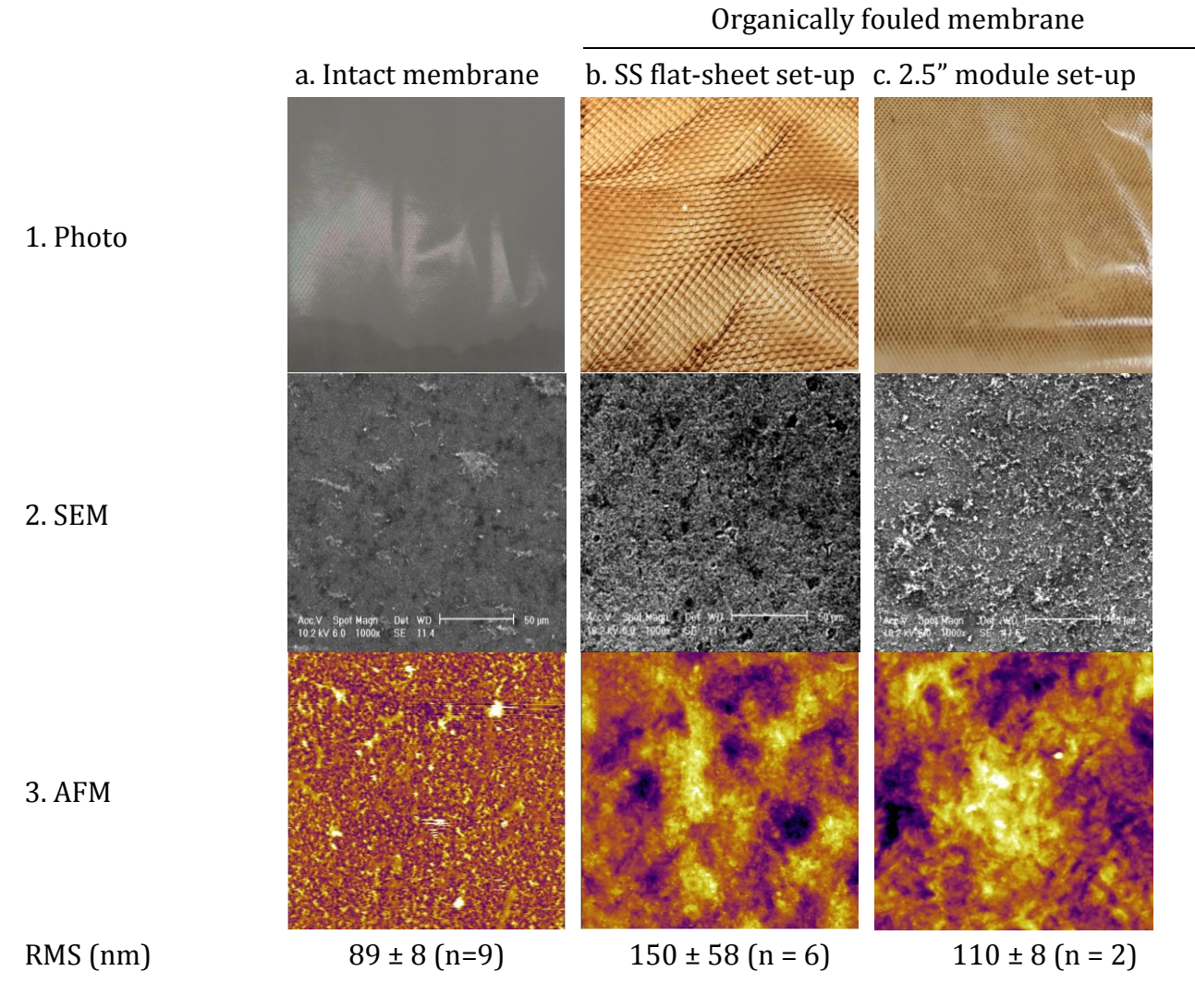
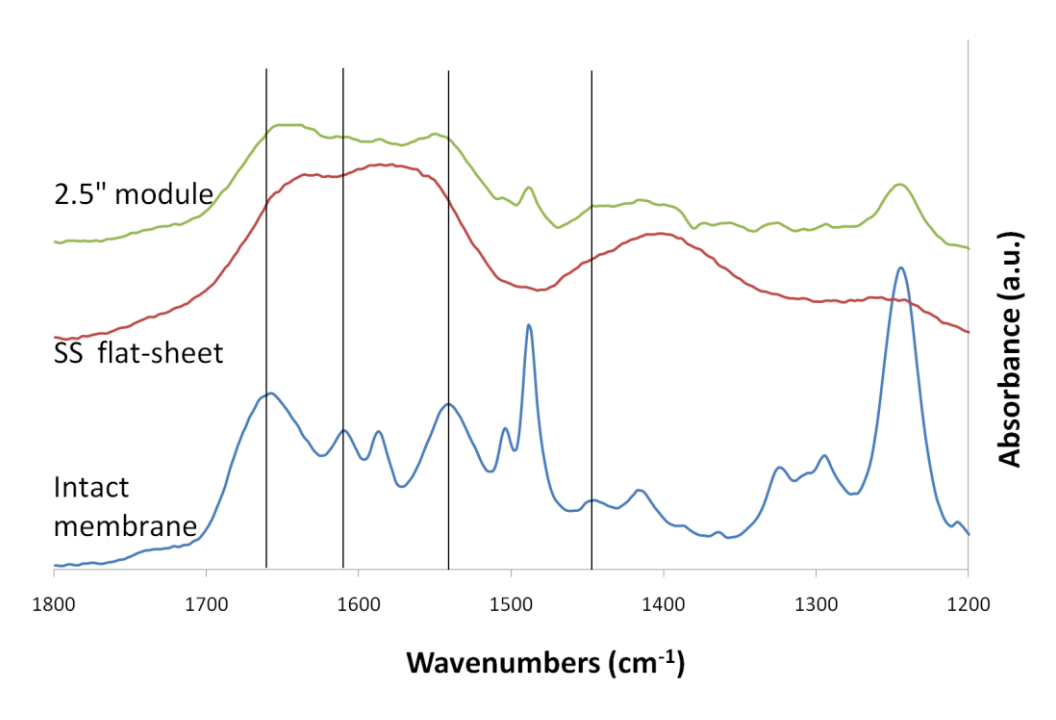


Figure 4.1: (1) Digital photographs, (2) SEM (bar scale = $50 \mu m$) and (3) AFM (30 x 30 μm , height scale bar: 300 nm) images of (a) intact and organically fouled membranes with (b) the SS flat-sheet set-up and (c) the 2.5" module set-up.



<u>Figure 4.2:</u> ATR-FTIR spectra of intact and organically fouled membranes with the SS flat-sheet set-up and the 2.5" module set-up. Vertical black lines = characteristic peaks of polyamide.

4.1.3. Rejection of virus surrogate and membrane integrity indicators

Figure 4.3 presents the LRV of the virus surrogate and the four indicators in the respective set-ups. Overall, the LRV increased statistically with the presence of organic fouling (Student's t-test, p-value < 0.05) on the surface of the membrane which is in accordance with the study of Lozier et al. (2003). However, the modification of the LRV could not be determined for MS2 phage and sulphate, due to the limit of quantification (LOQ) of the analytical techniques (i.e. qRT-PCR and ion chromatography, respectively).

From Figure 4.3, two groups of compounds can be defined: (i) particulate compound; and (ii) soluble compound. MS2 phage is a particle in contrast to the other ones who are soluble compounds. Due to its negative charge and its size (~ 25 nm), MS2 phage was well removed (LRV > 5.5) by the membrane filtration following size exclusion and charge repulsion mechanisms.

R-WT is a soluble fluorescent dye having a pKa value of 5.1 (Shiau et al., 1993). R-WT is negatively charged at water pH (pH_{water} > pKa_{R-WT}) which causes electrostatic repulsion between the molecule and the membrane. R-WT is highly water soluble with an octanol-

water partition coefficient (K_{ow}) close to zero. However, Vasudevan *et al.* (2001) showed that R-WT, especially the *meta*-isomer, was able to adsorb on humic acid-coated sand. The presence of organic fouling on RO membrane increased the R-WT rejection by more than 0.9 LRV with the SS flat-sheet set-up. With the 2.5" module set-up, the concentration of the permeate samples was below the LOQ of the fluorescence technique. Then, the LRV of the R-WT before and after organic fouling could not be determined with this set-up. The minimum LRV calculated from the LOQ of the technique was determined and showed in Figure 4.4.b (minimum LRV = 3.6).

EC measures all negative and positive charge, mono- and poly-valent ions in aqueous solution. Thus, positive and negative mono-valent ions go through the membrane which determines the LRV measured by this technique. The presence of organic fouling on RO membrane increased the salt rejection by more than 0.1 LRV.

Due to the detection limit of the ion chromatography technique, the maximum LRV of sulphate, that could be determined, was 2.5. In a previous plant study (internal data, not published), the average LRV of sulphate was of 2.6. Sulphate had a rejection close to R-WT even if its MW is five times smaller. The double negative charges of the sulphate ions probably allowed creating a strong charge repulsion force between sulphate ions and the organic fouled membrane.

DOM is a mix of solutes having different properties such as pKa, MW and size. Thus, an organic solute with a low MW and a pKa close to the water pH decreases the DOM removal. Regarding the DOM rejection of the different regions (region I to III noted DOM I, DOM II and DOM III), their rejection increased by more than 0.1 LRV. The cocktail of organic foulant had a similar EEM map than the pre-filtered secondary effluent. However, these foulants did not impact on the EEM map of the feed samples because the average of the three DOM regions was similar before and after fouling.

Several studies measured the zeta potential of organic foulants (NRMMC et al., 2006; Kim and Dempsey, 2013), and of the intact and organically fouled ESPA2 RO membranes (Fujioka et al., 2013) (Table 4.2). Intact membranes have a lower zeta potential value than organic foulants. Thus, the organic fouling layer decreases the negativity of the membrane surface by increasing the zeta potential value as reported in Table 4.2; and thereby decreases the charge repulsion effect between the fouled membrane and the negatively charged

compounds. The mechanisms of the development of organic fouling on low and high pressure membranes were studied by several researchers (Lee et al., 2006; Xu et al., 2006; Li et al., 2007; Mo et al., 2008; Contreras et al., 2009; Xu et al., 2010; Ang et al., 2011; Wang and Tang, 2011; Huang et al., 2012; Kim and Dempsey, 2013). It has been well defined that alginate binds with calcium ions (Ca²⁺) to create a gel which clogs the polyamide membrane cavities (van den Brink et al., 2009). Moreover, humic acids and BSA might adhere to the membrane cavities and surface causing pore constriction as determined by Huang *et al.* (2012). All of these cavity constrictions increase the removal of virus surrogate and indicators by size exclusion. R-WT is the indicator where the organic fouling had the biggest impact (more than 0.9 LRV). Due to the change of membrane surface by the presence of organic matter on the membrane, R-WT sorption might increase. Salt rejection increased (+ 0.1 LRV) with organic fouled membrane which is not in accordance with the DOW manual guidance (Dow, 2010). This increase might be due to the high concentration of foulants on the membrane which blocked the salt diffusion through the membrane.

<u>Table 4.2:</u> Zeta potential values of organic foulant solutions, intact and fouled ESPA2 RO membranes at pH 7.

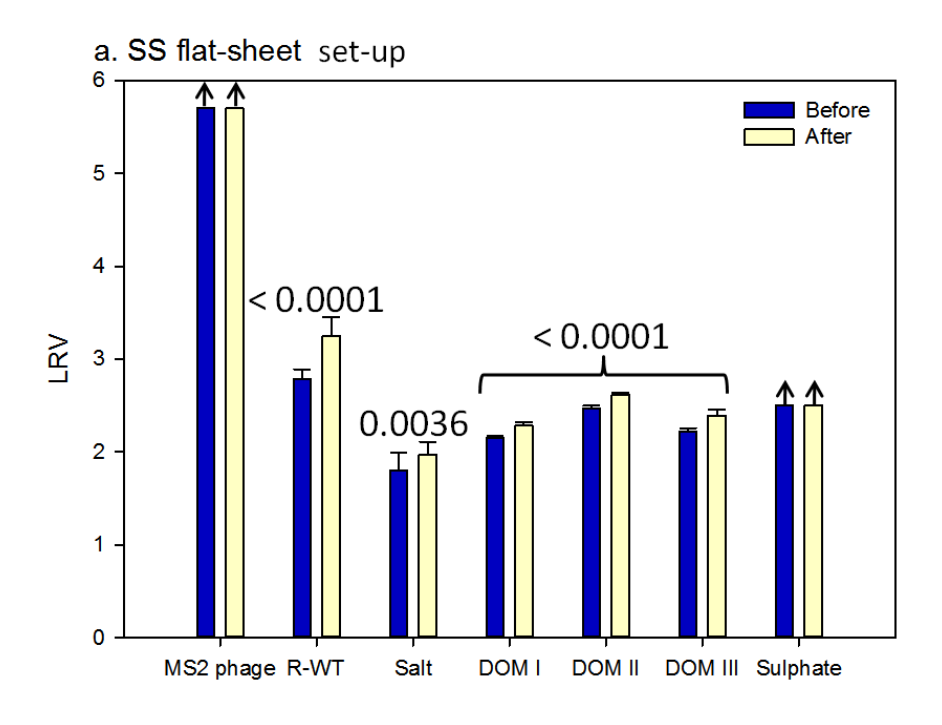
	Zeta potential (mV)			- nI	
	None	Ca ²⁺ 0.8 mM	KCl 1 mM	pl	
Alginate	- 20.9 ¹	- 13.8 ¹		~ 3.5 ²	
Humic acid	- 49.2 ¹	- 23.11		N/A	
BSA			- 12.9 ²	4.72	
Intact ESPA2			- 35.5		
ESPA2 fouled with BSA			- 10.9 ³		
ESPA2 fouled with Humic acid			- 29.1 ³		
ESPA2 fouled with 3ary effluent			- 11.4 ³		

N/A: not available.

¹ from (Kim and Dempsey, 2013).

² from (NRMMC et al., 2006).

³ from (Fujioka et al., 2013).



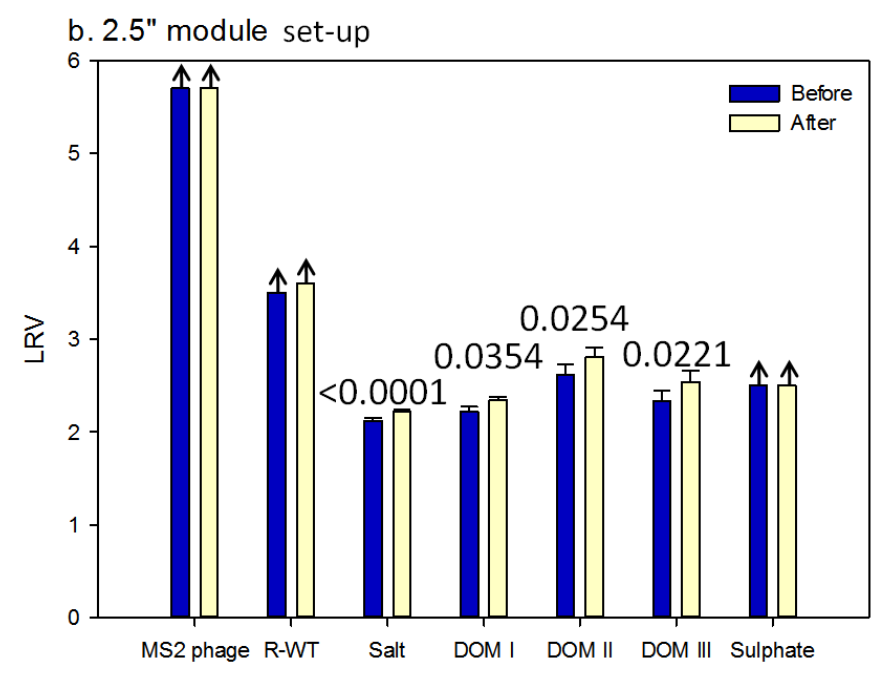


Figure 4.3: Comparison between MS2 phage, salt (EC), R-WT, DOM and sulphate rejections by intact and organically fouled membranes using (a) the SS flat-sheet and (b) the 2.5" module set-ups. Error bars = standard deviation, n = 9 (3 measurements/coupon, 3 membrane coupons) for SS flat-sheet set-up and n = 6 (1 membrane module) for the 2.5" module set-up. Black arrow (\rightarrow) = value determined limited by the LOQ of the analytical technique, i.e. permeate concentration below LOQ. Value above bar = t-test p-value.

To sum up, size exclusion was the principal mechanism to remove the different compounds. Indeed, even if the membrane surface was more positive, i.e. reduce the charge repulsion mechanism, the LRV of the different compounds increased to compare to the intact membrane.

4.2. Scaling

<u>Note:</u> the scaling layer was created from synthetic RO feed solution (mix of salt reconstituting natural RO feed without organic matter) without recirculating the permeate line.

4.2.1. Membrane characteristics

Table 4.3 presents the characteristics of each set-up before and after scaling impairment operating at a constant pressure of 7.5 bar and a cross-flow velocity of 10 cm·s⁻¹. The initial characteristics (before scaling) of the two set-ups were statistically different (p-value < 0.05). The 2.5" intact membrane module showed better salt rejection than the SS flat-sheet set-up (+1.1%). It has to be noted that the pure water permeability after scaling has not been determined in order to avoid the dissolution of the inorganic layer on the membrane surface. However, the water permeability between same feed compositions can be compared. In Table 4.3, the 1.5 g·L⁻¹ NaCl feed water permeability has been reported. As expected, the inorganic layer created a decrease of the water permeability (p-value < 0.05) which is due to the presence of an inorganic layer on the surface membrane (Antony et al., 2011). The salt rejection stayed stable with the SS flat-sheet set-up whereas the salt rejection decreased with the 2.5" module set-up. This variation might be explained by the difference between the two set-ups configuration. As presented in the previous part concerning organic fouling, the mass transfer of the two set-ups was different due to a difference in set-ups configuration and feed spacer height. Also, the permeate recovery has an impact on the scaling formation (Antony et al., 2011). High recovery increases the concentration polarization due to the solute concentration at the surface membrane. The recovery of the SS flat-sheet set-up was of 2% whereas the one of the 2.5" module set-up was of 10%. Thus, the 2.5" module set-up would be subject to scale more than the SS flat-sheet set-up. The reduction of the water permeability was more severe with the 2.5" module set-up than with the SS flat-sheet set-up. According to Hoek et al. (2003), the decrease of the water permeability is proportional to the decrease of

the salt rejection, and the presence of inorganic crystallizations on the membrane surface decrease the salt rejection by cake-enhanced concentration polarization.

<u>Table 4.3:</u> Comparison of water permeability and salt rejection before and after scaling at an applied pressure of 7.5 bar and a cross-flow velocity of 10 cm·s⁻¹. Temperature normalised at 25°C.

	-				
	SS cross-flow set-up		2.5" module set-up		
	Before	After	Before	After	
Water permeability (L·h-1·m-2·bar-1)	6.8 ± 0.2	N.A	9.4 ± 0.6	N.A	
Water permeability (L·h-1·m-2·bar-1) from NaCl feed solution	5.9 ± 0.3	4.9 ± 0.2	6.7 ± 0.3	1.9± 0.1	
NaCl rejection (%)	98.1 ± 0.4	98.4 ± 0.3	99.2 ± 0.1	97.1 ± 0.1	

N.A: not applicable.

SS flat-sheet set-up: average of six membrane coupons.

2.5" module set-up: average of six values of one membrane module.

4.2.2. Membrane autopsy

The comparison of SEM micrograph of intact and scaled membranes used in both set-ups shows heterogeneity on the surface of the impaired membranes (Figure 4.4). The EDS analysis detected the presence of carbon (81% for intact and 63% for scaled membrane), oxygen (around 10% for intact membrane, 15.5% and 11% for scaled membrane with SS flat-sheet and 2.5" module set-ups, respectively), calcium (around 0.1% for intact membrane, 3.5% and 10% for scaled membrane with SS flat-sheet and 2.5" module set-ups, respectively) and phosphate (around 0.3% for intact membrane, 2% and 5% for scaled membrane with the SS flat-sheet and the 2.5" module set-ups, respectively). Due to the presence of these elements, the formation of calcium carbonate (CaCO₃) and calcium phosphate (CaPO₄) scaling on the membrane surface can be concluded. After the experiments, the membranes were generally quickly washed with DI water in order to remove the virus surrogate and the indicators. This wash might remove some of the inorganic layer compounds as DI water is an excellent remover of inorganic scale which could explain the low intensity of the different ions. Also, after the pre-filtered secondary effluent experiment, the 2.5" module set-up was stopped to remove all the feed water in order to switch with the RO synthetic feed water to

analyse the rejection of MS2 phage, R-WT and salt. The re-start of the set-up could remove some scaling due to the change of the flow and the pressure.

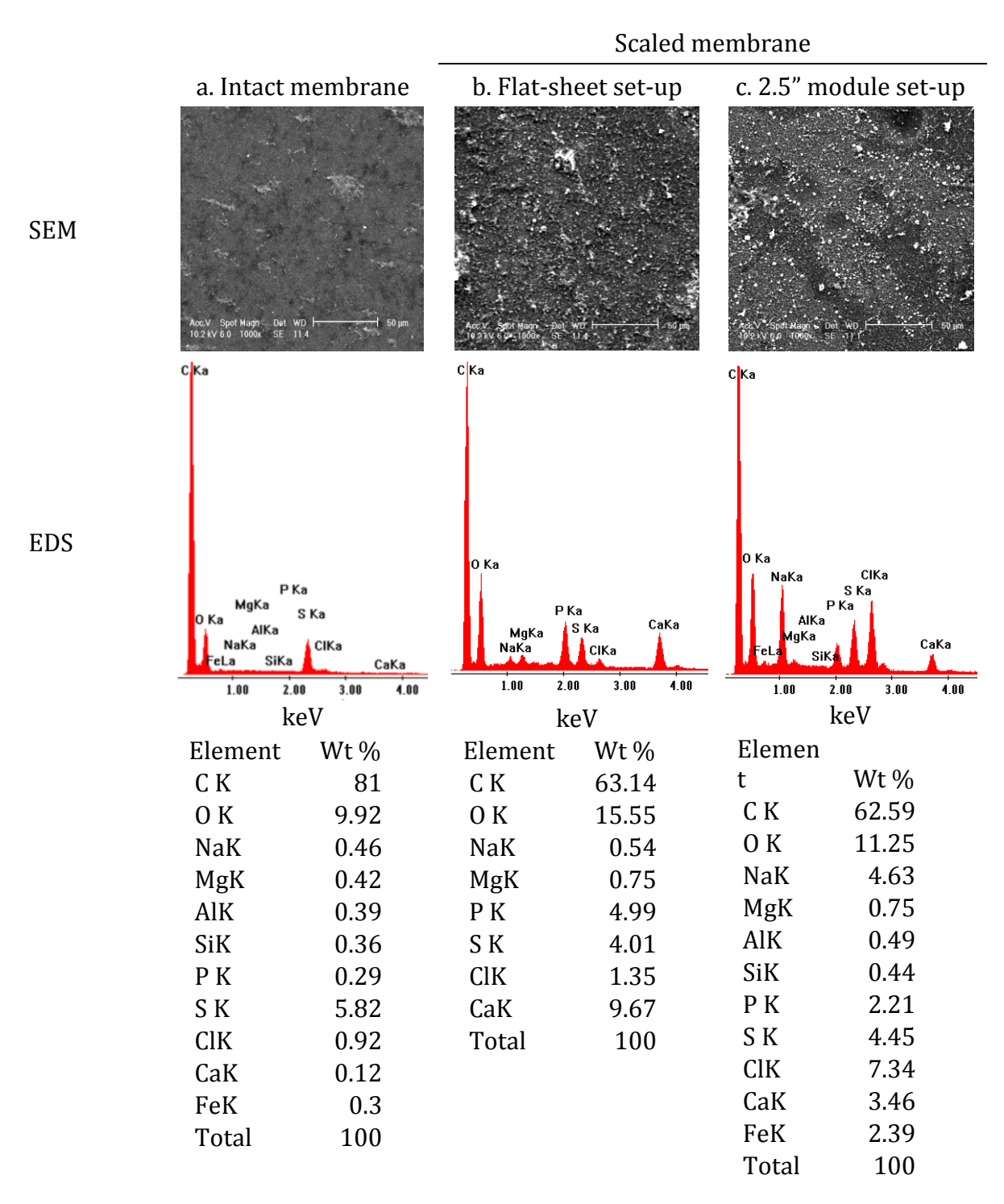


Figure 4.4: SEM images (bar scale = $50 \mu m$) and EDS results of (a) intact and scaled membranes with (b) the SS flat-sheet and (c) the 2.5" module set-ups.

4.2.3. Rejection of virus surrogate and membrane integrity indicators

Figure 4.5 shows the LRV of the virus surrogate and the four indicators analysed in this study. For both systems, the presence of inorganic ions on the membrane surface did not have an impact on the rejection of R-WT, DOM I and DOM II (Student's *t*-test, *p-value* > 0.05). Scaling had an impact on the rejection of salt and DOM III with the SS flat-sheet set-up whereas, no difference was observed with the 2.5" module set-up. However, due to the LOQ of the MS2 phage and sulphate analytical techniques, the effect of scaling on LRV could not be determined for them.

The salt rejection increased significantly with the SS flat-sheet set-up (Student's *t*-test, *p-value* < 0.05). This increase of salt rejection could be due to back diffusion phenomena. Salt could pass the porous inorganic layer but could be repulsed by the negatively charged polyamide membrane. The second explanation is the possible healing of the membrane by salt. At the initial state, intact membrane might have some tiny imperfections. By creating an inorganic layer on the membrane surface, these imperfections might be covered up and thus membrane would have a better rejection than initially. This observation is not in concordance with the one made during the membrane characteristics which showed a similar NaCl rejection with the two membrane states. The presence of other particles in the feed water might interact with the salt which could increase the salt rejection. It could explain why the salt rejection did not decrease with the 2.5" module set-up as observed with the NaCl rejection during the membrane characterisation. Moreover, no explanation has been found to justify the increase of DOM III with the SS set-up.

The decrease of salt rejection and the stability of the other compounds rejection from intact to scaled membrane are in accordance with the full-scale study presented in Chapter 3. Indeed during this study, it has been noted that the salt rejection decreased in the last stage of the RO train due to the possible presence of scaling. However, there was no impact on the DOM removal (Figure 3.4 a).

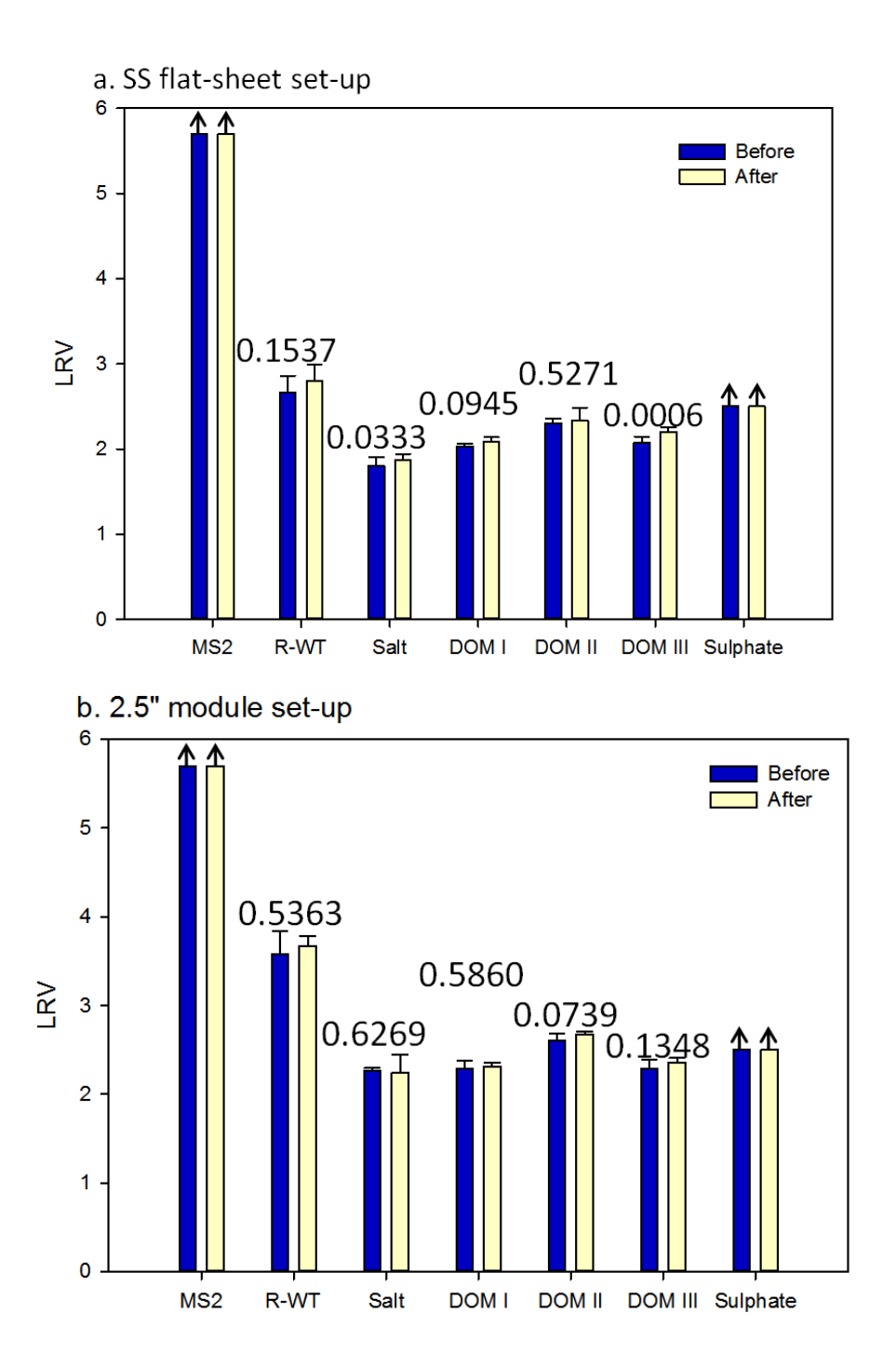


Figure 4.5: Comparison between the overall MS2 phage, conductivity, R-WT, DOM and sulphate rejections by intact and scaled membranes using (a) the SS cross-flow set-up and (b) the 2.5" module set-up. Error bars = standard deviation, n=9 (3 measurements/coupon, 3 membrane coupons) for SS flat-sheet set-up and n=6 (1 membrane module) for the 2.5" module set-up.

4.3. Conclusions

In this chapter, the impact of organically fouled and scaled membranes was studied.

It is generally assumed that organic fouling has a negative impact on the water treatment process causing a drop of the water permeability and an increase of the treatment cost. However, as shown in this study, organic fouling had also a positive impact by increasing the removal of the different compounds (minimum + 0.1 LRV). Indeed, the organic foulants created a cake layer on the membrane surface and blocked the membrane cavities which improved their removal by size exclusion even if this cake layer reduced the surface negativity. Thus, size exclusion mechanism played the main role on the removal of virus surrogate and indicators. Over time, the nature of organics can vary depending on the season and the initial wastewater influent. From the full-scale study presented in Chapter 3, it has been observed that the fluorescence EEM maps of the different RO feed water in the two AWTPs were similar over a sampling period of 18 months. Moreover, it has to be noted that for one AWTP (plant A), the secondary effluent originates from four different wastewater treatment plants at daily varying mixing ratios. Fluorescence EEM maps depend on the type of organics present in the sample, and thus by extrapolation depends on the type of wastewater process, water temperature and salt concentration. Before using this technique in a specific plant, it is recommended to do a fluorescence EEM analysis of the RO feed and permeate waters in order to select the most adequate regions of the samples.

Scaling had also a negative impact on the water treatment process causing a drop of the water permeability and a decrease of the NaCl rejection (only for 2.5" module set-up) and thus, an increase of the treatment cost. On the other hand, the presence of an inorganic layer on the membrane surface did not have any impact on the compounds removal except for the salt rejection. The presence of organic in the feed water might improve the rejection of salt.

To conclude, fouling had a negative impact on membrane process whereas it did not have a negative impact on the compounds studied except for salt removal. R-WT was the best indicator removed with intact and fouled membrane (LRV > 2.6). According to the high rejection of MS2 phage (> 5.5 LRV), R-WT might be an efficient indicator to monitor the integrity of RO membrane. However, this compound is not a good indicator to monitor the general integrity state of the RO process.

It has to be noted that the LRV parameter should not be the only parameter used to determine

the water quality. Indeed, even with a high process LRV, the concentration of compounds in the permeate water could be higher than the authorized concentration if the initial quality of the feed water is very poor. Thus, it is important to determine the concentration of the different compounds in the permeate water to protect public health.

5. Effect of membrane impairments:

Ageing

5.1.	Membrane characteristics.	106
5.2.	Membrane autopsy	109
5.3.	Rejection of virus surrogate and membrane integrity indicators	114
5.4.	Conclusions	118

In AWTP, chlorine as disinfectant is used to limit biofouling. Its long-term exposure can have an impact on the RO membrane integrity. In this chapter, the removal of the virus surrogate (MS2 phage) and the four indicators used in the previous chapter (R-WT, salt, DOM and sulphate) were analysed to monitor the integrity of RO membranes oxidised by chlorine. Feed and permeate waters from intact and aged membranes were analysed by different analytical techniques to determine the rejection of the virus surrogate and the different membrane integrity indicators with the SS flat-sheet, plastic flat-sheet and 2.5" module set-ups. The analytical methods and the three set-ups are described in detail in Chapter 2 Materials & methods. Accelerated ageing was performed using a solution of sodium hypochlorite at 560 mg·L⁻¹ (ppm), pH 7 for 16 h, targeting a total chlorine exposure of 9000 ppm·h. A chlorine exposure of 9000 ppm·h would correspond to 10 years of operation at a chlorine exposure concentration of 0.1 mg·L⁻¹ (Antony et al., 2010). The concentration of the total chlorine was determined from preliminary tests in order to determine changes of the salt and R-WT rejection by aged membranes with the SS flat-sheet set-up. The pH value was selected so that it matches the pH of RO feed water in South East Queensland AWTPs. Stainless-steel can be attacked by high chlorine applied during active ageing (filtration) whereas the materials used in the plastic flat-sheet set-up are chlorine resistant. Thus, this set-up allowed also comparing the impact of active and passive (soaking) ageing which was not possible with the two other set-ups (SS flat-sheet and 2.5" module set-ups), where only passive ageing can be monitored.

The objectives of this work are (i) to assess the performance of aged RO membranes to remove virus surrogate and indicators; and (ii) to better understand the virus surrogate removal mechanism with aged membrane.

5.1. Membrane characteristics

Table 5.1 presents the characteristics (water permeability and NaCl rejection) of the three filtration set-ups. The plastic set-up was operated at an applied pressure of 5 bar. The SS flat-sheet and the 2.5" module set-ups were operated at 7.5 bar. The concentrate flow of the three set-ups was selected in order to obtain a cross-flow velocity of 10 cm·s⁻¹ before and after ageing as described in Chapter 2 Materials & methods.

Before ageing, the performance of the membranes in the three chosen set-ups was different in terms of water permeability and salt rejection. The water permeability of the plastic set-up (3.6 L·h-1·m-2·bar-1) was approximately half of the one obtained from the SS flat-sheet set-up (6.2 L·h-1·m-2·bar-1). The water permeability of the 2.5" module set-up was the highest (8.7 L·h-1·m-2·bar-1). Following the measurement of water permeability with DI water, NaCl rejection was measured. The salt rejection of the two flat-sheet set-ups was similar (97.4 -97.8%) and around 1% lower than the salt rejection of the 2.5" module set-up (98.8%). As it has been explained in Chapter 4, the difference in water permeability and salt rejection between the three set-ups could be due to the set-up configuration such as the height of the feed spacer and the membrane manipulation. After ageing, the water permeability evolved in two steps. Firstly, the water permeability dropped significantly after ageing for all experimental systems by 89%, 74%, 66% and 83% for the plastic flat-sheet set-up active ageing, the plastic flat-sheet set-up passive ageing, the SS flat-sheet and the 2.5" module setups, respectively. Membrane oxidation by chlorine decreased also significantly (Student's ttest) the salt rejection for the plastic flat-sheet active ageing (5%, p-value = 0.0031), plastic flat-sheet passive ageing (9%, p-value = 0.0006), SS flat-sheet (4%, p-value = 5.188×10^{-9}) and 2.5" module set-ups $(0.6\%, p\text{-value} = 6.6988 \cdot 10^{-8})$, respectively. Then, during the recirculation of the feed water (from DI water to NaCl solution to RO feed synthetic or prefiltered secondary effluent), the water permeability increased and reached a steady-state higher than with the intact membrane as measured with compounds feed water or the NaCl solution ($K_{W,intact} < K_{W,aged}$). Figure 5.1 presents an example of the evolution of the water permeability during one experiment with the SS flat-sheet set-up. In this experiment, the NaCl rejection was measured after compound rejection. In the literature, the conclusions about the change of water permeability after ageing are controversial (Kwon and Leckie, 2006a; Antony et al., 2010; Dow, 2010; Do et al., 2012a; Do et al., 2012c; Donose et al., 2013). Shin et al. (2011) showed an increase of the water permeability after ageing (up to 25000 ppm·h, at pH 7 - 8) whereas Donose et al. (2013) concluded to a decrease or no change depending on the type of membrane (up to 6000 ppm·h, pH 7). Therefore, this phenomenon of water permeability reduction followed by an increase after ageing was also observed by Kwon et al. (2006b). From these observations, they proposed a mechanism of the chlorine attack on the polyamide layer. The first step of the initial water permeability drop was caused by the collapse or the compaction of the polyamide chains which blocked the water molecules due to high concentration of chlorine and low pH. Indeed, H-bonds of the polyamide layer appear to be broken by the chlorine attack which could be observed from ATR-FTIR (attenuated total reflection-Fourier transform infrared) analysis. Secondly, the

water permeability increased due to possible rearrangement of the flexible chlorinated polyamide layer.

<u>Table 5.1:</u> Comparison of water permeability (K_w ± standard deviation) and NaCl rejection (R_{salt} ± standard deviation) before and after ageing with the plastic flat-sheet (plastic) set-up at an applied pressure of 5 bar and a cross-flow velocity of 10 cm·s⁻¹; the SS flat-sheet (SS) and the 2.5" module (module) set-ups at an applied pressure of 7.5 bar and a cross-flow velocity of 10 cm·s⁻¹. Temperature normalised at 25°C.

		K _w (L·h-1·m-2·bar-1)		R _{salt} (%)	
Set-up	Mode	Before	After	Before	After
Plastic	Active	3.6 ± 0.6	0.4 ± 0.1	97.8 ± 0.8	92.5 ± 6.0
Plastic	Passive	3.7 ± 0.8	0.9 ± 0.1	97.8 ± 0.6	88.9 ± 2.3
SS	Passive	6.2 ± 0.5	2.1 ± 0.3	97.4 ± 0.4	93.4 ± 1.8
Module	Passive	8.7 ± 0.6	1.5 ± 0.1	98.8 ± 0.1	98.2 ± 0.1

Plastic flat-sheet set-up: average of eight membrane coupons.

SS flat-sheet set-up: average of four membrane coupons.

^{2.5&}quot; module set-up: average of six values of one membrane module.

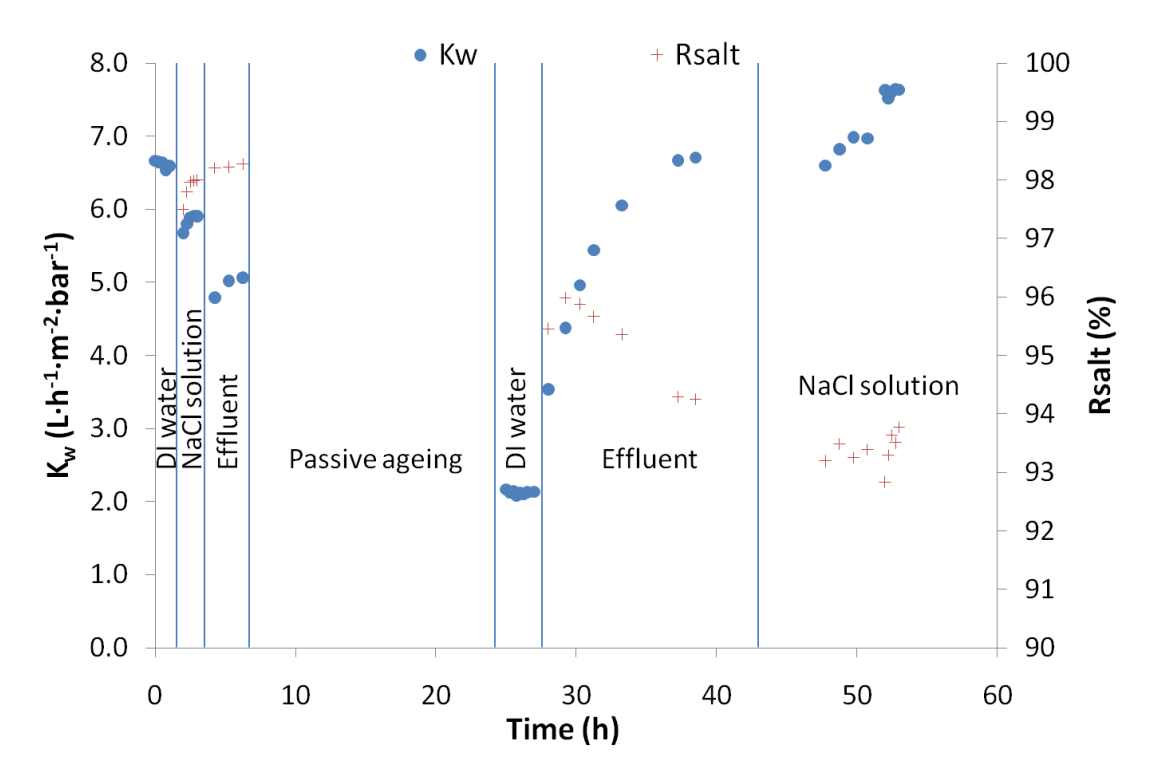


Figure 5.1: Evolution of water permeability (K_w , round) and salt rejection (R_{salt} , cross) with the SS cross-flow set-up (passive mode). System fed sequentially with DI water, NaCl solution (1500 mg·L⁻¹) and pre-filtered secondary effluent.

5.2. Membrane autopsy

Figures 5.2 and 5.3 show AFM (atomic force microscopy) micrographs and ATR-FTIR spectra of intact and aged membranes for the three set-ups. The two techniques were used to determine the surface roughness with AFM and the surface chemistry with ATR-FTIR. Table 5.2 presents the averaging RMS (root-mean-square) values from AFM images of the intact and aged membranes.

AFM:

Figure 5.2.a presents the AFM images of intact membrane used to filter RO synthetic feed (a.1. MS2 phage, R-WT and salt, RMS = 95, n = 1) and pre-filtered secondary effluent (a.2. DOM, sulphate and salt, RMS = 108, n = 1). The roughness of the different membranes was compared using the average of the RMS index calculated from AFM images (Table 5.2). From the image a.2, bacteria and other foulants were present on the surface of the membrane and caused an increase of the membrane roughness to compare to the not used intact

membrane (RMS = 89 ± 8 , n = 9). These bacteria and foulants were also present on the image of the SS flat-sheet set-up (RMS = 100 ± 31 , n = 3); ageing did not change the membranes roughness. Moreover, the high surface roughness variability between samples could be due to the structural non-uniformity of the entire membrane and the presence of foulants.

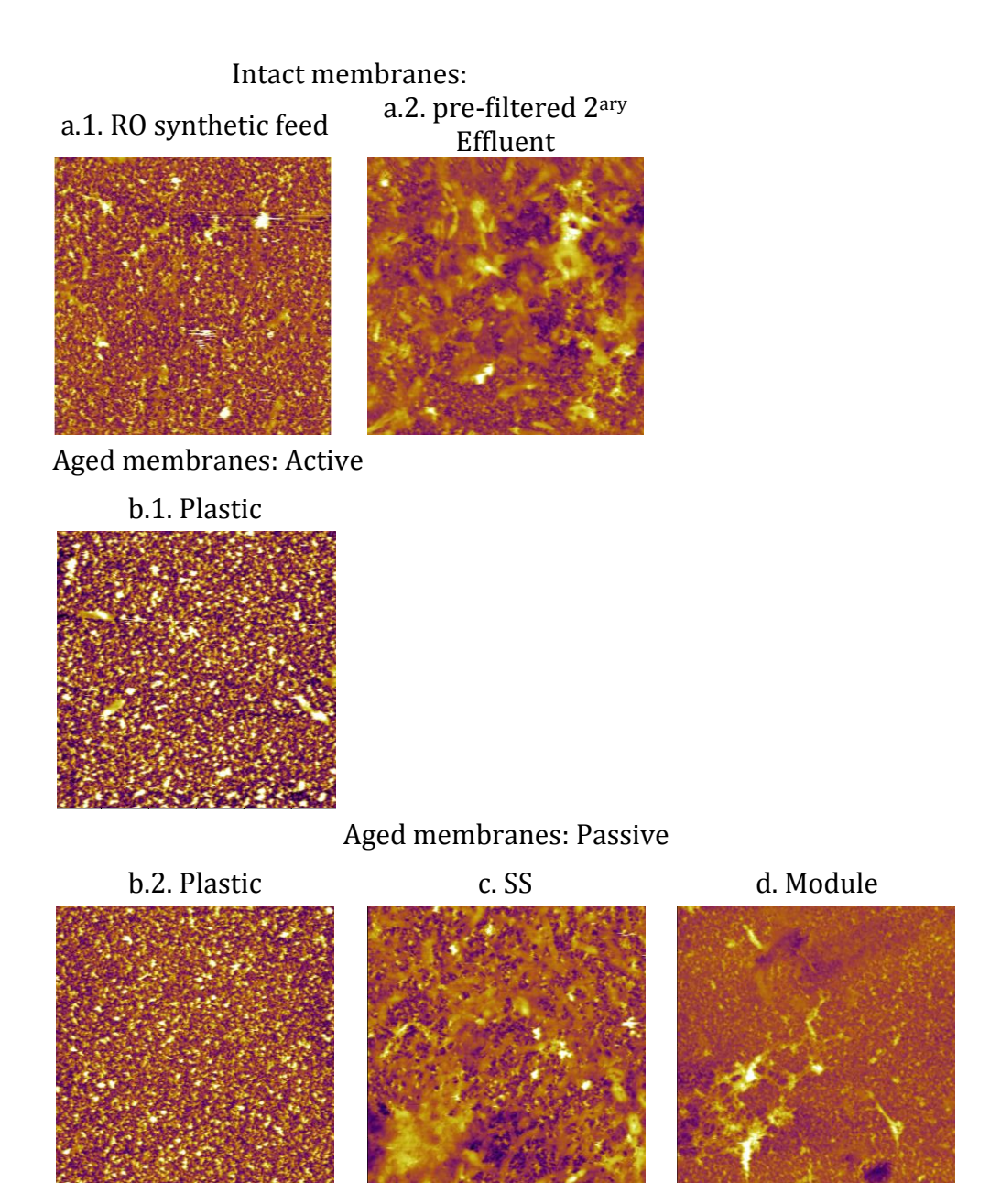


Figure 5.2: AFM images (30 x 30 μ m) of (a) intact membranes used to filtered (1) RO feed synthetic (MS2, R-WT and salt) and (2) pre-filtered secondary effluent (DOM, sulphate and salt), and aged membranes with (b) the plastic flat-sheet (1. active and 2. passive modes), (c) the SS flat-sheet and (d) the 2.5" module set-ups. Height scale bar: 300 nm for intact, 200 nm for active and passive ageing using the plastic flat-sheet set-up, and 400 nm for the SS flat-sheet and the 2.5" module set-ups.

<u>Table 5.2:</u> RMS (± standard deviation) as a function of the ageing conditions.

Membrane type	RMS
Intact membrane	89 ± 8 (n = 9)
Intact membrane used to filter RO synthetic feed	95 (n = 1)
Intact membrane used to filter pre-filtered secondary effluent	108 (n = 1)
Active ageing: Plastic flat-sheet set-up	115 ± 9 (n = 5)
Passive ageing: Plastic flat-sheet set-up	109 ± 19 (n = 13)
Passive ageing: SS flat-sheet set-up	$100 \pm 31 (n = 3)$
Passive ageing: 2.5" module set-up	108 (n = 1)

ATR-FTIR:

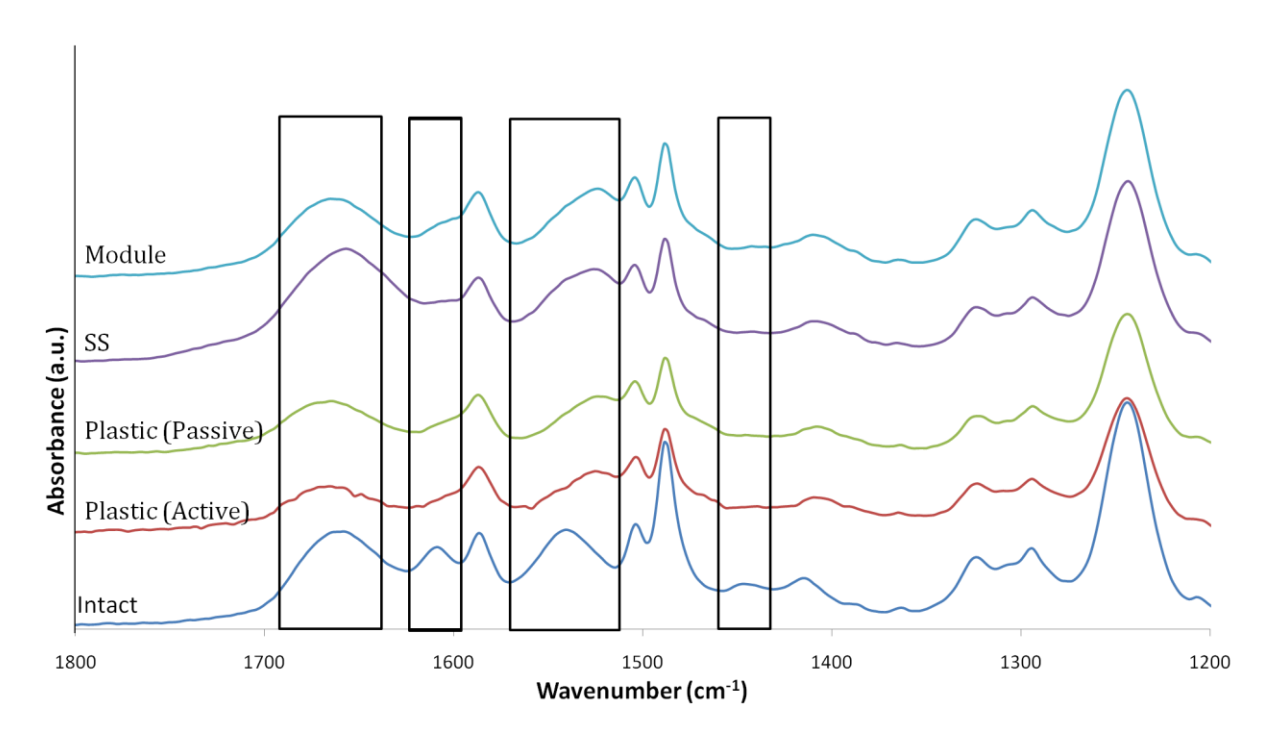
ATR-FTIR spectroscopy is a technique widely used to investigate the chemistry change of the polyamide RO membrane surface induced by chlorine (Kwon and Leckie, 2006a; Kang et al., 2007; Tang et al., 2007; Kwon et al., 2008; Antony et al., 2010; Kim et al., 2010; Cran et al., 2011; Ettori et al., 2011; Do et al., 2012a; Gu et al., 2012; Donose et al., 2013). ATR-FTIR scans the membrane surface from a few hundred nanometres depth to a few micrometres at different IR frequencies and measures their absorbance (Tang et al., 2009). The frequency band of vibration is specific to chemical groups representing the chemical composition of the polyamide and polysulfone layers. Table 5.3 summarises the principal peaks assignment specific to the polyamide layer.

<u>Table 5.3:</u> Principal peak assignment for FTIR of intact and aged polyamide RO membrane.

	Frequency (cm ⁻¹)		
Assignment	Intact membrane	Aged membrane	
Amide I band: C=O stretching, C-N stretching, C-C-N deformation vibration	~ 1660	Shift to higher frequency	
Aromatic amide groups: N-H deformation vibration, C=C ring stretching vibration	1609	Peak reduced	
Amide II band: N-H in-plane bending N-C stretching vibration	1541	Peak reduced	

Adapted from (Tang et al., 2009; Antony et al., 2010).

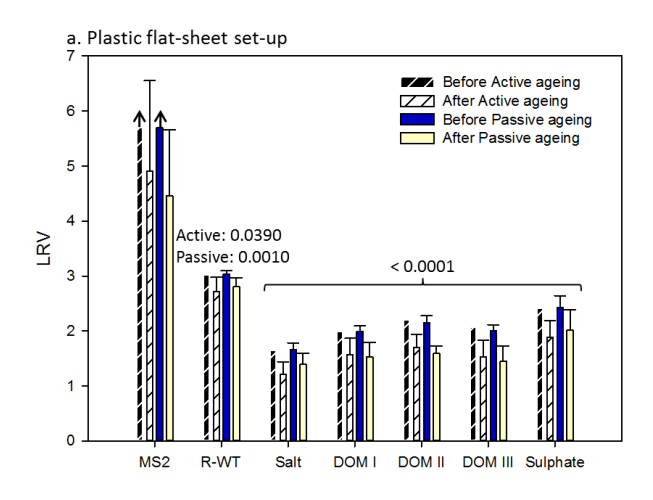
A decline of the absorbance peak at 1609 cm⁻¹ was observed and corresponded to chlorination of the aromatic ring and the resulting suppression of the C=C ring stretching vibration (Figure 5.3). In fact, one of the principal chemical changes on the polyamide layer during chlorine exposure is the aromatic ring chlorination by shifting the inter-molecular Hbonds to intra-molecular binding (Kwon and Leckie, 2006b; Kwon et al., 2008). Also, the observed destruction or the weakening of the H-bonds permitted the conversion of N-H to N-Cl groups which resulted in a reduction and a shift to lower frequencies of the 1541 cm⁻¹ peak. The reduction of the peaks at 1609 cm⁻¹ (aromatic amide groups) and 1541 cm⁻¹ (amide II band) are characteristic of chlorine attack. The peak at 1609 cm⁻¹ seemed to be more reduced with the active ageing mode than the passive mode. However, more analysis has to be done to confirm this statement. Antony et al. (2010) showed a difference between the two exposures type by a more pronounced change of the 1609 cm⁻¹ peak which might be caused by the feed applied pressure and the chlorine passage through the membrane. The peak at 1664 cm⁻¹ shifted to higher frequency might result from the breakage of the H-bonds between C=O and N-H groups (Kwon and Leckie, 2006b). A change of the peak at 1444 cm⁻¹ was also observed. This broad and weak peak corresponds to a combination of chemical bonds. Thus, its reduction or shift is very difficult to assess and more research (i.e. variation of pH and chlorine concentration, addition of analytical technique, etc.) has to be done in order to connect its change to a chemical modification of the polyamide membrane.



<u>Figure 5.3:</u> ATR-FTIR spectra of intact and aged membranes with the plastic flat-sheet (active and passive modes), the SS flat-sheet and the 2.5" module set-ups. Black boxes = peaks modified by the chlorine attack.

5.3. Rejection of virus surrogate and membrane integrity indicators

Figure 5.4 presents the LRV of the virus surrogate and the four indicators before and after ageing in the respective set-ups. Overall, Student's t-test performed at the 95% level (Student's t-test, p-value < 0.05) revealed a significant decrease of the LRV of the different compounds after chlorine ageing. However, due to the LOQ of the MS2 phage and the sulphate analytical techniques, dependent on the initial concentration of the compounds (feed water concentration), their LRV could not always be determined. However, a minimum LRV was calculated taking into account the LOQ of the technique used as the concentration of the permeate sample, i.e. 10^{-2} copies· μ L⁻¹ for qRT-PCR (MS2 phage) and 0.3 mg·L⁻¹ for the IC (sulphate).



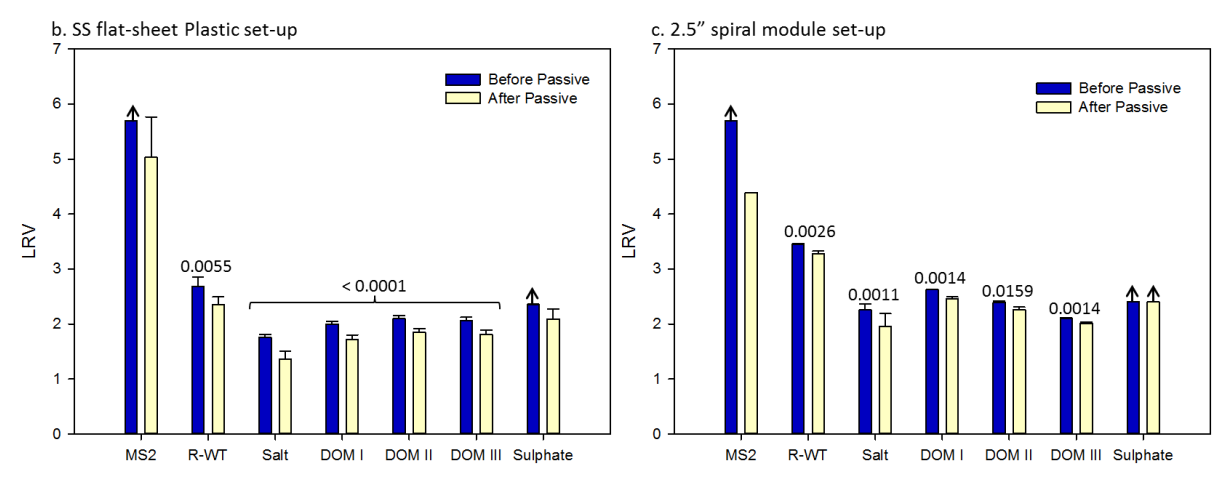


Figure 5.4: Comparison between MS2 phage, R-WT, salt (EC), DOM and sulphate rejections with intact and aged membranes using (a) the plastic flat-sheet, (b) the SS flat-sheet and (c) the 2.5" module set-ups. Error bars = standard deviation, n = 12 for the plastic flat-sheet set-up (3 measurements/coupon, 4 membrane coupons), n = 6 (3 measurements/coupon, 3 membrane coupons) for the SS flat-sheet set-up and n = 6 (1 membrane module; MS2 phage n = 1) for the 2.5" module set-up. Black arrow (\rightarrow) = LRV value determined limited by the LOQ of the analytical technique, i.e. permeate concentration below LOQ. Value above bars = t-test p-value.

After ageing, the rejection of MS2 phage decreased by more than 0.7 LRV depending on the set-up used, except for the SS flat-sheet set-up which could show only 0.3 LRV.

The decrease of all compounds removals were between 0.1 (DOM II and III with the 2.5" module set-up) to 0.6 (DOM II and III with the plastic flat-sheet set-up and passive mode) for all set-ups (except for the sulphate with the 2.5" module set-up which could not be measured)

as presented in Figure 5.4.

The 2.5" module set-up was the system where the membrane oxidation by chlorine had the least impact on compound rejection. There was no difference between active and passive ageing modes regarding the removal of virus surrogate and membrane integrity indicators. It would be expected that the active mode (filtration) would have more impacted the membrane characteristics (water permeability and salt rejection) and the contaminant removal than the passive mode as observed by Antony *et al.* (2010). Under pressurised system, the solution of chlorine is 'forced' to go through the membrane. Thus, the chlorine could attack the membrane deeper inside the polyamide layer. It might be possible that the concentration of the chlorine solution reach a maximum of induced damage into the membrane. The impact of chlorine attack seemed to have less impact on the 2.5" module set-up. This difference might be explained by the difference in the ageing protocol. Indeed, for the SS and plastic flat-sheet set-ups, the membrane coupons were entirely soaked in the solution. On the other hand, the solution of chlorine was passed along the 2.5" module set-up using a peristaltic pump (Figure 5.5). Thus, the ageing of the spiral-wound module might not be uniformed along the module.

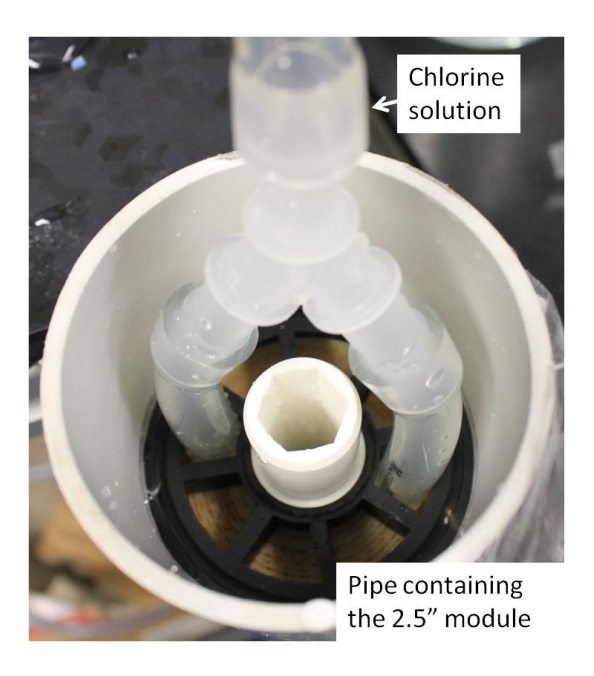


Figure 5.5: Picture of the 2.5" spiral-wound module ageing set-up.

Polyamide membrane has an isoelectric point of 3. Due to the dissociation of the functional groups within the intact membrane matrix, this type of membrane is negatively charged at

neutral pH. The equilibrium constant (pKa) of the acid/base couple [HOCl]/[OCl] of the ageing solution is equal to 7.5. Thus, at pH 7 (pH experimental), the hypochlorous acid HOCl is the predominant species. HOCl is more reactive and a stronger disinfectant than the basic hypochlorite species OCl⁻ (Deborde and von Gunten, 2008). HOCl passes the membrane due to its neutrality and small molecular size (low MW = 52.5 g·mol⁻¹); however the OCl⁻ species is partially rejected due to electrostatic charge repulsion between OCl⁻ and the membrane surface charge (Gu et al., 2012). During chlorination, N-Cl groups replaced N-H groups via electrophilic substitution which was confirmed by the suppression of the ATR-FTIR peak at 1609 cm⁻¹. The breakage of H-bonds between C=O and N-H formed additional carboxylic groups (COOH) by hydrolysis which at pH 7 increased the negative charge of the membrane (Do et al., 2012b). This mechanism was indicated by the shift to higher frequency of the ATR-FTIR peak at 1663 cm⁻¹. The polyamide membrane became more hydrophilic and the tertiary structure of the polyamide change due to the hydrolysis of C-N groups as it was demonstrated by measuring the contact angle in a previous study (Do et al., 2012a). The principal mechanism of virus surrogate rejection (MS2 phage: 25 nm, pI = 3.9) is size exclusion, and electrostatic repulsion helps to remove it in presence of membrane imperfections (Antony et al., 2012). Virus surrogate and membrane integrity indicators were less removed by the membrane due to a modification of the polyamide tertiary structure causing membrane swelling (increased of the size of the membrane cavities), even if the enhanced negative surface charge of the membrane was more important after ageing (Do et al., 2012a). The LRV of the virus surrogate by aged membrane was above four. The supporting layer under the polyamide layer has a MWCO of 15 kDa. Thus, this layer behaves like an UF membrane, which is able to remove virus (Jacangelo et al., 1995; Asano, 2007). However, the reliability of the results can be discussed. In fact, the rejection of MS2 phage decreased but the rejection of salt stayed around 1.5 LRV. On the hypothesis that the polyamide layer is destroyed by the chlorine attack, the salt should not be retained by the aged membrane as UF membrane does not remove salt. MS2 phage is highly unstable and can easily be adsorbed on the systems such as tubing and membrane. The decrease of virus surrogate rejection could be primarily due to a technical problem than a membrane integrity problem. Another hypothesis could be that if 0.01% of the feed flow goes through the membrane due to a swelling of the membrane, R-WT and salt will not be affected as their LRV are below three. However, this imperfection can set the MS2 phage removal to a maximum achievable LRV value of four.

5.4. Conclusions

To conclude, ageing had a negative impact on the water treatment process in general. Indeed, chlorine attack caused a drop of the water permeability by the blockage of the water molecules due to the breakage of H-bonds and the creation of Cl-bonds. However, after solution change (from DI water to NaCl solution to RO feed synthetic or pre-filtered secondary effluent), the water permeability increased due to the possible rearrangement of the flexible chlorinated polyamide layer. Ageing had also a negative impact on the rejection of MS2 phage, salt and other indicators. This is essentially due to chemical change inside the polyamide layer. Indeed, during ageing at pH 7, polyamide layer was hydrolysed causing a swelling of the membrane and permitted the compounds to pass the membrane more easily.

It would be expected that a decrease of membrane integrity over time, due to chlorine exposure for example, will slowly decrease the rejection of the different compounds. However, it has to be noted that the rejection of the different compounds would be different depending on the type of membrane impairment as MS2 phage and the four membrane integrity indicators have different properties such as surface charge and size. In contrast, a drop of the compounds' rejection would be more characteristic of the presence of leak(s) in the system.

At industrial scale, chlorine post-treatment is sometimes used to improve the RO membrane performance by increasing the water permeability and the salt rejection (Do et al., 2012b). However, the chlorine exposure is done at low chlorine concentration (lower than 2000 ppm·h) and at basic pH (9 - 10) not to destroy the polyamide membrane, by avoiding the passage of HOCl through the membrane which would break the H-bonds (Kwon and Leckie, 2006a, 2006b; Kang et al., 2007).

6. Statistical comparison of experimental set-ups & membrane impairments

6.1.	Correlation between the rejection of the different membrane integrity indicators .	.121
6.2.	Effect of membrane impairment and set-up	.123
6.3.	Comparison of the different lab-scale set-ups with the full-scale plant	.129
6.4.	Conclusions	.132

This chapter compares the previously discussed LRV results of R-WT, salt, DOM and sulphate measured with the different filtration systems and the different membrane impairments discussed in Chapters 4 and 5. The overall objectives of this chapter are (i) to select the best membrane integrity indicators or combination of membrane integrity indicators to monitor RO membrane integrity; and (ii) to estimate which lab-scale set-up was the most suitable to represent full-scale. In order to address the needs of these objectives, different statistical tools have been used such as:

- Pearson's correlation coefficient (*r*) to determine the correlation between the different indicators rejection;
- Two-way analysis of variance (ANOVA) to compare the average difference between indicators (called groups) depending on the type of set-up (SS flat-sheet, plastic flat-sheet or 2.5" module set-ups; called factor 1) and the type of membrane impairments (intact, organically fouled, scaled and aged; called factor 2);
- Box plots to graphically represent the variability of the different indicators rejection (LRV) as a function of the membrane impairments and the set-ups. *t*-tests were performed to statistically assess this variability;
- Box plots to graphically compare the variability of DOM and effluent salt, in all the setups with intact membrane, and in full-scale (data from Chapter 3 plant A). *t*-tests were performed to assess the statistical significance of this variability.

This chapter only analyses sulphate rejection determined with the ageing impairment in the plastic and SS flat-sheet set-ups, as permeate sulphate concentrations with organically fouled and scaled membranes (Chapter 4) and the 2.5" module set-up (Chapters 4 and 5) were below LOQ. The LRVs of MS2 phage were not included in this statistical analysis as the majority of the MS2 phage permeate samples had a concentration lower than the LOQ of the qRT-PCR technique. The LRV of salt was separated in two datasets: (i) LRV determined from RO synthetic feed (feed water used to analyse MS2 phage and R-WT) referred to as 'RO salt'; and (ii) LRV determined from secondary effluent (feed water used to analyse DOM and sulphate) referred to as 'effluent salt'. Table 6.1 summarises the membrane impairment experiments for each scale set-up.

6. Statistical comparison of experimental set-ups and membrane impairments

<u>Table 6.1:</u> Summary of the different experiments done for each scale.

_	Flat-sheet		_	
	SS	Plastic	2.5" module	Full-scale
Intact	X	X	X	X
Organic fouling	X		X	
Scaling	X		X	
Passive ageing	X	X	X	
Active ageing		X		

SS = stainless-steel flat-sheet cross-flow set-up.

Plastic = plastic flat-sheet cross-flow set-up.

Module = 2.5" spiral-wound module set-up.

6.1. Correlation between the rejection of the different membrane integrity indicators

The Pearson's correlation coefficient (r, n = sample size) between two indicators was determined by the function correlation (cor.test; Appendix B.1.1) of the R program and is summarised in Table 6.2. Appendix B.1.2 presents scatter plots with the calculated linear regression of combinations of the different indicators used in this study. The closer the value of r to 1 the greater is the correlation between the two variables. Thus, correlation can be classified in four groups depending on the r value (Onwuegbuzie et al., 2007):

- Weak or no correlation: r = 0 - 0.2;

- Weak correlation: r = 0.2 - 0.4;

- Moderate correlation: r = 0.4 - 0.6;

- Strong correlation: r = 0.6 - 0.8;

- Very strong correlation: r = 0.8 - 1.

Moreover, the *p-value* associated with the Pearson's correlation allows determination of the significance of a correlation. Thus, if the *p-value* is lower than 0.01 (*p-value* < 0.01), the correlation is significant at the 1% level.

According to the plots and regression coefficients, the LRV of DOM I, DOM II and DOM III were very strongly correlated ($r \ge 0.94$ for all combinations, p-value $< 2.2 ext{ } 10^{-16}$, n = 140).

DOM I to III correspond to three different regions of the map obtained by fluorescence EEM. These results suggest that DOM I to III had similar behaviour during RO filtration process. Baghoth et al. (2011) report strong correlation between different fluorescence EEM peaks such as tryptophan-like (λ_{ex} / λ_{em} < 250 / 360 nm) and tyrosine-like (λ_{ex} / λ_{em} 270 / 306 nm), and also with DOC and LC-OCD fractions in water samples from a drinking water treatment plant. Thus, the LRV of DOM II was used to interpret the general DOM LRV data. The choice of DOM II was due to its higher rejection tendency than the other DOM regions. The LRV of RO salt and effluent salt were very strongly correlated (r = 0.82, p-value $< 2.2 \times 10^{-16}$, n = 126). A stronger correlation was expected as both feed waters have similar ion species and in both cases salt rejection was measured by the same method (EC). The inherent differences between each experiment, such as the use of a new membrane coupon for each experiment, which introduces variability in water permeability and NaCl rejection; and the variability in initial characteristics of pre-filtered secondary effluent, could explain the lower than anticipated r value. However, the hypothesis that the membrane variability was the principal source of variability was not confirmed because even with the 2.5" module set-up, which used the same membrane module per type of impairment, the correlation was not as strong as expected (r = 0.83, p-value = 7.64 10^{-9} , n = 30). The variability in the LRV of RO salt and effluent salt might be explained by the difference in composition of the two feed waters. Some compounds present in the pre-filtered secondary effluent such as organic matter could interact with the effluent salt which could have an impact on its removal. The Pearson's correlation coefficient between the LRV of effluent salt and DOM II (r = 0.89, p-value $< 2.2 \cdot 10^{-16}$, n = 140), the LRV of effluent salt and sulphate (r = 0.90, p-value $< 2.2 \cdot 10^{-16}$, n = 59) and the LRV of DOM II and sulphate $(r = 0.89, p\text{-value} < 2.2 \cdot 10^{-16}, n = 63)$ were very strong. Conversely, RO salt - DOM and RO salt - sulphate were not analysed simultaneously which could explain lower LRV correlations (r = 0.70, p-value < 2.2 10^{-16} , n = 126 and r =0.63, p-value = $3.002 \cdot 10^{-6}$, n = 45, respectively) than with effluent salt. The lower correlation between the LRV of RO salt and sulphate could be explained by two facts. Firstly, there were less data values with sulphate than the other indicators as they were from only one type of membrane impairment (ageing) and two set-ups (SS and plastic flat-sheet set-ups). Since the sample size (n) has an impact on the r value the result from the pairing of RO salt and sulphate LRVs (n = 45) has less impact than the other indicators pairing (n > 126). Secondly and as explained previously, sulphate and RO salt were analysed in two different sets of experiments (see Chapter 2 Figure 2.1) which reduces their correlation due to the inherent variability between experiments. The LRV of R-WT had lower correlations with the LRV of other indicators (r = 0.65, p-value = 1.243 10^{-14} , n = 109 with RO salt, r = 0.61, p-value = 1.586 10^{-12} , n = 109 with DOM II, r = 0.63, p-value = 2.214 10^{-13} , n = 109 with effluent salt and r = 0.46, p-value = 0.0009, n = 46 with sulphate). This suggests that R-WT behaved differently during RO membrane filtration than the other indicators.

<u>Table 6.2:</u> Pearson's cross-correlation matrix for each combination of indicators (LRV).

	RO salt	DOM I	DOM II	DOM III	Effluent salt	Sulphate
R-WT	0.65*	0.63*	0.61*	0.61*	0.63*	0.46*
RO salt	1	0.72*	0.79*	0.70*	0.82*	0.63*
DOM I		1	0.96*	0.98*	0.85*	0.84*
DOM II			1	0.94*	0.89*	0.89*
DOM III				1	0.84*	0.80*
Effluent salt					1	0.90*

^{*} Significant r value (p-value < 0.01).

In conclusion, indicators from pre-filtered secondary effluent (i.e. DOM, effluent salt and sulphate) were very strongly correlated with each other (r > 0.80). RO salt was also strongly correlated with these indicators (r > 0.63). A Pearson's correlation coefficient closer to 1 was expected between RO salt and effluent salt as they are both of a similar ionic composition. The weaker correlation between RO salt and sulphate LRVs might be due to a lower number of experimental points which could increase the impact of experimental errors. Finally, from the correlation analyses it can be concluded that R-WT had a different behaviour than the other indicators.

6.2. Effect of membrane impairment and set-up

To determine the impact of the type of set-up (factor 1), the type of membrane impairment (factor 2) and their interaction on the rejection of indicators (R-WT, RO salt, DOM II and effluent salt), two-way ANOVA was used. Sulphate was not analysed due to permeate concentrations generally being below its LOQ. Nevertheless, the impact of the different factors on the LRV of effluent salt could be extrapolated to the LRV of sulphate because of their very high correlation (r = 0.90, p-value $< 2.2 ext{ } 10^{-16}$, n = 59). Table 6.3 sums up the p-

values of each indicator. The R program used for carrying out the two-way ANOVA and for determining the *p-values*, and the resulting two-way ANOVA tables are included in Appendix B.2.

<u>Table 6.3:</u> *p-values* of the indicators obtained from the two-way ANOVA.

		Groups			
Factors	R-WT	RO salt	DOM II	Effluent salt	
F1: Set-up	< 0.0001	< 0.0001	< 0.0001	< 0.0001	
F2: Membrane impairment	< 0.0001	< 0.0001	< 0.0001	< 0.0001	
Factors interaction	0.0242	0.0851*	0.0492	< 0.0001	

^{*} Comparison significantly equal (p-value > 0.05).

Overall, the type of membrane impairment had a significant impact on the rejection of all indicators (p-values < 0.05). This result was expected as in the previous chapters (Chapters 4 and 5) organic fouling and ageing impairments showed an impact on the rejection of the different indicators. The type of set-up also had an impact on the rejection of all indicators (p-values < 0.05). The three set-ups had different configurations (e.g. flat-sheet versus spiral-wound set-ups, different height of feed spacers) and were run at different experimental conditions (e.g. pressure of the SS flat-sheet and 2.5" module set-ups set at 7.5 bar, pressure of the plastic flat-sheet set-up set at 5 bar). All these differences played a role on the rejection of the indicators. The interaction effect between the two factors was significant for all indicators (p-values < 0.05) except for RO salt which had no significant factors interaction (p-value = 0.0851). Thus, for the indicators except RO salt, the combination of the type of membrane impairment and the type of set-up had an impact on its rejection.

Box plots permit to visualise these effects on indicators' rejection and are presented in Figures 6.1 (factor 1) and 6.2 (factor 2). The principle of box plots is to visualise the distribution of the samples for each parameter. The box represents the first quartile (lower horizontal line), the median (middle line) and the third quartile (top horizontal line). Top and bottom whiskers represent maximum and minimum value. Outliers are represented by dots. Appendix B.3 presents the R code used to create these box plots. According to Figure 6.1, the LRV of all indicators was the highest with the 2.5" module set-up and the lowest with the

plastic flat-sheet set-up except with R-WT which appeared to have a similar rejection between the SS and plastic flat-sheet set-ups. To determine statistically if there was a difference between the two set-ups, a t-test was performed. The homogeneity of the two groups of variance has to be determined beforehand using a Fisher's F-test in order to set the parameters of the t-test. If the p-value of the F-test is greater than 0.05 (p-value > 0.05), the two variances are homogeneous. Appendix B.4 presents the R code used to conduct the F-test and t-test for each case. Table 6.4 presents the results of the t-test for each indicator. For R-WT, there was a significant difference between the 2.5" module and the two flat-sheet set-ups (p-value < 0.05), whereas there was no significant variation between the two flat-sheet set-ups (p-value > 0.05). Conversely, there was a statistical difference between the three set-ups for RO salt, DOM II and effluent salt (p-value < 0.05).

<u>Table 6.4:</u> *p-values* of the *t*-tests for the comparison between the different types of setup.

	R-WT	RO salt	DOM II	Effluent salt
Module - Plastic	< 0.0001	< 0.0001	< 0.0001	< 0.0001
Module - SS	< 0.0001	< 0.0001	< 0.0001	< 0.0001
Plastic - SS	0.2958*	< 0.0001	< 0.0001	< 0.0001

^{*} Comparison significantly equal (p-value > 0.05).

Figure 6.2 shows an increase of the indicators' LRV with organically fouled membranes in contrast to their decrease with aged membranes as previously discussed in Chapters 4 and 5, respectively. The presence of an organic layer on the surface membrane covered up the cavities of the polyamide membrane as shown in Chapter 4, which improved the removal of indicators by size exclusion. In the case of ageing, chlorine hydrolysed the polyamide membrane which destroyed the cross-linked structure and thus caused an increase of the indicators passage. Table 6.4 presents the *p-values* of the *t*-test performed between the intact membrane and the different membrane impairments. Overall, organic fouling and ageing had an impact on the indicators LRV as discussed in Chapters 4 and 5. Scaling had an impact on the LRV of effluent salt, but not for the other indicators. In Chapter 4, results for the impact of scaling on salt rejection were inconclusive. Salt LRV increased with the SS flat-sheet set-up whereas it remained at the same level with the 2.5" module set-up. Thus, the *t*-test results presented in Table 6.5 could explain these differences. RO salt rejection increased in a

statistically significant manner with the 2.5" module set-up (p-value = 0.0013), whereas its rejection stayed equal with the SS flat-sheet set-up (p-value = 0.526). In contrast, the rejection of effluent salt by scaled membranes changed statistically with both set-ups (p-value = 0.0084 with the SS flat-sheet set-up, p-value = 5.79 10^{-5} with the 2.5" module set-up). However, these changes were conflicting. After scaling, salt rejection decreased with the 2.5" module set-up whereas effluent salt rejection increased with the SS flat-sheet set-up. It has to be noted that the commonly accepted behaviour is a decrease in salt rejection with a scaled membrane (Hoek and Elimelech, 2003; Dow, 2010).

<u>Table 6.5:</u> *p-values* of the *t*-tests for the comparison between the different types of impairment.

	R-WT	RO salt	DOM II	Effluent salt
Intact - Organic Fouling	0.0007	< 0.0001	0.0002	0.0018
Intact - Scaling	0.7141*	0.0909*	0.5525*	0.0022
Intact - Passive Ageing	0.0390	< 0.0001	< 0.0001	< 0.0001
Intact - Active Ageing	0.0010	< 0.0001	< 0.0001	< 0.0001

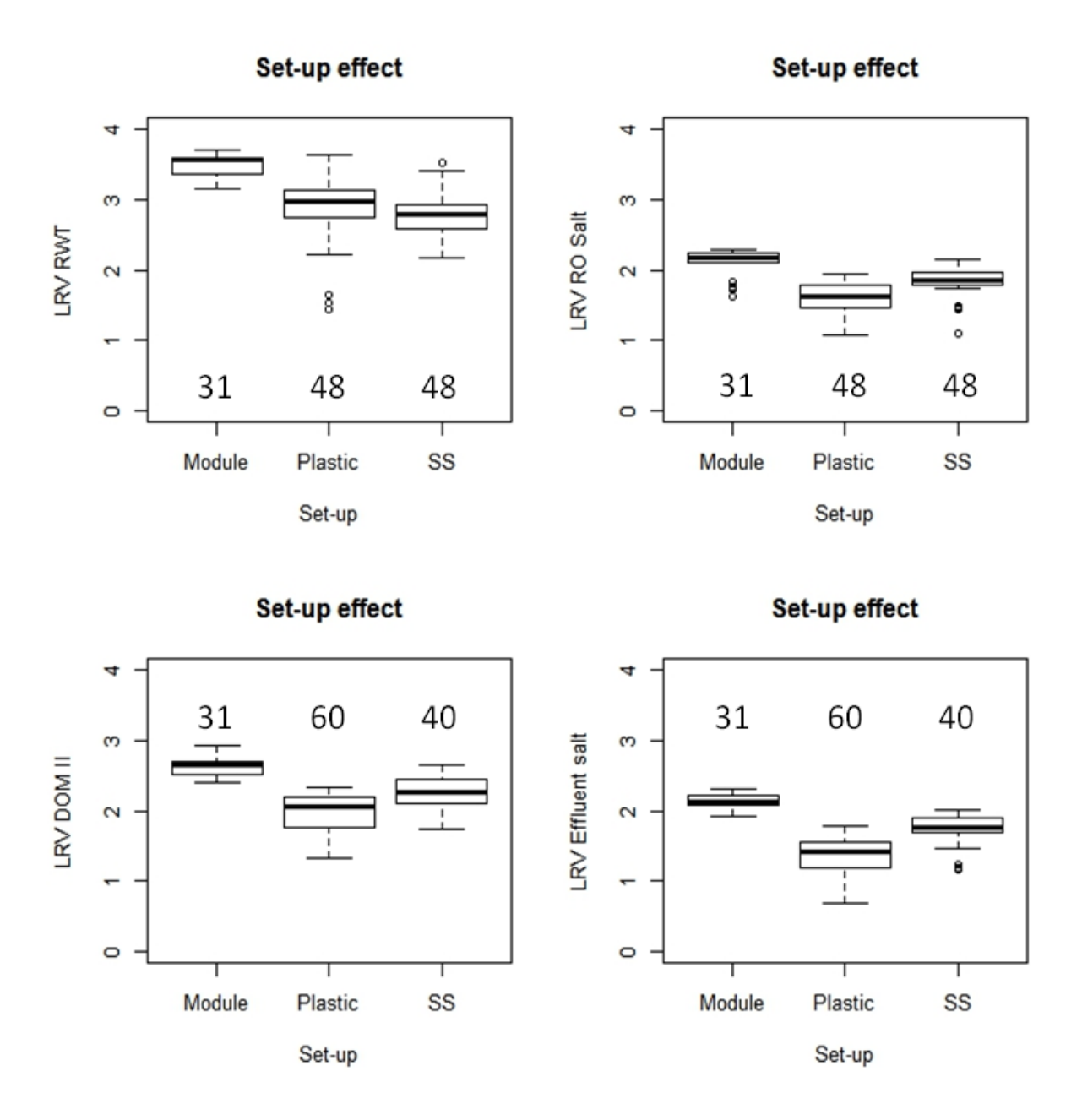
^{*} Comparison significantly equal (p-value > 0.05).

DOM and R-WT followed the same trend of rejection by membrane impairments; however the active membrane surface size variation between the two flat-sheet set-ups seemed not to have an impact on the rejection of R-WT. Between the two flat-sheet set-ups, the active membrane surface area was not the only difference. The pressure (i.e. 5 bar versus 7.5 bar for the plastic and SS flat-sheet set-ups, respectively), the feed spacers (i.e. no feed spacer for the plastic flat-sheet set-up) and the material composition of the different parts of the set-up (i.e. stainless-steel versus plastic material composition) were also different. All these differences could have an impact on the indicators' rejection. The sorption of R-WT on the plastic material could also increase its rejection and thus decrease the difference in behaviour between the two set-ups. MS2 phage was well retained by all intact membranes, which therefore eliminates the possibility of leaks through the seals of the systems.

The high variability of the R-WT LRV by the different impairments was due to the variability of the rejection between the two flat-sheet set-ups and the 2.5" module set-up (Figure 6.2). Also, the LRV of R-WT was always higher than the DOM and salt. DOM and salt had the

6. Statistical comparison of experimental set-ups and membrane impairments

same trend in behaviour with the size of the system and also in LRV value (1 - 2 LRV). Effluent salt indicators were the most sensitive to the variation in type of membrane impairments. This indicator is a good membrane integrity indicator of the current state of the membrane (i.e. intact, fouled or aged). However, this indicator underestimates the potential efficiency of the membrane to remove virus as its LRV is below those of the virus surrogate (MS2 phage). With regards to public health, it is better to underestimate the integrity of the membrane than to overestimate it.



<u>Figure 6.1:</u> Effect of the set-up scales on the LRV of indicators. Module = 2.5" spiral-wound module set-up, Plastic = plastic flat-sheet cross-flow set-up, SS = stainless-steel flat-sheet cross-flow set-up. The numbers in the graphs = number of sample per impairment.

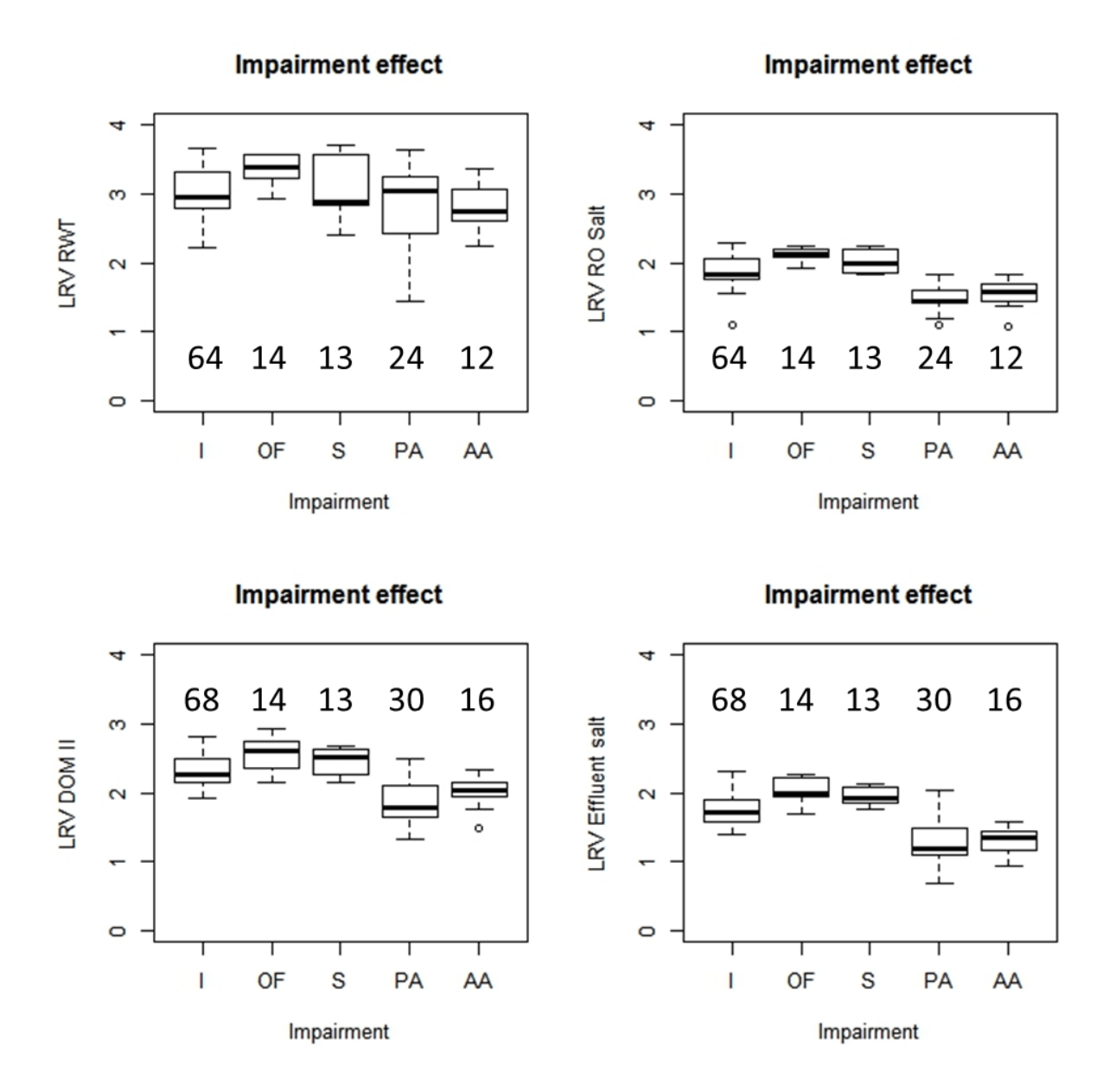


Figure 6.2: Effect of the different impairments on the LRV of indicators. I = intact membrane, OF = organic fouling impairment, S = scaling impairment, PA = passive ageing impairment and AA = active ageing impairment. The numbers in the graphs = number of sample per impairment.

6.3. Comparison of the different lab-scale set-ups with the full-scale plant

Figure 6.3 represents the comparison of the DOM and effluent salt rejections with intact membranes using the three lab-scale set-ups and the full-scale plant A (presented in Chapter 3). Table 6.6 presents the *t*-test results for the comparison of the different lab-scales with the full-scale for the rejection of DOM and effluent salt. None of the lab-scale set-ups was

statistically equal to the full-scale in terms of effluent salt removal (p-value < 0.05), with the SS set-up the closest to full-scale (p-value = 0.0268). The SS flat-sheet set-up was the only set-up having a statistically equal DOM rejection than the full-scale plant (p-value = 0.2757). Thus, the SS flat-sheet set-up was the most representative of full-scale. This conclusion is surprising as we expected the 2.5" module to best represent full-scale due to its spiral-wound configuration. The full-scale plant was operational for around four years (intermittent operation), and data obtained from this plant are therefore from used membranes. This could explain the lower in DOM and salt rejections compared to the new membranes. Another reason could be the effect of the system recovery. The total permeate recovery of the full-scale system is around 85% (i.e. around 55% per stage) compared with 10% for the 2.5" module set-up. It has been proven that the percentage of recovery has an impact on the removal of contaminants (Chellam and Taylor, 2001). Indeed, the rejection of the contaminants decreases as permeate water recovery is lowered due to the increase of the gradient concentration across the membrane. During membrane filtration:

- The pressure decreases due to the friction (i.e. pressure is the main driving force for separation);
- The concentration of solutes increases due to the passage of pure water through the membrane caused by the concentration gradient;
- The osmotic pressure increases which decreases the water permeation.

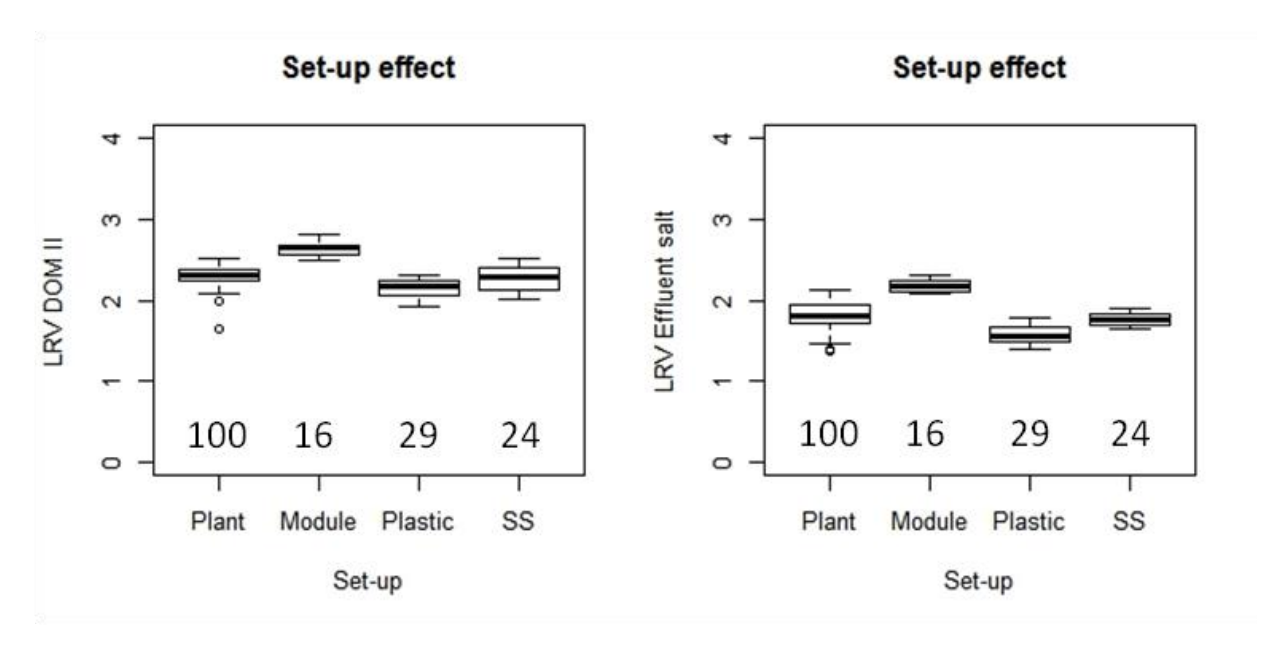
These phenomenon lead to:

- Decrease in the permeate flux and thus a greater diffusive flux compared with the water flux;
- Decrease in the cross-flow velocity across the module due to a decrease in turbulence and therefore an increase in concentration polarization which cause a decrease in solute rejection.

The flat-sheet systems had a very low permeate recovery (< 2%). However, their efficiency to remove indicators was lower than the 2.5" module set-up. This might be explained by the difference of ratio between the membrane surface and the volume of feed water ($1070 - 3570 \, \text{L·m}^{-2}$ for the flat-sheet set-ups versus 42 L·m⁻² for the 2.5" module set-up). The 2.5" module set-up possesses more sorption sites than the flat-sheet set-up for a lower ratio of

6. Statistical comparison of experimental set-ups and membrane impairments

foulants (feed mass $\mu g \cdot cm^{-2}$) which improved the rejection.



<u>Figure 6.3:</u> Effect of the different set-ups on the LRV of DOM II and effluent salt with intact membranes. Module = 2.5" spiral-wound module set-up, Plastic = plastic flat-sheet cross-flow set-up, SS = stainless-steel flat-sheet cross-flow set-up. Numbers in graphs = number of sample per impairment.

<u>Table 6.6:</u> *p-values* of the *t*-tests for the comparison between the full-scale and lab-scale set-ups.

	DOM II	Effluent salt
Full-scale - Module	< 2.2 10 ⁻¹⁶	< 2.2 10 ⁻¹⁶
Full-scale - Plastic	9.395 10 ⁻⁹	3.527 10 ⁻¹⁴
Full-scale - SS	0.2757*	0.0268

^{*} Comparison significantly equal (p-value > 0.05).

Module = 2.5" spiral-wound module set-up.

Plastic = plastic flat-sheet cross-flow set-up.

SS = stainless-steel flat-sheet cross-flow set-up.

6.4. Conclusions

Data analysis by different statistical tools allows evaluating (i) the correlation between the indicator removals; and (ii) the effect of the type of membrane impairment and set-up on the rejection of the indicators. Due to the high correlation between DOM, salt and sulphate, DOM II could be the most suitable indicator used to monitor the integrity of RO membranes. R-WT was the indicator having the lowest correlation with the other indicators. However, it could be the best indicator of those analysed in this thesis to monitor membrane integrity in regards to virus rejection as R-WT consistently had the highest rejection of the tested indicators but at the same time had a lower rejection than MS2 phage. A possible combination of DOM and R-WT measurement could be a viable option. Indeed, DOM is naturally present in RO feed effluent, which has several advantages. Its removal (or rather its fluorescent components) could be measured periodically or continuously by fluorescence spectrometry. When a breach of the system is suspected by DOM measurement, the integrity could be further tested by adding R-WT to the feed water, which is measured easily and sensitively by fluorescence in order to determine the possible impact of the observed malfunction to virus removal.

7. Conclusions & recommendations for future research

7.1.	Conclusions	.134
7.2.	Recommendations for future research	.136

7.1. Conclusions

This PhD thesis aimed at:

- Assessing the suitability of dissolved organic matter (DOM) for using it as a membrane integrity indicator and;
- Understanding the rejection behaviour of viruses (i.e. MS2 phage) and currently used membrane integrity indicators (i.e. rhodamine WT (R-WT), salt as measured by electrical conductivity and sulphate). This was realised using intact and differently impaired RO membranes (i.e. organic fouling, scaling and ageing) and various process set-ups.

It was expected that this information would help to select a single or a combination of compounds to monitor the performance of RO systems effectively.

DOM naturally present in RO feed water was evaluated as a potential membrane integrity indicator for virus rejection. The analysis of DOM from two RO full-scale plants by recording fluorescence excitation emission matrices (EEM) coupled with the so-called fluorescence regional integration (FRI) technique identified three different fluorescent regions as being of particular relevance. From these regions, DOM rejection was calculated in order to monitor the RO process. In combination with conductivity profiling, the use of DOM could detect the presence of defects in individual pressure vessels more reliably than conductivity profiling alone confirming the suitability of measuring DOM rejection as a new monitoring technique to ascertain RO membrane integrity.

During operation membrane fouling and ageing may compromise the integrity of an RO process. The filtration of MS2 bacteriophage employed as a virus surrogate and the four indicators (R-WT, DOM, salt and sulphate) by impaired membranes allowed improving our understanding on compunds removal mechanisms.

No effect on MS2 phage and sulphate rejection could be observed, possibly due to their analytical methods' limit of quantification (LOQ) imposing restrictions on determining their respective LRVs. The minimum LRV calculable from the LOQ of the analytical techniques showed a high LRV for MS2 phage (LRV > 5.7) with intact, organically fouled and scaled membranes.

Organic fouling is known to have a negative impact on the RO process leading to an increase

in operational costs (i.e. drop of the water permeability, higher energy demand and frequency for chemical cleaning). However, this impairment had a positive impact on the rejection of virus surrogate and indicators by increasing their log removal value (LRV). A cake layer formed by organic foulants covered up the cavities of the membrane and blocked the passage of the compounds by improving the size exclusion mechanism. Also, the presence of organic foulants could enable sorption of R-WT.

Inorganic scaling is a second potential fouling problem of the RO process. Like organic fouling, scaling caused a drop of the water permeability, whereas the rejection of R-WT, DOM and sulphate remains the same. Moreover, the results of the rejection of salt were controversial between the two systems. With the stainless-steel (SS) flat-sheet set-up, the NaCl rejection stayed equal but salt rejection from compounds' effluent increased. In contrast, with the 2.5" module set-up, the NaCl rejection decreased but salt rejection from compounds' effluent remained the same. This variation between the two systems might be due to the difference in system configuration. The 2.5" module set-up was more scaled than the SS flat-sheet set-up due to its higher permeate recovery which can be observed by the higher decrease of its water permeability and thus proportionally to a decrease of salt rejection by cake-enhanced concentration polarization (Hoek and Elimelech, 2003). Regarding the increase of the salt rejection from RO feed water, the presence of organic in the solution might interact with the salt improving its rejection.

Ageing by chlorine exposure modified the chemistry of the polyamide layer by introducing chlorine into the molecular structure. These changes in molecular structure can lead to all of the following: (i) breakage of amide bonds and H-bonds that are an integral part of the tertiary structure of the molecule and the RO membrane; and (ii) either swelling increasing permeability or a collapse of the structure leading to decreased permeability. In the experiments performed in this thesis this structural rearrangement resulted in an increase of permeability and a decrease of virus surrogate and indicators rejection by limiting the size exclusion mechanism or by inhibiting the steric hindrance mechanism by the possible appearance of larger defects in the membrane.

In summary, the general mechanisms of virus surrogate and indicators rejection are size exclusion followed by electrostatic repulsion and in some case sorption (R-WT). Depending on the state of the membrane, these mechanisms are enhanced (e.g. organic fouling) or reduced in their efficiency (e.g. ageing).

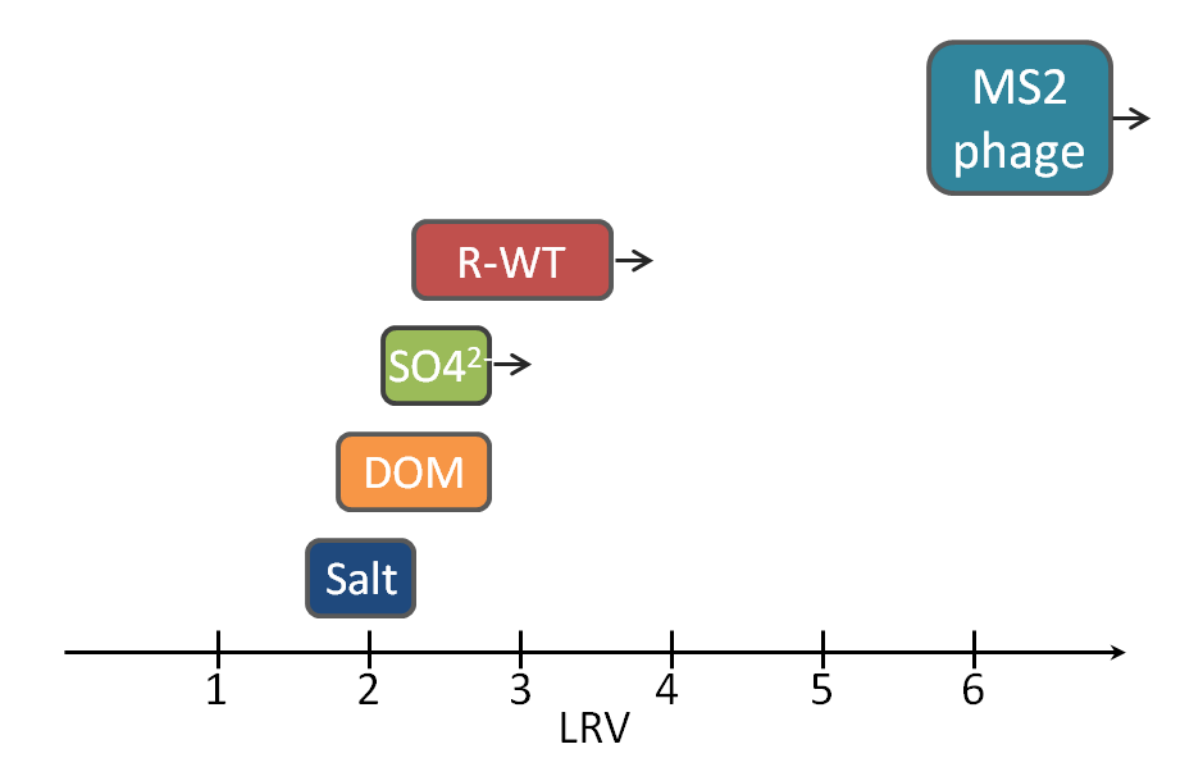
Finally, a statistical comparison between the indicators' removals comparing the set-ups and the impairments showed a very strong correlation for DOM, salt and sulphate removal, and a weaker correlation between R-WT and the other indicators. From this analysis, we proposed a combination of DOM and R-WT as suitable indicators to monitor RO membrane integrity. Indeed, DOM is naturally present in RO feed water and was better rejected than salt measured by conductivity as demonstrated in Chapter 3; and R-WT had the highest rejection of the indicators tested but at the same time had a lower rejection than MS2 phage. A comparison of the different lab-scale set-ups (i.e. plastic and SS flat-sheet cross-flow set-ups, and 2.5" spiral-wound module set-up) with the full-scale plant showed an equal rejection of DOM with the SS flat-sheet set-up. Thus and surprisingly, this set-up would be the most suitable set-up to imitate the full-scale for RO membrane study, if the experimental results were to be used directly without further modelling aiming at correcting for different process recoveries in lab-scale and full-scale processes.

7.2. Recommendations for future research

MS2 phage is a good virus surrogate, because it is non-hazardous for humans and easy to culture. The LOQ of the plaque-assay and quantitative reverse transcriptase-polymerase chain reaction (qRT-PCR) can be improved by either increasing the volume of sample or concentrating the sample. However, MS2 phage might be difficult to use at full-scale essentially due to the difficulty in working very clean in a full-scale plant environment, which makes it difficult to measure accurately very different concentrations in feed and permeate without the risk of cross-contamination. In addition, there is also a high analytical cost, considerable time needed to obtain results and the requirement of highly skilled staff to handle and analyse MS2 phage.

• Figure 7.1 represents the LRV of the different surrogates used in this thesis. The virus surrogates used in this thesis are less well rejected than MS2 phage creating a big gap (around 2 LRV) between their rejection and the real virus rejection causing an underestimation of the virus removal efficiency by RO membrane. New virus surrogates could be developed in order to reduce this gap while still be rejected less than viruses maintaining an overall conservative behaviour compared to viruses. Virus-like-particles (VLPs) and organic dendrimers might be two good potential surrogates.

- VLPs are composed of viral proteins without the genetic material. The advantage of this particle is to have the same specificities than viruses regarding size, shape and isoelectric point. VLPs could be built with chemical function to facilitate their detection. For example, a fluorescent group can be linked to VLPs and facilitate their detection. Thus, VLPs would be easier to detect than MS2 phage because of potential online detection. Moreover, due to the absence of genetic material, this particle is not pathogenic. Another advantage of VLPs would be their constant concentration in the system (except their potential deterioration by chemical oxidation for example) to compare to MS2 phage which can multiply or die in the system. Nowadays, different enteric virus and MS2 phage VLPs have been produced (Chuan et al., 2008; Peabody et al., 2008; Chung et al., 2010; Sano et al., 2010; Ashley et al., 2011; Caldeira and Peabody, 2011; Rodríguez-Limas et al., 2011; Tan et al., 2011). However, they often cannot be produced at industrial scale yet and are still expensive to use in full-scale (Liew et al., 2010; Imai et al., 2011). Nevertheless, research should firstly test them at the lab-scale to ascertain their suitability, e.g. with the SS flat-sheet set-up which was the system best mimicking the full-scale in our study;
- Dendrimers are organic compounds which can be entirely created incorporating the surface functional groups needed to mimic viruses and markers for the type of detection method wanted. Up-to-date, the most efficient and easiest detection method for dendrimers is fluorescence.



<u>Figure 7.1:</u> LRV of MS2 phage and membrane integrity indicators by intact RO membranes based on this thesis results.

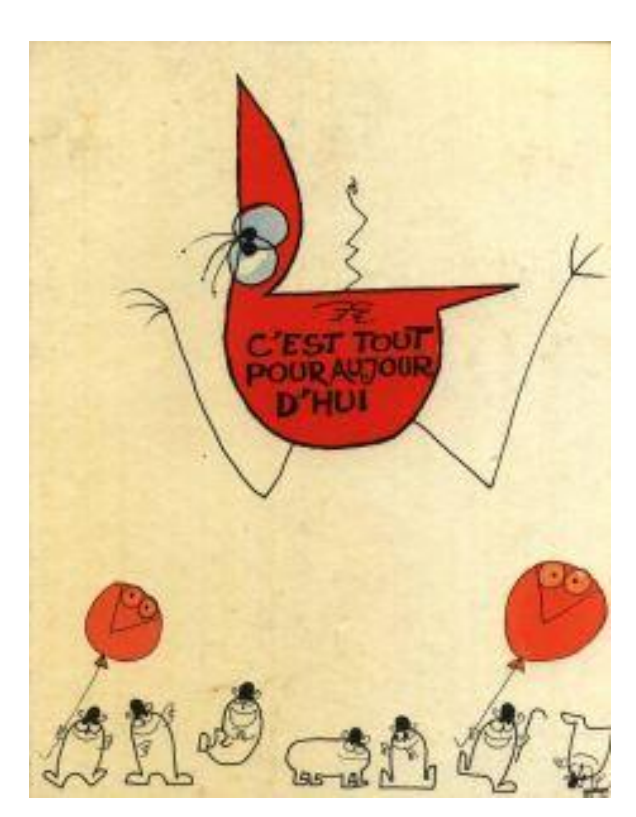
• An alternative would be to develop new online measurement techniques using surrogates naturally present in RO feed water such as online sulphate or DOM monitoring. In this thesis, sulphate has been analysed. However, due to the high LOQ of the ion chromatography technique, the concentration of sulphate in the permeate samples could not be determined with intact, organically fouled and scaled membrane. However, it has been proven that the potential sulphate LRV in full-scale plant is around 2.6 (data not published). Thus, sulphate monitoring with a low detection limit would be more effective than conductivity profiling. DOM rejection could also be monitored by employing size exclusion chromatography (SEC) to further monitor more selectively those DOM fractions that have the highest rejection. In Chapter 3 of this thesis, it was shown that this is a feasible approach and a LRV that was around one unit higher was determined compared to direct measurement of the untreated sample by fluorescence. However, the current approach is complex and may be difficult to standardize. Further research should explore this approach including suitable preconcentration techniques in more detail.

The virus counter, a new technique based on flow cytometry directly measuring the concentration of virus, might also have a potential use for the assessment of the integrity of

RO membranes. However, research is needed to assess the LOQ of this technique in the RO feed and RO permeate matrix and determine the potential impact of the presence of organic matter or other possible interferences in this technique.

- The impact of membrane ageing by chlorine and especially the impact of the chlorinated polyamide membrane on the rejection of MS2 phage and membrane integrity indicators were studied. Depending on the type of fouling, acids such as citric acid at pH 2 or base such as sodium hydroxide at pH 11 are used to remove scaling or organic fouling, respectively. While polyamide membranes should be tolerant to high and low pH, still more study on the tolerance limit of the polyamide layer should be performed to enlarge our understanding on the membrane ageing mechanism. The impact of the long-term chemical cleaning exposure on RO membrane and their effect on membrane change need investigation regarding virus rejection. An opportunity and requirement for future research would definitely be to assess the impact of the membrane damage from a material science point of view, e.g. how the mechanic properties of the membrane may be impacted including the structural elements of the membrane like the poly (ether) sulfone and polyester backing of the polyamide, and what impact this has on the likelihood of leaks to be appear during operation.
- Finally, not only new research but also consolidation of existing knowledge is required. It is well known that virus rejection is linked to membrane integrity. However, to date, different monitoring techniques such as conductivity and TOC are used without standardized validation protocols. A detailed understanding of the formation of membrane impairments and their frequency is necessary to develop a validation guideline and simplify the validation and operational monitoring of the RO process.

In analogy, guidelines for other water treatment processes such as rapid filtration, membrane bioreactor or advanced oxidation processes and other risks such as chemical contaminant are also needed. Research and practitioners should collaborate to develop adequate frameworks to develop such guidance in practical, efficient and understandable, and therefore manageable ways.



(http://www.lesshadoks.com/)

- Adham S, Gagliardo P, Smith D, Ross D, Gramith K, Trussell R. 1998a. Monitoring the integrity of reverse osmosis membranes. Desalination 119:143-150.
- Adham S, Trussell S, Gagliardo P, Trussell R. 1998b. Rejection of MS-2 virus by RO membranes. Journal AWWA 90:130-135.
- Alford T, Feldman L, Mayer J. 2007a. Radiative Transitions and the Electron Microprobe. In: Fundamentals of Nanoscale Film Analysis: Springer US. p 214-233.
- Alford T, Feldman L, Mayer J. 2007b. Scanning Probe Microscopy. In: Fundamentals of Nanoscale Film Analysis: Springer US. p 277-290.
- Ang WS, Elimelech M. 2007. Protein (BSA) fouling of reverse osmosis membranes: Implications for wastewater reclamation. Journal of Membrane Science 296:83-92.
- Ang WS, Elimelech M. 2008. Fatty acid fouling of reverse osmosis membranes: Implications for wastewater reclamation. Water Research 42:4393-4403.
- Ang WS, Tiraferri A, Chen KL, Elimelech M. 2011. Fouling and cleaning of RO membranes fouled by mixtures of organic foulants simulating wastewater effluent. Journal of Membrane Science 376:196-206.
- Angelakis AN, Spyridakis S. 1996. The status of water resources in Minoan times: a preliminary study. In: Angelakis AN, Issar A, editors. Diachronic climatic impact on water resources in mediterranean region. Heidelberg, Germany: Springer-Verlag.
- Antony A, Blackbeard J, Leslie G. 2012. Removal Efficiency and Integrity Monitoring Techniques for Virus Removal by Membrane Processes. Critical Reviews in Environmental Science and Technology 42:891-933.
- Antony A, Fudianto R, Cox S, Leslie G. 2010. Assessing the oxidative degradation of polyamide reverse osmosis membrane--Accelerated ageing with hypochlorite exposure. Journal of Membrane Science 347:159-164.
- Antony A, Low JH, Gray S, Childress AE, Le-Clech P, Leslie G. 2011. Scale formation and control in high pressure membrane water treatment systems: A review. Journal of Membrane Science 383:1-16.
- Arkhangelsky E, Gitis V. 2008. Effect of transmembrane pressure on rejection of viruses by ultrafiltration membranes. Separation and Purification Technology 62:619-628.
- Asano T, editor. 2007. Water reuse: issues, technologies, and applications.
- Asano T, Levine AD. 1996. Wastewater reclamation recycling and reuse: past, present and futur. Water Science and Technology 33:1-14.

- Ashley CE, Carnes EC, Phillips GK, Durfee PN, Buley MD, Lino CA, Padilla DP, Phillips B, Carter MB, Willman CL, Brinker CJ, Caldeira JdC, Chackerian B, Wharton W, Peabody DS. 2011. Cell-Specific Delivery of Diverse Cargos by Bacteriophage MS2 Virus-like Particles. ACS Nano 5:5729-5745.
- Baghoth SA, Sharma SK, Amy GL. 2011. Tracking natural organic matter (NOM) in a drinking water treatment plant using fluorescence excitation-emission matrices and PARAFAC. Water Research 45:797-809.
- Bakhshayeshi M, Jackson N, Kuriyel R, Mehta A, van Reis R, Zydney AL. 2011. Use of confocal scanning laser microscopy to study virus retention during virus filtration. Journal of Membrane Science 379:260-267.
- Bartels C, Franks R, Rybar S, Schierach M, Wilf M. 2005. The effect of feed ionic strength on salt passage through reverse osmosis membranes. Desalination 184:185-195.
- Barty-King H. 1992. Water the book, an illustrated history of water supply and wastewater in the United Kingdom. London, UK.
- Bastian R. 2006. The future of water reuse. BioCycle 47:25-27.
- Bixio D, Wintgens T, editors. 2006. Water reuse system management manual Aquarec.
- Bosch A, Guix S, Sano D, Pinto RM. 2008. New tools for the study and direct surveillance of viral pathogens in water. Current Opinion in Biotechnology 19:295-301.
- Buch PR, Jagan Mohan D, Reddy AVR. 2008. Preparation, characterization and chlorine stability of aromatic–cycloaliphatic polyamide thin film composite membranes. Journal of Membrane Science 309:36-44.
- Buffle J, Leppard GG. 1995a. Characterization of Aquatic Colloids and Macromolecules. 1. Structure and Behavior of Colloidal Material. Environmental Science & Technology 29:2169-2175.
- Buffle J, Leppard GG. 1995b. Characterization of Aquatic Colloids and Macromolecules. 2. Key Role of Physical Structures on Analytical Results. Environmental Science & Technology 29:2176-2184.
- Buffle J, Wilkinson KJ, Stoll S, Filella M, Zhang J. 1998. A Generalized Description of Aquatic Colloidal Interactions: The Three-colloidal Component Approach. Environmental Science & Technology 32:2887-2899.
- Bustin SA, Mueller R. 2005. Real-time reverse transcription PCR (qRT-PCR) and its potential use in clinical diagnosis. Clin Sci 109:365-379.

- Caldeira JC, Peabody DS. 2011. Thermal Stability of RNA Phage Virus-Like Particles Displaying Foreign Peptides. Journal of Nanobiotechnology 9.
- Chellam S, Taylor JS. 2001. Simplified Analysis of Contaminant Rejection During Groundand Surface Water Nanofiltration Under the Information Collection Rule. Water Research 35:2460-2474.
- Chen W, Westerhoff P, Leenheer JA, Booksh K. 2003. Fluorescence excitation-emission matrix regional integration to quantify spectra for dissolved organic matter. Environmental Science and Technology 37:5701-5710.
- Chuan YP, Fan YY, Lua L, Middelberg APJ. 2008. Quantitative analysis of virus-like particle size and distribution by field-flow fractionation. Biotechnology and Bioengineering 99:1425-1433.
- Chung C-Y, Chen C-Y, Lin S-Y, Chung Y-C, Chiu H-Y, Chi W-K, Lin Y-L, Chiang B-L, Chen W-J, Hu Y-C. 2010. Enterovirus 71 virus-like particle vaccine: Improved production conditions for enhanced yield. Vaccine 28:6951-6957.
- Coble PG. 1996. Characterization of marine and terrestrial DOM in seawater using excitation-emission matrix spectroscopy. Marine Chemistry 51:325-346.
- Contreras AE, Kim A, Li Q. 2009. Combined fouling of nanofiltration membranes: Mechanisms and effect of organic matter. Journal of Membrane Science 327:87-95.
- Cran MJ, Bigger SW, Gray SR. 2011. Degradation of polyamide reverse osmosis membranes in the presence of chloramine. Desalination 283:58-63.
- da Silva MK, Tessaro IC, Wada K. 2006. Investigation of oxidative degradation of polyamide reverse osmosis membranes by monochloramine solutions. Journal of Membrane Science 282:375-382.
- Deborde M, von Gunten U. 2008. Reactions of chlorine with inorganic and organic compounds during water treatment—Kinetics and mechanisms: A critical review. Water Research 42:13-51.
- Deluhery J, Rajagopalan N. 2008. Use of paramagnetic particles in membrane integrity testing. Journal of Membrane Science 318:176-181.
- Do VT, Tang CY, Reinhard M, Leckie JO. 2012a. Degradation of Polyamide Nanofiltration and Reverse Osmosis Membranes by Hypochlorite. Environmental Science & Technology 46:852-859.

- Do VT, Tang CY, Reinhard M, Leckie JO. 2012b. Effects of Chlorine Exposure Conditions on Physiochemical Properties and Performance of a Polyamide Membrane—Mechanisms and Implications. Environmental Science & Technology 46:13184-13192.
- Do VT, Tang CY, Reinhard M, Leckie JO. 2012c. Effects of hypochlorous acid exposure on the rejection of salt, polyethylene glycols, boron and arsenic (V) by nanofiltration and reverse osmosis membranes. Water Research.
- Donose BC, Sukumar S, Pidou M, Poussade Y, Keller J, Gernjak W. 2013. Effect of pH on the ageing of reverse osmosis membranes upon exposure to hypochlorite. Desalination 309:97-105.
- Dow. 2010. FILMTEC Reverse Osmosis Membranes. In: Manual T, editor.
- Dreier J, Stormer M, Kleesiek K. 2005. Use of bacteriophage MS2 as an internal control in viral reverse transcription-PCR assays. Journal of clinical microbiology 43:4551-4557.
- du Pisani PL. 2006. Direct reclamation of potable water at Windhoek's Goreangab reclamation plant. Desalination 188:79-88.
- Ettori A, Gaudichet-Maurin E, Schrotter J-C, Aimar P, Causserand C. 2011. Permeability and chemical analysis of aromatic polyamide based membranes exposed to sodium hypochlorite. Journal of Membrane Science 375:220-230.
- Farahbakhsh K, Smith DW. 2004. Removal of coliphages in secondary effluent by microfiltration—mechanisms of removal and impact of operating parameters. Water Research 38:585-592.
- Foley J, Batstone D, Keller J. 2007. The Challenges of Water Recycling: Technical and Environmental Horizons. In. Brisbane: AWMC.
- Fujioka T, Khan SJ, McDonald JA, Henderson RK, Poussade Y, Drewes JE, Nghiem LD. 2013. Effects of membrane fouling on N-nitrosamine rejection by nanofiltration and verse osmsosis membranes. Journal of Membrane Science 427:311-319.
- Furiga A, Pierre G, Glories M, Aimar P, Roques C, Causserand C, Berge M. 2011. Effects of ionic strength on bacteriophage MS2 behavior and their implications for the assessment of virus retention by ultrafiltration membranes. Applied and Environmental Microbiology 77:229-236.

- Gabelich CJ, Frankin JC, Gerringer FW, Ishida KP, Suffet IH. 2005. Enhanced oxidation of polyamide membranes using monochloramine and ferrous iron. Journal of Membrane Science 258:64-70.
- Gerba CP, Gramos DM, Nwachuku N. 2002. Comparative inactivation of Enteroviruses and Adenovirus 2 by UV light Applied and Environmental Microbiology 68:5167-5189.
- Gerba CP, Naranjo JE, Jones EL. 2008. Virus Removal from Water by a Portable Water Treatment Device. Wilderness & Environmental Medicine 19:45-49.
- Gitis V, Adin A, Nasser A, Gun J, Lev O. 2002. Fluorescent dye labeled bacteriophages—a new tracer for the investigation of viral transport in porous media: 1. Introduction and characterization. Water Research 36:4227-4234.
- Gitis V, Haught RC, Clark CM, Gun J, Lev O. 2006. Nanoscale probes for the evaluation of the integrity of ultrafiltration membranes. Journal of Membrane Science 276:199-207.
- Glater J, Hong S-k, Elimelech M. 1994. The search for a chlorine-resistant reverse osmosis membrane. Desalination 95:325-345.
- Glater J, Zachariah MR. 1985. Mechanistic study of halogen interaction with polyamide reverse-osmosis membranes. ACS Symposium Series 345-358.
- Golmohammadi R, Valegård K, Fridborg K, Liljas L. 1993. The Refined Structure of Bacteriophage MS2 at 2·8 Å Resolution. Journal of Molecular Biology 234:620-639.
- Grant SB, Saphores J-D, Feldman DL, Hamilton AJ, Fletcher TD, Cook PLM, Stewardson M, Sanders BF, Levin LA, Ambrose RF, Deletic A, Brown R, Jiang SC, Rosso D, Cooper WJ, Marusic I. 2012. Taking the "Waste" Out of "Wastewater" for Human Water Security and Ecosystem Sustainability. Science 337:681-686.
- Gu J-E, Jun B-M, Kwon Y-N. 2012. Effect of chlorination condition and permeability of chlorine species on the chlorination of a polyamide membrane. Water Research 46:5389-5400.
- Guan X-H, Shang C, Chen G-H. 2006. ATR-FTIR investigation of the role of phenolic groups in the interaction of some NOM model compounds with aluminum hydroxide. Chemosphere 65:2074-2081.
- Guo H, Wyart Y, Perot J, Nauleau F, Moulin P. 2010a. Application of magnetic nanoparticles for UF membrane integrity monitoring at low-pressure operation. Journal of Membrane Science 350:172-179.
- Guo H, Wyart Y, Perot J, Nauleau F, Moulin P. 2010b. Low-pressure membrane integrity tests for drinking water treatment: A review. Water Research 44:41-57.

- Guo W, Ngo H-H, Li J. 2012. A mini-review on membrane fouling. Bioresource Technology 122:27-34.
- Hambly AC, Henderson RK, Storey MV, Baker A, Stuetz RM, Khan SJ. 2010. Fluorescence monitoring at a recycled water treatment plant and associated dual distribution system
 Implications for cross-connection detection. Water Research 44:5323-5333.
- Havelaar AH, Melse JM. 2003. Quantifying public health risk in the WHO Guidelines for Drinking-Water Quality: A burden of disease approach. In: National Institute for Public Health and the Environment of the Netherlands.
- Henderson RK, Baker A, Murphy KR, Hambly A, Stuetz RM, Khan SJ. 2009. Fluorescence as a potential monitoring tool for recycled water systems: A review. Water Research 43:863-881.
- Henderson RK, Stuetz RM, Khan SJ. 2010. Demonstrating ultra-filtration and reverse osmosis performance using size exclusion chromatography. Water Science and Technology 62:2747-2753.
- Her N, Amy G, Chung J, Yoon Y. 2008. Characterizing dissolved organic matter and evaluating associated nanofiltration membrane fouling. Chemosphere 70:495-502.
- Herath G, Yamamoto K, Urase T. 1999. Removal of viruses by microfiltration membranes at different solution environments. Water Science and Technology 40:331-338.
- Hewitt J, Leonard M, Greening GE, Lewis GD. 2011. Influence of wastewater treatment process and the population size on human virus profiles in wastewater. Water Research 45:6267-6276.
- Hoek EMV, Elimelech M. 2003. Cake-Enhanced Concentration Polarization: A New Fouling Mechanism for Salt-Rejecting Membranes. Environmental Science and Technology 37:5581–5588.
- Huang H, Young TA, Schwab KJ, Jacangelo JG. 2012. Mechanisms of virus removal from secondary wastewater effluent by low pressure membrane filtration. Journal of Membrane Science 409–410:1-8.
- Huber SA, Balz A, Abert M, Pronk W. 2011. Characterisation of aquatic humic and non-humic matter with size-exclusion chromatography organic carbon detection organic nitrogen detection (LC-OCD-OND). Water Research 45:879-885.
- Hurlimann A, Dolnicar S. 2010. When public opposition defeats alternative water projects The case of Toowoomba Australia. Water Research 44:287-297.

- Hurlimann A, Dolnicar S. 2012. Newspaper coverage of water issues in Australia. Water Research 46:6497-6507.
- Hydranautics. 2001. What is membrane performance normalization? Technical Service Bulletin January.
- IAWPRC. 1991. Bacteriophages as model viruses in water quality controlag. Water Research 25:529-545.
- Iborra MI, Lora J, Alcaina MI, Arnal JM. 1996. Effect of oxidation agents on reverse osmosis membrane performance to brackish water desalination. Desalination 108:83-89.
- Imai T, Sano D, Miura T, Okabe S, Wada K, Masago Y, Omura T. 2011. Adsorption characteristics of an enteric virus-binding protein to norovirus, rotavirus and poliovirus. BMC Biotechnology 11:123.
- ISO. 1995. Water quality detection and enumeration of bacteriophages. In: Part 1: enumeration of F-specific RNA bacteriophages. Geneva, Switzerland: International Organisation of Standardization.
- Jacangelo JG, Adham SS, Laine JM. 1995. Mechanism of Cryptosporidium, Gardia, and MS2 virus removal by MF and UF. Journal AWWA 87:107-121.
- Jaddi N, Vij DR. 2006. Fourier transform infrared spectroscopy. In: US S, editor. Handbook of Applied solid state spectroscopy. p 411-490.
- Kaiser G. 2009. Size and Shapes of Virus. In: http://faculty.ccbcmd.edu/courses/bio141/lecguide/unit3/viruses/ssvir.html, editor.
- Kang G-D, Gao C-J, Chen W-D, Jie X-M, Cao Y-M, Yuan Q. 2007. Study on hypochlorite degradation of aromatic polyamide reverse osmosis membrane. Journal of Membrane Science 300:165-171.
- Kaufman Y, Kasher R, Lammertink RGH, Freger V. 2012. Microfluidic NF/RO separation: Cell design, performance and application. Journal of Membrane Science 396:67-73.
- Kawaguchi T, Tamura H. 1984. Chlorine-resistant membrane for reverse osmosis. I. Correlation between chemical structures and chlorine resistance of polyamides. Journal of Applied Polymer Science 29:3359-3367.

- Khan S, Roser D. 2007. Risk Assessment and Health Effects Studies of Indirect Potable Reuse Schemes Final report. In: Centre for Water and Waste Technology.
- Kim H-C, Dempsey BA. 2013. Membrane fouling due to alginate, SMP, EfOM, humic acid, and NOM. Journal of Membrane Science 428:190-197.
- Kim YK, Lee SY, Kim DH, Lee BS, Nam SY, Rhim JW. 2010. Preparation and characterization of thermally crosslinked chlorine resistant thin film composite polyamide membranes for reverse osmosis. Desalination 250:865-867.
- Kitis M, Lozier JC, Kim J-H, Mi B, Marinas BJ. 2003. Microbial removal and integrity of RO and NF membranes. Journal AWWA 95:105-119.
- Kubista M, Andrade JM, Bengtsson M, Forootan A, Jonák J, Lind K, Sindelka R, Sjöback R, Sjögreen B, Strömbom L, Ståhlberg A, Zoric N. 2006. The real-time polymerase chain reaction. Molecular Aspects of Medicine 27:95-125.
- Kumar M, Adham S, DeCarolis J. 2007. Reverse osmosis integrity monitoring. Desalination 214:138-149.
- Kwon Y-N, Leckie JO. 2006a. Hypochlorite degradation of crosslinked polyamide membranes: I. Changes in chemical/morphological properties. Journal of Membrane Science 283:21-26.
- Kwon Y-N, Leckie JO. 2006b. Hypochlorite degradation of crosslinked polyamide membranes: II. Changes in hydrogen bonding behavior and performance. Journal of Membrane Science 282:456-464.
- Kwon Y-N, Tang CY, Leckie JO. 2006. Change of membrane performance due to chlorination of crosslinked polyamide membranes. Journal Of Applied Polymer Science 102:5895-5902.
- Kwon Y-N, Tang CY, Leckie JO. 2008. Change of chemical composition and hydrogen bonding behavior due to chlorination of crosslinked polyamide membranes. Journal of Applied Polymer Science 108:2061-2066.
- Langlet J, Gaboriaud F, Duval JFL, Gantzer C. 2008. Aggregation and surface properties of F-specific RNA phages: Implication for membrane filtration processes. Water Research 42:2769-2777.
- Lapworth DJ, Kinniburgh DG. 2009. An R script for visualising and analysing fluorescence excitation–emission matrices (EEMs). Computers & Geosciences 35:2160-2163.

- Lawaetz AJ, Stedmon CA. 2009. Fluorescence Intensity Calibration Using the Raman Scatter Peak of Water. Applied Spectroscopy 63:936-940.
- Lebleu N, Roques C, Aimar P, Causserand C. 2009. Role of the cell-wall structure in the retention of bacteria by microfiltration membranes. Journal of Membrane Science 326:178-185.
- Lee S, Ang WS, Elimelech M. 2006. Fouling of reverse osmosis membranes by hydrophilic organic matter: implications for water reuse. Desalination 187:313-321.
- Lee S, Lee CH. 2005. Scale formation in NF/RO: mechanism and control. Water Science & Technology 51:267-275.
- Leenheer JA, Croue JP. 2003. Characterizing dissolved aquatic organic matter. Environmental Science and Technology January 1:19A-26A.
- Li Q, Xu Z, Pinnau I. 2007. Fouling of reverse osmosis membranes by biopolymers in wastewater secondary effluent: Role of membrane surface properties and initial permeate flux. Journal of Membrane Science 290:173-181.
- Liew MWO, Rajendran A, Middelberg APJ. 2010. Microbial production of virus-like particle vaccine protein at gram-per-litre levels. Journal of Biotechnology 150:224-231.
- Liu M, Chen Z, Yu S, Wu D, Gao C. 2011. Thin-film composite polyamide reverse osmosis membranes with improved acid stability and chlorine resistance by coating N-isopropylacrylamide-co-acrylamide copolymers. Desalination 270:248-257.
- Loeb S, Sourirajan S. 1962. Sea water demineralization by means of an osmotic membrane. Advances in Chemistry Series 38:117-132.
- Lohwacharin J, Takizawa S. 2009. Effects of nanoparticles on the ultrafiltration of surface water. Journal of Membrane Science 326:354-362.
- Lovins III WA, Taylor JS, Hong SK. 2002. Micro-organism rejection by membrane systems. Environmental Engineering Science 19:453-465.
- Lozier JC, Kitis M, Colvin CK, Kim JH, Mi B, Marinas BJ. 2003. Microbial removal and integrity monitoring in high-pressure membranes. Denver: AWWA research foundation.
- Lukasik J, Scott TM, Andryshak D, Farrah SR. 2000. Influence of Salts on Virus Adsorption to Microporous Filters. Applied and Environmental Microbiology 66:2914-2920.
- Madaeni SS. 1997. Mechanism of virus removal using membranes. Filtration and Separation Jan/Feb:61-65.

- Malaeb L, Ayoub GM. 2011. Reverse osmosis technology for water treatment: State of the art review. Desalination 267:1-8.
- Maruyama T, Katoh S, Nakajima M, Nabetani H, Abbott TP, Shono A, Satoh K. 2001. FT-IR analysis of BSA fouled on ultrafiltration and microfiltration membranes. Journal of Membrane Science 192:201-207.
- Masclaux FG, Hotz P, Friedli D, Savova-Bianchi D, Oppliger A. 2013. High occurrence of hepatitis E virus in samples from wastewater treatment plants in Switzerland and comparison with other enteric viruses. Water Research 47:5101-5109.
- Mi B, Eaton CL, Kim JH, Colvin CK, Lozier JC, Marinas BJ. 2004. Removal of biological and non-biological viral surrogates by spiral-wound reverse osmosis membrane elements with intact and compromised integrity. Water Research 38:3821-3832.
- Michen B, Graule T. 2010. Isoelectric points of viruses. Journal of Applied Microbiology 109:388-397.
- Mitrouli ST, Karabelas AJ, Isaias NP. 2010. Polyamide active layers of low pressure RO membranes: Data on spatial performance non-uniformity and degradation by hypochlorite solutions. Desalination 260:91-100.
- Mo H, Tay KG, Ng HY. 2008. Fouling of reverse osmosis membrane by protein (BSA): Effects of pH, calcium, magnesium, ionic strength and temperature. Journal of Membrane Science 315:28-35.
- Murphy KR, Butler KD, Spencer RGM, Stedmon CA, Boehme JR, Aiken GR. 2010.

 Measurement of Dissolved Organic Matter Fluorescence in Aquatic Environments:

 An Interlaboratory Comparison. Environmental Science and Technology 44:9405-9412.
- NRMMC, EPHC, NHMRC. 2006. Australian guidelines for water recycling: Managing health and environemental risks (phase 1). In: NRMMC, EPHC, NHMRC, editors. Canberra.
- NRMMC, EPHC, NHMRC. 2008. Australian guidelines for water recycling: managing health and environmental risks (phase 2). Augmentation of water supplies. In. Canberra: Biotext Pty Ltd.

- Ogorzaly L, Gantzer C. 2006. Development of real-time RT-PCR methods for specific detection of F-specific RNA bacteriophage genogroups: Application to urban raw wastewater. Journal of Virological Methods 138:131-139.
- Oh BS, Jang HY, Jung YJ, Kang JW. 2007. Microfiltration of MS2 bacteriophage: Effect of ozone on membrane fouling. Journal of Membrane Science 306:244-252.
- Oh H-J, Choung Y-K, Lee S, Choi J-S, Hwang T-M, Kim JH. 2009. Scale formation in reverse osmosis desalination: model development. Desalination 238:333-346.
- Onwuegbuzie AJ, Daniel L, Leech NL. 2007. Pearson Product-Moment Correlation Coefficient. In: Salkind. NJ, editor. Encyclopedia of Measurement and Statistics. Thousand Oaks, CA: SAGE Reference. p 750-755.
- Orton KJP, Jones WJC. 1909. Primary interaction of chlorine and acetanilides. Journal of the Chemical Society, Transactions 95:1456–1464.
- Orton KJP, Soper FG, Williams G. 1928. The chlorination of anilides. Part III. N-chlorination and C-chlorination as simultaneous side reactions. Journal of the Chemical Society (resumed):998-1005.
- Ottoson J, Hansen A, Björlenius B, Norder H, Stenström TA. 2006. Removal of viruses, parasitic protozoa and microbial indicators in conventional and membrane processes in a wastewater pilot plant. Water Research 40:1449-1457.
- Peabody DS, Manifold-Wheeler B, Medford A, Jordan SK, do Carmo Caldeira J, Chackerian B. 2008. Immunogenic Display of Diverse Peptides on Virus-like Particles of RNA Phage MS2. Journal of Molecular Biology 380:252-263.
- Peeters JMM, Boom JP, Mulder MHV, Strathmann H. 1998. Retention measurements of nanofiltration membranes with electrolyte solutions. Journal of Membrane Science 145:199-209.
- Peiris RH, Budman H, Moresoli C, Legge RL. 2010a. Understanding fouling behaviour of ultrafiltration membrane processes and natural water using principal component analysis of fluorescence excitation-emission matrices. Journal of Membrane Science 357:62-72.
- Peiris RH, Hallé C, Budman H, Moresoli C, Peldszus S, Huck PM, Legge RL. 2010b. Identifying fouling events in a membrane-based drinking water treatment process using principal component analysis of fluorescence excitation-emission matrices. Water Research 44:185-194.

- Peter-Varbanets M, Margot J, Traber J, Pronk W. 2011. Mechanisms of membrane fouling during ultra-low pressure ultrafiltration. Journal of Membrane Science 377:42-53.
- Peterson RJ, Cadotte JE, Buettner JM. 1982. Development of FT-30 membrane in spiral wound modules. In: Report to office of water research and technology.
- Pontius FW, Crimaldi JP, Amy GL. 2011. Virus passage through compromised low-pressure membranes: A particle tracking model. Journal of Membrane Science 379:249-259.
- Radcliffe JC. 2004. Water recycling in Australia. In: Engineering AAoTSa, editor. Victoria state.
- Reid CE, Breton EJ. 1959. Water and Ion Flow Across Cellulosic Membranes. Journal of Applied Polymer Science 1:133-143.
- Rodríguez-Limas WA, Tyo KEJ, Nielsen J, Ramírez OT, Palomares LA. 2011. Molecular and process design for rotavirus-like particle production in Saccharomyces cerevisiae. Microbial Cell Factories 10:33.
- Rodriguez C, Van Buynder P, Lugg R, Blair P, Devine B, Cook A, Weinstein P. 2009. Indirect Potable Reuse: A Sustainable Water Supply Alternative. International Journal of Environmental Research and Public Health 6:1174-1209.
- Roh IJ, Kim J-J, Park SY. 2002. Mechanical properties and reverse osmosis performance of interfacially polymerized polyamide thin films. Journal of Membrane Science 197:199-210.
- Salinas Rodriguez SG, Kennedy MD, Schippers JC, Amy GL. 2009. Organic foulants in estuarine and bay sources for seawater reverse osmosis Comparing pre-treatment processes with respect to foulant reductions. Desalination and Water Treatment 9:155-164.
- Sano D, Wada K, Imai T, Masago Y, Omura T. 2010. Norovirus-binding proteins recovered from activated sludge micro-organisms with an affinity to a noroviral capsid peptide. Journal of Applied Microbiology 109:1923-1928.
- Semiat R. 2008. Energy Issues in Desalination Processes. Environmental Science & Technology 42:8193-8201.
- Seqwater. 2011. How water is purified. In: http://www.previous.seqwater.com.au/public/sites/default/files/userfiles/file/pdfs/201 11207% 20How% 20water% 20is% 20purified% 20FINAL.pdf.

- Shafer JA. 1970. Directing and activating effects of the amido group. In: Zabicky J, editor. The Chemistry of Amides. New York: Wiley Interscience. p 685-729.
- Shannon MA, Bohn PW, Elimelech M, Georgiadis JG, Marinas BJ, Mayes AM. 2008. Science and technology for water purification in the coming decades. Nature 452:301-310.
- Shemer H, Semiat R. 2011. Impact of halogen based disinfectants in seawater on polyamide RO membranes. Desalination 273:179-183.
- Shiau B-J, Sabatini DA, Harwell JH. 1993. Influence of Rhodamine WT properties on sorption and transport in subsurface media. Ground water 31:913-920.
- Shin DH, Kim N, Lee YT. 2011. Modification to the polyamide TFC RO membranes for improvement of chlorine-resistance. Journal of Membrane Science 376:302-311.
- Shintani T, Matsuyama H, Kurata N. 2007. Development of a chlorine-resistant polyamide reverse osmosis membrane. Desalination 207:340-348.
- Shintani T, Matsuyama H, Kurata N. 2009. Effect of heat treatment on performance of chlorine-resistant polyamide reverse osmosis membranes. Desalination 247:370-377.
- Simon A, Nghiem LD, Le-Clech P, Khan SJ, Drewes JE. 2009. Effects of membrane degradation on the removal of pharmaceutically active compounds (PhACs) by NF/RO filtration processes. Journal of Membrane Science 340:16-25.
- Singh S, Henderson RK, Baker A, Stuetz RM, Khan SJ. 2009. Distinguishing stage 1 and 2 reverse osmosis permeates using fluorescence spectroscopy. Water Science and Technologie 60:2017-2023.
- Sorber CA, Malina JF, Sagik BP. 1972. Virus rejection by the reverse osmosis-ultrafiltration processes. Water Research 6:1377-1388.
- Soussan L, Guigui C, Alfenore S, Mathe S, Cabassud C. 2011a. A new biosynthetic tracer for the inline measurement of virus retention in membrane processes: Part I Synthesis protocol. Analytica Chimica Acta 690:190-198.
- Soussan L, Guigui C, Alfenore S, Mathe S, Cabassud C. 2011b. A new biosynthetic tracer for the inline measurement of virus retention in membrane processes: Part II Biochemical and physicochemical characterizations of the new tracer. Analytica Chimica Acta 690:199-208.
- Stoffel CL, Kathy RF, Rowlen KL. 2005. Design and characterization of a compact dual channel virus counter. Cytometry Part A 65A:140-147.

- Takimoto T, Chano T, Shimizu S, Okabe H, Ito M, Morita M, Kimura T, Inubushi T, Komatsu N. 2010. Preparation of Fluorescent Diamond Nanoparticles Stably Dispersed under a Physiological Environment through Multistep Organic Transformations. Chemistry of Materials 22:3462-3471.
- Tan M, Huang P, Xia M, Fang P-A, Zhong W, McNeal M, Wei C, Jiang W, Jiang X. 2011.
 Norovirus P Particle, a Novel Platform for Vaccine Development and Antibody Production. Journal of Virology 85:753-764.
- Tang CY, Chong TH, Fane AG. 2011. Colloidal interactions and fouling of NF and RO membranes: A review. Advances in Colloid and Interface Science 164:126-143.
- Tang CY, Kwon Y-N, Leckie JO. 2007. Probing the nano- and micro-scales of reverse osmosis membranes—A comprehensive characterization of physiochemical properties of uncoated and coated membranes by XPS, TEM, ATR-FTIR, and streaming potential measurements. Journal of Membrane Science 287:146-156.
- Tang CY, Kwon Y-N, Leckie JO. 2009. Effect of membrane chemistry and coating layer on physiochemical properties of thin film composite polyamide RO and NF membranes:I. FTIR and XPS characterization of polyamide and coating layer chemistry.Desalination 242:149-167.
- Tantipolphan R, Rades T, McQuillan AJ, Medlicott NJ. 2007. Adsorption of bovine serum albumin (BSA) onto lecithin studied by attenuated total reflectance Fourier transform infrared (ATR-FTIR) spectroscopy. International Journal of Pharmaceutics 337:40-47.
- UNESCO, WRQA. 2009. Virus particle removal by membrane based water recycling plants:

 Development of testing protocols and understanding long-term operational performance. Phase1: Literature review. In.
- USEPA. 2005. Membrane filtration guidance manual. In. Cincinnati.
- USEPA. 2012. Guidelines for water reuse. In. Washington, D.C.
- van den Brink P, Zwijnenburg A, Smith G, Temmink H, van Loosdrecht M. 2009. Effect of free calcium concentration and ionic strength on alginate fouling in cross-flow membrane filtration. Journal of Membrane Science 345:207-216.

- van der Bruggen B, Schaep J, Wilms D, Vandecasteele C. 2000. A Comparison of Models to Describe the Maximal Retention of Organic Molecules in Nanofiltration. Separation Science and Technology 35:169-182.
- van Voorthuizen EM, Ashbolt NJ, Schäfer AI. 2001. Role of hydrophobic and electrostatic interactions for initial enteric virus retention by MF membranes. Journal of Membrane Science 194:69-79.
- Vasudevan D, Fimmen RL, Francisco AB. 2001. Tracer-Grade Rhodamine WT: Structure of Constituent Isomers and Their Sorption Behavior. Environmental Science & Technology 35:4089-4096.
- Vrouwenvelder JS, Kruithof JC, Van Loosdrecht MCM. 2010. Integrated approach for biofouling control. Water Science & Technology 62:2477-2490.
- Vrouwenvelder JS, van Paassen JAM, van Agtmaal JMC, van Loosdrecht MCM, Kruithof JC. 2009. A critical flux to avoid biofouling of spiral wound nanofiltration and reverse osmosis membranes: Fact or fiction? Journal of Membrane Science 326:36-44.
- Wang Y-N, Tang CY. 2011. Protein fouling of nanofiltration, reverse osmosis, and ultrafiltration membranes--The role of hydrodynamic conditions, solution chemistry, and membrane properties. Journal of Membrane Science 376:275-282.
- Watnick P, Kolter R. 2000. Biofilm, City of Microbes. Journal of Bacteriology 182:2675-2679.
- WHO. 2011. Guidelines for drinking-water quality Fourth edition. In.
- Wilf M, editor. 2010. The Guidebook to Membrane Technology for Wastewater Reclamation.
- Wolf G, Almeida JS, Pinheiro C, Correia V, Rodrigues C, Reis MAM, Crespo JG. 2001. Two-dimensional fluorometry coupled with artificial neural networks: A novel method for on-line monitoring of complex biological processes. Biotechnology and Bioengineering 72:297-306.
- Xu P, Bellona C, Drewes JE. 2010. Fouling of nanofiltration and reverse osmosis membranes during municipal wastewater reclamation: Membrane autopsy results from pilot-scale investigations. Journal of Membrane Science 353:111-121.

- Xu P, Drewes JE, Kim T-U, Bellona C, Amy G. 2006. Effect of membrane fouling on transport of organic contaminants in NF/RO membrane applications. Journal of Membrane Science 279:165-175.
- Zhao Y, Song L, Ong SL. 2010. Fouling behavior and foulant characteristics of reverse osmosis membranes for treated secondary effluent reclamation. Journal of Membrane Science 349:65-74.
- Zornes GE, Jansen E, Lozier JC. 2010. Validation testing of the reverse osmosis system at Gippsland water factory. In: Sydney 2010.

Appendix A. Résumé en français

A.1. Introduction
A.2. Objectifs de la thèse
A.3. Principaux résultats et discussions
A.3.1. Evaluation de la mesure des DOM comme nouvelle technique de surveillance de l'intégrité des procédés d'OI
A.3.2. Effet des colmatages sur la rétention d'un substitut de virus et d'indicateur d'intégrité membranaire
A.3.2.1. Colmatage organique
A.3.2.2. Colmatage inorganique ou entartrage
A.3.3. Effet du vieillissement des membranes sur la rétention d'un substitut de virus et d'indicateur d'intégrité membranaire
A.3.4. Impact des systèmes d'étude et des défauts membranaires sur la rétention des composés
A.4. Conclusions

A.1.Introduction

La réutilisation des eaux usées est une des sources alternatives d'eau potable pour pallier les déficits des sources conventionnelles que sont les eaux de surface et souterraine (Shannon et al., 2008; Grant et al., 2012). Cette réutilisation peut cependant engendrer des risques par la présence de contaminants chimiques et microbiologiques. Afin de limiter au mieux ces risques, les stations de traitement des eaux usées utilisent différentes barrières dont des procédés membranaires comme la microfiltration (MF) ou l'ultrafiltration (UF) et l'osmose inverse (OI), mais aussi des procédés de désinfection comme les ultraviolets (UV) (Radcliffe, 2004). Les eaux de sortie de ces stations de traitement sont ensuite acheminées vers un réservoir qui joue un rôle de barrière environnementale (USEPA, 2012). Ce système de barrières multiples est un moyen de réduire les risques chimiques et microbiologiques à un niveau acceptable. Les risques microbiologiques sont associés à l'ingestion d'eau contaminée par des fèces humaines et animales, mais aussi à la présence d'organismes pathogènes capables de se développer dans les canalisations (ex : Legionella) (WHO, 2011). Dans l'objectif de protéger les consommateurs et d'améliorer l'acceptation publique, ces procédés de retraitement doivent être validés suivant des normes strictes mentionnées dans les textes réglementaires des pays concernés.

Les textes réglementaires australiens pour le recyclage des eaux sont basées sur l'évaluation des risques depuis les eaux usées jusqu'à leur réutilisation indirecte à titre d'eau potable. Ces textes exigent un abattement de plus de 9,5 log pour les virus pathogènes et de plus de 8 log pour les bactéries et les deux protozoaires : *Giardia* et *Cryptosporidium*. Les procédés de filtrations membranaires contribuent à l'élimination des micro-organismes incluant les bactéries et les virus avec des performances variables. La MF est capable d'éliminer les bactéries de 1 à > 7 log et les virus de 0 à 2 log (Jacangelo et al., 1995; Lovins III et al., 2002; Lebleu et al., 2009). L' UF est capable de rejeter de 1,5 à > 7 log les bactéries et les virus (Jacangelo et al., 1995; Asano, 2007). Leur efficacité à éliminer les pathogènes dépend du type de membrane et de la qualité des eaux usées. Le procédé d'OI est généralement utilisé dans le traitement tertiaire des eaux usées en tant que dernier procédé physique de filtration grâce à sa capacité théorique à retenir intégralement les virus (Shannon et al., 2008). Plusieurs études ont cependant démontré le passage des virus au travers de ces membranes, dû essentiellement à des problèmes d'intégrité des membranes d'OI (Adham et al., 1998b; Kitis et al., 2003; Lozier et al., 2003; Mi et al., 2004). A l'heure actuelle, la conductivité est la

méthode de surveillance des procédés d'OI en ligne. Cette technique n'est toutefois ni assez robuste (1,7 - 2 log) aux regards des objectifs réglementaires, ni un bon indicateur d'élimination des virus (Kitis et al., 2003) au regard de ses propriétés physico-chimiques (taille, charge). Il est aussi nécessaire de comprendre les mécanismes d'élimination des virus par des membranes intactes et défectueuses afin de développer des méthodes plus efficaces de contrôle d'intégrité pour ce système.

A.2. Objectifs de la thèse

Cette thèse est structurée autour des trois objectifs décrits ci-dessous. Ces trois objectifs constituent les quatre chapitres résultats et discussions.

<u>Objectif 1 :</u> Utilisation de l'analyse des matières organiques dissoutes pour évaluer l'effet de défaillances des procédés d'OI (Chapitre 3).

Au cours du fonctionnement d'un procédé d'OI, des connecteurs ou des joints peuvent rompre ce qui provoque une diminution de l'abattement des sels mesurés par la conductivité. Or, ce type de défaillance n'entraine pas forcément une diminution de l'abattement des virus. L'utilisation des matières organiques dissoutes (DOM) comme nouvelle méthode de surveillance des procédés d'OI a été suggérée par Henderson et al. (2009). Leur composition et leur concentration sont très variables et dépendent de la qualité des eaux d'alimentation (Chen et al., 2003; Leenheer and Croue, 2003). L'analyse des DOM se réalise généralement par fluorescence tridimensionnelle. De nombreuses études ont utilisé cette technique dans le but de différencier la qualité des eaux traitées par différents procédés (Her et al., 2008; Singh et al., 2009; Hambly et al., 2010; Peiris et al., 2010a; Peiris et al., 2010b). En 2009, Singh et al. ont prouvé que la différence de qualité des perméats au cours des étapes d'un même procédé d'OI pouvait être suivie par fluorescence tridimensionnelle. Le premier objectif de cette thèse est donc consacré à la mesure des DOM naturellement présentes dans les eaux d'alimentation par fluorescence tridimensionnelle. L'objectif est ici de valider la possibilité d'utiliser l'abattement des DOM comme nouvelle technique de surveillance et de comparer leur rétention à celle obtenue par la conductivité dans deux stations de traitements des eaux appelées 'échelle industrielle'.

<u>Objectif 2</u>: comprendre l'effet des défauts membranaires sur la rétention d'un substitut de virus et d'indicateurs d'intégrité membranaire (Chapitres 4 & 5).

Les principaux défauts membranaires des procédés d'OI sont les colmatages organique et inorganique. Afin d'éviter ou d'éliminer ces colmatages, différents produits chimiques sont utilisés. L'utilisation du chlore dans les stations de traitement des eaux est généralement une solution choisie afin de limiter le bio colmatage même si cela peut avoir un impact sur l'intégrité des membranes à long terme. Dans cette partie de la thèse, l'effet du colmatage organique et inorganique (Chapitre 4) et l'effet du vieillissement des membranes (Chapitre 5) sur la rétention des virus et de leurs substituts sont étudiés. Pour cela, un substitut de virus (phage MS2) et quatre indicateurs d'intégrité membranaire (rhodamine WT, DOM, sulfate et sels) sont utilisés sur trois systèmes à échelle laboratoire. Deux types de systèmes à flux tangentiel sont utilisés :

- Deux systèmes à membrane plane : (i) une cellule d'OI métallique ayant une surface membranaire de 140 cm² utilisée pour tous les défauts membranaires et appelé 'système métallique', et (ii) deux cellules en résine montées en parallèle ayant chacune une surface membranaire de 42 cm² utilisée uniquement pour les expériences de vieillissement des membranes et appelé 'système plastique';
- Un module à membrane à spirale : système en métal ayant une surface membranaire de 2,4 m² utilisé pour tous les défauts membranaires et appelé 'module à spirale'.

Le virus modèle et les quatre substituts sont :

- Les phages MS2 : c'est le substitut de virus classiquement utilisé dans les études sur les procédés membranaires. Dans cette étude, il a joué le rôle de témoin (contrôle) et tous les composés lui sont comparés. Sa concentration est déterminée par culture bactérienne communément appelée méthode UFP (Unités Formant Plages). Les échantillons d'entrée et de perméats sont quantifiés par la méthode de PCR (réaction de polymérisation en chaine) quantitative en temps réel, car cette méthode est plus sensible que la méthode UFP;
- La rhodamine WT (R-WT): son utilisation est autorisée dans les eaux potables par l'agence de protection américaine (USEPA, 2005). Ce marqueur est facilement quantifiable par fluorescence;

- Les sels mesurés par conductivité: la conductivité mesurée dans les eaux est liée à la présence d'ions et principalement d'ions monovalents. C'est la méthode standard actuelle de surveillance des membranes d'OI même si cette technique démontre une efficacité de 1,7 - 2 log d'abattement;
- Les DOM: l'analyse par fluorescence des DOM comme méthode de surveillance a été démontrée au cours du précédent objectif. Dans cette partie de la thèse, son utilisation possible en tant qu'indicateur d'intégrité de membrane est évaluée;
- Les sulfate (SO₄²⁻): cet ion doublement chargé est présent naturellement dans les eaux d'alimentation naturelles des procédés d'OI est mesuré par chromatographie ionique.
 La mesure des sulfates est actuellement évaluée dans les stations de traitement des eaux afin de contrôler périodiquement l'intégrité des membranes d'OI. Il est intéressant de comparer leur abattement à celui du phage MS2 et d'évaluer leur corrélation.

L'objectif de cette partie est donc d'évaluer l'impact des défauts membranaires sur la rétention d'un substitut de virus et d'indicateurs d'intégrité membranaire et d'identifier ainsi les principaux facteurs ou mécanismes qui influencent cette rétention.

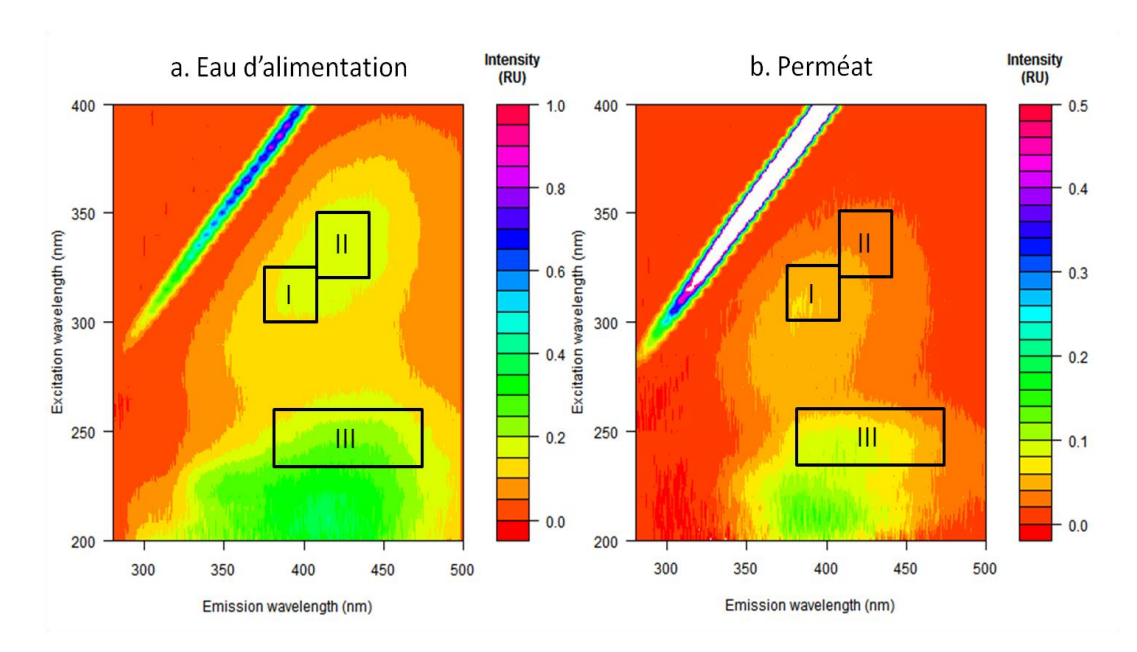
Objective 3 : comparaison des différentes échelles et composés utilisés (Chapitre 6).

Deux échelles ont été utilisées lors des expérimentations: l'échelle industrielle (Chapitre 3) et l'échelle de laboratoire (Chapitres 4 & 5). Trois systèmes à échelle laboratoire sont utilisés ayant différentes tailles de surface membranaire et/ou différentes configuration (deux systèmes à membrane plane et un module à membrane à spirale). Ces systèmes de laboratoire sont comparés au système industriel. Un test de Student est utilisé pour déterminer le système de laboratoire le plus représentatif de l'échelle industrielle. De plus, une analyse de variance à deux facteurs (ANOVA) nous permet de comparer les types de système et les types de défaut membranaire en fonction des abattements des composés. Enfin, une comparaison statistique (*t*-test) des différents abattements des composés est effectuée afin de déterminer le composé ou la combinaison de composés capable de contrôler efficacement l'intégrité des membranes d'OI.

A.3. Principaux résultats et discussions

A.3.1. Evaluation de la mesure des DOM comme nouvelle technique de surveillance de l'intégrité des procédés d'OI

Dans ce chapitre, deux procédés d'OI à trois étages présents sur deux stations différentes sont étudiés. Les influents et les perméats de différents tubes de pression ont été échantillonnés à chaque étage. L'abattement des sels et des DOM est calculé à partir des mesures réalisées par la conductivité et la fluorescence tridimensionnelle. La comparaison des spectres de fluorescence entre les influents et les perméats permet de délimiter trois régions notées régions I, II et III (Figure A.1). La région I est spécifique aux perméats, la région II est spécifique aux eaux d'alimentation et la région III est commune aux deux types d'eaux mais à des intensités de fluorescence différentes. La répartition entre ces trois régions, ramenée au volume total de fluorescence, calculée d'après la méthode d'intégration régionale (Chen et al., 2003), est commune aux deux stations. La région I est de 25% pour les influents et de 33% pour les perméats, la région II est de 31% et de 22% et la région III, qui est de 43%, reste stable entre les deux types d'échantillons. De plus, il est constaté que l'abattement des DOM reste stable au cours du procédé (99% pour la région I, 99,5% pour la région II et 99,2% pour la région III), tandis que l'abattement en sel diminue étage par étage (de 98% à 97% environ). Le taux de rétention des sels varie de 0,1à 1,5% pour un unique tube de pression aux cours des différents échantillonnages. Cette diminution peut être due à (i) une perte des performances membranaires due au colmatage ou au vieillissement des membranes; ou (ii) une fuite autour d'un joint, de la colle ou tout autre défaut physique membranaire. En théorie, la rétention des DOM est similaire au sein d'un même étage. La variation de leur abattement dans un même étage peut ainsi aider à identifier les fuites plus sensiblement qu'avec la conductivité seule, car la rétention des DOM est plus élevée que celle des sels. Cette amélioration de la sensibilité est importante si une élimination importante des virus est le but du traitement.



<u>Figure A.1</u>: Spectre de fluorescence tridimensionnelle (a) d'une eau d'alimentation diluée 50 fois et (b) d'un perméat non dilué. Les trois régions (notées I, II et III) sont délimitées par des rectangles.

Dans une même campagne d'échantillonnage, une diminution de 1,3% de l'abattement en sels entre les étages 2 et 3 d'un rack d'OI est observée, alors que celui des DOM reste constant. Par opposition, dans un autre rack d'OI, l'abattement des sels et des DOM diminue de plus de 1% entre les étages 2 et 3. Les principaux mécanismes de rétention des DOM sont l'exclusion par la taille et la répulsion électrostatique. Cette rétention peut également être influencée par d'autres propriétés moléculaires comme l'hydrophobicité qui peut être élevée tant que l'intégrité des membranes est conservée. Un connecteur cassé a été découvert dans le tube de pression ayant une diminution des abattements en sels et en DOM, ce qui provoque une fuite d'eaux d'alimentation contaminant le perméat. L'abattement en sels est plus variable que celui des DOM. Ainsi, l'utilisation des DOM est plus pertinente pour détecter les fuites.

En conclusion, cette étude prouve la faisabilité d'utiliser la fluorescence tridimensionnelle couplée à la technique d'intégration régionale pour calculer l'abattement en DOM au sein des procédés d'OI. La région II a été identifiée comme la région la plus retenue par les membranes (autour de 99,5%) tout au long des trois étages du procédé.

De plus, l'utilisation de la fluorescence en combinaison de la conductivité permet de détecter

plus sensiblement la présence de défaut dans un tube de pression. L'abattement des DOM pourrait être utilisé comme nouvelle technique de surveillance afin de satisfaire les législations en vigueur pour protéger la santé publique. Cependant, d'autres recherches doivent être menées afin de confirmer une corrélation entre les comportements des virus et des DOM pendant leurs filtrations.

A.3.2. Effet des colmatages sur la rétention d'un substitut de virus et d'indicateur d'intégrité membranaire

Cette étude a été effectuée en laboratoire utilisant deux systèmes : le système métallique et le module à spirale.

A.3.2.1. Colmatage organique

Le colmatage organique est créé à partir d'un mélange de 5 mg C.L⁻¹ d'acide humique, de 0,25 mg C.L⁻¹ de sérum albumine bovine (composé modèle pour le colmatage des protéines) et de 0,25 mg C.L⁻¹ d'alginate de sodium (composé modèle pour le colmatage des polysaccharides) et est identifié par différentes techniques microscopique et spectroscopique. Ce type de colmatage recouvre les cavités de la membrane d'OI (Ang and Elimelech, 2007; Ang et al., 2011; Kim and Dempsey, 2013) et provoque une diminution de la perméabilité à l'eau de plus de 36%. Ce colmatage change également les propriétés chimiques de la membrane telle que la charge de la surface.

Les abattements - exprimé en log (LRV = log removal value) - des phages MS2 et des indicateurs (R-WT, sels, DOM et sulfate) sont présentés dans la Figure A.2. Le colmatage organique augmente significativement les abattements des différents composés (Student t-test, p-value < 0.05) en cohérence avec l'étude de Lozier et al. (2003).

A partir de la Figure A.2, deux groupes peuvent être définis : (i) le phage MS2 et (ii) les composés solubles. Le phage MS2 est bien retenu par la membrane (LRV > 5,7) de par sa taille (effet stérique) et sa charge négative (répulsion électrostatique).

La R-WT est un colorant fluorescent soluble de 487 mol. L^{-1} chargé négativement à pH environnemental (pH_{eau} > pKa_{R-WT}). Le mécanisme de rétention de la R-WT par les membranes intactes est la répulsion électrostatique. Vasudevan *et al.* (2001) ont montré l'adsorption de la R-WT sur du sable revêtu d'acide humique. La présence d'acide humique

sur la membrane augmente l'abattement de la R-WT (+ 0.9 LRV). Les mécanismes de rétention de la R-WT par les membranes colmatées sont l'effet stérique et l'adsorption.

La mesure de conductivité englobe tous les ions présents dans l'échantillon. Le passage des ions monovalents positif et négatif au travers de la membrane diminuent l'abattement des sels mesurés par cette technique. Le colmatage organique augmente l'abattement en sels par blocage de leur diffusion à travers la membrane.

La DOM est un mélange de solutés avec différents pKa, masses molaires et tailles. La couche organique présente sur la membrane augmente leur abattement (+ 0.1 LRV) par le mécanisme d'exclusion stérique.

En conclusion, l'effet stérique est le premier mécanisme de rétention des composés lors du colmatage organique.

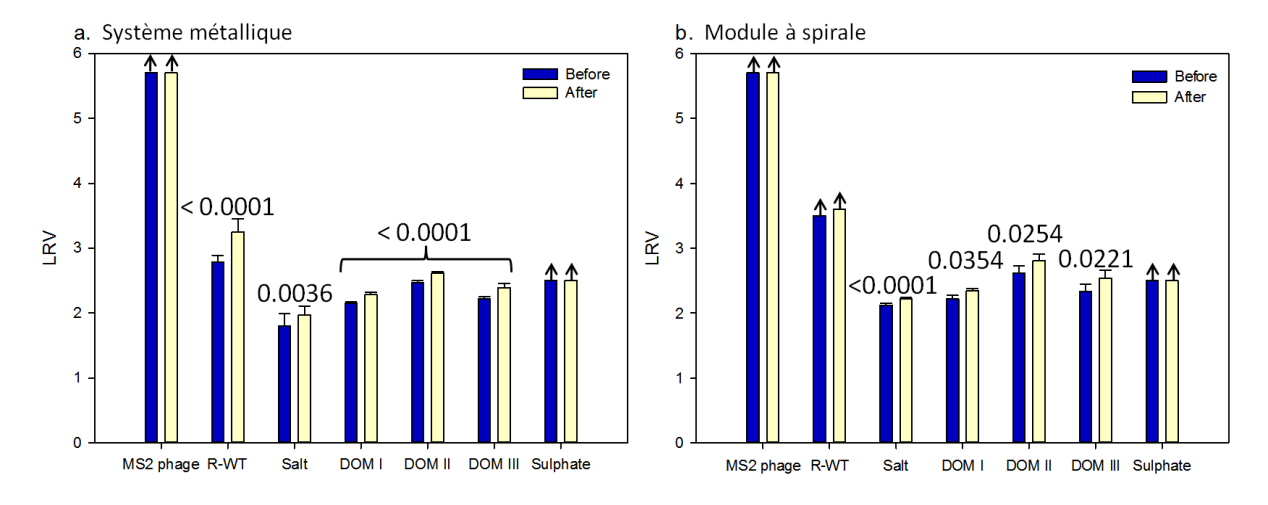


Figure A.2: Comparaison entre les abattements des phages MS2, sels (conductivité), R-WT, DOM et sulfate par les membranes intactes et colmatées organiquement avec (a) le système métallique à membrane plane et (b) le module à membrane à spirale. Expériences menées à un flux d'entrée constant, 7,5 bar et à une cross-flow vélocité de 10 cm.s^{-1} . Barres d'erreur = écart-type, n=9 (3 mesures/membrane, 3 membranes) pour le système à membrane plane et n=6 (1 module membranaire) pour le module à membrane à spirale. Flèche noire (\rightarrow) = valeur limite calculée avec la limite de quantification (LOQ) des méthodes analytiques (concentration des perméats en dessous de la LOQ pour les échantillons correspondants). Valeur au-dessus des barres = p-value du t-test.

A.3.2.2. Colmatage inorganique ou entartrage

Le colmatage inorganique est créé en utilisant un mélange de sels correspondant à la composition moyenne d'une eau d'alimentation naturelle et est caractérisé par microscopie couplée à une analyse chimique élémentaire. La couche de sels diminue la perméabilité à l'eau (*p-value* < 0.05). La majorité des abattements des substituts ne varie pas entre les membranes intactes et entartrées (*p-value* > 0.05) (Figure A.3). Les sels sont les seuls substituts à avoir subi un effet de l'entartrage des membranes sur leur abattement. Les résultats obtenus entre les deux systèmes sont contradictoires. Les abattements en sels calculés à partir du système métallique augmentent statistiquement (*p-value* < 0.05) après entartrage de la membrane, tandis que les abattements restent similaires avec le module à spirale. Cette variation entre les deux systèmes peut être expliquée par leur différence de configuration (membrane plane et membrane spiralée), mais aussi par la manipulation et le stockage des membranes planes.

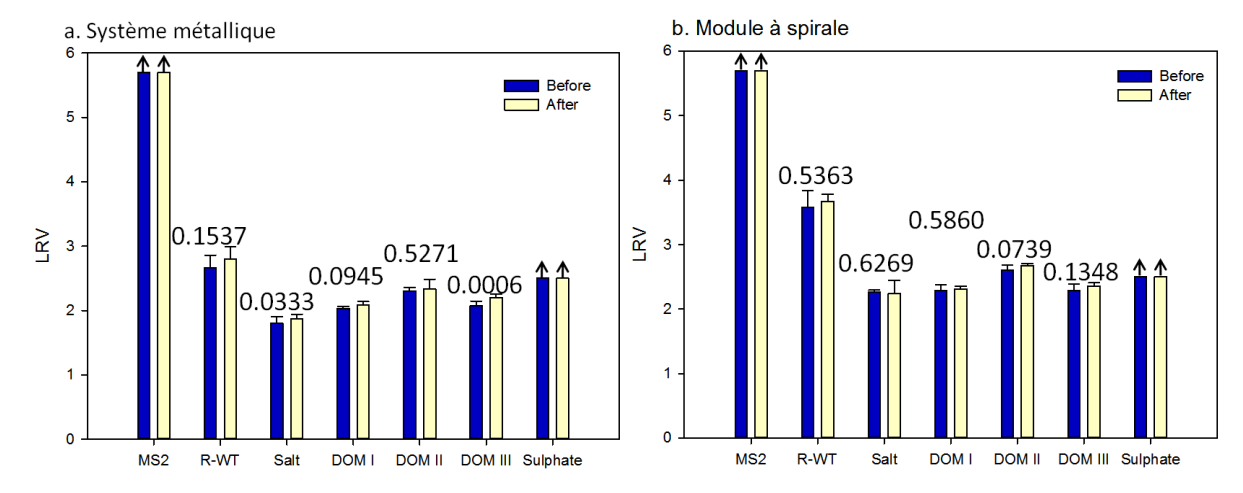


Figure A.3: Comparaison entre les abattements des phages MS2, sels (conductivité), R-WT, DOM et sulfate par les membranes intactes et entartrées avec (a) le système métallique à membrane plane et (b) le module à membrane à spirale. Expériences menées à un flux d'entrée constant, 7,5 bar et à une cross-flow vélocité de 10 cm.s⁻¹. Barres d'erreur = écart-type, n=9 (3 mesures/membrane, 3 membranes) pour le système à membrane plane et n = 6 (1 module membranaire) pour le module à membrane à spirale. Flèche noire (\rightarrow) = valeur limite calculée avec la limite de quantification (LOQ) des méthodes analytiques (concentration des perméats en dessous de la LOQ pour les échantillons correspondants). Valeur au-dessus des barres = p-value du t-test.

En conclusion, l'effet stérique reste le premier mécanisme de rétention des composés lors de l'entartrage suivi par la répulsion électrostatique.

Pour conclure sur ces deux expériences de colmatage, les abattements des composés sont soit inchangés, soit augmentés par la présence d'une couche organique ou inorganique sur la membrane qui vient bloquer le passage des composés.

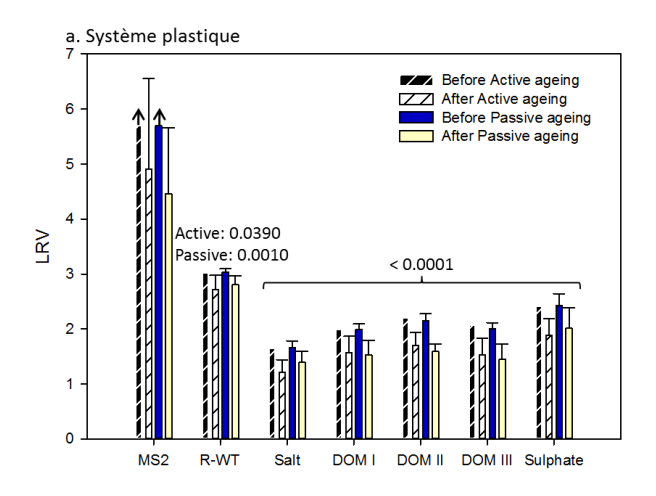
A.3.3. Effet du vieillissement des membranes sur la rétention d'un substitut de virus et d'indicateur d'intégrité membranaire

Les membranes sont vieillies artificiellement en utilisant une solution de chlore libre à 560 mg.L⁻¹ à pH 7. Le temps total d'exposition est de 16 h afin d'obtenir une exposition totale en chlore de 9000 ppm.h en mode passif (immersion) pour les trois systèmes à échelle de laboratoire et en mode actif (filtration) pour le seul système en plastique.

Le chlore attaque la structure chimique en polyamide des membranes d'OI. Ces modifications chimiques sont observées grâce à la spectroscopie infrarouge à transformée de Fourier (FTIR), couplée avec la technique de réflexion totale atténuée ou réflexion interne (ATR-FTIR) : elles provoquent une diminution ou un déplacement des pics des spectres d'IR spécifiques à la couche en polyamide. Le pKa du couple [HOCl]/[OCl] est égal à 7,5. A pH 7, l'acide hypochloreux [HOCl] est l'espèce majoritaire. Cette molécule est une espèce non chargée de faible poids moléculaire (52,5 g.mol⁻¹) ce qui lui permet de passer aisément au travers de la membrane. Pendant la chloration, les liaisons N-H sont rompues et l'atome d'hydrogène est remplacé par un atome de Cl par substitution électrophile. La formation de groupe carboxylique (COOH) est favorisée par la rupture des liaisons hydrogènes entre les groupes C=O et N-H augmentant le nombre de charges négatives à la surface de la membrane. La membrane devient également plus hydrophobe due à la rupture des liaisons C-N (Do et al., 2012a). Ces ruptures et formations de groupes provoquent un changement de la structure polyamide aromatique réticulée en structure linéaire, ce qui provoque dans un premier temps une diminution de la perméabilité à l'eau. Dans un deuxième temps, la perméabilité à l'eau augmente du fait du potentiel de flexibilité de la structure en polyamide (Kwon and Leckie, 2006b).

L'attaque au chlore provoque une diminution de l'abattement du phage MS2 et des indicateurs (Figure A.4). Ces changements de structure, de charge et d'hydrophobicité de la membrane ont provoqué une augmentation de la taille des cavités membranaires permettant

ainsi le passage facilité des composés, l'effet stérique est donc réduit.



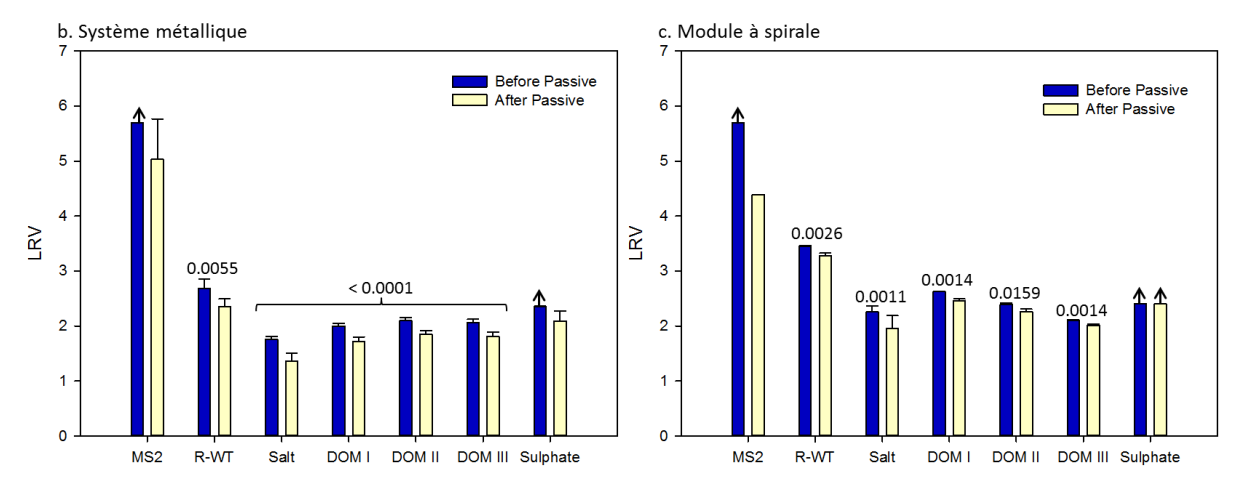


Figure A.4: Comparaison entre les abattements des phages MS2, sels (conductivité), R-WT, DOM et sulfate par les membranes intactes et vieillies avec les systèmes (a) en plastique et (b) métallique à membrane plane et (c) le module à membrane à spirale. Expériences menées à un flux d'entrée constant, à un cross-flow vélocité de 10 cm.s^{-1} , une pression de 5 bar pour le système en plastique et 7,5 bar pour le système métallique à membrane plane et le module à membrane à spirale. Barres d'erreur = écart-type, n=12 pour le système plastique (3 mesures/membrane, 4 membranes), n= 6 pour le système à membrane plane et n = 6 (1 module à membrane spiralée, n phage MS2 = 1) pour le module à membrane à spirale. Flèche noire (\rightarrow) = valeur limite calculée avec la limite de détection (LOQ) des méthodes analytiques (concentration des perméats en dessous de la LOQ pour les échantillons correspondants). Valeur au-dessus des barres = p-value du t-test.

A.3.4. Impact des systèmes d'étude et des défauts membranaires sur la rétention des composés

Le coefficient de Pearson (r) détermine le poids de corrélation entre deux abattements de composés. Ce coefficient r calculé entre les abattements des DOM, sels, R-WT et sulfate démontre une très forte corrélation entre les abattements des DOM, sels et sulfate (r > 0.7). Les corrélations entre les abattements de la R-WT et des autres substituts sont quant à elles beaucoup plus faibles (r < 0.65) et tendent à montrer une différence de comportement de la R-WT pendant la filtration comparativement aux autres composés.

L'ANOVA à deux facteurs prouve que le type de défaut membranaire et le type de système à échelle laboratoire utilisés ont un effet sur la rétention des composés.

Le système métallique à membrane plane est démontré comme étant le plus proche en termes de comportement que le procédé étudié à l'échelle industrielle (*t*-test *p-value* > 0,05). Ce résultat est surprenant, car le module à membrane à spirale semblait être le plus proche de l'échelle industrielle (même configuration membranaire). Le module à membrane à spirale est le procédé retenant le plus efficacement les composés. Le rendement de production d'eau de très haute qualité joue un rôle sur la capacité du système à retenir les contaminants : plus le rendement est élevé, moins les contaminants sont retenus à cause de la diminution de la pression et à l'augmentation de la concentration en contaminants le long d'un module par exemple. Ceci ne peut pas être appliqué aux systèmes à membrane plane, car la surface membranaire est trop faible.

En conclusion, la comparaison du comportement général des composés au cours de la filtration montre que les DOM sont le meilleur indicateur pour surveiller efficacement l'intégrité des membranes du fait de leur présence naturelle dans les eaux d'alimentation et de son abattement. Au cours de ces expériences, l'abattement de la R-WT est le plus élevé mais reste toujours plus faible que l'abattement du phage MS2. Une combinaison DOM/R-WT pourrait ainsi être envisagée.

A.4. Conclusions

Les principales conclusions de cette thèse sont :

- En combinaison avec la conductivité, l'analyse par fluorescence des DOM peut être utilisée pour détecter la présence de défaut dans un tube à pression. Ce résultat confirme l'utilisation potentielle de l'abattement des DOM pour surveiller l'intégrité des procédés d'OI.
- Le colmatage organique bloque les cavités des membranes d'OI. L'abattement des composés est alors amélioré grâce à un effet stérique amplifié.
- L'entartrage des membranes ne modifie pas l'abattement des composés sauf pour les sels sur une seule des configurations testées.
- Le vieillissement des membranes utilisant une exposition totale en chlore de 9000 ppm.h diminue l'abattement des composés. Les modifications chimiques relatives à ce vieillissement sur la membrane en polyamide, et observées lors de son autopsie, semblent modifier ses propriétés de rétention sans qu'il soit possible de savoir s'il y a modification des propriétés de surface ou cassure telle que la formation de trous.
- Le type de défaut membranaire et le type de système influencent la rétention des indicateurs d'intégrité membranaire. Le système métallique à membrane plane est le système représentant le mieux l'échelle industrielle. Finalement, ces informations permettent de sélectionner la meilleure combinaison d'indicateurs utilisés dans ce projet pour contrôler l'efficacité des procédés d'OI qui est : DOM/R-WT. Cette combinaison est un compromis entre :
 - Les DOM : suivi potentiel 'en ligne' (présence naturelle des DOM dans les eaux d'alimentation), faisabilité de la technique (fluorescence), la robustesse de cet indicateur par rapport à la méthode conductivité (même si forte corrélation entre les sels et DOM) ;
 - La R-WT : abattement plus élevé, car la R-WT a le même mécanisme de répulsion électrostatique que le phage MS2. Mais due à sa masse moléculaire, la R-WT est plus faiblement retenu par le mécanisme stérique, mais peut être adsorbée sur la membrane.

Appendix B. R program

B.1.	Pea	rson's correction coefficient (r)	174
B.1	.1.	R program code	174
B.1	.2.	Plot and linear regression	175
B.2.	Two	o-way ANOVA	179
B.2	2.1.	R program code	179
B.2	2.2.	Two-way ANOVA results	180
B.3.	Box	x plot	182
B.4.	Fish	ner's F-test and t-test	183

B.1. Pearson's correction coefficient (*r*)

The purpose of this section is to present the different code used in the software R for Chapter 6 Section 6.1 in order to:

- calculate the Pearson's correlation coefficient (*r*) to determine the relationship between two paired samples;
- plot the data and do a linear regression in order to visualise this relationship.

B.1.1. R program code

#Example of a Pearson's correlation coefficient table:

Pearson's product-moment correlation

data: Group[,1] and Group[,2]

Degree of freedom = n -1

t = 8.0188, df = 29, p-value = 7.64e-09

alternative hypothesis: true correlation is not equal to 0

95 percent confidence interval:

0.6741339 0.9152711

sample estimates:

cor

0.8301693

r correlation coefficient

#Graph plot:

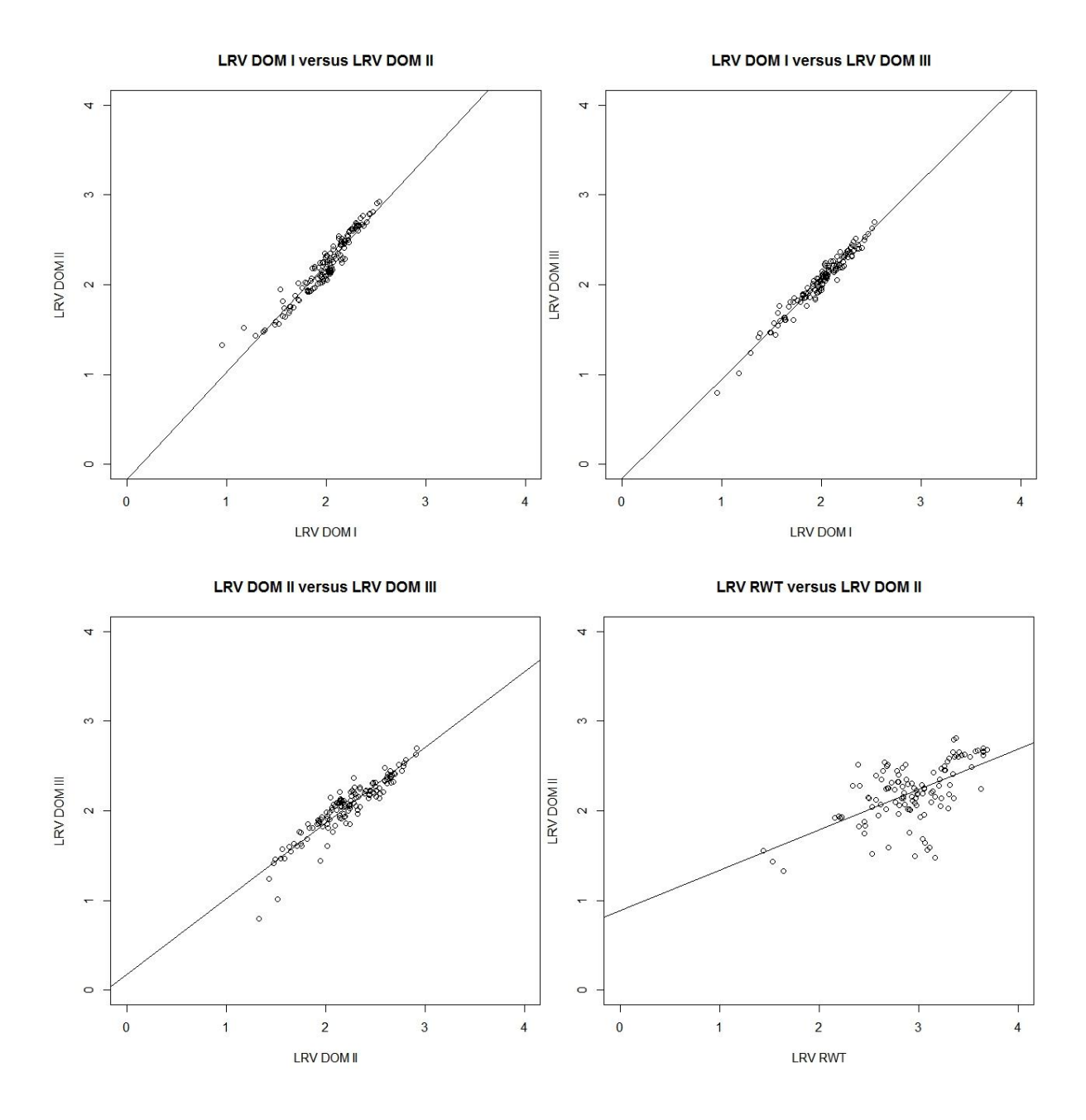
plot(Group[,1], Group[,2], xlab=" LRV Compound 1 ", ylab="LRV Compound 2", main="Compound 1 versus Compound 2", xlim = c(0,4), ylim = c(0,4))

#Add regression linear line and calculate regression coefficients:

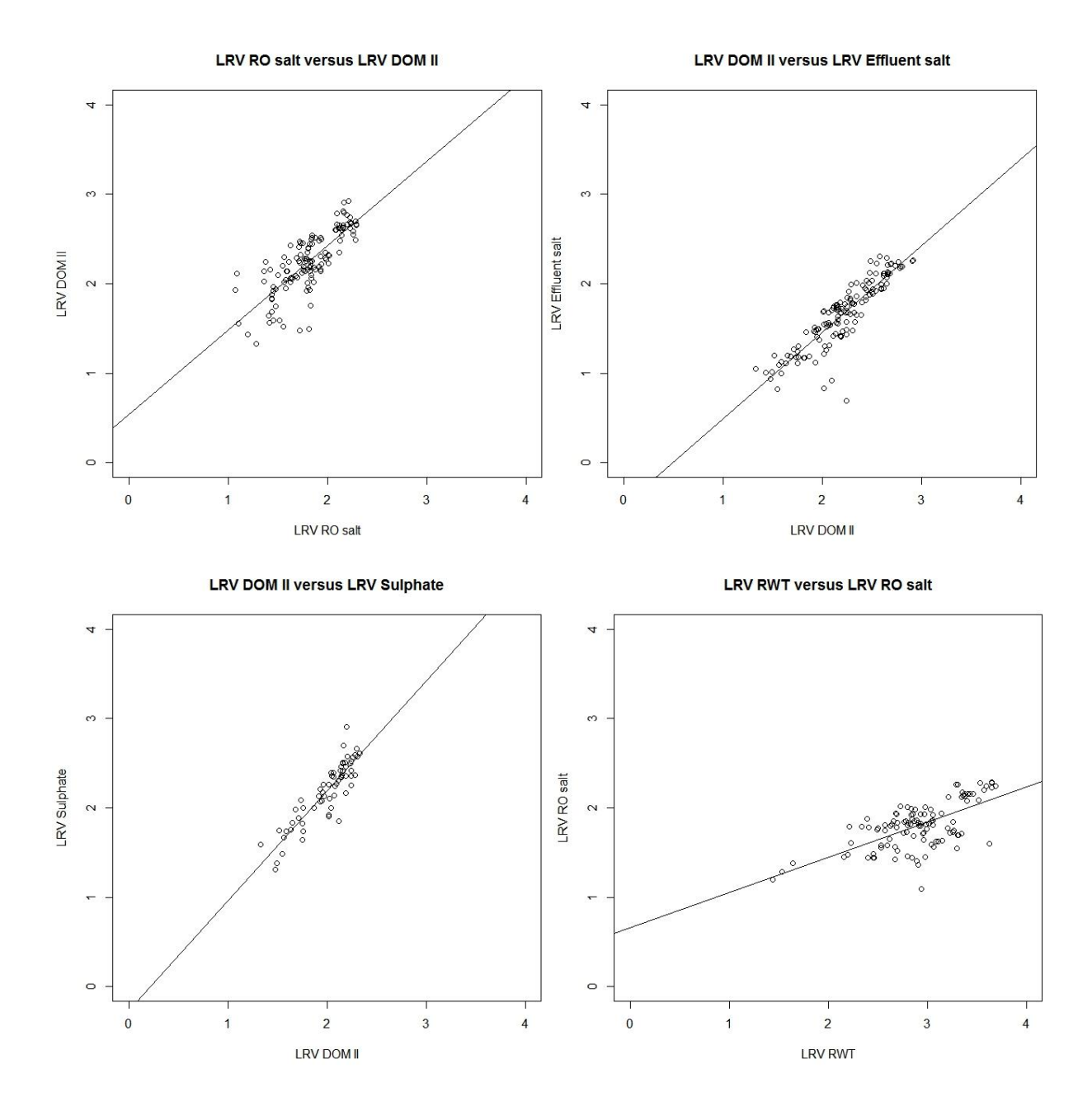
lm.r=lm(Group [,2]~Group [,1])
abline(lm.r)
coef(lm.r)
summary(lm.r)\$r.squared

B.1.2. Plot and linear regression

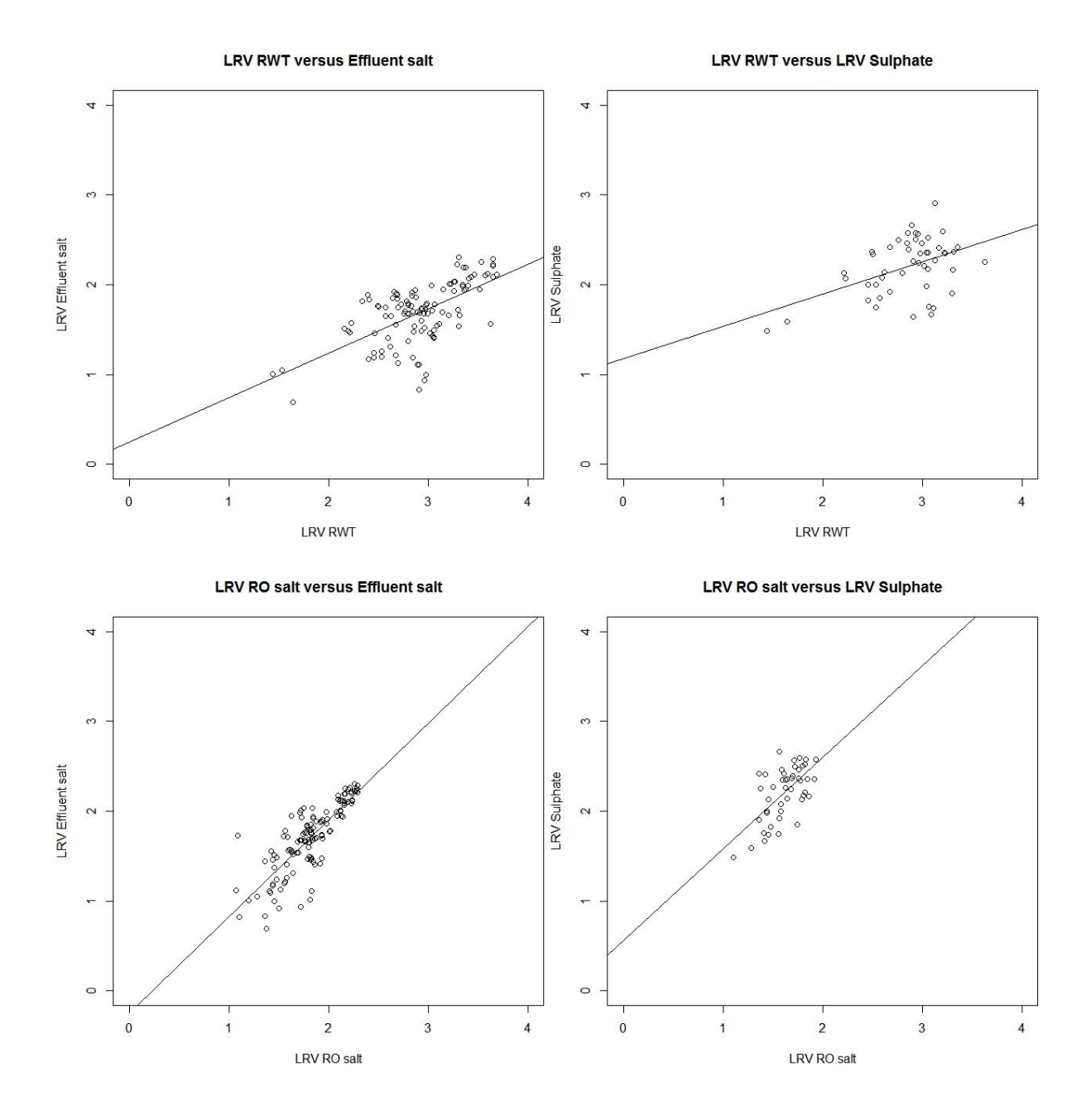
From the R program code "plot" and "abline", the plots of the different compounds rejection combinations have been obtained and are presented below.



<u>Figure B.1:</u> Plots with linear regression of different combinations of compounds (expressed in LRV).



<u>Figure B.1:</u> Plots with linear regression of different combinations of compounds (expressed in LRV) (continued).



<u>Figure B.1:</u> Plots with linear regression of different combinations of compounds (expressed in LRV) (continued).

B.2. Two-way ANOVA

The purpose of this section is to present the different two-way ANOVA codes used for the software R and the table results for Chapter 6 Section 6.2. Two-way ANOVA was used to determine the effect of set-up (factor 1) and membrane impairment (factor 2) on the compounds rejection.

B.2.1. R program code

```
#Read the data into R and saves as some name:
Group<-read.csv("group_ANOVA.csv", header = TRUE)
Factor<-read.csv("factor_ANOVA.csv", header = TRUE)
#Determine first row as label row:
row.names(Group)<- Group [,1]</pre>
Group <- Group [,-1]
row.names(Factor)<- Factor [,1]</pre>
Factor <- Factor [,-1]
#Allow the factors within the data to be accessible to R:
attach(Factor)
attach(Group)
#Two-way ANOVA:
anova(lm(Groups[,X]~Factors[,1]*Factors[,2]))
       # If p-value > 0.05 = no effect of the factor
       # If p-value < 0.05 = effect of the factor
```

B.2.2. Two-way ANOVA results

#Analysis of Variance Table

#Factor 1 = Set-ups

#Factor 2 = Impairments

#Response: R-WT:

Analysis of Variance Table

Response: Group[, 1]

	Df	Sum Sq	Mean Sq	F value	Pr (>F)	
Factor[, 1]	2	10.2017	5.1008	56.1206	< 2.2e-16	***
Factor[, 2]	4	5.4159	1.3540	14.8969	7.474e-10	***
Factor[, 1]: Factor[, 2]	4	1.0615	0.2654	2.9197	0.02418	*
Residuals	116	10.5346	0.0909			

Signif. codes: 0 '***' 0.001 '**' 0.01 '*' 0.05 '.' 0.1 ' '1

#Response: RO salt:

Analysis of Variance Table

Response: Group[, 2]

	Df	Sum Sq	Mean Sq	F value	Pr (>F)	
Factor[, 1]	4	4.8474	2.42372	149.263	< 2e-16	***
Factor[, 2]	4	3.2745	0.81862	50.414	< 2e-16	***
Factor[, 1]: Factor[, 2]	4	0.1365	0.03412	2.101	0.08511	
Residuals	116	1.8836	0.01624			

Signif. codes: 0 '*** 0.001 '** 0.01 '* 0.05 '.' 0.1 ' ' 1

#Response: DOM I:

Analysis of Variance Table

Response: Group[, 3]

	Df	Sum Sq	Mean Sq	F value	Pr (>F)	
Factor[, 1]	2	4.5800	2.29001	103.8838	< 2e-16	***
Factor[, 2]	4	2.7331	0.68328	30.9964	< 2e-16	***
Factor[, 1]: Factor[, 2]	4	0.2787	0.06967	3.1604	0.01623	*
Residuals	130	2.8657	0.02204			

Signif. codes: 0 '*** 0.001 '** 0.01 '* 0.05 '.' 0.1 ' ' 1

#Response: DOM II:

Analysis of Variance Table

Response: Group[, 4]

	Df	Sum Sq	Mean Sq	F value	Pr (>F)	_
Factor[, 1]	2	8.6344	4.3172	163.0480	< 2e-16	***
Factor[, 2]	4	3.8731	0.9683	36.5687	< 2e-16	***
Factor[, 1]: Factor[, 2]	4	0.2597	0.0649	2.4524	0.04915	*
Residuals	130	3.4422	0.0265			

Signif. codes: 0 '*** 0.001 '** 0.01 '* 0.05 '.' 0.1 ' ' 1

#Response: DOM III:

Analysis of Variance Table

Response: Group[, 5]

	Df	Sum Sq	Mean Sq	F value	Pr (>F)	_
Factor[, 1]	2	5.7782	2.88909	104.3294	< 2.2e-16	***
Factor[, 2]	4	3.3255	0.83137	30.0221	< 2.2e-16	***
Factor[, 1]: Factor[, 2]	4	0.5650	0.14124	5.1005	0.0007531	***
Residuals	130	3.6000	0.02769			

Signif. codes: 0 '*** 0.001 '** 0.01 '* 0.05 '.' 0.1 ' ' 1

#Response: Effluent salt:

Analysis of Variance Table

Response: Group[, 6]

	Df	Sum Sq	Mean Sq	F value	Pr (>F)	-
Factor[, 1]	2	12.5824	6.2912	429.3865	< 2.2e-16	***
Factor[, 2]	4	4.3017	1.0754	73.4000	< 2.2e-16	***
Factor[, 1]: Factor[, 2]	4	0.4917	0.1229	8.3901	4.718e-06	***
Residuals	130	1.9047	0.0147			

Signif. codes: 0 '*** 0.001 '** 0.01 '* 0.05 '.' 0.1 ' 1

B.3. Box plot

Box plots were used in Chapter 6 Sections 6.2 and 6.3 in order to visualise the effect of the type of set-up and the type of membrane impairment on the rejection of the compounds.

#Read the data into R and saves as some name:

Group<-read.csv("groups.csv", header = TRUE)

Factor<-read.csv("factors.csv", header = TRUE)

#Determine first row as label row:

row.names(Group)<- Group [,1]</pre>

Group <- Group [,-1]

row.names(Factor)<- Factor [,1]</pre>

Factor <- Factor [,-1]

#Allow the factors within the data to be accessible to R:

attach(Factor)

attach(Group)

```
#Open R graphics window, determine number of line and number of graph per line:
par(mfrow=c(1,1))
#To select a specific order for the box plots x axis:
Factor [,1] = factor(Factor [,1], unique(Factor [,1]))
#Box plot:
boxplot(Group[,1]~Factor[,1], xlab="Factor", ylab="Group", main="Title", ylim = c(0,4))
B.4. Fisher's F-test and t-test
#Read the data into R and saves as some name:
LRV<-read.csv("LRV virus.csv", header = TRUE)
#Allow the factors within the data to be accessible to R:
attach(LRV)
#Fisher: proved that the samples were homogenous if p-value > 0.05 (H0 hypothesis):
var.test(LRV [,1], LRV [,2])
              #If p-value > 0.05: t.test var.equal = TRUE
              #If p-value < 0.05: t.test var.equal = FALSE
```

#Example of F-test:

F test to compare two variances

```
data: LRV [, 1] and LRVmodule[, 2]
               Degree of
                             Degree of
                                              Homogenous
 Fisher's F for freedom of
                            freedom of
                                              variance
 alpha = 0.05 numerator
                             denominator
     F = 0.9488, num df = 10, denom df = 9, p-value = 0.928
     alternative hypothesis: true ratio of variances is not equal to 1
     95 percent confidence interval:
      0.2393611 3.5854615
     sample estimates:
     ratio of variances
          0.9487952
               #Verify H0:
pf(0.95,num df,denom df)
              \#If pf > F = acceptation of the H_0 of homogeneity of variances
       #t-test:
              #If pf < F:
t.test(LRV [,1], LRV [,2], var.equal=FALSE, paired=FALSE)
               #If pf > F:
t.test(LRV [,1], LRV [,2], var.equal=FALSE, paired=TRUE)
```

 $\#If \ p\text{-}value > 0.05 = averages of two groups are significantly similar$

#Example of *t*-test:

Welch Two Sample t-test

data: LRV [, 1] and LRV [, 2] averages of two groups t-test value Degree of freedom significantly similar t = -1.9982, df = 7.984, p-value = 0.08082 alternative hypothesis: true difference in means is not equal to 0 95 percent confidence interval: -0.28438947 - 0.02038947 sample estimates: mean of x mean of y 2.280 - 2.412

#Verify H₀:

pt(0.975,df)

 $\#If\ pf > t = acceptation\ of\ the\ H_0\ of\ variances\ of\ equality\ of\ the\ means$



MONITORING REVERSE OSMOSIS MEMBRANE INTEGRITY AND VIRUS REJECTION IN WATER REUSE

This study shows the impact of fouling and ageing of reverse osmosis (RO) membranes on the rejection of different compounds to improve our understanding on virus rejection mechanisms. Dissolved organic matter (DOM) is generally used as an indicator of water quality. Thus, in combination with electrical conductivity profiling, the potential monitoring of DOM by three-dimensional fluorescence to detect membrane breaches was firstly investigated. It has been demonstrated that DOM could be used as new membrane integrity indicator. Then, the rejection of one virus surrogate (MS2 phage) and four membrane integrity indicators (DOM, rhodamine WT, sulphate and salt) has been studied with intact and impaired membranes using lab-scale set-ups. It has been concluded that the presence of organic foulants on the membrane surface causes a decrease of the water permeability and an increase of compounds rejection by improving size exclusion mechanism. On the other hand, scaling does not have an impact on their rejection even if the water permeability decreases. Moreover, a chlorine exposure of 9000 ppm.h NaOCl at pH 7 causes a drop of the water permeability and compounds rejection. However, the exact modifications of the membrane surface chemistry caused by chlorine exposure are still not well understood. To conclude, statistical analysis of the data obtained using the full- and lab-scales permits to propose a new combination of monitoring techniques to monitor RO membrane.

DEFENDED ON 18TH DECEMBER 2013 AT:





WITH THE FINANCIAL SUPPORT OF:







INSTITUT NATIONAL DE LA RECHERCHE AGRONOMIQUE

Unité de recherche (UR0050) - Laboratoire de Biotechnologie de l'Environnement

Avenue des Etangs F 11100 - Narbonne France Tél.:+33468425151

Courriel: Ibe-contact@supagro.inra.fr www.montpellier.inra.fr/narbonne

